Microbial and Immune Control of Intestinal Stem Cells

by

Meghan Patricia Ferguson

A thesis submitted in partial fulfillment of the requirements for the degree of

Doctor of Philosophy

Department of Cell Biology
University of Alberta

Abstract

Intestinal epithelial damage and homeostatic cell shedding sends evolutionarily conserved growth signals to activate division programs in stem cells, which renews the epithelium to maintain barrier integrity[1]. In addition to conserved growth and stress signaling, microbes and innate immune pathways regulate stem cell function during homeostasis and disease. For instance, the microbiome promotes stem cell proliferation and differentiation while overactive innate immune signaling causes stem cell hyperproliferation and exacerbates tumorigenesis[2]. It is clear bacteria and immune pathways are important regulators of stem cell function, however the complexity of the microbiome has made it difficult to elucidate the specific effects individual bacterial species have on stem cells. In addition, the intestine is a heterologous tissue composed of multiple different specialized cell types, including intestinal stem cells, absorptive enterocytes and secretory enteroendocrine cells. Given the heterogeneity of cell types in the intestine and the limitations of vertebrate genetics, cell-type specific contributions of immune pathway activation on intestinal growth have been hard to determine, especially the impact of immune activity in stem cells.

To determine how individual bacterial species and immune pathways impact stem cell function I used *Drosophila melanogaster* as a model system. *Drosophila* provides a number of advantages for this work. For example, *Drosophila* can be easily reared without a microbiome and associated with single bacterial species to determine their effects. In addition, *Drosophila* genetics allow for the perturbation of immune signaling in distinct cell types of the intestine, including stem cells. Using *Drosophila*, I identified the commensal bacteria *Lactobacillus brevis* as a potent stimulator of stem cell divisions and tumorigenesis. *L. brevis* altered the expression and intracellular localization of integrins in stem cells, leading to symmetric stem cell expansion. Next, I asked what

the consequences of immune signaling in stem cells are by activating or inhibiting the immune deficiency (IMD) pathway. Activation of IMD in progenitor cells resulted in intestinal hyperplasia and exacerbation of tumorigenesis. Furthermore, inhibition of IMD reduced homeostatic proliferation and disrupted differentiation. Finally, I asked if the NF-κB family transcription factor Relish acts in stem cells to modulate damage response. Damage of the intestine results in elevated stem cell divisions to repair the injury. However, stem cell specific Relish depletion caused stem cells and their progeny to undergo apoptosis, rendering intestines incapable of effective epithelial repair, leading to host lethality. Thus, bacterial species can have profound effects on stem cell physiology and that immune pathways act directly in stem cells to modify proliferation, tumorigenesis, differentiation and epithelial repair responses.

Preface

This thesis contains original work from Meghan Ferguson as well as the work of Minjeong Shin and Kristina Petkau from the Foley lab. In each case Dr. Edan Foley was the supervisory author involved in concept formation and manuscript composition. Content from published sources are reused with permission and include:

- **Ferguson, M.**, & Foley, E., (2021). Microbial recognition regulates intestinal epithelial growth in homeostasis and disease. *FEBS*. 1-26. Review article written by myself, the content of which is used in the introductory Chapter 1.
- **Ferguson, M**., Petkau, K., Shin, M., Galenza, A., Fast, D., & Foley, E. (2021). Differential effects of commensal bacteria on progenitor cell adhesion, division symmetry and tumorigenesis in the *Drosophila* intestine. *Development*. 148(5): 1-14. Data from this manuscript are shown in Chapter 3 with the exception of Figure 3.12 which is unpublished. I performed all experiments, analysis and manuscript composition while KP, MS, AG, and DF helped with dissections for the FACS RNA-seq experiment.
- Petkau, K., **Ferguson, M**., Guntermann, S., & Foley, E. (2017). Constitutive Immune Activity Promotes Tumorigenesis in *Drosophila* Intestinal Progenitor Cells. *Cell Reports* 20: 1784-1793. Data from this manuscript are in Chapter 4. Data in Figures 4.2-4.5 were generated by KP and SG while data in figure 4.6 was generated by myself.
- Shin, M., **Ferguson, M.,** Willms, R. J., Jones, L. O., Petkau, K., & Foley, E. (2022). Immune regulation of intestinal stem cell function in *Drosophila*. *Stem Cell Reports.* 17(4):741-755. Data in Figures 4.1, 4.7A-C H-J and L-N, 4.8 and 4.11 A-G were generated by MS. Data in Figures 4.9, 4.10 and 4.11H-I were generated by myself. RW, LJ and KP helped with intestinal dissections. MS did remaining data analysis and manuscript composition alongside EF.

This thesis also contains original work by Meghan Ferguson that is in preprint form and currently sent for review at Stem Cell Reports:

- **Ferguson, M.,** Shin, M., & Foley, E. (2022). Relish/NF-κB acts in intestinal stem cells to promote epithelial repair in *Drosophila*. *Biorxiv* **doi:** https://doi.org/10.1101/2022.09.29.510182. Data from this manuscript are shown in Chapter 4 Figure 4.7 D-G and K, and Chapter 5 Figures 5.1-5.9. MS helped with intestinal dissections while I generated all data, performed analysis and composed the manuscript.

Dedication

To all the women in STEM

"Life is not easy for any of us. But what of that? We must have perseverance and above all confidence in ourselves. We must believe that we are gifted for something and that this thing must be attained."
~ Marie Curie ~

Acknowledgments

Throughout the course of this PhD I received support and guidance from numerous sources, without which this immense amount of work would not be possible. I would like to begin by thanking my supervisor Dr. Edan Foley for being an amazing mentor over the years. Thank you for being a spark of joy in the lab and for always being there to discuss science or otherwise. I always thought of you more of a colleague than a supervisor and will be forever grateful to you for creating a positive and inclusive atmosphere for the future generations to thrive. I consider myself lucky to have had the opportunity to study in your lab and hope to carry on the lessons I have learned to advance science and inspire others.

Thank you to the Foley lab, past and present, for your valuable help and friendship over the years. Special shout out to past members Saeideh Davoodi, Anthony Galenza and David Fast, now all successful PhDs, for their comradery and guidance navigating the graduate program when I joined the lab. Certain experiments only happened with the helping hands of my amazing lab mates. The great dissection party of 2017 would not have been possible without the efforts of Anthony Galenza, David Fast, Minjeong Shin and Kristina Petkau. Thank you for helping me dissect 1200 fly intestines for my sequencing project! Another huge thanks to Minjeong Shin for helping me dissect, again, for my single cell sequencing project. Many hands make for light work! I also had the pleasure of collaborating with Kristina Petkau and Minjeong Shin closely for their papers and have included some of these data in this thesis. I would also like to thank our technicians Brittany Fraser and Lena Jones for their dedication, friendship and help in making everything in the lab run smoothly over the years. And to the current students; Reegan Willms, Mckenna Ecklund, Xinyue Xu, Derrick De Leon, and Eduardo Bueno; I'm very grateful for the support, intellectual conversations about bugs and guts and immunity, all the treats, and laughs. I hope the best for you all as you continue down this path. Finally, thank you to all Foley lab members over the years for dealing with my weird singing and random bird noises, I'm sure it will be missed.

The numerous core facilities at the University of Alberta were paramount for the completion of my PhD. I'd like to thank all the staff at the Alberta Diabetes Institute cryosectioning facility, Molecular Biology Facility (MBSU), Faculty of Medicine and Dentistry (FoMD) Cell Imaging Centre, and FoMD high content analysis core for their invaluable services.

I'd like to thank the amazing fly community for the engaging talks and generosity. Whenever I needed certain flies or reagents I could always count on the community to provide.

Special thank you to my committee members Dr. Andrew Simmonds and Dr. Lynne Postovit for creating a supportive environment and for their valuable discussion. And thank you to my external examiners Dr. Rob Ingham and Dr. Julia Cordero for your contributions to the thesis examining process.

Thank you to the Medical Microbiology and Immunology department and Cell Biology department students and staff. Navigating graduate school would not have been possible without your guidance and efforts.

Finally, I am forever grateful to my friends and family for their support over the years. Thank you to my partner Noah who was always there to talk, good or bad, when I needed it. Thank you to my friend Dan for all the chats and strolls on campus. And thank you to my family, without your support none of this would be possible.

Financial support for these projects was provided by Alberta Innovates Technology Futures and the National Science and Engineering Research Council.

Last but not least I would like to thank the humble *Drosophila* for being an amazing teacher. I learned so much about genetics, stem cell biology, host-microbe interactions, and immunity from the fly and it allowed me to gain experience in techniques I love, like microscopy and bioinformatics. I will forever be grateful for my time spent with the fly and hope to carry on these lessons to my next model organism!

Table of Contents

List of Tables

List of Figures

Chapter 1: Introduction

Chapter 3: Commensal bacteria modify intestinal stem cell adhesion, division symmetry and tumorigenesis

Chapter 5: The NF-κB transcription factor Relish acts in stem cells to regulate intestinal repair

Chapter 6: Discussion

List of Abbreviations – in order of appearance

MAMPS	Microbe associated molecular patterns
TLR	Toll-like receptor
IBD	Inflammatory bowel disease
ISC	Intestinal stem cell
PM	Peritrophic matrix
EC	Enterocyte
EE	Enteroendocrine cell
EB	Enteroblast
TA zone	Transit amplifying zone
BMP	Bone morphogenic protein
JNK	Jun N-terminal kinase
JAK-STAT	Janus kinase/signal transducer and activator of transcription
EGF	Epidermal growth factor
IMD	Immune deficiency pathway
NOD	Nucleotide binding oligomerization domain
PGN	Peptidoglycan
AMPs	Antimicrobial peptides
ROS	Reactive oxygen species
Ecc15	*Erwinia caratovora caratovora 15*
T6SS	Type six secretion system
TARGET	Temporal and regional gene expression
MARCM	Mosaic analysis with a repressible cell marker
LPS	Lipopolysaccharide
DSS	Dextran sodium sulfate
TNF	Tumor necrosis factor
GF	Germ-free
CR	Conventionally reared
PH3	Phospho-histone 3

Nomenclature

Table 1.0 *Drosophila* nomenclature

Type	**Notation**	**Example**
Gene	Italics	*Delta* or *relish*
Protein	Non-italics, first letter capitalized	Relish
Pathway	All capitalized	IMD
Chromosome	, (comma) separates genes within a chromosome	*esg-GAL4, UAS-GFP*
Chromosome	/ (forward slash) separates genes on homologous chromosomes	esg^{ts}/rel^{RNAi}
Chromosome	; (semi colon) separates genes on heterologous chromosomes	$RasN17;ISC^{ts}$
Chromosome	+ (plus) denotes a wild-type chromosome	$esg^{ts}/+$
Transgene	> (greater than) denotes expression with the GAL4 UAS system	$esg^{ts}>ImdCA$

Chapter 1

Introduction

This chapter contains content from the following sources:

- **Ferguson, M.**, & Foley, E., (2021). Microbial recognition regulates intestinal epithelial growth in homeostasis and disease. *FEBS*. 1-26.
- **Ferguson, M.**, Petkau, K., Shin, M., Galenza, A., Fast, D., & Foley, E. (2021). Differential effects of commensal bacteria on progenitor cell adhesion, division symmetry and tumorigenesis in the *Drosophila* intestine. *Development*. 148(5): 1-14

1.1 Summary

The intestine is a dynamic tissue that is constantly exposed to environmental insults. In response to such challenges, intestinal homeostasis must be tightly regulated to maintain epithelial integrity. In addition to dietary inputs, the intestinal lumen is inhabited by a dense consortium of microbes that aid intestinal digestion, direct the maturation of immune cells and alter epithelial growth[3,4]. For example, commensal bacteria promote intestinal proliferation in flies, fish and mice[5–9]. Observations like these suggest animals have evolved mechanisms that integrate microbial cues to modulate intestinal epithelial proliferation and adapt to the constantly changing lumen environment. Evolutionarily conserved innate immune pathways act in epithelial tissues to directly respond to microbe associated molecular patterns (MAMPs) and dictate the action of downstream immune effectors. Innate immune pathways are essential for animals to tolerate commensal microbes while limiting the persistence and damage caused by pathogenic microbes. In addition to immune functions, innate immune pathways play important roles in intestinal homeostasis and disease[2,10]. For instance, Toll-like receptor (TLR) signaling in mice is required for the differentiation of mucus-secreting goblet cells in the intestine[11] and in humans, microbial dysbiosis and hyper activation of immune pathways correlate with the onset of intestinal diseases such as inflammatory bowel disease (IBD) and colorectal cancer [12–16]. Therefore, intestinal immune signaling must be appropriately balanced to limit intestinal disease while allowing for proper intestinal development.

The intestine contains multiple specialized cell types with distinct functions. For instance, multipotent intestinal stem cells (ISCs) divide and differentiate to generate all absorptive and secretory lineages in the intestine[17–19]. ISCs are essential for epithelial maintenance. Upon ageing or damage, mature cells are shed from the epithelium and must be replaced by the proliferative actions of ISCs. ISCs integrate cues from the surrounding epithelium and lumen to adapt their division programs to effectively maintain an epithelial barrier. Given the important role microbes and immunity plays in directing intestinal growth, ISCs may directly integrate microbial cues to dictate their actions. However, it is not yet understood how microbes specifically alter the function and physiology of ISCs. In addition, we still do not know if innate immune pathways function within ISCs to regulate intestinal growth in the context of homeostasis or disease.

To answer these questions, I used *Drosophila melanogaster* as a model organism. *Drosophila* is a popular system to study microbial and immune control of intestinal homeostasis and disease given its cultivable microbiome and the evolutionary conservation of immune, stress and growth pathways. In addition, the abundance of genetic tools in *Drosophila* allows us to investigate the function of immune pathways in targeted cell types of the intestine, including ISCs. Using this model, I identified a commensal species of bacteria that alters ISC cell adhesion, promotes the division and expansion of ISCs, and exacerbates tumorigenesis. In addition, I discovered that innate pathways act in ISCs to regulate cell survival, proliferation, differentiation, and facilitate tumorigenesis and repair. Together, my work identifies microbes and innate immune pathways as critical regulators of ISC function with important implications for intestinal health.

1.2 The *Drosophila* intestine

1.2.1 Intestinal anatomy

The vinegar fly, *Drosophila melanogaster*, has become a pivotal model to understand intestinal physiology and function. The adult *Drosophila* intestine, although much simpler than vertebrate intestines, contains intestinal regions with physiologically similar functions[20,21]. It is divided into three main regions: the foregut, midgut, and hindgut. The foregut stores and regulates the passage of food into the midgut. The midgut shares similar functions to the human small intestine and is further subdivided into five regions differing in morphology and function. The anterior R1 and R2 regions express enzymes to metabolize proteins and lipids[20]. The R3 or copper cell region contains specialized cells that maintain an acidified stomach-like region to aid in food breakdown and control bacterial abundance[22,23]. The posterior midgut R4 and R5 regions are highly proliferative and where most studies focus to understand stem cell biology[20,23–25]. The hindgut is similar to the human large intestine and regulates the passage of waste out of the intestinal tract.

Unlike human or mouse intestines, the fly gut is a pseudostratified epithelium that lacks folds, villi, or crypts. However, the fly intestine is composed of equivalent cell types to vertebrates[19] (Fig. 1.1). Like vertebrates, fly intestines contain absorptive enterocytes and secretory enteroendocrine cells that are maintained by multipotent intestinal stem cells (ISCs)[26–28] (Fig. 1.1A). Enterocytes make up the majority of the intestinal landscape and absorb nutrients from the intestinal lumen, while enteroendocrine cells produce and secrete peptide hormones. A chitinous membrane, the

peritrophic matrix, limits direct contact with bacteria in the lumen and functions similarly to vertebrate mucus[29] (Fig. 1.1). *Drosophila* ISCs reside basally in close proximity to the supporting visceral muscle layer, an important source of signals that regulate ISC division[30,31]. Similarly, mouse ISCs reside basally in crypts as two populations, +4 slowly cycling, damage resistant ISCs and actively cycling crypt base columnar cells specified by the expression of the Wnt target gene Lgr5[32,33] (Fig. 1.1). The majority of ISC divisions in *Drosophila* occur asymmetrically to produce a post-mitotic enteroblast and an ISC[34–37]. The enteroblast then undergoes a maturation process and fully integrates into the epithelium as a mature enterocyte. Collectively, *Drosophila* ISCs and enteroblasts are known as progenitors. Although the *Drosophila* intestine contains major cell lineages, such as progenitors that give rise to secretory and absorptive lineages, they lack specific vertebrate cell types such as Paneth cells, goblet cells, tuft cells, and M cells (Fig. 1.1B). In addition, *Drosophila* lacks structures like Peyer's patches for the recruitment and organization of immune cells, although innate immune cells associate with the intestine and influence ISC function[38,39].

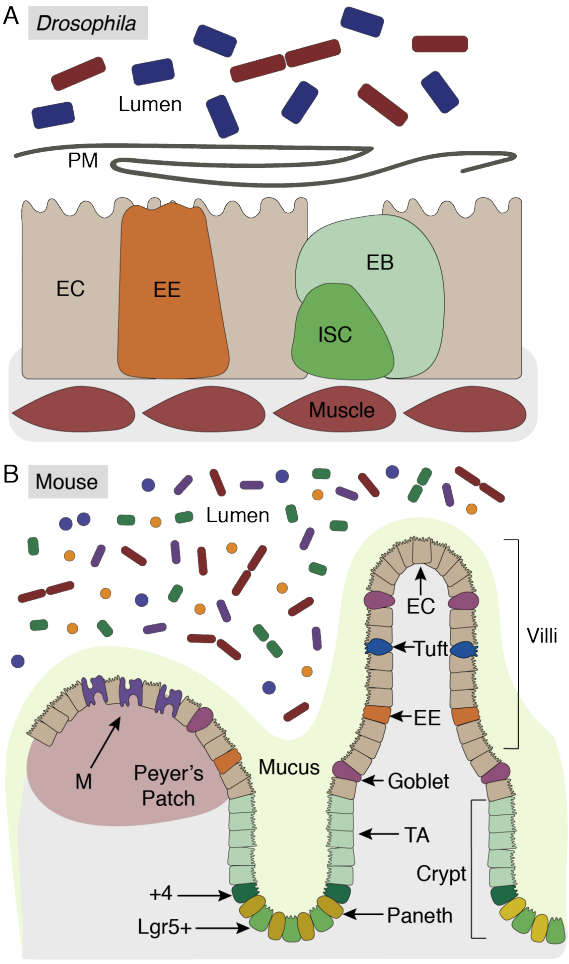

Figure 1.1 Comparison of fly and mouse intestines. (A) *Drosophila* intestine limits bacterial contact with the peritrophic matrix (PM). The epithelium is composed of absorptive enterocytes (EC), secretory enteroendocrine cells (EE) and progenitors, which include multipotent intestinal stem cells (ISC) and post-mitotic enterocyte precursors called enteroblasts (EB). The epithelium is supported by a layer of visceral muscle. **(B)** The mouse intestine is organized into villi and crypts and limits contact with microbes with a layer of mucus. Mature cells types include enterocytes (EC), enteroendocrine cells (EE), tuft, goblet and antigen capturing M cells. Multipotent Lgr5+ stem cells, secretory Paneth cells, +4 stem cells and transit amplifying progenitors reside in crypts.

1.2.2 Intestinal growth in *Drosophila*

Key regulators of intestinal homeostasis are evolutionarily conserved between flies and vertebrates[21]. For example, vertebrate and fly ISCs reside basally in a niche that uses related growth factors to direct stem cell division and differentiation[17,40,41]. Integrins are particularly important niche regulators of ISC division. Integrins anchor fly ISCs to the basal extracellular matrix, orienting the mitotic spindle at an angle to the basement membrane, and ensuring polarized distribution of cell fate determinants[36,42]. In asymmetric divisions, the apical daughter exits the niche and terminally differentiates as a mature epithelial cell, whereas the basal daughter remains within the niche and retains 'stemness'[26–28,43]. Depletion of integrins from the fly midgut diminishes asymmetric division frequency, promoting symmetric expansion of stem cell lineages and epithelial dysplasia[36,44,45]. Notably, relationships between integrins and ISC growth are evolutionarily conserved, as integrin loss also causes hyperplasia in the mouse intestine[46].

In addition to niche factors like integrins, growth pathways regulate intestinal division and differentiation in flies and vertebrates. Intestinal homeostasis is governed by evolutionarily conserved pathways, such as wingless (Wg), bone morphogenic protein (BMP), and Notch signaling pathways. Wg, orthologous to the proto-oncogene Wnt in vertebrates, is produced by the visceral muscle and promotes ISC maintenance and division[47–49] (Fig. 1.2). In humans, Wnt mutations are commonly associated with colorectal cancer, and in *Drosophila*, hyperactivation of the Wg pathway results in intestinal hyperplasia and tumorigenesis[50–53]. BMP signaling also plays an important role in stem cell maintenance and division[54,55]. BMP ligands are produced and secreted by enterocytes, trachea, and visceral muscle, which become basally sequestered by the extracellular matrix[55–57]. BMP activity promotes regional specification of the intestine and limits ISC renewal [57–59](Fig. 1.2). In humans, mutations in BMP pathway genes are associated with juvenile polyposis syndrome and an increased risk for colorectal cancer[60]. Similarly, in *Drosophila*, loss of BMP results in intestinal hyperplasia and tumorigenesis[61].

In flies, most asymmetric divisions generate a post-mitotic enteroblast that differentiates as a large, absorptive enterocyte in response to Notch pathway signals[27,62–66]. The Delta ligand on *Drosophila* ISCs interacts with the Notch receptor on neighboring enteroblasts to activate Notch and promote enterocyte differentiation[27,64] (Fig. 1.2). Previously, it was thought that enteroblasts could develop into either an enterocyte or enteroendocrine cell depending on Notch activity

levels[26,27,67]. However, it was more recently discovered that enteroblasts are committed to become enterocytes, while enteroendocrine cells arise from a separate secretory-committed progenitor cell[63–65]. Loss of Notch from stem cell/ enteroblast progenitor pairs leads to rapid growth of epithelial tumors characterized by hyperplastic stem cells, absence of enterocytes, and accumulation of secretory enteroendocrine cells[68]. Disruptions to Notch cause similar dysplastic phenotypes in fish and mice[69,70], and spontaneous accumulation of mutations at the Notch locus is linked to age-dependent development of intestinal tumors in adult *Drosophila*[71].

Upon injury, *Drosophila* ISCs increase their rate of division to replace damaged cells and maintain barrier integrity. Stress and growth pathways such as the Jun N-terminal kinase (JNK), Hippo, Janus kinase/signal transducer and activator of transcription (JAK-STAT), and epidermal growth factor (EGF) signaling pathways are key to mediate crosstalk between damaged epithelial cells and ISC divisions[1]. Epithelial damage and stress induce JNK activity and inhibit Hippo, which results in the production of unpaired (Upd) cytokines and EGF ligands[5,72–75] (Fig. 1.2). Upd cytokines released from damaged enterocytes activate JAK-STAT signaling in ISCs in a paracrine manner to promote cell division[76]. Similarly, EGF ligands secreted by damaged enterocytes and visceral muscle bind to the EGF receptor (EGFR) on progenitors (Fig. 1.2) which initiates both Ras-ERK and PI3K-Akt signaling to promote cell proliferation and facilitate repair[23,30,31,75,77].

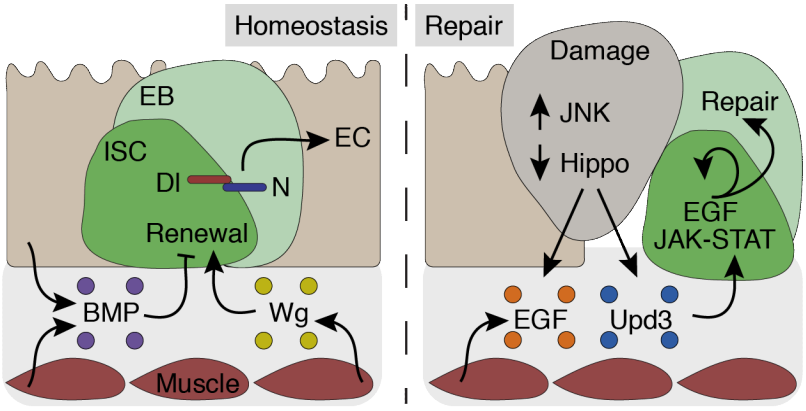

Figure 1.2 Growth of the *Drosophila* intestine during homeostasis and repair. Under homeostasis BMP ligands produced by enterocytes and the visceral muscle inhibit ISC renewal and promote differentiation. Wg is produced by muscle to activate WNT and promote ISC renewal. Delta on ISCs activates Notch on enteroblasts (EB) to promote enterocyte differentiation. During repair, damage activates JNK and inhibits Hippo, resulting in the production of EGF ligands and Upd cytokines. This results in EGF and JAK-STAT activation in ISCs, stimulating ISCs divisions to facilitate repair.

1.3 Microbes and Immunity in the *Drosophila* intestine

1.3.1 The *Drosophila* microbiome

Drosophila has become a useful model to understand host-microbe interactions[3]. The microbiome of *Drosophila* is dominated by bacteria from the phyla Firmicutes and Proteobacteria[78–80]. Although wild and lab raised strains have slight differences in microbial composition, the main bacterial commensals commonly associated with the fly are of the species *Acetobacter* and *Lactobacillus*, which are easily cultivated in the lab[79,81,82]. While the *Drosophila* microbiome does not fully represent the complex bacterial communities of the mammalian intestine, the simplicity allows researchers to tease apart taxon specific effects on gut physiology. *Drosophila* embryos can be surface sterilized on a large scale to generate cohorts of axenic flies that lack a microbiome throughout development and adult life[81]. Similarly, a simple antibiotic cocktail can be added to fly food to generate germ-free adult flies. Gnotobiotic flies, those with a defined microbiome, are easily generated by feeding bacterial species back to the axenic or germ-free flies[81]. These manipulations in *Drosophila* are readily accessible and have been paramount in understanding how host–microbe interactions shape gut physiology.

1.3.2 The Immune Deficiency pathway

Like vertebrates, fly cells are equipped with pattern recognition receptors that respond to bacterial MAMPs and activate downstream immune pathways. One such pathway in *Drosophila* is the immune deficiency (IMD) pathway. IMD is required in the fly intestine to mount an effective antimicrobial response against pathogenic bacteria and to coordinate host responses to commensal microbes[6,83,84]. In addition to IMD, Toll signaling is an important innate immune pathway in *Drosophila*, however activation of Toll does not appear to occur in the intestine due to the acidic pH and enzymes present[5,85]. Similar to vertebrate TLR and nucleotide binding oligomerization domain (NOD) pathways, IMD directly detects bacterial patterns to initiate downstream signaling. *Drosophila* express two IMD pathway receptors. Membrane-associated peptidoglycan recognition protein–LC (PGRP-LC) recognizes y-D-glutamyl-meso-diaminopimelic acid (DAP) type peptidoglycan, and cytosolic PGRP-LE recognizes monomeric DAP-type peptidoglycan[86] (Fig. 1.3). Upon peptidoglycan (PGN) recognition, PGRP-LC and PGRP-LE activate a signaling cascade similar to vertebrate tumor necrosis factor α (TNFα) receptor signaling[86]. Receptor activation promotes

recruitment of a signaling complex composed of Imd, the adapter protein Fas-associated with death domain (Fadd) which results in cleavage of Imd by the caspase Dredd and subsequent Tak1 activation[86] (Fig. 1.3). Tak1 activates the *Drosophila* IKK complex, Kenny and Ird5 (orthologs of vertebrate NEMO/IKKγ and IKKβ, respectively). Active IKK phosphorylates the NF-κB like transcription factor Relish (vertebrate p100/p105 ortholog), which allows for its cleavage by the caspase Dredd and nuclear translocation of the N-terminal Rel homology domain[86] (Fig. 1.3). Once in the nucleus, Rel activates transcription of antimicrobial peptides (AMPs), such as the *attacins* and *diptericins*, and negative regulators of the IMD pathway, such as *pirk* and *PGRP-LB*[86] (Fig. 1.3). Tak1 also induces JNK activation, AP-1 transcription factor nuclear localization, and transcription of genes involved in stress response and cytoskeletal rearrangement[87] (Fig. 1.3). All cell types within the intestinal epithelium encode IMD pathway components, and enterocytes, enteroblasts and enteroendocrine cells upregulate expression of AMPs in response to infectious microbes[25]. Although Relish is one of the most highly expressed transcription factors in ISCs, they do not appear to express AMPs in response to infection[25,88]. This suggests that IMD may have non-bactericidal roles in cells such as ISCs in response to pathogenic microbes, or in homeostasis.

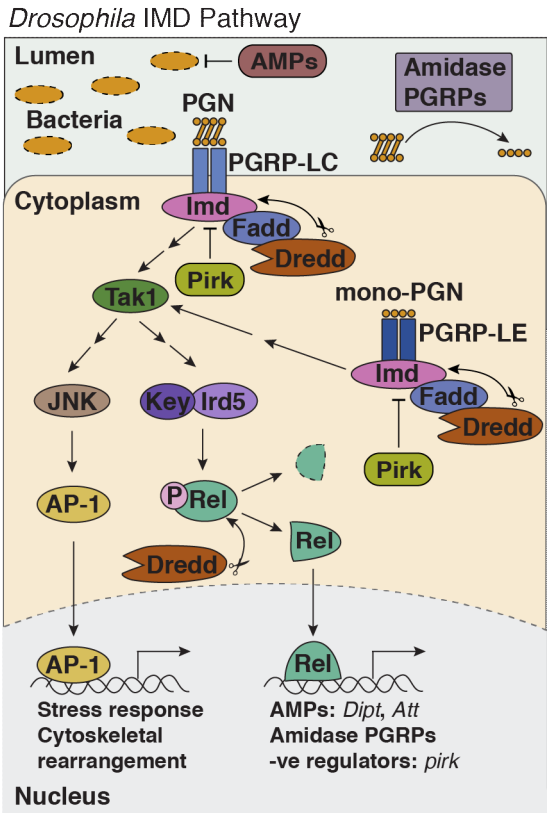

Figure 1.3 The *Drosophila* IMD pathway. Polymeric bacterial peptidoglycan (PGN) is detected by cell surface PGRP-LC while monomeric PGN is detected by intracellular PGRP-LE. PGN detection assembles the Imd, Fadd and Dredd complex. Dredd cleaves Imd which activates Tak1. Tak1 activates JNK and results in AP-1 dependent transcription of stress and cytoskeletal genes. Tak1 also activates the IKK complex (Kenny and Ird5). Active IKK phosphorylates Relish, targeting it for cleavage by Dredd. Upon cleavage, Relish enters the nucleus and activates expression of antimicrobial peptides (AMPs), Amidase PGRPs and negative regulators like Pirk.

IMD components are regionally expressed in the intestine. PGRP-LC is enriched in the post-mitotic foregut and hindgut, while PGRP-LE is enriched throughout the midgut[89,90]. Downstream Relish targets are also regionally expressed in the intestine. AMPs are mainly expressed in the anterior midgut, while negative regulators such as Pirk and PGRP amidases that breakdown lumenal peptidoglycan to limit IMD activation are enriched in the middle and posterior midgut[20]. This spatial regionalization of IMD components suggests that antimicrobial immune responses predominate in the anterior midgut, while tolerance mechanisms are favored in the middle and posterior midgut. In agreement with this, activation of IMD differs in response to pathogenic and commensal bacteria. Infection with pathogenic microbes elevates expression of AMPs in a PGRP-LC-dependent manner in the anterior midgut, while PGRP-LE is required for AMP expression in the copper cell region and posterior midgut[90]. Commensal bacteria, however, do not evoke a strong AMP response and instead induce expression of negative regulators of the IMD pathway, such as Pirk and PGRP-LB, in a PGRP-LE-dependent manner[90]. The distinctive transcriptional outputs of the IMD pathway in response to pathogens and commensals are partly regulated by factors such as the transcriptional repressor Caudal, which is enriched in the posterior midgut and selectively represses Relish-dependent AMP expression in response to commensal microbes[91]. Together, this suggests that IMD is regulated on multiple levels in the intestine to allow for appropriate responses to pathogens while tolerating the microbiome.

1.3.3 Bacterial modulation of intestinal physiology

Drosophila has become an important model to understand the effects of bacteria on intestinal health and disease. Given the ease of manipulation, researchers have uncovered sophisticated dynamics of bacterial association and effects on the animal as a whole as well as direct effects on the intestine. For instance, the microbiome of *Drosophila* modulates host feeding behaviour, reproduction, metabolism, immunity, and intestinal homeostasis[3,85]. In addition to IMD pathway activation, one of the initial responses to bacteria in the intestine is the production of reactive oxygen species (ROS)[92–96] (Fig. 1.4). Both commensals and pathogens activate ROS production through either the NADPH oxidase (Nox) or dual oxidase (Duox). For instance, commensal *Lactobacillus plantarum* activates Nox in the intestine to produce ROS[93,94,96] while the commensal *Lactobacillus brevis* and the pathogen *Erwinia caratovora caratovora 15* (*Ecc15*)

activate Duox to produce ROS[95]. Since ROS production damages the intestine and results in increased ISC division to repair the damage, ROS is proposed to be a mechanism for bacteria to modify intestinal growth[97–99] (Fig. 1.4).

Comparison of flies with and without a microbiome have revealed the importance of bacteria on intestinal physiology. Flies raised in the absence of a microbiome have decreased ISC divisions and are characterized by reduced expression of JAK/STAT, JNK, EGF and Notch pathway components[5,6] (Fig. 1.4). Interestingly, over 50% of genes induced by the microbiome are dependent on the NF-κB family transcription factor Relish, indicating that the IMD pathway is the main modulator of intestinal physiology in response to the microbiome[6]. Pathogens stimulate similar growth pathways but to a heightened extent due to the increased nature of damage associated with infectious microbes[5].

In addition to proliferative effects, the microbiome and pathogens alter intestinal differentiation. Flies without a microbiome have decreased numbers of enteroblasts and increased levels of enteroendocrine cells, indicating that the microbiome supports the differentiation of enterocytes in the intestine[6,100] (Fig. 1.4). Conversely, infection with the pathogen *Ecc15* increases the numbers of enteroendocrine cells in the intestine[100]. Here, commensal microbes activate IMD/Relish to promote enterocyte differentiation whereas upon infection with a pathogen, overt JAK-STAT activation overrides the actions of IMD to instead promote enteroendocrine production[100]. These observations suggest different bacteria impact intestinal differentiation dependent on the level of immune activation and the concurrent levels of stress signaling.

Although the microbiome as a whole has growth promoting effects on the intestine, individual bacterial species can fail to stimulate or actively inhibit intestinal growth. For instance, monoassociation with the common commensal *L. plantarum* damages the intestine without compensatory ISC divisions, leading to premature host death[101]. Similarly, infection with the pathogen *Vibrio cholerae* causes extensive damage to the intestinal epithelium, inhibits ISC divisions and results in fly lethality[102,103]. Interestingly, ISC divisions and survival are enhanced upon depletion of the microbiome or mutation of the *V. cholerae* Type six secretion system (T6SS), a molecular syringe that transfers toxic effectors into prokaryotic or eukaryotic cells[102,103]. This suggests that *V. cholerae* interacts with the microbiome using its T6SS to inhibit ISC divisions and disrupt epithelial repair mechanisms. Together, microbes have a profound impact on intestinal

physiology although we are still lacking a characterization of how microbes specifically alter cell-type specific processes, especially those in ISCs.

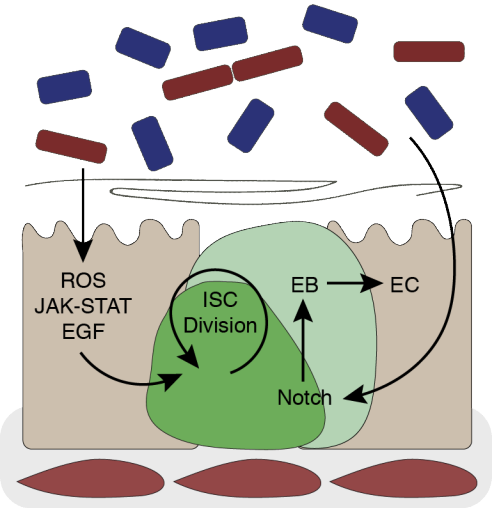

Figure 1.4 Microbes alter intestinal proliferation and differentiation. In response to commensal bacteria, the intestinal epithelium produces ROS and activates JAK-STAT and EGF to promote ISC divisions. Commensal bacteria also activate Notch to promote enterocyte differentiation.

1.4 *Drosophila* genetic tools to study ISC biology

A major advantage to using *Drosophila* is the extensive genetic toolkit. There are libraries of transgenic and mutant fly lines readily available to researchers around the world[104]. These include genome-wide CRISPR induced mutants, RNAi libraries, tissue- and cell type-specific drivers, and various tools such as fluorescent reporter lines. One of the most popular tools is the temporal and regional gene expression (TARGET) system that allows researchers to manipulate any gene in any cell for a specific amount of time[105]. The TARGET system uses cell type specific promoters to drive the expression of GAL4 adopted from yeast, which can then bind to upstream activating sequences (UAS) and activate the expression of transgenes of interest (Fig. 1.5A). Also built into this system is the ubiquitous expression of the temperature sensitive GAL80 variant, which inhibits GAL4 at lower temperatures and allows the researcher to turn transgene expression on or off at any time (Fig. 1.5A). This system and other genetic tools have allowed *Drosophila* researchers to determine gene function within specific cell types making important discoveries that have later been found to be true in vertebrates. Importantly, the TARGET system has been used extensively in the intestine and multiple cell type specific TARGET drivers have been developed to modulate gene function exclusively in intestinal ISCs, progenitor cells (enteroblasts and ISCs), enteroendocrine cells, or enterocytes.

Therefore, *Drosophila* presents an important platform to resolve cell-type specific novel discoveries of gut biology.

In addition to cell-type specific drivers, many tools exist to study ISC function. One such tool is mosaic analysis with a repressible cell marker (MARCM) which generates homozygous mutant clones surrounded by wild-type tissue[106,107]. For instance, heterozygous flies are generated that contain an FRT recombination site upstream of a mutation or transgene of interest on one chromosome and an FRT site upstream of the GAL80 inhibitor on the other chromosome (Fig. 1.4B). In heterozygosity, GAL80 represses the induction of GAL4 driven transgenes that encode fluorescent reporters, resulting in unmarked tissue. Heat shock activates FLP recombinase and induces mitotic recombination at the FRT sites in progenitors to segregate GAL80 away from the mutation/transgene (Fig. 1.5B). Mitotic recombination results in homozygous daughter cells that are either unlabelled wild-type or labelled mutant/transgenic (Fig. 1.5B). Different versions of MARCM label wild-type/heterozygous tissue and have unlabelled mutant tissue. Resulting clones can be tracked for lineage analysis, cell competition, morphogen diffusion range and to study gene function.

Versions of MARCM also allow for twinspot analysis, where heterozygous precursor cells distribute two separate fluorescent reporters into homozygous daughter cells[35,108] (Fig. 1.5C). The resulting clones can then be assessed to determine whether the mitotic event that initiated the clone was asymmetric or symmetric. Here, asymmetric divisions would generate a mature post-mitotic epithelial cell plus a mitotic ISC. Therefore, asymmetric clones would contain a multicellular cluster of one color next to a single cell of the other color (Fig. 1.5C). Conversely, symmetric divisions would generate either two post-mitotic daughter cells or two ISCs. This generates either two single cell clones of different colors or two multicellular clones of different colors next to each other (Fig. 1.5C). Researchers can then assess the frequency of asymmetric and symmetric outcomes to determine how ISC division is altered in response to environmental perturbations. Together, these tools allow us to investigate stem cell dynamics and the role of ISC intrinsic immune pathways.

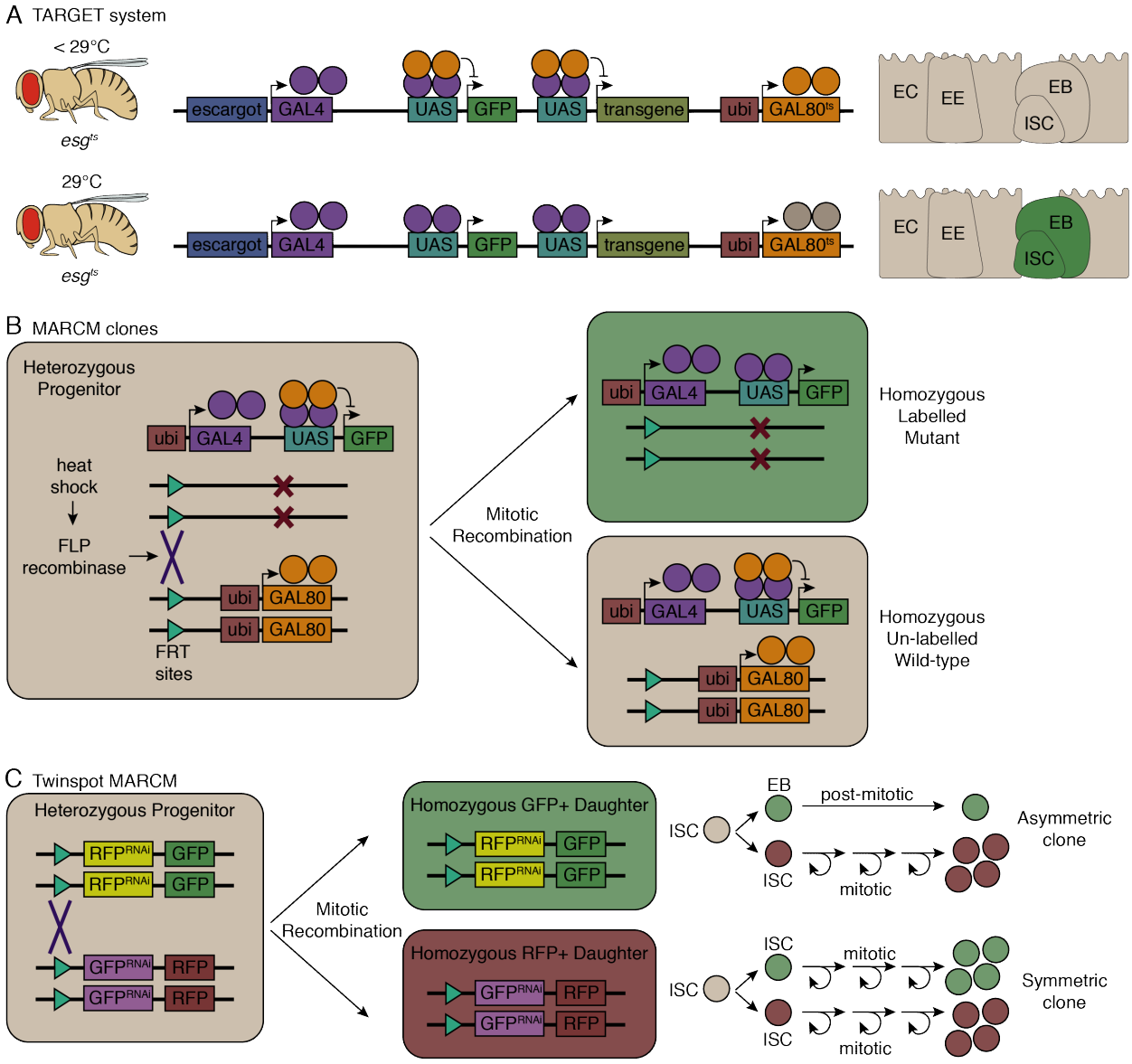

Figure 1.5. *Drosophila* genetic tools to study ISC biology. (A) The *esg*^{ts} driver as an example of the TARGET system. The *escargot* promoter induces expression of GAL4 in intestinal progenitor cells. GAL4 binds to UAS and activates the expression of downstream transgenes such as GFP. A temperature sensitive version of the GAL4 inhibitor GAL80 (GAL80^{ts}) is expressed ubiquitously and is active at lower temperatures. Raising flies at temperatures below 29°C permits GAL80^{ts} activity and inhibits cell-type specific expression of transgenes. Raising flies at 29°C inactivates GAL80^{ts}, allowing GAL4 dependent induction of transgenes and progenitor specific expression of GFP and any additional transgenes. **(B)** MARCM clones start with a heterozygous progenitor cell. One chromosome contains an FRT recombination site upstream of a mutation or transgene while the

other chromosome contains an FRT site and the GAL80 inhibitor. On a separate chromosome GAL4 is expressed ubiquitously to drive expression of GFP. In heterozygosity GAL80 prevents GFP expression. Upon heat shock, FLP recombinase induces mitotic recombination at the FRT sites. This results in homozygous daughter cells, a mutant/transgenic GFP labelled daughter cell and a wild-type unlabelled daughter cell. **(C)** Twinspot MARCM starts with a heterozygous progenitor that has two separate fluorescent tags on separate chromosomes. Each chromosome also contains a repressor for the fluorescent tag located on the opposite chromosome. In heterozygosity, the repressors result in unlabelled cells. Upon heat shock and FLP dependent recombination at FRT sites, the repressors are segregated away from their target allowing each daughter cell to express a separate fluorescent tag. The resulting clones can be assessed to determine if the original mitotic event was asymmetric or symmetric.

1.5 Immune regulation of ISC function

1.5.1 Immune regulation of homeostatic intestinal proliferation

Intestinal growth and differentiation are controlled by evolutionarily conserved pathways and are influenced by the microbiome. This suggests that immune pathways are a critical factor in intestinal homeostasis. In *Drosophila*, the microbiome induces basal levels of JAK-STAT and EGF cytokines to promote homeostatic growth[5,6]. Cytokine production is Relish-independent, suggesting that growth factors induced by the microbiome do not require NF-κB activity. In support of this hypothesis, *relish* mutant intestines have increased levels of proliferation compared with WT flies, but this difference is not seen in flies without a microbiome[6]. However, this does not completely rule out IMD in transducing microbial pro-growth signals as a known activator of growth, JNK, is also downstream of IMD. In addition, the complex regulatory nature of IMD may impact growth phenotypes. For instance, deletion of IMD-negative regulators such as Pirk and PGRP amidases results in hyperactive IMD, which increases JAK-STAT activity to promote intestinal proliferation[109] (Fig. 1.6A). Interestingly, components that limit IMD activation, such as PGRP amidases and Caudal, are highly enriched in the posterior midgut, a region characterized by EGF, JAK-STAT, Wnt activity, and elevated ISC proliferation[20,25]. Therefore, IMD may be specifically downregulated in the posterior midgut to dampen proliferative signals. Along these lines, overexpression of PGRP-LC in enterocytes induces Relish-dependent proliferation in the posterior

midgut[110] (Fig. 1.6A). Together, this suggests that IMD activation in the intestinal epithelium may promote proliferation in a Relish-dependent manner alongside IMD-independent JNK activation, although normally, negative regulators act to limit IMD-dependent proliferation.

The microbiome of zebrafish promotes intestinal proliferation in a MyD88-dependent manner, the adapter required for TLR signaling, indicating that microbial sensing through TLRs induces ISC division[7]. In mice however, different TLRs have distinct impacts on proliferation. For instance, TLR2-/- intestines have decreased proliferation while TLR1-/- mutants have increased proliferation[111,112]. In addition, epithelial TLR4 inhibits or promotes proliferation in different settings. For example, lipopolysaccharide (LPS) inhibits β-catenin signaling and subsequent proliferation in a TLR4-dependent manner in the mouse small intestine[113]. In contrast, TLR4 overexpression in the intestinal epithelium of mice increases β-catenin nuclear accumulation, increases the number of Lgr5+ stem cells, and promotes proliferation[114]. These discrepancies may be due to differences in the microbiome between laboratories, or due to the subcellular location of TLR4 signals. For example, LPS injected into mice access the basal side of the epithelium, whereas in homeostasis, lumenal LPS would have limited access to the basolateral side of the epithelium. Therefore, TLR4 may play an important role in modifying proliferation upon barrier disruption, but a role for TLR4 in homeostatic proliferation is unclear.

Similar to TLR4, TNFα can either promote or inhibit intestinal proliferation dependent on the level of TNFα in the intestine. Mouse colon cells exposed to low dose TNFα had increased levels of proliferation, whereas high doses of TNFα decreased proliferation[115]. This indicates that physiological levels of TNFα promotes proliferation while pathological levels of TNFα inhibits proliferation. The discrepancies between low and high doses of TNFα on proliferation are likely due to the differential activation of the two TNFα receptors, since TNFR1 agonist antibody inhibited proliferation while TNFR2 blocking antibody prevented the proliferation induced by low dose TNFα[115]. Together, evidence from flies, fish and mice suggest that immune signals in the intestinal epithelium dictate the division of ISCs, however it is still unclear which cell types immune pathway activity is required to impact ISC function.

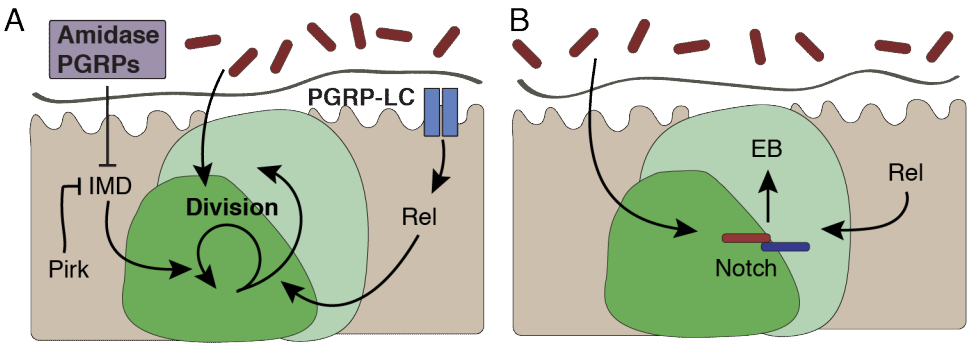

Figure 1.6 Microbes and the IMD pathway alter intestinal proliferation and differentiation. (A) The microbiome promotes ISC divisions. PGRP-LC activation promotes ISC divisions in a Relish dependent manner. IMD negative regulators dampen IMD activity to reduce ISC divisions. **(B)** The microbiome and Relish promote Notch activity and production of enteroblasts.

1.5.2 Immune regulation of intestinal differentiation

Germ-free mice and fish have decreased numbers of secretory goblet and enteroendocrine cells relative to conventionally reared counterparts[116–118]. Conversely, germ-free *Drosophila* have increased numbers of secretory enteroendocrine cells and decreased numbers of enterocyte precursors[6]. These discrepancies are likely attributed to differences in Notch signaling in the intestines of flies compared with vertebrates. For instance, while in *Drosophila*, Delta on ISCs interacts with the Notch receptor on post-mitotic enteroblasts[27,64], in mice, the Notch receptor resides on mitotic ISCs and progenitors in the transit amplifying zone where it promotes absorptive lineage specification[119–121]. Despite these differences, microbes alter Notch to influence lineage specification in the intestines of flies and vertebrates. In *Drosophila*, the microbiome promotes Notch activity to induce enterocyte differentiation, and *relish* mutants have decreased expression of Notch targets in response to the microbiome[6] (Fig. 1.6B). This indicates that the microbiome promotes Notch signaling downstream of Relish.

Immune pathways in vertebrates also influence Notch activity to modify intestinal differentiation. The zebrafish microbiome promotes differentiation of secretory cells in a MyD88-dependent manner[118]. Likewise in mice, LPS stimulation of colonoids increases goblet cell number, suggesting that TLR4 activation inhibits Notch to induce differentiation of secretory cells[122]. Conversely, epithelium-specific TLR4 deletion in the small intestine decreases Notch activity, resulting in increased expression of secretory cell determinants and decreased expression of

absorptive cell determinants[11]. This suggests that TLR4 can activate or inhibit Notch signaling depending on the context. Nucleotide oligomerization domain (NOD) signaling also impacts intestinal differentiation. Specifically, NOD1 and NOD2 agonists in combination promote goblet cell differentiation[123]. Together, immune pathways such as IMD, TLR and NOD are important regulators of intestinal differentiation.

1.5.3 Immune regulation of intestinal repair

Intestinal injury can cause epithelial cell death, and efficient tissue repair requires coordinated regulation of stress and growth pathways. Microbes modulate repair responses in *Drosophila* and vertebrates; however, immune pathways can either promote or inhibit epithelial repair depending on the pathway and the context of the damage. Therefore, a balance of microbial response, inflammation, and proliferation are key to repair intestinal injury.

In *Drosophila*, the role of IMD in epithelial repair is unclear. Infection with the oral pathogen *Ecc15* activates the IMD pathway and causes enterocyte delamination in an IMD and Relish-dependent manner[110] (Fig. 1.7). However, Relish is not required for proliferative repair even though it is required for enterocyte Upd2 production[83,110] (Fig. 1.7). Instead, JNK activity is required for ISC division in response to *Ecc15* through the induction of EGF and Upd ligands[5,110] (Fig. 1.7). IMD has also been shown to modulate repair in response to other pathogens. For example, *V. cholerae* damage the fly intestine and inhibit intestinal proliferation in an IMD-dependent manner, resulting in defective repair and early death[102,103,124] (Fig. 1.7). In contrast, *Staphylococcus aureus*, a pathogen that does not induce IMD, is more lethal in *imd* and *relish* mutants, suggesting a protective role for basal levels of IMD activity[125] (Fig. 1.7). Similarly, Trypanosoma infection induces ISC divisions in an IMD and Relish-dependent manner to repair the intestine and survive infection[126] (Fig. 1.7). Together, these observations suggest that IMD has a protective or deleterious effect on repair mechanisms dependent on the pathogen present; however, it is unclear whether these differences reflect regional effects, cell type-specific requirements, levels of IMD activity, or differences between feeding procedures and microbiomes between laboratories. In addition, we still do not know whether IMD plays a role in injury or repair in response to nonmicrobial damaging agents.

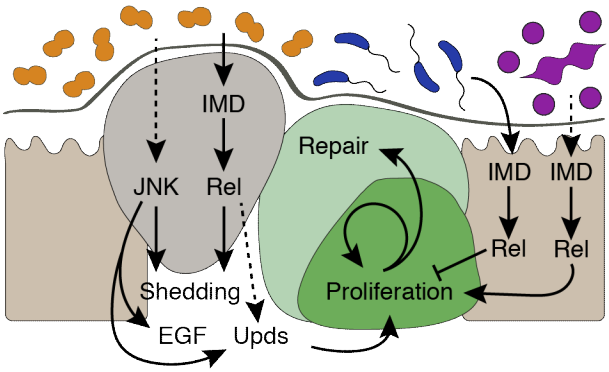

Figure 1.7 IMD influences repair upon pathogenic infection. Upon infection with *Ecc15* (yellow) JNK, IMD and Rel cooperate to promote enterocyte shedding, induce Upd and EGF secretion and activate ISC divisions to repair the damage. Infection with *V. cholerae* (blue) activates IMD and Rel to inhibit proliferation and repair. Infection with *S. aureus* or Trypanosoma (pink) requires IMD to survive infection and for proliferative repair.

In mice, dextran sodium sulfate (DSS) is commonly used to study colitis-like injury and repair. Germ-free mice are more susceptible to DSS injury than conventionally reared counterparts, due to reduced mucus thickness, decreased proliferation, and unresolved inflammation, suggesting that microbes protect the epithelium upon damage[127,128]. Along these lines, mice mutant for MyD88, TLR1, TLR2, TLR4, TLR5, TLR9, NOD1, or NOD2 are more susceptible to DSS-induced colitis[112,129–136]. TLRs limit initial injury by improving barrier integrity. For example, administration of TLR2 agonists preserves tight junctions and blocks apoptosis in response to DSS[131] and TLR5-/- intestines have increased intestinal permeability and develop spontaneous colitis[137]. However, inhibition of TLR4 signaling decreases intestinal injury during DSS challenge[138]. Interestingly, epithelium-specific expression of a constitutively active form of IKK induces proliferation and inflammatory cytokine/chemokine production but does not induce damage unless exposed to the TLR4 agonist LPS[139]. In this case, LPS induces TNFα, which causes extensive crypt apoptosis and injury. This suggests that TLRs such as TLR2 and TLR5 enhance the epithelial barrier to limit TLR4 activation and reduce colitis-induced injury.

After DSS exposure, TLR mutants display decreased proliferation and increased apoptosis, suggesting that TLR signaling promotes repair after injury. For instance, TLR4 is required for the production of cytokines and growth factors that activate EGF and JAK-STAT to promote proliferation

and repair in response to DSS[129,140]. Together, TLR signaling modulates initial injury caused by DSS and promotes epithelial repair after DSS exposure. Similarly, NOD1 and NOD2 mutants are more susceptible to DSS-induced colitis, but this is generally attributed to changes in the microbiome and hyperactivation of TLR signaling in intestinal immune cells[135,136,141,142].

TNF signaling plays an important role in IBD[143]. Patients with IBD have elevated TNFα levels in serum and TNFα monoclonal inhibitory antibodies are used as a treatment for IBD[144–147]. Similarly, mouse models of colitis have increased levels of TNFα in the intestine and mice with chronic overproduction of TNFα spontaneously develop Crohn's like inflammation[148,149]. Along these lines, TNFα-/- mice are less susceptible to chronic DSS colitis but are more susceptible to acute DSS colitis[150,151]. This indicates that TNFα has a beneficial effect during acute colitis but a detrimental effect with chronic colitis. The various downstream effectors of TNFα likely give rise to these discrepancies under different inflammatory contexts. For example, TNFα disrupts tight junctions in mice, induces cell shedding and apoptosis from the epithelium, and increases intestinal permeability, a process known to fuel inflammation and exacerbate IBD[152]. On the other hand, TNFα induces the expression of ErbB4, a receptor part of the ErbB family of receptor tyrosine kinases, of which EGFR is also a part of[153]. ErbB4 expression and signaling activates downstream Akt and ERK, reduces epithelial apoptosis, and facilitates wound healing[153,154]. Therefore, TNFα has beneficial and deleterious effects on the intestine during damage which merits further investigation on a cell-type specific level. Together, immune pathways modulate initial injury and subsequent repair of the intestine although it is still unclear whether immune pathways act specifically within ISCs to alter repair dynamics.

1.5.4 Immune regulation of intestinal tumorigenesis

The microbiome has an inhibitory or stimulatory effect on tumor growth depending on the context. For example, germ-free mice have increased tumor growth in response to AOM/DSS, a model for inflammatory colitis-associated cancer, due to insufficient repair and unresolved inflammation[155]. Conversely, germ-free *Apc^{min}/+* mice have decreased tumor growth, a model dependent on overactive Wnt signaling instead of overt inflammation[8]. Similarly, microbes in *Drosophila* promote growth of BMP-deficient and Notch-deficient tumors[61,156]. These

observations suggest the microbiome protects against inflammation-mediated tumorigenesis, while promoting non-inflammatory tumor growth.

In *Drosophila*, immune activity positively correlates with tumor growth. For example, pathogenic microbes, such as *Pseudomonas entomophila*, promote growth of Ras mutant, or Notch-deficient tumors[156]. Increased tumor growth is generally attributed to activation of stress-induced JNK, not IMD. Since JNK is downstream of IMD, it is possible that pathogenic microbes activate JNK, at least partially, via IMD to promote tumorigenesis, although this has yet to be directly tested and JNK is activated in response to multiple upstream signaling events. Therefore, microbes may activate JNK in both IMD-dependent and IMD-independent ways to promote tumor growth (Fig. 1.8). IMD may also have cell-specific effects on tumor growth. For instance, IMD promotes enterocyte delamination, a process which stimulates tumor growth[76,110]. Since microbes promote tumorigenesis, and over 50% of the intestinal transcriptional response to the microbiome is mediated by Relish, it is possible that Relish may mediate microbial effects on tumorigenesis (Fig. 1.8) [6]. However, the role of Relish in tumorigenesis is unknown. In addition, whether immune pathways act in progenitors to modify tumor growth has yet to be explored.

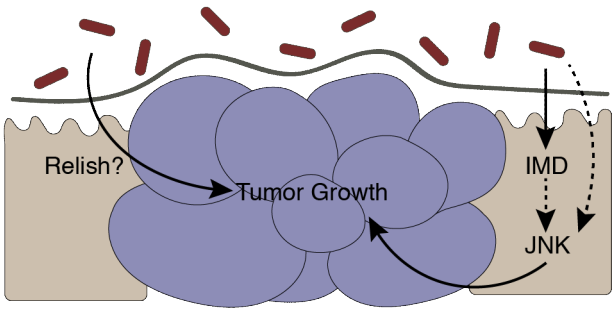

Figure 1.8 Microbes promote tumorigenesis via immune activation. The microbiome promotes growth of intestinal tumors potentially through Relish. Pathogenic microbes promote tumorigenesis through the activation of JNK, via potential IMD dependent or independent mechanisms.

The microbiome of mice protects against colitis-associated tumorigenesis but promotes noninflammatory tumor growth[8,155]. Along these lines, MyD88-/- mouse intestines have reduced tumor growth in Apc^{min}/+ mice, but increased tumor growth in the inflammatory AOM/DSS model[157,158]. Similarly, TLR2-/-, NOD1-/-, and NOD2-/- mice have increased tumor growth in the AOM/DSS model characterized by increased JAK-STAT activation, increased β-catenin, increased proliferation, and decreased apoptosis[136,159,160]. Increased tumor growth in TLR2 and NOD

mutant intestines is generally attributed to lack of repair upon exposure to DSS, exacerbating inflammation, and leading to increased tumorigenesis. Although TLR2 and NODs protect against inflammatory tumorigenesis, TLR4 activity exacerbates tumorigenesis. In contrast to TLR2 and NOD mutants, TLR4-/- mice have decreased tumor growth in response to AOM/DSS due to decreased expression of EGF factors[161]. In agreement with this, expression of a constitutively active form of TLR4 in the intestinal epithelium of mice increases tumor incidence via EGFR activation[162]. Together, these results suggest that attenuation of TLR4 activity and the activation of TLR2 and NOD pathways act to prevent inflammatory tumorigenesis.

Under non-inflammatory settings, TLR activation promotes tumorigenesis. For instance, *Apc^{min}/+ MyD88-/-* intestines have decreased EGF and JAK-STAT activity and smaller, fewer tumors[157]. Interestingly, in the absence of carcinogens or oncogenic mutations, overexpression of TLR4 in the intestinal epithelium of mice results in spontaneous tumor formation[114]. Mechanistically, intestinal TLR4 overexpression activates β-catenin in a cell-autonomous fashion, independent of Wnt, resulting in increased Lgr5+ stem cell numbers, elevated proliferation, and tumorigenesis[114].

Aberrant TNFα signaling promotes intestinal tumorigenesis. Patients with colorectal adenomas have increased levels of TNFα and TNFα positively correlates with the severity of colorectal cancer[163–165]. Similarly in mice, AOM/DSS treatment results in increased TNFα production and mice mutant for the TNFR1 receptor have decreased inflammation and tumor growth[166]. Mechanistically, TNFα inhibition reduces intestinal damage, immune cell infiltration, β-catenin nuclear localization and EGF ligand expression, important mediators of tumor growth[166]. In addition to these *in vivo* observations, TNFα induces the malignant transformation of ISCs *in vitro* through the activation of NF-κB and Wnt/β-catenin pathways[167]. These observations suggest that immune pathways modulate intestinal tumorigenesis dependent on the inflammatory context of the intestine.

1.5.5 Immune pathways directly modulate progenitor function

It is unclear whether immune pathways affect progenitors or crypt dynamics directly or indirectly. Many phenotypes can be explained by an indirect non-autonomous effect. For instance, TLR4 promotes epithelial secretion of growth factors, such as EGF ligands, that act in a paracrine

manner on crypts to activate proliferation[140]. However, TLRs, NODs, and components of the IMD pathway are enriched in crypts and ISCs, indicating potential roles for direct modification of progenitor and crypt dynamics[25,88,161,168–170].

In *Drosophila*, several lines of evidence hint at potential cell-autonomous roles for IMD in regulating progenitor division and differentiation. However, significant discrepancies arise between different labs. In one set of experiments, knockdown of *relish* specifically in progenitors increased stem cell divisions (Fig. 1.9A) [124]. Conversely, in a separate investigation, knockdown of *relish* in progenitors decreased proliferation, while overexpression of Relish in progenitors increased proliferation (Fig. 1.9A) [126]. The discrepancy between these experiments may be due to differences in microbiomes or feeding methods across laboratories. Recent work has also established a pivotal role for Relish in dictating progenitor differentiation. Specifically, knockdown of *relish* in progenitor cells increased the proportion of enteroendocrine cells in the intestine[100]. This suggests that Relish acts within progenitors to promote enterocyte differentiation (Fig. 1.9A). Together, these observations indicate that IMD and the downstream transcription factor Relish act in progenitors to modulate homeostatic proliferation and differentiation. As a caveat to the above-mentioned studies, the *esg*^{ts} TARGET promoter system used allows transgene expression in both stem cells and post-mitotic enteroblasts. Therefore, additional experiments are required to distinguish between IMD activity in stem cells and in enteroblasts.

In the mouse large intestine, crypt-specific core microbiota limit proliferation in a TLR4-dependent manner, suggesting that microbes activate TLR signaling in crypts to inhibit division[122]. Along these lines, TLR4 is expressed by Lgr5+ stem cells in the mouse intestine, and in mouse organoids, LPS-mediated activation of TLR4 induces apoptosis and inhibits stem cell proliferation[171]. In an elegant study by Neal et al., the authors generated mice where TLR4 is deleted specifically within Lgr5+ stem cells using a tamoxifen-inducible Cre/Lox system[171]. While this technique initially deletes TLR4 specifically in Lgr5+ ISCs, resulting progeny inherit this mutation. They induced TLR4 deletion and performed *in vivo* experiments at a time where TLR4 mutation was contained to crypts. This approach generated a mosaic pattern within intestines where some crypts lost TLR4, while others retained TLR4, allowing direct comparisons in the same individual. Similar to results with organoids, injection of LPS into these mice induced apoptosis and inhibited proliferation in crypts that retained TLR4[171]. However, crypts deficient for TLR4 did not respond to LPS:

Apoptosis and proliferation were unchanged compared with saline-injected animals. Therefore, LPS activates TLR4 in crypts to inhibit proliferation, and promote apoptosis (Fig. 1.9B). However, since this genetic approach ultimately generates mutant ISCs and progeny, additional experimentation is required to determine whether these effects are due to cell-autonomous effects of TLR4 directly in ISCs.

There is little evidence to suggest TNFα signaling acts directly on ISCs to modulate their function. However, exposure of isolated Lgr5+ stem cells to TNFα induces NF-κB, Wnt/β-catenin, and PI3K/Akt signaling, known modifiers of cell death, proliferation and differentiation in the intestine[167]. This suggests that TNFα may act directly on Lgr5+ ISCs to modify division programs. However, effects of TNF pathway activation specifically in ISCs *in vivo* have yet to be characterized.

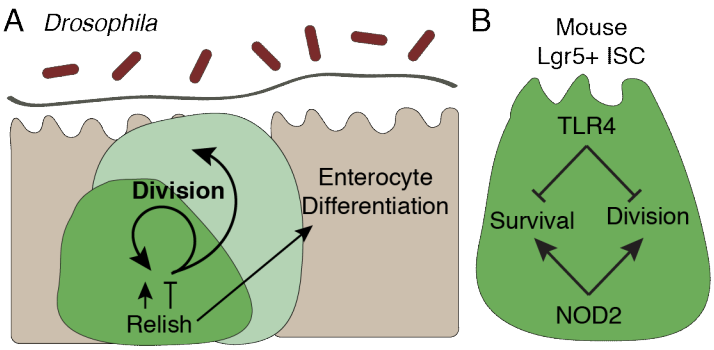

Figure 1.9 Immune pathways act directly in progenitors to alter their function. (A) Relish acts in progenitors to either promote or inhibit ISC division in different contexts. Progenitor specific Relish promotes enterocyte differentiation. **(B)** In mouse Lgr5+ stem cells, TLR4 inhibits cell survival and division while NOD2 promotes survival and division.

Recently, an important role for NOD2 in ISCs has been discovered. NOD2 is highly expressed in Lgr5+ stem cells, and organoids grown in the presence of the NOD2 agonist MDP have increased viability[170]. In mice, NOD2 agonists protect crypts against oxidative stress and NOD2-/- crypts have increased apoptosis and decreased proliferation (Fig. 1.8B), suggesting that NOD2 has a protective effect on stem cells[170]. Subsequent work showed that, upon irradiation, NOD2 expression increases in stem cells and protects from irradiation-induced apoptosis[172]. Together with the TLR4 data, this suggests that NOD2 and TLR4 have opposing roles in stem cell survival and proliferation (Fig. 1.9B). This implies that stem cells must balance NOD2 and TLR4 activation for

appropriate responses to stimuli and that perhaps NOD2 promotes stem cell maintenance in response to commensals, while TLR4 promotes stem cell death in response to invasive microbes.

1.6 Objective

Microbes and immune pathways modulate the function of ISCs. However, we know little about the direct effects individual bacterial species have on ISCs. In addition, it is unclear whether immune pathways act specifically within ISCs to direct their function. Within the scope of my thesis, I aimed to answer these questions. Specifically, I asked how individual commensal species alter ISC proliferation under homeostasis and during tumorigenesis (Fig. 1.10). I also determined the role of the IMD pathway in progenitors and ISCs in the context of proliferation, differentiation, tumorigenesis and repair (Fig. 1.10). Given the fundamental role ISCs play in intestinal maintenance and the impact of microbes and immunity on intestinal health, it is imperative we understand the complex interplay between ISCs, microbes and immunity.

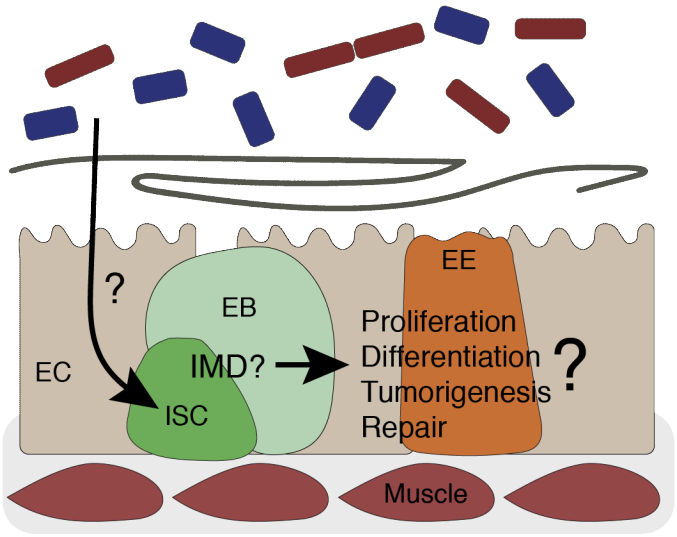

Figure 1.10 Thesis objectives. How do individual commensal bacteria modify ISC physiology and function? Does the IMD pathway act specifically within progenitors and ISCs to alter intestinal proliferation, differentiation, tumorigenesis and repair?

Chapter 2

Materials and Methods

This chapter contains content from the following sources:

- **Ferguson, M**., Petkau, K., Shin, M., Galenza, A., Fast, D., & Foley, E. (2021). Differential effects of commensal bacteria on progenitor cell adhesion, division symmetry and tumorigenesis in the *Drosophila* intestine. *Development*. 148(5): 1-14
- Petkau, K., **Ferguson, M**., Guntermann, S., & Foley, E. (2017). Constitutive Immune Activity Promotes Tumorigenesis in *Drosophila* Intestinal Progenitor Cells. *Cell Reports* 20: 1784-1793.
- Shin, M., **Ferguson, M.,** Willms, R. J., Jones, L. O., Petkau, K., & Foley, E. (2022). Immune regulation of intestinal stem cell function in *Drosophila*. *Stem Cell Reports*. 17(4):741-755.

2.1 *Drosophila* husbandry

2.1.1 *Drosophila* stocks and handling

Drosophila stocks and crosses were setup and maintained at 18-25°C on standard corn meal food (Nutri-Fly Bloomington formulation; Genesse Scientific) with a 12:12 light:dark cycle. All experimental flies were virgin female flies except when noted. Upon eclosion, flies were kept at 18°C then shifted to the appropriate temperature once 25-30 flies per vial was obtained. Fly lines used in this study are noted in Table 2.1. Twin-spot clones were induced by a 37°C heatshock for 1 hour immediately after transferring flies to fresh food after the overnight monoassociation protocol. Flies were then shifted back to 29°C for 8 days before dissecting and counting clones from 30 intestines per treatment. Standard MARCM clones were generated by raising flies at 18°C for 5-6 days, heatshock at 37°C for 2 hours and raised for an additional 8-10 days at 25°C. Mitotic clones using the *esgF/O* system were induced by raising flies at 18°C for 3 days, shifted to 29°C for 16hr then raised at 25°C for an additional 9 days. The *imd* and *UAS-ImdCA* lines had been backcrossed into the Foley lab wild-type w^{1118} background. Foley lab w^{1118} stock was used as controls in chapter 3 and chapter 4 figures 4.1-4.5. VDRC w^{1118} stock was used as controls in chapter 4 figures 4.7-4.11 and chapter 5.

Table 2.1 Fly lines used in this study

Fly line	Genotype	Origin	ID Number
esg^{ts}	*w;esg-GAL4,tubGAL80^{ts},UAS-GFP*	Bruce Edgar	
Notch RNAi	*UAS-N^{RNAi}*	VDRC	100002
Myo1A^{ts}	w;*Myo1A-GAL4;tubGAL80^{ts},UAS-GFP*	Bruce Edgar	
Imd mutant	*imd*	Bruno Lemaitre	
Foley w stock	w^{1118}	Foley stock	
ImdCA	*UAS-ImdCA*	Foley stock	
esg^{ts},UAS-CFP,Su(H)-GFP	*w;esg-GAL4,UAS-CFP, Su(H)-GFP;tubGal80^{ts}*	Lucy O'Brien	

Twinspot MARCM	*hsFLP;FRT40A,UAS-CD2-RFP,UAS-GFP-miRNA*	Lucy O'Brien	
Twinspot MARCM	*FRT40A,UAS-CD8-GFP,UAS-CD2-miRNA;tubGAL4*	Lucy O'Brien	
cg^{ts}	*cgGAL4;GAL80^{ts}*	Bloomington	7011,7018
Dredd mutant	*dredd*	Bruno Lemaitre	
MARCM	*hsFLP,UAS-GFP;neoFRT40A*	Lucy O'Brien	
MARCM	*tubGAL80,neoFRT40A;tubGAL4*	Foley stock	
ISC^{ts}	*w;esg-GAL4,UAS-2xEYFP;Su(H)GBE-GAL80,tub-GAL80^{ts}*	Bruce Edgar	
FADD RNAi	*UAS-FADD^{RNAi}*	VDRC	7926
VDRC w	*w^{1118}*	VDRC	60000
$esg^{F/O}$	*esg-GAL4,tubGAL80ts,UAS-GFP;UAS-flp,Act>CD2>GAL4*	Bruce Edgar	
$Su(H)^{ts}$	*w;Su(H)GBE-GAL4,UAS-GFP;ubi-GAL80^{ts}*	Bruce Edgar	
PGRP-LE RNAi	*UAS-PGRP-LE^{RNAi}*	VDRC	108199
PGRP-LC RNAi	*UAS-PGRP-LC^{RNAi}*	VDRC	101636
Relish RNAi	*UAS-rel^{RNAi}*	VDRC	49413
Kenny RNAi	*UAS-key^{RNAi}*	VDRC	7723
RelVP16	*UAS-relVP16*	Bloomington	36547
RasN17	*UAS-RasN17*	Bloomington	4845
RasV12	*UAS-RasV12*	Bloomington	4847

2.1.2 Germ-free and gnotobiotic rearing

Germ-free and mono-associated flies were generated as previously described [101]. To generate germ-free flies, freshly eclosed flies were fed autoclaved food with antibiotics (Ampicillin (100μg/mL), Neomycin (100μg/mL), Vancomycin (50μg/mL) and Metronidazole (100μg/mL)) for 5 days at 25°C. Conventionally reared controls were fed autoclaved food without antibiotics for 5 days

at 25°C. To generate mono-associated animals, flies were made germ-free as above then were fed 1mL OD_{600}=50 of *L. brevis* or *L. plantarum* resuspended in sterile 5% sucrose/PBS on a cotton plug overnight at 25°C. During this overnight feeding, CR and GF controls were fed sterile 5% sucrose/PBS without bacteria. The following morning, CR and mono-associated conditions were transferred to fresh autoclaved food at 29°C for the remainder of the experiment, while GF flies were maintained on autoclaved food with antibiotics. Sterility and mono-association were confirmed in each experimental vial by plating fly homogenate or fly food on MRS. Vials found to be contaminated were discarded from the experiment.

2.1.3 Lifespan analysis

For the data in chapter 3 (Fig. 3.3E) virgin female flies were mono-associated with *L. brevis* or raised with a conventional microbiome as described. After mono-association, flies were distributed to sterile vials with autoclaved food at a density of 10 flies/vial and shifted to 29°C for the remainder of the experiment. Dead flies were counted every 1-3 days and vials were transferred 3 times per week to fresh autoclaved food.

For the data in chapter 4, esg^{ts} and esg^{ts}/*ImdCA* flies were raised at 29°C for two days then fed *V. cholerae* on a cotton plug for the remainder of the experiment (Fig. 4.2D). Fly deaths were counted every 2-12 hours. For esg^{ts} and esg^{ts}/*ImdCA* longevity flies were shifted to 29°C and dead flies were counted every 1-3 days and vials were flipped 3 times per week to normal food (Fig. 4.4C).

For the data in chapter 5, 30 virgin females per vial for each genotype (esg^{ts}/+ and esg^{ts}/rel^{RNAi}) were raised at 29°C and dead flies were counted every 1-3 days and vials were flipped 3 times per week to fresh standard food (Fig. 5.2E). For DSS survival experiments ISC^{ts}/+ and ISC^{ts}/rel^{RNAi} flies were placed on fresh 10% DSS daily for the course of the survival experiment and deaths were counted daily (Fig. 5.2F).

2.2 Microbial analysis

2.2.1 Bacterial strains and growth conditions

L. brevis^{EF} (DDBJ/EMBL/GeneBank accession LPXV00000000) and *L. plantarum*^{KP} (DDBJ/EMBL/GenBank chromosome 1 CP013749 and plasmids 1-3 CP013750, CP013751, and CP013752) were both isolated from our *Drosophila* lab stocks and have been previously described

[173]. Both bacteria were streaked out on MRS (deMan, Rogosa, and Sharpe) plates (BD; 288210) and aerobically grown at 29°C. Single colonies were picked for growth in MRS broth (Sigma; 69966) at 29°C (*L. brevis* for 2 days and *L. plantarum* for 1 day). To generate dead *L. brevis*, liquid culture was spun down, washed twice with sterile water then resuspended in sterile water before heating to 95°C for 30min. After heating, the killed bacteria were spun again and resuspended to 10mg/mL in sterile 5% yeast, 5% sucrose in PBS.

To extract the cell wall, *L. brevis* was heat killed as above, let cool on ice, then run through a French Press at 20,000 psi three times to lyse the bacterial cells. After lysis, any remaining whole cells were collected and discarded by two successive spins at 2000g. To collect the cell wall, the supernatant was spun at 10,000g for 30 minutes, washed twice with 1M NaCl and twice with sterile water before resuspending in sterile 5% yeast, 5% sucrose in PBS. Germ-free flies were fed a 10mg/mL cell wall solution on filter paper disks on top of sterile food alongside 10mg/mL dead *L. brevis* and sterile 5% yeast, 5% sucrose PBS without any *L. brevis* extracts. Dead bacteria and cell wall were continuously fed to flies during the experiment, with fresh extracts provided every second day. Sterility of dead *Lb* and cell wall was confirmed by plating 100uL of extract on MRS.

V. cholerae C6706 strain [174] was grown in Lysogeny broth (LB) (1% tryptone, 0.5% yeast extract, 0.5% NaCl) at 37°C with shaking in the presence of 100μg/mL streptomycin. *Erwinia caratovora caratovora 15* [175] was grown in LB (Difco Luria Broth Base, Miller, 241420 supplemented with 4.75g NaCl per 500mL broth) at 29°C with shaking for 20-24 hours.

2.2.2 Quantification of Bacterial CFUs

Five flies were randomly selected from a single vial of flies for each biological replicate and surface sterilized by washing in 10% bleach and 70% ethanol. Flies were then homogenized in MRS, serially diluted and 10μL of each dilution was plated on MRS. Colonies were counted from 10μL streaks that had 10-200 colonies and the colony forming units (CFU) per fly calculated.

2.2.3 Oral infection and DSS treatment

For *V. cholerae* infection, freshly eclosed flies were raised at 18°C for 5 days then switched to 29°C for two days. 24hr prior to infection 100μL of *V. cholerae C6706* glycerol stock was spread on LB agar plates and grown at 29°C. Flies were starved 2hr before infection. Bacterial lawn was

scraped off the plate, mixed with LB broth and diluted to an optical density 600 of 0.125. Flies were fed 3mL of bacterial suspension on a cotton plug throughout the infection.

DSS was prepared by dissolving DSS (Sigma 42867) in a PBS 5% sucrose solution, filter sterilized and kept in the freezer for up to two weeks. A 3% DSS solution was used for Figures 5.1-5.4, 5.6-5.8 and 5.5A and a 5% DSS solution was used for Figure 5.5B-D and 5.9 for a more robust proliferative response. *Ecc15* was prepped by streaking then incubating LB plates at 29°C overnight, then inoculating LB broth with single colonies and grown with shaking at 29°C for ~20-24hr. The liquid culture was spun down at 1250g for 10min and the bacterial pellet was resuspended in residual LB and diluted 1:1 in PBS 5% sucrose. DSS or *Ecc15* vials were prepped by covering normal fly food with circular filter paper (Whatman, Grade 3, 23mm, 1003-323) and adding 150µL of the DSS, *Ecc15* or unchallenged (PBS 5% sucrose) solution. Flies were flipped daily onto fresh DSS, *Ecc15* or control solution for 48hr for all experiments except for DSS survival which was over the course of 10 days.

2.3 Imaging

2.3.1 Immunofluorescence

Intestines were dissected in PBS, fixed in 8% formaldehyde for 20 minutes, washed in PBS 0.2% Triton-X (PBST) then blocked in PBST with 3% BSA for 1hr at room temperature. Primary antibodies were incubated in PBST with BSA overnight at 4°C. The following day guts were washed in PBST then secondary antibody incubations were done in conjunction with DNA stain for 1 hour at room temperature in PBST with BSA, washed with PBST then again with PBS. Antibodies and DNA stains used are noted in Table 2.2.

Table 2.2. List of Antibodies and dyes used in this study

Antibody/Dye	Dilution	Company	Cat Number
Mouse anti-prospero	1/100	DSHB	MR1A
Mouse anti-armadillo	1/100	DSHB	N2 7A1
Mouse anti-mys	1/100	DSHB	CF.6G11
Rabbit anti-GFP	1/1000	Thermo Fisher	G10362
Mouse anti-GFP	1/2000	Invitrogen	PA1-9533

Rabbit anti-PH3	1/1000	Millipore	06-570
Mouse anti-Delta	1/100	DSHB	C594.9B
Rabbit anti-pERK	1/1000	Millipore	05-797R
Goat anti-chicken 488	1/1000	Invitrogen	A11039
Goat anti-mouse 568	1/1000	Invitrogen	A11004
Goat anti-rabbit 568	1/1000	Invitrogen	A11011
Goat anti-mouse 647	1/1000	Invitrogen	A21235
Goat anti-rabbit 647	1/1000	Invitrogen	A21244
Hoescht DNA stain	1/1000	Molecular Probes	H-3569
DRAQ5 DNA stain	1/500	Invitrogen	65-0880-96

To prepare the intestinal sections, the posterior midgut was extracted, flash frozen on dry ice in frozen section compound (VWR 95057-838), sectioned to 10μm and slides were stained using the same parameters as whole guts. To determine the apical and basal mys intensity, I drew a line of 10 pixel width from the basal side to the apical (lumen side) side across GFP+ progenitor cells. I defined apical and basal progenitor cell borders as 50% of the maximum GFP intensity, as this GFP intensity coincides with the basal mys intensity peak. I determined the intensity of GFP and mys across the progenitors using the function plot profiles, copied these values into Excel and determined the apical and basal mys intensities.

Apoptotic cells were detected in dissected guts using the TMR red In Situ Cell Death Detection Kit (Roche; 12156792910) following standard kit staining protocol. Briefly, guts were washed in PBS following secondary antibody then stained with 100μL of TUNEL solution for 1hr at 37°C then washed twice with PBS. GFP primary antibody was used for the TUNEL experiment and cryosectioning experiments to retain GFP signal from the esg promoter.

Intestines were mounted on slides using Fluoromount (Sigma; F4680). For every experiment, images were obtained of the posterior midgut region (R4/5) of the intestine with a spinning disk confocal microscope (Quorum WaveFX). PH3+ cells were counted through the entire midgut. All image stacking, intensity and area calculations were done using Fiji software [176].

2.3.2 Transmission Electron Microscopy

Intestines were dissected from virgin female flies that had been at 29°C for 8 days following germ-free and bacterial association protocols. Posterior midguts were excised and fixed with 3% paraformaldehyde with 3% glutaraldehyde. Fixation, contrasting, sectioning, and visualization were performed at the Faculty of Medicine and Dentistry Imaging Core at the University of Alberta. Midgut sections were visualized with Hitachi H-7650 transmission electron microscope at 60Kv in high contrast mode.

2.4 Expression profile preparation

2.4.1 Intestinal progenitor cell isolation and RNA sequencing

Progenitor cell isolation by fluorescence activated cell sorting (FACS) was adapted from previously described protocols [177]. In brief, three biological replicates consisting of 100 fly midguts per replicate were dissected into DEPC PBS and placed on ice. Guts were dissociated with 1mg/ml of elastase at 27°C with gentle shaking and periodic pipetting for 1 hour. Progenitors were sorted based on GFP fluorescence and size with the BD FACSAria III sorter. All small GFP positive cells were collected into DEPC PBS. Cells were pelleted at 1200g for 5 minutes and then resuspended in 500µl of Trizol. Samples were stored at -80°C until all samples were collected. RNA was isolated via a standard Trizol chloroform extraction and the RNA was sent on dry ice to the Lunenfeld-Tanenbaum Research Institute (Toronto, Canada) for library construction and sequencing. The sample quality was evaluated using Agilent Bioanalyzer 2100. TaKaRa SMART-Seq v4 Ultra Low Input RNA Kit for Sequencing was used to prepare full length cDNA. The quality and quantity of the purified cDNA was measure with Bioanalyzer and Qubit 2.0. Libraries were sequenced on the Illumina HiSeq3000 platform.

2.4.2 Single-cell sequencing sample prep

Preparation of single-cell intestinal suspension was made following previous methods [88,178]. For the ImdD30A experiments flies were raised at 18°C for 5 days then shifted to 29°C for an additional 10 days prior to dissection. For the DSS experiments flies were raised for 10 days at 29°C then treated with 3% DSS or unchallenged solution for 48hrs. Batches of five *Drosophila* midguts were dissected at once then transferred to 1% BSA in DEPC treated PBS. Once 30 midguts

were obtained for each condition they were transferred to a 1.5mL tube with 200μL of DEPC/PBS with 1mg/mL Elastase (Sigma, E0258) and chopped into pieces with small dissecting scissors. After mechanical disruption, tubes were incubated at 27°C for 40min with gentle pipetting every 10min. 22μL of 10%BSA in DEPC/PBS solution was added to stop the enzymatic digestion then cells were pelleted by spinning at 300g for 15min at 4°C. Cell pellet was resuspended in 200μL of 0.04% BSA in DEPC/PBS then filtered through a 70μM filter. Live cells were enriched using OptiPrep Density Gradient Medium (Sigma, D1556). Filtered cells were mixed with 444μL of 40% iodixanol (2:1 OptiPrep:0.04% BSA DEPC/PBS) then transferred to a 15mL tube. Another 5.36mL of 40% iodixanol was added and mixed. A 3mL layer of 22% iodixanol was added on top then an additional 0.5mL layer of 0.04% BAS in PBS/DEPC was added. Tubes were spun at 800g for 20min at 20°C then the top interface containing live cells (~500μL) was collected. Live cells were diluted with 1mL of 0.04% BSA in DEPC/PBS. Remaining iodixanol was removed by pelleting cells at 300g for 10min at 4°C and removing supernatant. Cell pellet was resuspended in remaining 0.04% BSA DEPC/PBS solution (~40μL) and cell counts and viability was determined using a hemocytometer. Libraries were generated using 10X Genomics Single-cell Transcriptome Library kit and sent to Novogene for sequencing.

2.4.3 Microarray

Microarray studies were performed with the GeneChip *Drosophila* Genome 2.0 Array (Affymetrix) in triplicate on virgin flies that were raised on regular or antibiotic food for 10–11 days at 18°C. Flies were then shifted to 29°C for another 2 days, after which guts were dissected for RNA extraction (5 females and 5 males per sample). 100 ng purified RNA was used to make labeled cRNA using the GeneChip 30 IVT Plus Reagent Kit (Affymetrix). Preliminary analysis was done with the Transciptome Analysis Console (TAC) software (Affymetrix). We analyzed gene expression data using FlyMINE [179] and Panther [180].

2.4.4 Bacterial 16S sequencing

For 16S deep-sequencing, we raised freshly eclosed virgin females flies on antibiotic medium for 5 days at 18°C and then switched to sterile antibiotic-free food for 1 day. We fed flies a homogenate prepared from w^{1118} flies for 16 hr. Afterward, we raised flies on sterile food at 18°C for

7 days, and 29°C for another 7 days, and dissected 10 guts per sample. We extracted microbial DNA with the UltraClean Microbial DNA Isolation Kit (Mol Bio Laboratories) and amplified 16S DNA with Platinum PFX Taq (Invitrogen) and the 16S primers (Forward AGAGTTTGATCCTGGCTCAG, Reverse GGCTACCTTGTTACGACTT) followed by purification with the QIAquick PCR Purification Kit (QIAGEN). We measured concentration on the Qubit 2.0 (Invitrogen) and used 1 ng for library preparation. Libraries were prepared using the Nextera XT DNA Library Preparation Kit (Illumina). We purified libraries with Ampure Beads (QIAGEN). Pooled libraries were loaded on the MiSeq (illumina) using the MiSeq Reagent Kit v3 (600-cycle). 16S sequences were assembled using DNASTAR Navigator and annotated with the Greengenes database.

2.4.5 Quantitative PCR

RNA was isolated from 10 flies using Trizol Invitrogen) according to manufacturers recommendations. RNA was treated with DNase I (Invitrogen) and Superscript III (Invitrogen) was used to generate cDNA using 5μg of RNA and random primers (Invitrogen). Transcript amplification was performed in an Eppendorf realplex 2 PCR machine using PerfeCTa SYBR Green FastMix (Quanta Biosciences). Primers for *att*: Forward AGTCACAACTGGCGGAAC, Reverse TGTTGAATAAATTGGCATGG. Primers for *dpt*: Forward ACCGCAGTACCCACTCAATC, Reverse ACTTTCCAGCTCGGTTCTGA. Primers used for actin (control): Forward TGCCTCATCGCCGACATAA, Reverse CACGTCACCAGGGCGTAAT.

2.5 Bioinformatics

2.5.1 Bulk RNA Sequencing data processing and analysis

FASTQC was used to evaluate the quality of raw paired-end sequencing reads (http://www.bioinformatics.bbsrc.ac.uk/projects/fastqc, version 0.11.3). Adaptors and reads of less than 36 base pairs in length were trimmed from the raw reads using Trimmomatic (version 0.36) [181]. Reads were aligned to the *Drosophila* transcriptome- bdgp6 (https://ccb.jhu.edu/software/hisat2/index.shtml) with HISAT2 (version 2.1.0) [182]. The resulting BAM files were converted to SAM flies using Samtools (version 1.8) [183]. The converted files were counted using Rsubread (version 1.24.2) [184] and loaded into EdgeR (version 3.16.5) [185]. In EdgeR, genes with counts less than 1 count per million were filtered and libraries were normalized

for size. Normalized libraries were used to call genes that were differentially expressed among treatments. Genes with P-value < 0.01 and FDR < 5% were defined as differentially expressed genes.

Principle component analysis was performed on normalized libraries using Factoextra (version 1.0.5). Gene Ontology enRIchment anaLysis and visuaLizAtion tool (GORILLA) was used to examine Gene Ontology (GO) term enrichment[186]. Specifically, differentially expressed genes (defined above) were compared in a two-list unraked comparison to all genes output from edgeR as a background set. Redundant GO terms were removed.

2.5.2 Single-cell Sequencing data processing

Raw sequencing data from Novogene was aligned to the *Drosophila* reference transcriptome (FlyBase, r6.30) using Cell Ranger v3.0, with the EYFP sequence appended for the DSS experiment, to generate feature-barcode matrices. The resulting matrices were analyzed using Seurat (v3.2.3 for ImdD30A experiment and v4.1.0 for DSS experiment)[187,188] in R. For ImdD30A experiment, cells with <500 or >2500 features were removed. For DSS experiment, cells with <200 or >3500 features and cells with >20% mitochondrial reads were removed to reduce number of low quality cells or doublets. Expression values were normalized and data clustering was performed at a resolution of 0.5 and 15 PCA for the ImdD30A experiment and 0.4 with 30 PCA for the DSS experiment. Clusters were identified using established markers and previous *Drosophila* intestine single-cell analysis (www.flyrnai.org/scRNA)[88,178]. GO term analysis was performed using Gorilla using unranked two list.

For Pseudotime analysis we used Monocle3 (version 0.2.0) [189]. Specifically, we converted the existing Seurat data from each genotype separately into a Monocle cell data set of midgut epithelial cells and performed trajectory analysis. We manually assigned the root node of the trajectory to the node at the tip of the Progenitor cluster for each genotype. We then subset the trajectory branch that explains pseudotime within the Progenitor population to perform all subsequent gene level analysis. Here, we manually assessed expression of genes along pseudotime with known functions in ISC identity, division, and differentiation including genes that were differentially expressed based off our Seurat analysis.

2.6 Data visualization and Statistical analysis

Figures were constructed using R (version 3.3.1) via R studio (version 1.1.442) with easyggplot2 (version 1.0.0.9000), with the exception of GO term figures and lineplots where ggplot2 (version 3.0.0) was used. Longevity graphs were made in Prism software along with the stats for figures 3.3E, 4.2D, and 4.4C. Longevities in 5.2E-F were made in R. All other statistical analysis was performed in R. Figures were assembled in Adobe Illustrator.

2.7 Data availability

Gene expression data for RNA sequencing of FACS isolated progenitors from germ-free, *L. brevis* and *L. plantarum* associated esg^{ts} and esg^{ts}/N^{RNAi} flies has been deposited to the NCBI GEO database accession GSE138555. Microarray data from esg^{ts} and esg^{ts}/*ImdCA* flies have been submitted to the NCBI GEO database (GEO: GSE89445). Single cell sequencing expression data of esg^{ts}/+ and esg^{ts}/*ImdD30A* intestines is deposited at GEO: SuperSeries GSE141897 (GSE171001 and GSE141896). Single cell sequencing expression data from DSS and unchallenged ISC^{ts}/+ and ISC^{ts}/rel^{RNAi} intestines is deposited on NCBI under the accession number PRJNA873108.

Chapter 3

Commensal bacteria modify intestinal stem cell adhesion, division symmetry and tumorigenesis

Data in this chapter have been published in:

- **Ferguson, M**., Petkau, K., Shin, M., Galenza, A., Fast, D., & Foley, E. (2021). Differential effects of commensal bacteria on progenitor cell adhesion, division symmetry and tumorigenesis in the *Drosophila* intestine. *Development*. 148(5): 1-14

3.1 Summary

Microbial factors influence the homeostatic and oncogenic growth of the intestine. For instance, germ-free flies, fish and mice have reduced intestinal proliferation, and bacterial dysbiosis correlates with colorectal cancer progression in humans[5–9,13,16]. However, little is known about how individual bacterial species impact intestinal tumorigenesis and the direct effects of bacteria on stem cell division programs.

To determine how commensal bacteria modify tumorigenesis I monitored tumor growth in the *Drosophila* intestine in the presence of single commensal species. I identified *Lactobacillus brevis* as a potent driver of tumor growth while *Lactobacillus plantarum* had low levels of tumor severity. Mechanistically, *L. brevis* disrupted the expression and subcellular localization of integrins in intestinal progenitor cells. Since integrins are important regulators of stem cell maintenance and division symmetry I asked whether *L. brevis* altered stem cell numbers and the occurrence of symmetric divisions in the intestine. *Drosophila* associated with *L. brevis* contained elevated stem cell numbers and higher proportion of symmetric divisions, increasing the replicative capacity of the intestine. Collectively, these data highlight the impact of individual bacterial species on the division and maintenance of the intestinal progenitor compartment.

3.2 Results

3.2.1 *L. brevis* promotes tumor growth in the *Drosophila* intestine.

To study bacterial effects on intestinal tumors, I used the *escargot-GAL4, GAL80^{ts}, UAS-GFP* (*esg^{ts}*) transgenic fly line to express an inducible *Notch* RNAi construct (*UAS-N^{RNAi}*) in ISCs and enteroblasts (collectively referred to as progenitor cells). With this *esg^{ts}* line, the progenitor specific promoter *esg* drives expression of GAL4, which allows the expression of transgenes downstream of UAS sequences. In addition, the temperature sensitive GAL80 inhibits the activity of GAL4 at low temperatures, but upon raising flies at 29°C, GAL80 becomes inactive and allows the GAL4 dependent activation of transgene expression. Intestines of control *esg^{ts}/+* females contained evenly distributed GFP-positive progenitors and prospero-positive enteroendocrine cells in a simple epithelium dominated by large, polyploid enterocytes (Fig. 3.1A, 3.2B). Similar to previous reports[68], I found that depletion of *Notch* (*esg^{ts}/N^{RNAi}*) caused the formation of multilayered midgut tumors populated by excess progenitor and enteroendocrine cells (Fig. 3.1B, 3.2C). As

enteroendocrine and progenitor rich (level IV) tumors were evident in female intestines, but largely absent from males (Fig. 3.1C), I performed all subsequent experiments on adult female posterior midguts.

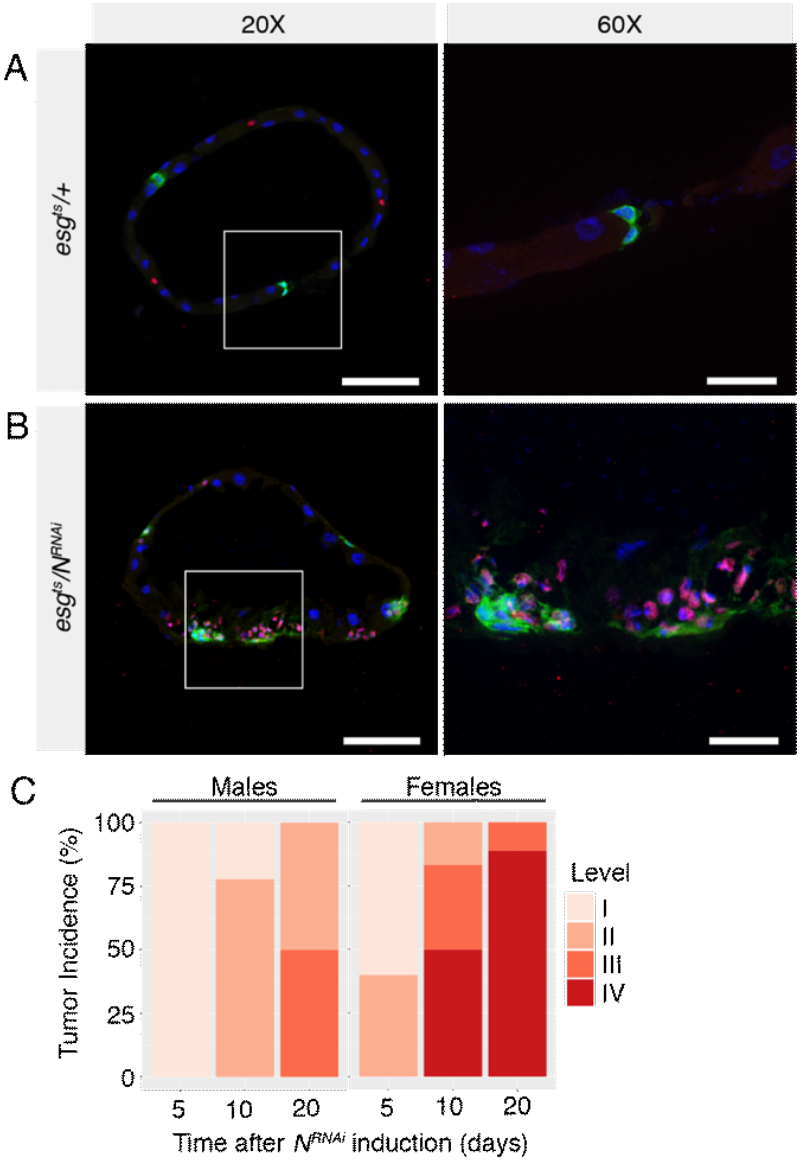

Figure 3.1 Multilayered Notch-deficient tumors form in the female *Drosophila* intestine. **(A)** Cross section of *esg*^{ts}/+ posterior midgut and **(B)** cross section of *esg*^{ts}/*N*^{RNAi} showing multilayered tumors composed of enteroendocrine cells labelled by Prospero (red) and progenitors (green). DNA labelled with Hoechst (blue). Scale bars: 20X = 50μm 60X = 15μm. **(C)** Incidence of tumors in male and virgin female *esg*^{ts}/*N*^{RNAi} intestines 5, 10 and 20 days after *Notch* knockdown in intestinal progenitors based off the grading system in Figure 1.2G.

In contrast to intestines with a conventional microbiome, Notch-deficient tumors rarely appeared in age-matched, germ-free (GF) flies, indicating microbial requirements for tumor growth (Fig. 3.2C-D), although the possibility that tumors eventually form in GF flies with age cannot be excluded. To identify bacterial species that promote tumors, I examined posterior midguts of adult *esg*^{ts}/*N*^{RNAi} flies that I associated exclusively with common species of *Lactobacillus* commensals, a dominant genus

within the fly microbiome[79,82]. To focus on adult tumors, I raised esg^{ts}/N^{RNAi} larvae with a conventional microbiome under conditions that permit wild-type Notch activity. Upon eclosion, I fed adults an antibiotic cocktail that depleted the bacterial microbiome below detectable levels, and re-associated flies with either *Lactobacillus brevis* (*Lb*), or *Lactobacillus plantarum* (*Lp*) (Fig. 3.2A) and shifted flies to 29°C to inhibit Notch. These two strains of bacteria were isolated from wild-type flies in the Foley lab and have been previously described[173]. I compared each mono-association to conventionally reared (CR) esg^{ts}/N^{RNAi} flies that contained a poly-microbial native gut microbiota. Mono-association of esg^{ts}/N^{RNAi} flies with *Lp* resulted in few visible tumors (Fig. 3.2E). In contrast, mono-association with *Lb* caused multiple, large tumors throughout the posterior midgut (Fig. 3.2F), indicating that *Lb* is sufficient for tumor development.

I then quantified impacts of bacterial association on midgut tumors. First, I developed a four-point system to classify intestines, ranging from no visible defects (level I) to intestines with progenitor and enteroendocrine-rich tumors (level IV, Fig. 3.2G). In a blinded assay, I categorized 85% of CR esg^{ts}/N^{RNAi} intestines as level IV, whereas only 20% of GF intestines belonged to the same category (Fig. 3.2H), confirming bacterial effects on gut tumors. Consistent with my initial observations, GF and *Lp*-associated intestines had similarly mild levels of tumor incidence (Fig. 3.2H). In contrast, all intestines associated with *Lb* had level IV tumors within five days of Notch inactivation. To measure total tumor size per midgut, I quantified the posterior midgut area occupied by progenitor and enteroendocrine cells in the respective groups. Association with *Lb* significantly enhanced accumulation of progenitors and enteroendocrine cells in esg^{ts}/N^{RNAi} intestines compared to CR, GF or *Lp* mono-associated flies, supporting a role for *Lb* in promoting tumors (Fig. 3.2I). To determine if the larger tumor areas in *Lb*-associated flies are a result of increased tumor initiation, or accelerated tumor growth I quantified the number of tumors in each intestine. Similar to my assessment of tumor size, association with *Lb* had a significant impact on tumor numbers, resulting in approximately three times as many tumors per gut as CR counterparts (Fig. 3.2J). Collectively, my data indicate that association with the common commensal *L. brevis* increases the frequency of midgut tumor initiation, whereas *L. plantarum* does not.

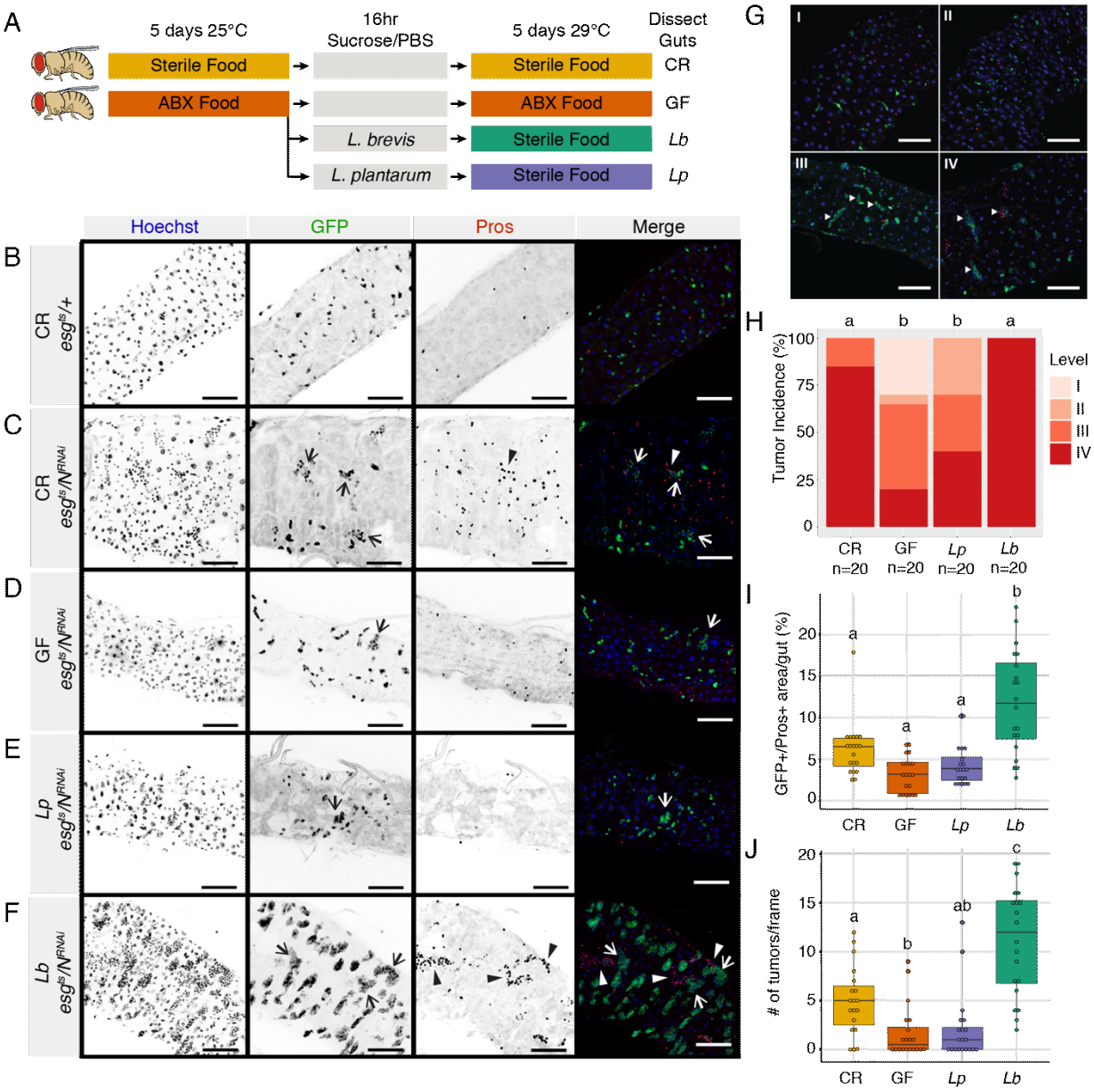

Figure 3.2. *L. brevis* promotes tumor growth in the *Drosophila* intestine. (A) Scheme for generating GF and gnotobiotic flies alongside CR controls. ABX = food with antibiotic cocktail **(B)** Images of wild-type CR *esg*^{ts}*/+* intestines **(C-F)** Images of *esg*^{ts}*/N*^{RNAi} posterior midguts 5 days after *Notch* knockdown and microbial manipulation. Hoechst marks DNA (blue), GFP marks esg+ progenitor cells (green) and Pros marks enteroendocrine cells (red). Level III tumours (open arrowheads) and level IV tumours (closed arrowheads). Scale bars = 50μm. **(G)** Tumor incidence grading system. I – healthy intestine, II – intestinal dysplasia without tumorigenesis, III – tumors populated by progenitors, IV – tumors populated by progenitors and enteroendocrine cells. **(H)**

Tumor incidence in CR, GF, *Lp* and *Lb* mono-associated intestines after 5 days of *Notch* depletion. Different letters denote significant difference of level IV tumor incidence of $p<0.01$ with Chi-squared test **(I)** Tumor burden in CR, GF, *Lp* and *Lb* mono-associated intestines after 5 days of Notch depletion. Burden is calculated as the percent area of the intestine that is GFP+ and Pros+. **(J)** Number of tumors per frame of the posterior midgut after 5 days of microbial manipulation and Notch depletion. Different letters in I-J denote significant difference of $p<0.05$ with ANOVA followed by multiple pairwise Tukey tests.

To determine which factors from *Lb* promote tumors, I measured tumors in flies that I continuously fed heat-killed *Lb* or cell wall derived from *Lb* for five days. GF esg^{ts}/N^{RNAi} flies fed heat-killed *Lb* mixed with sterile food had similar tumor levels (Fig. 3.3A), and similar progenitor and enteroendocrine cell expansions as *Lb* mono-associated flies raised on sterile food (Fig. 3.3B), indicating that structural components of *Lb* are sufficient to promote tumors. To determine if *Lb* cell wall mediated these effects, I measured tumors in GF flies fed sterile *Lb* extracts in PBS/sucrose on filter paper. While esg^{ts}/N^{RNAi} GF flies fed sterile PBS/sucrose alone had low levels of intestinal tumors, flies fed *Lb* cell wall extract had significantly increased tumor levels (Fig. 3.3C), and accumulated progenitor and enteroendocrine cells to similar levels as GF counterparts fed dead *Lb* (Fig. 3.3D). Finally, I noticed that esg^{ts}/N^{RNAi} flies mono-associated with *Lb* died significantly faster than CR counterparts, while *Lb* did not shorten the lifespan of $esg^{ts}/+$ controls (Fig. 3.3E), arguing that cell wall components from *L. brevis* promote initiation of Notch-deficient tumors, resulting in premature host death.

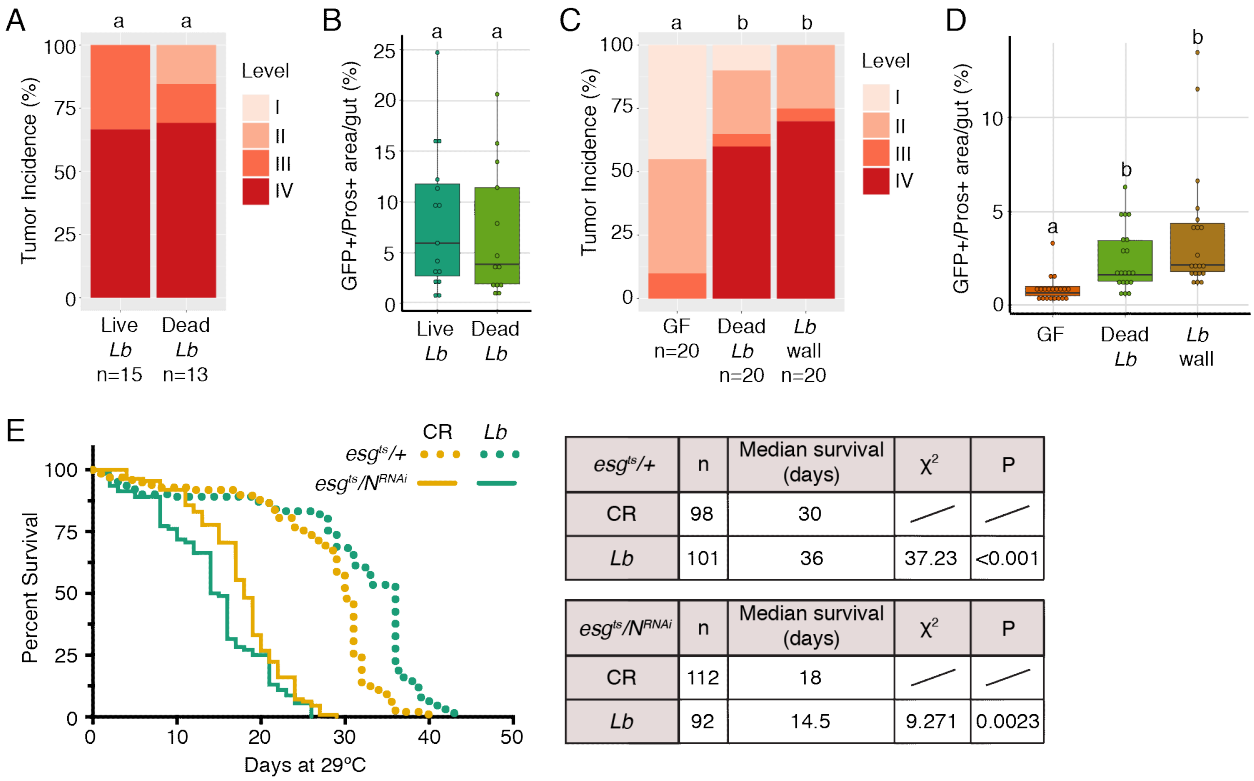

esg^ts/+	n	Median survival (days)	χ^2	P
CR	98	30		
Lb	101	36	37.23	<0.001

esg^ts/N^RNAi	n	Median survival (days)	χ^2	P
CR	112	18		
Lb	92	14.5	9.271	0.0023

Figure 3.3. *L. brevis* cell wall is sufficient to promote tumor growth. Tumor incidence **(A)** and burden **(B)** of *esg*^{ts}/*N*^{RNAi} flies colonized with live *Lb* or GF *esg*^{ts}/*N*^{RNAi} fed heat killed *Lb* mixed into sterile food. Same letters denote no significant difference between level IV tumor incidence at p = 0.05 with Chi squared test **(A)** or tumor burden using pairwise Wilcoxon test **(B).** Tumor incidence **(C)** and burden **(D)** of GF *esg*^{ts}/*N*^{RNAi} flies fed heat killed *Lb* or cell wall extract in PBS/sucrose on filter paper. Different letters denote significant difference of p < 0.05 with Chi squared test **(C)** or pairwise Wilcoxon test **(D). (E)** Fly lifespan of CR (yellow) and Lb colonized (teal) *esg*^{ts}/+ and *esg*^{ts}/*N*^{RNAi} flies was monitored after switching to the permissive temperature of 29°C. Statistical analysis performed in Prism software using Log-rank Mantel-Cox test.

3.2.2 Notch inactivation modifies expression of growth, differentiation, and immunity regulators in progenitors

To determine how *Lb* affects Notch-deficient progenitors, I used RNA-sequencing to identify the transcriptional profiles of FACS-purified, GFP-positive progenitors from *Lb*-associated *esg*^{ts}/+ and *esg*^{ts}/*N*^{RNAi} intestines (Fig. 3.4A). As controls, I sequenced transcriptomes of *esg*^{ts}/+ and *esg*^{ts}/*N*^{RNAi}

progenitors from GF flies, or flies that I mono-associated with *Lp*. Principal Component Analysis (PCA) revealed that Notch-deficient progenitors segregate from wild-type progenitors along PC1, regardless of bacterial association (Fig. 3.4B). Differential gene expression analysis showed that the majority of gene expression profiles altered by Notch-depletion were shared between GF, *Lb*-associated and *Lp*-associated intestines (Fig. 3.4C), indicating the existence of a microbe-independent core response to Notch reduction in progenitors. GO term analysis of the core Notch-deficient response revealed significant upregulation of biological processes involved in cell division (Fig. 3.4D), and diminished expression of Notch-responsive *Enhancer of split (E(spl))* complex genes required for enteroblast differentiation (Fig. 3.4E). In addition to effects on growth and differentiation, I observed unexpected downregulation of immune pathway regulators in progenitors that lacked *Notch* (Fig. 3.4D-E). Decreased expression of immune regulators is not secondary to tumor development, as I saw similar changes in intestines of GF, and *Lp*-associated flies. In each case, Notch inactivation diminished expression of essential components of the IMD pathway such as *imd*, and *rel*, as well as prominent IMD response genes such as *pirk*, and multiple PGRP family members (Fig. 3.4E). These data suggest a genetic link between Notch signaling and immune responses in the progenitor compartment and match previous reports that mutation or activation of the IMD pathway alters expression of Notch pathway genes in the fly intestine[6].

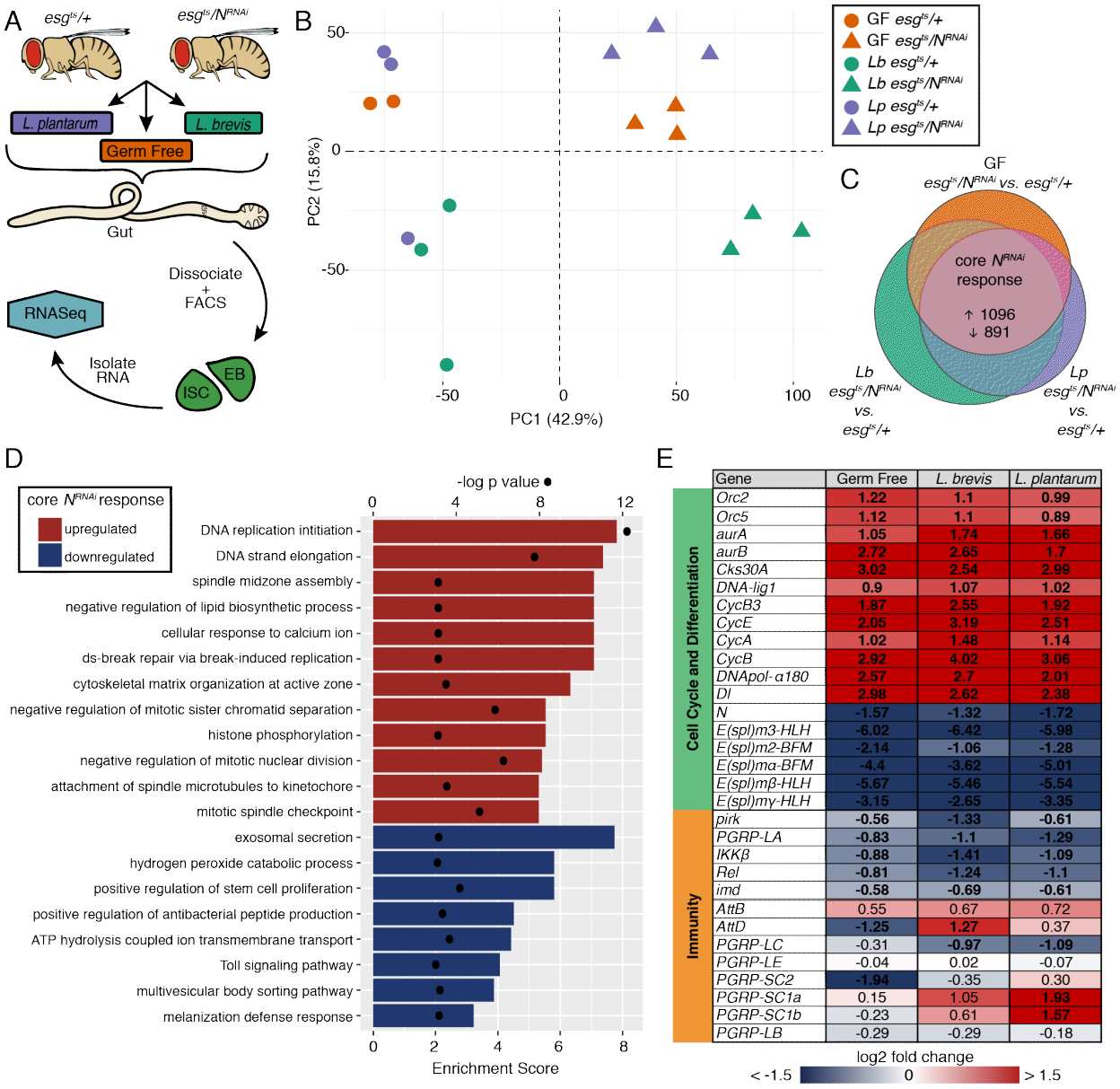

	Gene	Germ Free	*L. brevis*	*L. plantarum*
Cell Cycle and Differentiation	*Orc2*	**1.22**	**1.1**	**0.99**
	Orc5	**1.12**	**1.1**	**0.89**
	aurA	**1.05**	**1.74**	**1.66**
	aurB	**2.72**	**2.65**	**1.7**
	Cks30A	**3.02**	**2.54**	**2.99**
	DNA-lig1	**0.9**	**1.07**	**1.02**
	CycB3	**1.87**	**2.55**	**1.92**
	CycE	**2.05**	**3.19**	**2.51**
	CycA	**1.02**	**1.48**	**1.14**
	CycB	**2.92**	**4.02**	**3.06**
	DNApol-α180	**2.57**	**2.7**	**2.01**
	Dl	**2.98**	**2.62**	**2.38**
	N	**-1.57**	**-1.32**	**-1.72**
	E(spl)m3-HLH	**-6.02**	**-6.42**	**-5.98**
	E(spl)m2-BFM	**-2.14**	**-1.06**	**-1.28**
	E(spl)mα-BFM	**-4.4**	**-3.62**	**-5.01**
	E(spl)mβ-HLH	**-5.67**	**-5.46**	**-5.54**
	E(spl)mγ-HLH	**-3.15**	**-2.65**	**-3.35**
Immunity	*pirk*	**-0.56**	**-1.33**	**-0.61**
	PGRP-LA	**-0.83**	**-1.1**	**-1.29**
	IKKβ	**-0.88**	**-1.41**	**-1.09**
	Rel	**-0.81**	**-1.24**	**-1.1**
	imd	**-0.58**	**-0.69**	**-0.61**
	AttB	0.55	0.67	0.72
	AttD	**-1.25**	**1.27**	0.37
	PGRP-LC	-0.31	**-0.97**	**-1.09**
	PGRP-LE	-0.04	0.02	-0.07
	PGRP-SC2	**-1.94**	-0.35	0.30
	PGRP-SC1a	0.15	1.05	**1.93**
	PGRP-SC1b	-0.23	0.61	**1.57**
	PGRP-LB	-0.29	-0.29	-0.18

Figure 3.4. Notch inactivation decreases expression of immunity regulators in intestinal progenitors. (A) Workflow for the RNA-Seq of intestinal progenitors upon *Notch* knockdown and *Lb* colonization. **(B)** PCA plot from RNA-Seq project. Circles represent *esg*^{ts}*/+* and triangles represent *esg*^{ts}*/N*^{RNAi} replicates. Different colors represent GF (orange), *Lb* (teal) or *Lp* (purple). **(C)** Genes altered by *Notch* knockdown (p<0.01, FDR <5%) in each microbial context showing the core response to knockdown of *Notch*. **(D)** Biological process GO terms enriched in the core *Notch* response. Enrichment score shown as bars and p values shown as dots. **(E)** Log2 fold change of *Notch* response genes involved in cell cycle/differentiation and immunity. Values in bold are significantly altered genes with a p<0.01 and FDR 5%. All genes above the double line are part of

the core Notch response whereas genes below (*AttB* to *PGRP-LB*) are immune genes not included in the core response. Each column is a direct comparison of esg^{ts}/N^{RNAi} to $esg^{ts}/+$ under GF, *Lb* or *Lp* conditions.

3.2.3 Notch-deficiency promotes intestinal association with *L. brevis*.

As tumor growth frequently involves shifts in microbiota composition, I determined effects of Notch inactivation on host association with *Lb* and *Lp*. First, I measured the intestinal bacterial load of $esg^{ts}/+$ and esg^{ts}/N^{RNAi} flies that I mono-associated with the respective strains for five days. In these experiments, I quantified bacterial load in the same cohort of flies that I used to measure tumors in Figure 3.2, allowing me to determine if host-microbe associations correlate with midgut tumors. For *Lb* and *Lp*, I observed significantly increased bacterial loads in Notch-deficient intestines compared to wild-type controls (Figure 3.5A), suggesting effects of host genotype on bacterial association. Importantly, there were no differences between *Lp* or *Lb* loads in Notch-deficient guts. Thus, the identity of associated bacteria, not the abundance, determines tumors in the host.

As bacterial association is higher in Notch-deficient intestines than wildtype intestines (Fig. 3.5A), and Notch knockdown diminishes expression of IMD pathway components, I asked if IMD affects host association with *Lb*. Consistent with a role for IMD in the control of intestinal *Lb*, I found that *imd* mutants had significantly higher *Lb* loads than wild-type controls ten days after mono-association with *Lb* (Fig. 3.5B). Conversely, constitutive activation of IMD in enterocytes ($Myo1A^{ts}$/*ImdCA*) reduced *Lb* load to approximately 4% of that found in *imd* mutants (Fig. 3.5B). These data support a role for IMD in regulation of intestinal *Lb*. However, it is important to note that the increased bacterial abundance in *imd* mutants is considerably less pronounced than that observed upon *Notch* knockdown (compare Fig. 3.5A and 3.5B). Thus, I believe that additional, IMD-independent mechanisms control bacterial numbers in esg^{ts}/N^{RNAi} intestines that require identification.

Finally, I measured the effects of Notch inactivation on host association with *Lactobacillus* commensals. Here, I completed a longitudinal measurement of bacterial load in intestines of $esg^{ts}/+$ and esg^{ts}/N^{RNAi} flies that I mono-associated with *Lp* or *Lb*. In general, my data match earlier reports that total numbers of intestinal bacteria increase in flies with age[190,191]. In wild-type $esg^{ts}/+$ intestines, the rates of increase in host-association with *Lp* and *Lb* are nearly indistinguishable, with *Lb* associating to lower levels at all times tested (Fig. 3.5C). Initially, *Lb* also associated with

esg^{ts}/*N*^{RNAi} intestines to lower levels than *Lp*. However, I noted substantial effects of Notch inactivation on subsequent progressions in host-microbe association. In this case, association with *Lp* increased at a considerably slower rate than association with *Lb* (Fig. 3.5D). Exponential regression analysis revealed that host-associated *Lb* loads double at similar rates in intestines of *esg*^{ts}/+ (0.87d) and *esg*^{ts}/*N*^{RNAi} (0.78d) flies. In contrast, host-associated-*Lp* loads double at a considerably slower rate in Notch-deficient intestines (2.54d, Fig. 3.5D), than wild-type intestines (0.97d, Fig. 3.5C), suggesting that Notch knockdown hinders host association with *Lp*, but has minimal effects on association with *Lb*.

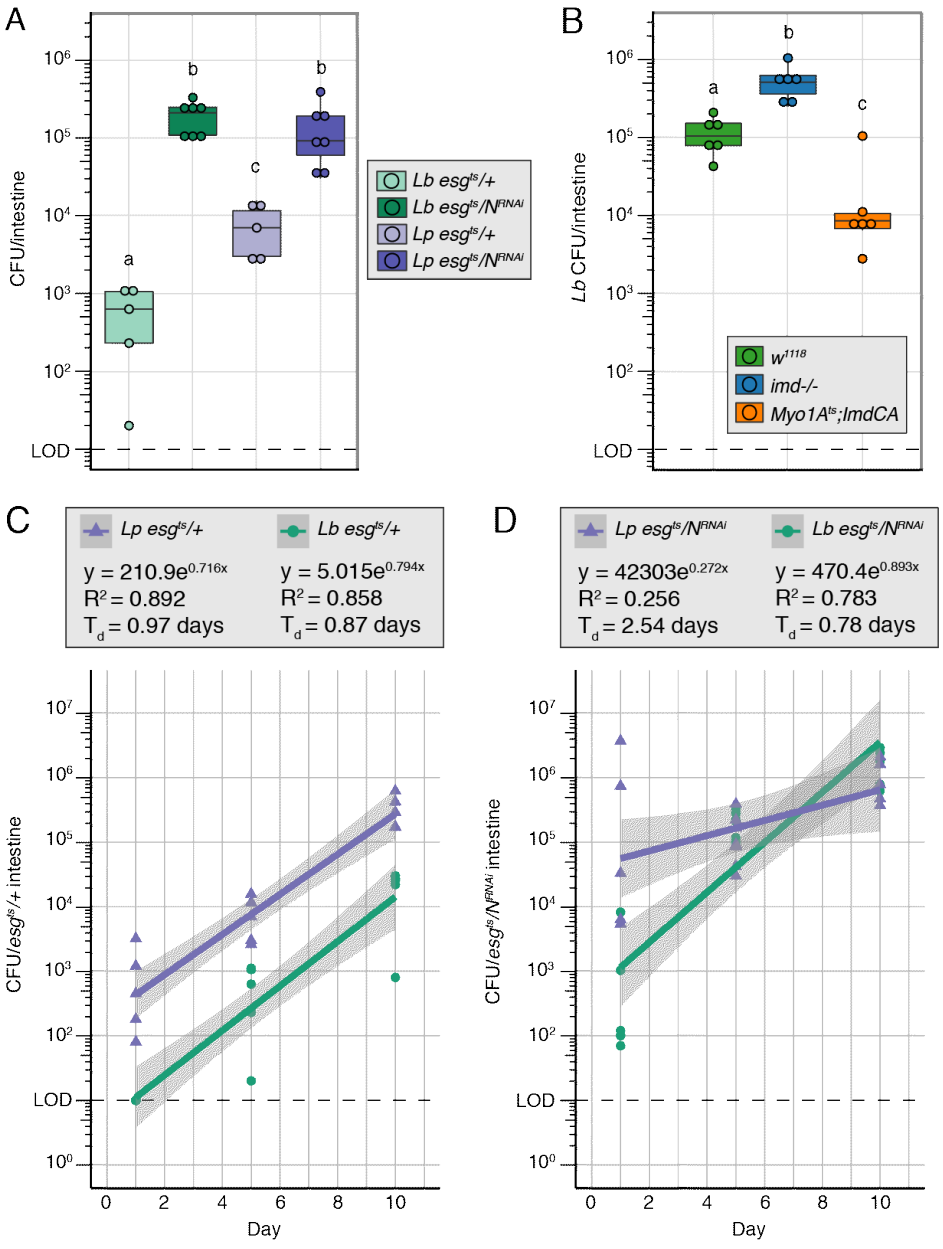

Figure 3.5 Notch-deficiency promotes intestinal association with *L. brevis*. **(A)** Colony forming units (CFU) of *Lb* (green) and *Lp* (purple) per fly intestine in mono-associated $esg^{ts}/+$ and esg^{ts}/N^{RNAi} 5 days after transgene expression and bacterial colonization. **(B)** CFU of *Lb* per fly intestine 10 days after transgene expression/bacterial colonization in *Lb* mono-associated wild-type (w^{1118}), *imd-/-*, and *Myo1A^{ts};ImdCA*. For **(A)** and **(B),** different letters denote significance at $p<0.05$ with multiple pairwise Wilcoxon tests. **(C)** CFU of *Lb* (green) and *Lp* (purple) over time in $esg^{ts}/+$ intestines. **(D)** CFU of *Lb* (green) and *Lp* (purple) over time in esg^{ts}/N^{RNAi} intestines. For **(C)** and **(D)**, x axis is days post transgene expression/bacterial colonization and line represents exponential trendline with shaded region being a 95% confidence interval. T_d = doubling time. LOD = Limit of detection.

3.2.4 *L. brevis* decreases expression of integrins in progenitor cells.

As *Lb* grows effectively in Notch-deficient intestines, where it promotes tumors, I hypothesized that *Lb* will have distinct division-enhancing effects on progenitor cells. To test this hypothesis, I looked for progenitor cell transcriptional events that were specific to association with *Lb*. PCA identified a transcriptional response that is unique to *Lb* in wild-type and *Notch*-deficient progenitors (Fig. 3.4B, Fig. 3.6A-B). For example, *Lb* changed the expression of 1208 genes in esg^{ts}/N^{RNAi} progenitors compared to GF while *Lp* only changed 98 genes (Fig. 3.6B). Regardless of host genotype, association with *Lb* specifically increased expression of genes required for cell division, such as DNA replication, and mitotic spindle organization (Fig. 3.6C), as well as prominent cell cycle and growth regulators (Fig. 3.7A), consistent with growth-promoting effects of gut-associated bacteria in *Drosophila*[5,6]. In addition to effects on cell cycle and growth pathways, I noticed a particularly striking inhibitory effect of *Lb* on expression of genes involved in cell-cell adhesion, cell-matrix adhesion and cell polarity (Fig. 3.6C), especially genes that encode integrin complex proteins (Fig. 3.6D). For example, association with *Lb* led to diminished expression of the alpha and beta-integrins *scab* and *myospheroid* (*mys*), the talin ortholog, *rhea*, and the integrin extracellular matrix ligand, *LanA* (Fig. 3.7A). The effects of *Lb* on expression of genes associated with stem cell adhesion were independent of host genotype, as I observed the same phenotypes in progenitors of *Lb*-associated $esg^{ts}/+$ and esg^{ts}/N^{RNAi} flies (Fig. 3.7A).

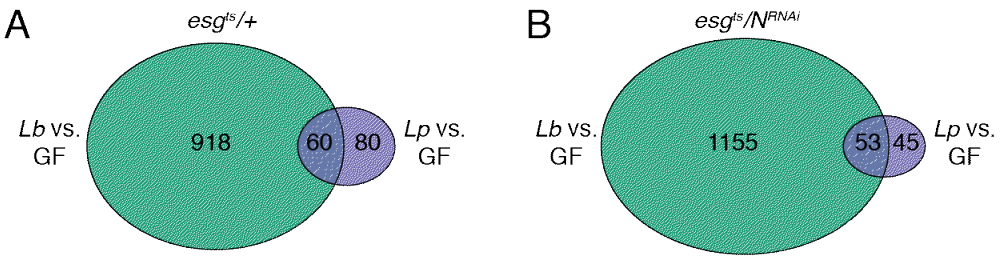
A
esg^ts/+
Lb vs. GF
918
60
80
Lp vs. GF
B
esg^ts/N^RNAi
Lb vs. GF
1155
53
45
Lp vs. GF

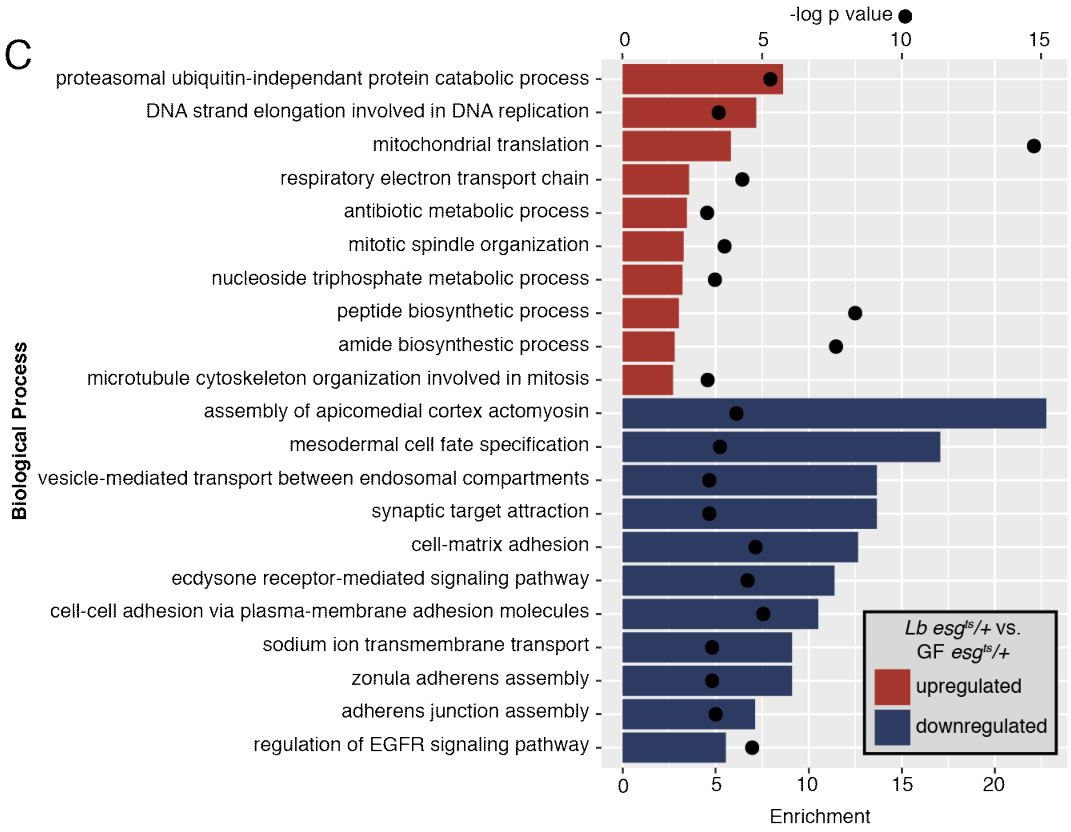
C
-log p value
0
5
10
15
proteasomal ubiquitin-independant protein catabolic process
DNA strand elongation involved in DNA replication
mitochondrial translation
respiratory electron transport chain
antibiotic metabolic process
mitotic spindle organization
nucleoside triphosphate metabolic process
peptide biosynthetic process
amide biosynthestic process
microtubule cytoskeleton organization involved in mitosis
assembly of apicomedial cortex actomyosin
mesodermal cell fate specification
vesicle-mediated transport between endosomal compartments
synaptic target attraction
cell-matrix adhesion
ecdysone receptor-mediated signaling pathway
cell-cell adhesion via plasma-membrane adhesion molecules
sodium ion transmembrane transport
zonula adherens assembly
adherens junction assembly
regulation of EGFR signaling pathway
Biological Process
Lb esg^ts/+ vs. GF esg^ts/+
upregulated
downregulated
0
5
10
15
20
Enrichment

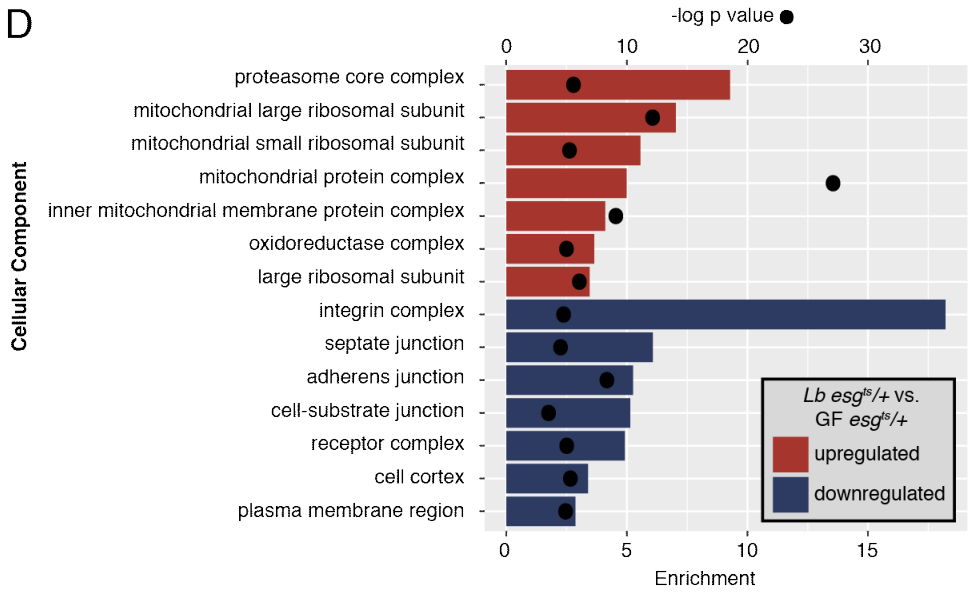
D
-log p value
0
10
20
30
proteasome core complex
mitochondrial large ribosomal subunit
mitochondrial small ribosomal subunit
mitochondrial protein complex
inner mitochondrial membrane protein complex
oxidoreductase complex
large ribosomal subunit
integrin complex
septate junction
adherens junction
cell-substrate junction
receptor complex
cell cortex
plasma membrane region
Cellular Component
Lb esg^ts/+ vs. GF esg^ts/+
upregulated
downregulated
0
5
10
15
Enrichment

Figure 3.6 Specific effect of *L. brevis* on the expression of growth and cell adhesion regulators

(A-B) Number of significant genes (p<0.01, FDR<5%) differentially expressed in progenitors upon *Lb* or *Lp* mono-association in comparison with GF. **(A)** Comparisons from $esg^{ts}/+$. **(B)** Comparisons from esg^{ts}/N^{RNAi}. **(C)** Biological process GO terms enriched in progenitors from $esg^{ts}/+$ colonized with *Lb* compared to GF. Enrichment score shown as bars and p values shown as dots. **(D)** Cellular component GO terms enriched in progenitors from $esg^{ts}/+$ colonized with *Lb* compared to GF. Enrichment score shown as bars and p values shown as dots.

Given the positive effects of *Lb* on expression of ISC division regulators in $esg^{ts}/+$ and esg^{ts}/N^{RNAi} progenitors, I asked if *Lb* activates ISC division of wild-type progenitors. To answer this question, I mono-associated GF wild-type ($esg^{ts}/+$) flies with *Lb* and quantified phospho-histone 3-positive (PH3+) mitotic cells in adult midguts. Similar to effects on tumors, *Lb* stimulated division of wild-type progenitors to significantly higher levels than CR, GF, or *Lp*-mono-associated flies (Fig. 3.7B). Thus, my data indicate that association with *Lb* diminishes expression of genes required for progenitor adhesion to the extracellular matrix, and induces expression of genes required for epithelial growth, promoting ISC division in wild-type and Notch-deficient progenitors.

A

	Gene	Function	*L. brevis* compared to Germ Free		*L. brevis* compared to *L. plantarum*	
			$esg^{ts}/+$	esg^{ts}/N^{RNAi}	$esg^{ts}/+$	esg^{ts}/N^{RNAi}
Cell Adhesion/Polarity	*rhea*	Integrin adapter	-0.43	**-0.47**	**-0.81**	**-0.91**
	mys	β Integrin	**-0.47**	**-0.28**	**-0.56**	**-0.36**
	ItgβV	β Integrin	**-0.42**	-0.24	**-0.31**	**-0.31**
	scab	α Integrin	**-0.60**	**-0.43**	**-0.74**	**-0.80**
	ItgaPS4	α Integrin	**-1.37**	**-0.68**	**-0.79**	**-1.20**
	Dg	ECM	**-0.42**	-0.10	**-0.76**	**-0.53**
	trol	ECM	**-0.59**	-0.13	**-0.82**	**-0.40**
	LanA	ECM	-0.44	**-0.92**	**-0.56**	**-0.96**
	LanB2	ECM	-0.12	**-0.57**	**-0.48**	**-0.79**
	Ndg	ECM	-0.44	**-1.19**	**-0.63**	**-1.51**
Growth	*scrib*	Septate Junction	**-0.94**	**-0.51**	**-0.71**	**-0.87**
	ed	Adherens Junction	**-0.52**	-0.16	**-0.59**	-0.31
	crb	Hippo	**-0.74**	**-0.50**	**-0.61**	**-0.73**
	sdt	Hippo	**-0.88**	-0.33	-0.44	**-0.76**
	Pez	Hippo	**-0.84**	-0.32	**-1.00**	**-0.85**
	kibra	Hippo	-0.28	**-0.45**	**-1.42**	**-0.40**
	ex	Hippo	-0.33	**-0.68**	**-0.60**	**-0.95**
	wts	Hippo	**-0.64**	**-0.65**	-0.35	**-0.45**
	Socs36E	JAK/STAT	0.27	**0.90**	0.05	**0.60**
Cell Cycle	*CycE*	Replication	-0.15	**0.99**	0.03	**0.71**
	Cdk2	Replication	**0.89**	**0.78**	0.32	**1.00**
	E2f2	Replication	0.23	**0.56**	**0.46**	**0.58**
	Orc2	Replication	**0.99**	**0.87**	**0.64**	**0.75**
	PCNA	Replication	**1.08**	**0.85**	0.37	**0.60**
	Mcm5	Replication	**1.01**	**0.94**	**0.89**	**0.62**
	CycA	Replication/Mitosis	0.13	**0.59**	0.19	**0.52**
	CycB	Mitosis	0.08	**1.17**	-0.18	**0.78**
	Cdk1	Mitosis	**0.55**	**0.88**	0.21	**0.87**
	Cks30A	Mitosis	**1.27**	**0.79**	**1.09**	**0.63**

log2 FC: > 1.5, 0, < -1.5

B

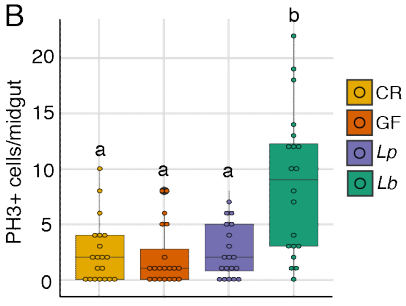

Figure 3.7 *L. brevis* decreases expression of integrins in progenitor cells and promote ISC divisions. **(A)** Log2 fold change of genes involved in cell adhesion/polarity, Growth and Cell cycle affected by *Lb* in comparison to either GF or *Lp* colonization in $esg^{ts}/+$ and esg^{ts}/N^{RNAi} progenitors. Bolded values are those with a p value <0.05 and FDR<5%. **(B)** Number of PH3+ cells per $esg^{ts}/+$ midgut in gnotobiotic flies 8 days after colonization. Different letters denote significant difference of p<0.01 by multiple pairwise Wilcoxon tests.

3.2.5 *L. brevis* colonization disrupts integrin localization independent of division.

I was particularly intrigued by effects of *Lb* on expression of integrins that anchor progenitors within the niche. Therefore, I asked what effects *Lb* has on progenitor cell adhesion and morphology. In a preliminary experiment, I used transmission electron microscopy to visualize posterior midguts of CR, and *Lb*-associated wild-type flies. CR intestines contained basal progenitors in close association with the extracellular matrix (Fig. 3.8A-B). Mono-association with *Lb* appeared to disrupt intestinal organization, generating round progenitors that shifted apically relative to the extracellular matrix, and lacked discernible contact with larger enterocytes or extracellular matrix (Fig. 3.8C-D). These morphological changes appear specific to progenitors, as no defects were apparent in the shape, or relative position, of surrounding enterocytes.

The apparent shift in progenitor localization in *Lb*-associated intestines prompted me to ask if *Lb* modifies integrin distribution. To answer this question, I determined the subcellular localization of the β-integrin, myospheroid (mys), in sagittal sections of GF intestines, or intestines that I associated with *Lb*. In GF $esg^{ts}/+$ flies, I detected basolateral enrichment of mys in GFP-positive progenitors (Fig. 3.9A). Similar to my electron microscopy results, I found that *Lb* colonization caused progenitors to round up and adopt a more apical position within the epithelium (Fig. 3.9B). Furthermore, association with *Lb* had visible impacts on mys localization, characterized by discontinuous basolateral distribution, and atypical apical enrichment of mys (Fig. 3.9B, arrowheads). To directly measure effects of *Lb* on subcellular distribution of integrins, I developed an immunofluorescence-based assay that allowed me to quantify apical:basolateral ratios of mys in progenitors (Fig. 3.9D-E). With this assay, I detected basal enrichment of mys in GF progenitors (Fig. 3.9F). Association with *Lb* shifted the distribution of mys, resulting in significant increases in apical mys (Fig. 3.9F). To determine if *Lb*-dependent effects on integrin subcellular distribution are

downstream consequences of ISC division, I blocked division in progenitors of *Lb*-associated flies by expressing the cell cycle inhibitor *dacapo* (*esg*^{ts}*/dap*) (Fig. 3.9G). Notably, when I examined division-impaired midguts, I found that *Lb* continued to cause increases in apical mys (Fig. 3.9C, 3.9F), indicating that *Lb* alters apicobasal integrin distribution independent of ISC divisions.

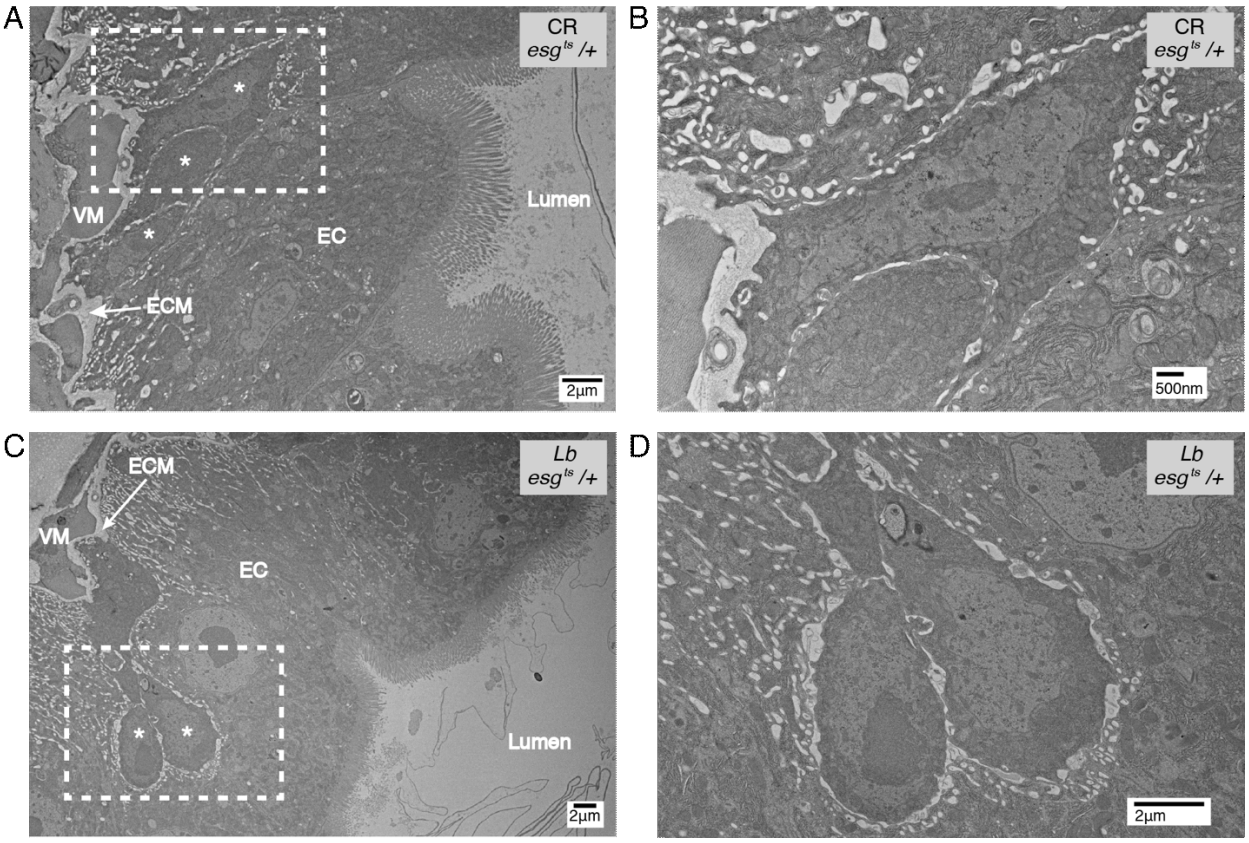

Figure 3.8 *L. brevis* disrupts progenitor morphology (A-D) TEM images of posterior midgut cross sections from *esg*^{ts}*/+* CR (A-B) and *Lb* mono-associated (C-D) intestines. VM = visceral muscle, ECM = Extracellular matrix, EC = Enterocyte, * = progenitors. Dashed boxes in (A) and (C) showed zoomed areas of (B) and (D) respectively.

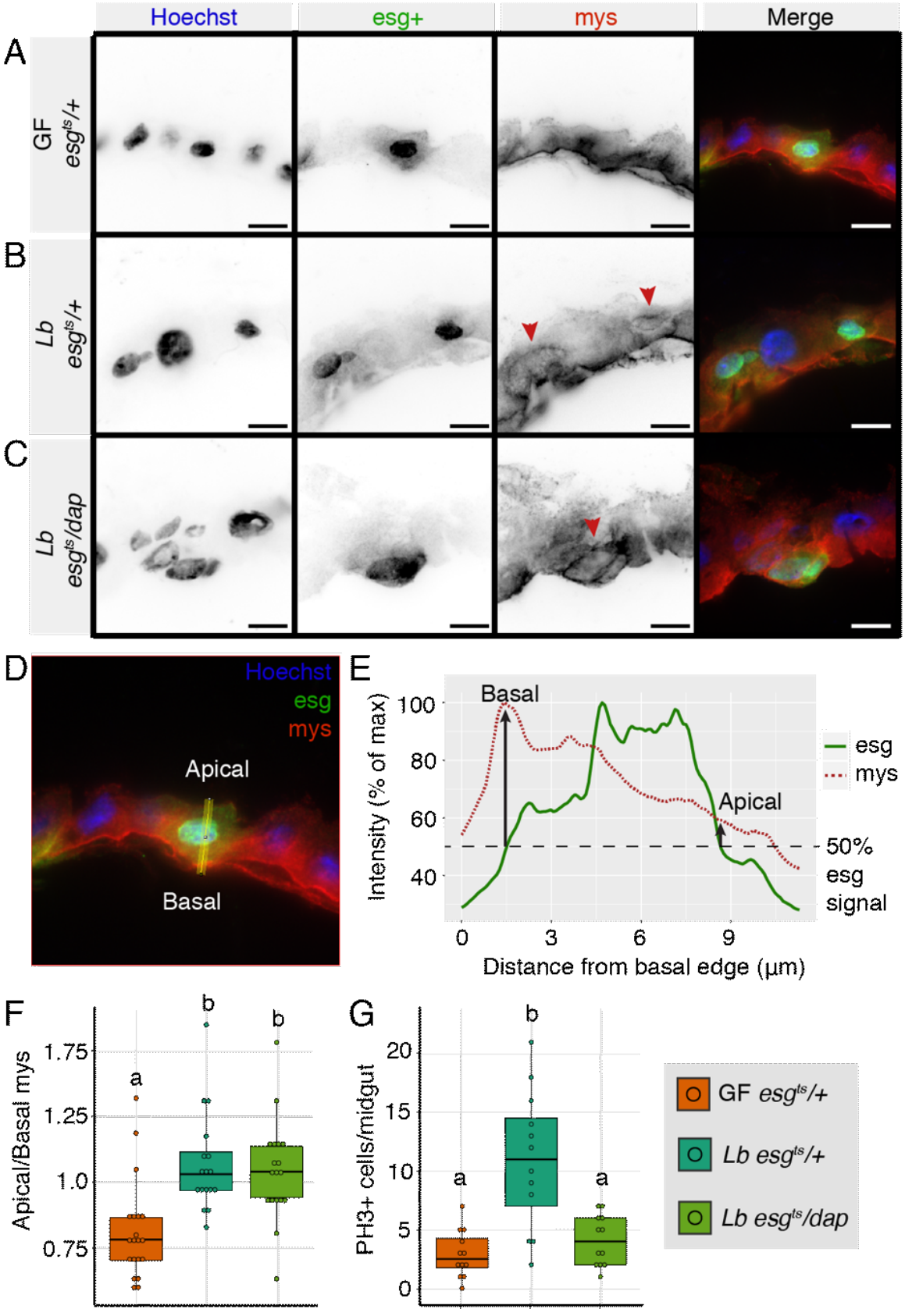
Hoechst
esg+
mys
Merge
A
GF esgts/+
B
Lb esgts/+
C
Lb esgts/dap
D
Hoechst
esg
mys
Apical
Basal
E
Basal
Apical
50% esg signal
esg
mys
Intensity (% of max)
100
80
60
40
0
3
6
9
Distance from basal edge (µm)
F
Apical/Basal mys
1.75
1.25
1.0
0.75
a
b
b
G
PH3+ cells/midgut
20
15
10
5
0
a
b
a
GF esgts/+
Lb esgts/+
Lb esgts/dap

Figure 3.9. *L. brevis* colonization disrupts integrin localization independent of division. (A-C) Immunofluorescence images of posterior midgut sagittal sections from GF (A) and *Lb* (B) mono-associated *esg^{ts}/+* and *Lb* mono-associated *esg^{ts}/dap* (C) flies after 8 days of transgene expression and bacterial colonization. Hoescht marks DNA (blue), esg marks progenitors (green) and mys marks integrins (red). Top of image is the apical/luminal side, bottom of image is the basal side of the epithelium. Red arrowheads = apical integrin mis-localization. Scale bars = 10μm **(D)** Example image of intestinal cross section where intensities of mys (red) and GFP (progenitors) were measured along the yellow line from basal to apical edges of progenitors. **(E)** Plot showing the normalized intensities of GFP (solid line) and mys (dashed line) across the yellow line in (A). The basal and apical edges of progenitors were defined as 50% of the maximum esg GFP intensity and mys intensity was determined at each of these edges. **(F)** Quantification of apical/basal progenitor cell mys intensity ratio from images captured from conditions in E-G. **(G)** Number of PH3+ cells per midgut of GF and *Lb* mono-associated *esg^{ts}/+* and *Lb* mono-associated *esg^{ts}/dap* intestines after 8 days of transgene expression/bacterial colonization. For F and G, different letters denote significant difference of $p<0.01$ with ANOVA followed by multiple pairwise Tukey tests.

3.2.6 *L. brevis* alters progenitor cell identity and promotes symmetric expansion of stem cell lineages.

Loss of intestinal integrins results in aberrant stem cell divisions with substantial effects on organization of the progenitor compartment[36]. Therefore, I asked what effects *Lb* has on midgut progenitor cells. I first stained intestines of GF flies, or flies that I mono-associated with *Lb* for the ISC marker Delta (Fig. 3.10A-B). Compared to GF intestines, *Lb* association significantly increased the proportion of Delta+ cells within the *esg+* progenitor pool (Fig. 3.10C). In support of an effect of *Lb* on ISCs I also noted that association with *Lb* increased expression of genes involved in stem cell identity, maintenance and differentiation, such as *Dl* and *Enhancer of split (E(Spl))* complex genes (Fig. 3.10D). To better understand effects of *Lb* on the progenitor compartment, I quantified marker expression in midguts of *esg^{ts},UAS-CFP,Su(H)-GFP* flies that I raised under conventional conditions, germ-free conditions, or mono-associated with *Lb* (Fig. 3.10E-G). In this line, stem cells that express the progenitor cell marker *esg* are visible as CFP single-positive cells. In contrast, progenitors that

express the enteroblast marker *Su(H)*, are visible as CFP/GFP double-positive cells. I found that CR flies had approximately equal numbers of *Su(H)*-positive and *Su(H)*-negative progenitors, suggesting a 1:1 distribution of stem cells and enteroblasts in midguts of conventional flies (Fig. 3.10H). Removal of the microbiome increased the proportion of Su(H)+ cells, whereas mono-association with *Lb* had the opposite effect (Fig. 3.10H). Specifically, I measured a significant decrease in the proportion of Su(H)+ cells within the esg+ population of *Lb*-associated flies (Fig. 3.10H). Combined with quantification of Dl+ stem cells (Fig. 3.10A-C), my data indicate that compared to CR or GF flies, *Lb* increases the proportion of stem cells relative to enteroblasts within the progenitor compartment.

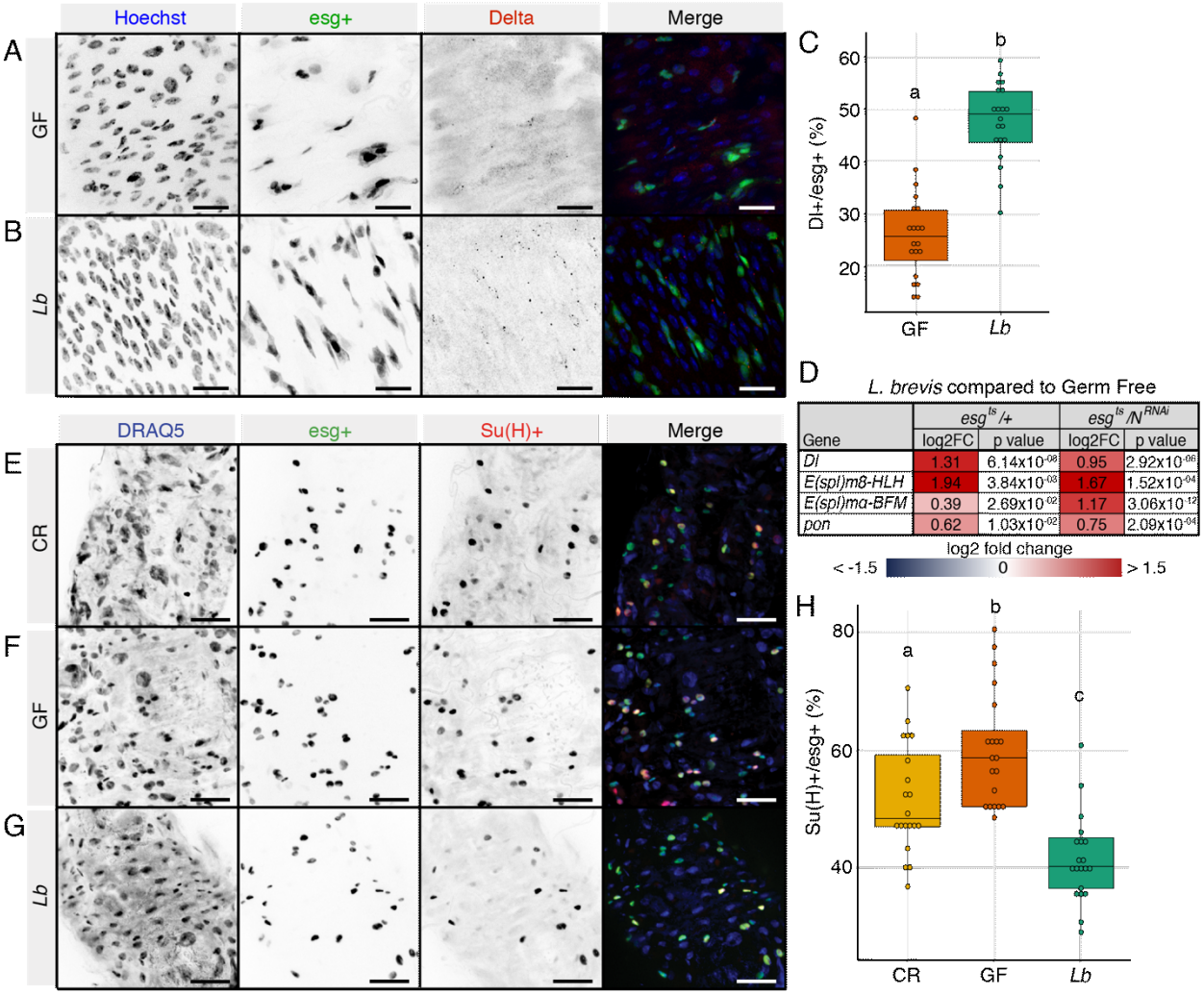

Gene	esg^{ts}/+ log2FC	esg^{ts}/+ p value	esg^{ts}/N^{RNAi} log2FC	esg^{ts}/N^{RNAi} p value
Dl	1.31	$6.14x10^{-08}$	0.95	$2.92x10^{-06}$
E(spl)m8-HLH	1.94	$3.84x10^{-03}$	1.67	$1.52x10^{-04}$
E(spl)ma-BFM	0.39	$2.69x10^{-02}$	1.17	$3.06x10^{-12}$
pon	0.62	$1.03x10^{-02}$	0.75	$2.09x10^{-04}$

Figure 3.10 *L. brevis* promotes intestinal stem cell expansion (A-B) Posterior midgut of esg^{ts}/+ GF and *Lb* mono-associated flies where Delta puncta (red) labels presumptive stem cells. Hoescht labels DNA (blue) and esg labels progenitors (green). Scale bars = 15µm **(C)** Percentage of Dl+ cells within the esg+ progenitor population in GF and *Lb* esg^{ts}/+. Different letters denote significance of p<0.01

by ANOVA followed by Tukey test. **(D)** Genes differentially expressed in *esg^{ts}/+* and *esg^{ts}/N^{RNAi}* progenitor cells upon *Lb* colonization **(E-G)** Posterior midgut of CR, GF or *Lb* mono-associated *esg^{ts},UAS-CFP,Su(H)-GFP* flies where DRAQ5 labels DNA (blue), esg labels all progenitors (green) and Su(H) labels presumptive enteroblasts (red). Scale bars = 25μm. **(H)** Proportion of Su(H)+ cells within the esg+ progenitor population from CR, GF and *Lb* mono-associated *esg^{ts},UAS-CFP,Su(H)-GFP* intestines. Different letters denote significance at $p<0.01$ by ANOVA followed by multiple pairwise Tukey tests.

I did not see elevated levels of cell death (Fig. 3.11A), or increased expression of apoptosis regulators (Fig. 3.11B) within progenitor cells of *Lb* mono-associated flies compared to CR or GF controls. Thus, I do not believe that *Lb* affects cell-type composition within the progenitor compartment by preferentially promoting enteroblast death[192], however I cannot rule out the possibility that *Lb* affects relative enteroblast numbers by increasing the rate of terminal differentiation. As an alternative, I tested the hypothesis that *Lb* increases stem cell proportions by promoting symmetric stem cell divisions. For this assay, I used twin-spot MARCM to visualize and quantify symmetric and asymmetric divisions in intestines of CR, GF, and *Lb* mono-associated flies. In this fly line, a stem cell division differentially labels daughter cells with heritable GFP and RFP markers[35,108]. In an asymmetric division, the marked enteroblast differentiates into a single marked enterocyte, while the stem cell undergoes rounds of division and differentiation that generate a multi-lineage clone of cells that bear the opposing marker (Figure 3.11C). In contrast, symmetric divisions generate sister cells of the same identity; ultimately producing neighboring clones of approximately equal size (Fig. 3.11D). To measure the effects of *Lb* on division symmetry, I induced recombination immediately after mono-association. I then allowed marked clones to develop for 8 days prior to visualization. I rarely spotted symmetric divisions that generated two enteroblasts. Instead, most symmetric clones contained large and small nuclei, regardless of the associated microbes, confirming that symmetric ISC divisions generated predominantly multi-lineage clones in each case (Fig. 3.11C). Consistent with earlier reports[35,193,194], approximately 23% of all clones were products of symmetric divisions in CR flies (Fig. 3.11E). Removal of the microbiome decreased the percentage of clones with symmetric signatures (Fig. 3.11E), indicating that gut bacteria promote symmetric stem cell divisions in conventional flies. Importantly, mono-association

with *Lb* significantly increased the frequency of multi-lineage symmetric clones compared to either GF or CR flies (Fig. 3.11E). Thus, my data indicate that association with *Lb* promotes symmetric stem cell divisions within the adult midgut.

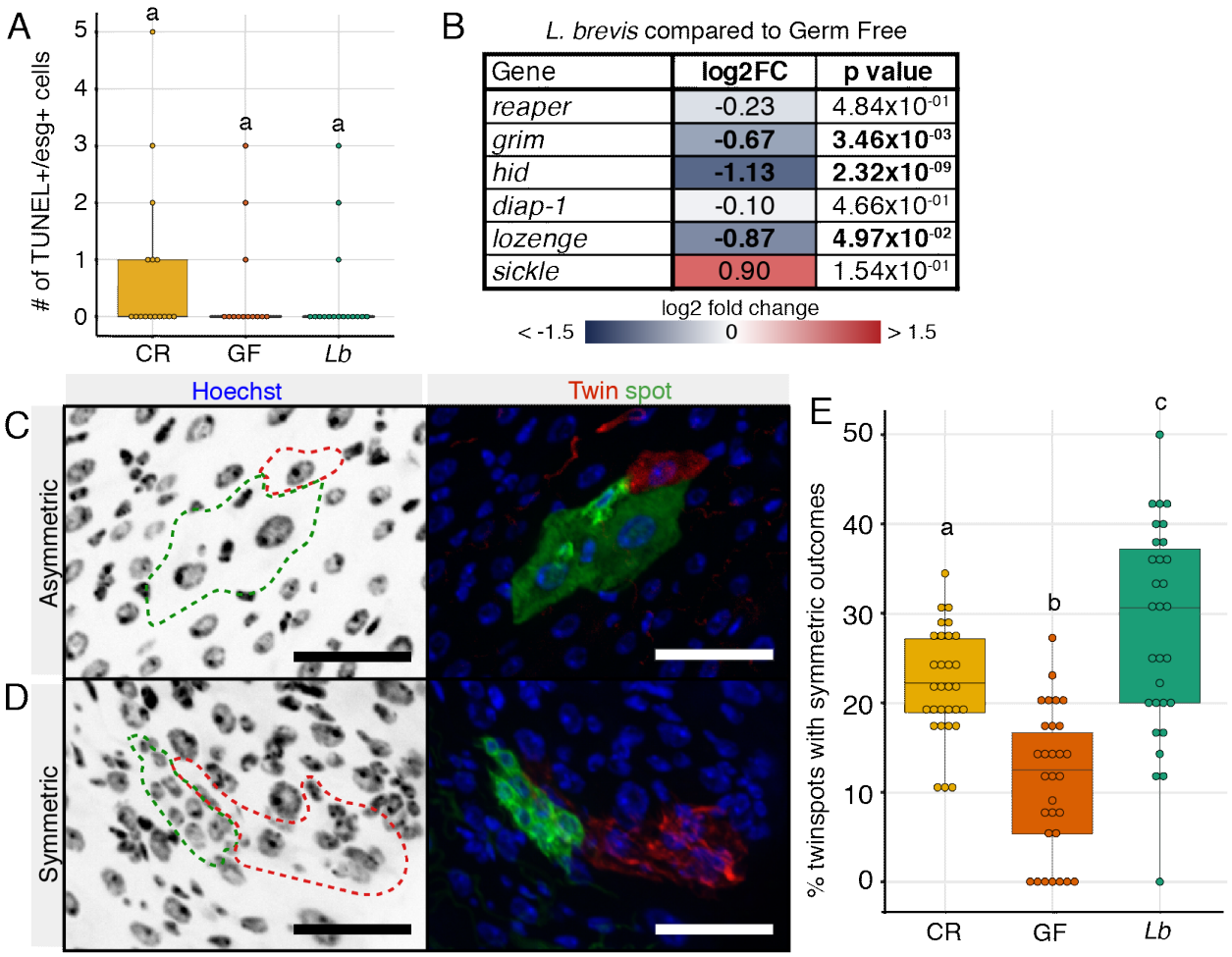

Gene	log2FC	p value
reaper	-0.23	$4.84x10^{-01}$
grim	**-0.67**	**$3.46x10^{-03}$**
hid	**-1.13**	**$2.32x10^{-09}$**
diap-1	-0.10	$4.66x10^{-01}$
lozenge	**-0.87**	**$4.97x10^{-02}$**
sickle	0.90	$1.54x10^{-01}$

Figure 3.11. *L. brevis* promotes symmetric stem cell divisions. (A) Total number of TUNEL positive progenitor cells in the posterior midgut of CR, GF and *Lb* mono-associated *esg^{ts}/+* flies. **(B)** Apoptotic gene expression from FACS isolated intestinal progenitor cells in response to *Lb* colonization. Bolded values are significant at p<0.05, FDR <5%. **(C-D**) Representative images of asymmetric (C) and symmetric (D) clones from twin-spot (*hsFLP;FRT40A,UAS-CD2-RFP,UAS-GFP-miRNA/FRT40A,UAS-CD8-GFP,UAS-CD2-miRNA;tubGAL4/+)* flies 8 days after clone induction. Hoescht labels DNA (blue) and dotted outlines show nuclei contained within twin-spot clones (red and green). Scale bars = 25μm **(E)** Percentage of twin-spot clones with symmetric signatures in the

midguts of CR, GF, or *Lb* mono-associated flies 8 days after bacterial manipulation and clone induction. Individual dots represent the proportion of clones with symmetric signatures in a single intestine. 30 midguts for each condition were analyzed and produced 463 (CR), 322 (GF) and 263 (*Lb*) total clones. Different letters denote significance at $p<0.01$ by ANOVA followed by pairwise Tukey tests.

3.2.7 The IMD pathway is required for *L. brevis* mediated intestinal proliferation

Since cell wall extract from *Lb* promotes the growth of intestinal tumors I hypothesized that immune pathways that respond to bacterial cell wall components are involved in *Lb* mediated intestinal growth. Therefore, I asked whether *Lb* acts through the IMD pathway to promote intestinal proliferation. Of the genes differentially expressed by *Lb* in progenitors I noted that IMD response genes were some of the most highly upregulated. For instance, the peptidoglycan scavengers *PGRP-SC1a* and *PGRP-SC1b* were the sixth and seventh most highly upregulated genes in wild-type progenitors, and the first and third most highly upregulated genes in Notch-deficient progenitors upon *Lb* association (Fig. 3.12A). This indicates that *Lb* induces a robust IMD response in intestinal progenitors. To determine whether the IMD pathway is required for *Lb*-induced proliferation I monitored the number of PH3+ cells in the midguts of wild-type w^{1118} and *imd-/-* flies that were either raised GF or in the presence of *Lb*. Similar to the results with $esg^{ts}/+$ and esg^{ts}/N^{RNAi} flies, *Lb* increased proliferation in wild-type w^{1118} flies compared to GF controls (Fig. 3.12B). However, this did not occur in *imd* mutants. Instead, *Lb* failed to induce proliferation in *imd-/-* and had similar levels of PH3+ cells as GF flies (Fig. 3.12B). Together, this suggests that the IMD pathway is required for *L. brevis* induced ISC divisions and highlights the importance of immune signaling in transducing bacterial signals to direct the function of ISCs.

A

Gene	$esg^{ts}/+$		esg^{ts}/N^{RNAi}	
	log2FC	p value	log2FC	p value
PGRP-SC1a	3.44	$5.24x10^{-06}$	4.34	$3.62x10^{-11}$
PGRP-SC1b	3.17	$1.35x10^{-05}$	4.02	$2.46x10^{-10}$

B

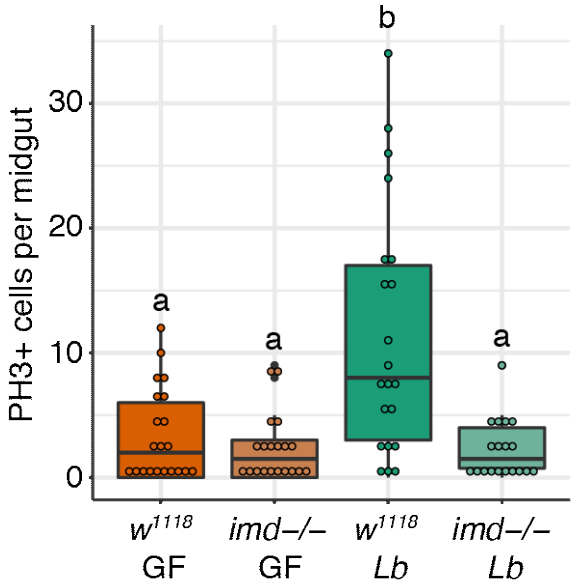

Figure 3.12. The IMD pathway is required for *L. brevis* mediated proliferation. (A) IMD response genes differentially expressed by *Lb* in FACS isolated $esg^{ts}/+$ and esg^{ts}/N^{RNAi} progenitors compared to GF controls **(B)** Number of PH3+ cells per w^{1118} or imd-/- midgut in GF or Lb mono-associated flies. Different letters denote significant difference of $p<0.01$ with ANOVA followed by multiple pairwise Tukey tests.

3.3 Conclusions

Microbial dysbiosis supports the development of inflammatory diseases and the hyperplastic expansion of cells that bear oncogenic lesions. To understand how gut bacteria cause progenitor dysplasia, I measured tumor growth and stem cell dynamics in adult *Drosophila* intestines mono-associated with common *Lactobacillus* commensals. I identified *L. brevis* as a potent stimulator of intestinal tumor growth. Interestingly, *L. plantarum* did not promote tumorigenesis even though it grew to similar levels in the intestine as *L. brevis*, suggesting that the strain of *L. plantarum* used fails to stimulate or actively inhibits ISC divisions. Comparison of bacterial levels in wild-type and tumor-prone intestines revealed that disruptions to Notch signaling promotes the accumulation of *L. brevis*, which fuels continued expansion of Notch-deficient progenitors. This suggests that Notch-deficient progenitors establish a feed forward loop with *L. brevis*, each enhancing the growth of the other (Fig. 3.13).

In an attempt to understand how *L. brevis* alters progenitor cell dynamics to promote intestinal growth, I characterized transcriptional responses to *L. brevis* in wild-type and tumor-prone progenitors. I observed significant effects on the expression and subcellular localization of integrins,

crucial regulators of stem cell niche interactions. Importantly, integrin depletion is associated with increased levels of symmetric divisions in the intestine, a mechanism for adaptive growth in the face of extrinsic challenges[35,36]. In line with the effect of integrins on division symmetry, I found that *L. brevis* enhances symmetric stem cell divisions, leading to increased numbers of stem cells (Fig. 3.13).

Interestingly, cell wall extracts from *L. brevis* are sufficient to promote tumorigenesis, suggesting a role for bacterial recognition pathways in intestinal growth. Consistent with this hypothesis, *L. brevis* failed to induce proliferation in intestines mutant for *imd*. Based on these observations, I speculate that *L. brevis* damages the intestine and activates epithelial IMD, resulting in subsequent reparative responses that promote ISC division (Fig. 3.13). In parallel with or downstream of epithelial stress, *L. brevis* decreases integrin expression in ISCs, which promotes the symmetric expansion of stem cells and increases the regenerative capacity of the intestine as a mechanism for adaptive growth (Fig. 3.13). Upon Notch knockdown, immunity is suppressed leading to *L. brevis* overgrowth and exacerbation of tumorigenesis (Fig. 3.13). Due to the evolutionary conservation of intestinal homeostatic regulators, *Drosophila* will be a fruitful model to uncover additional mechanisms of how gut-resident bacteria influence intestinal progenitor function.

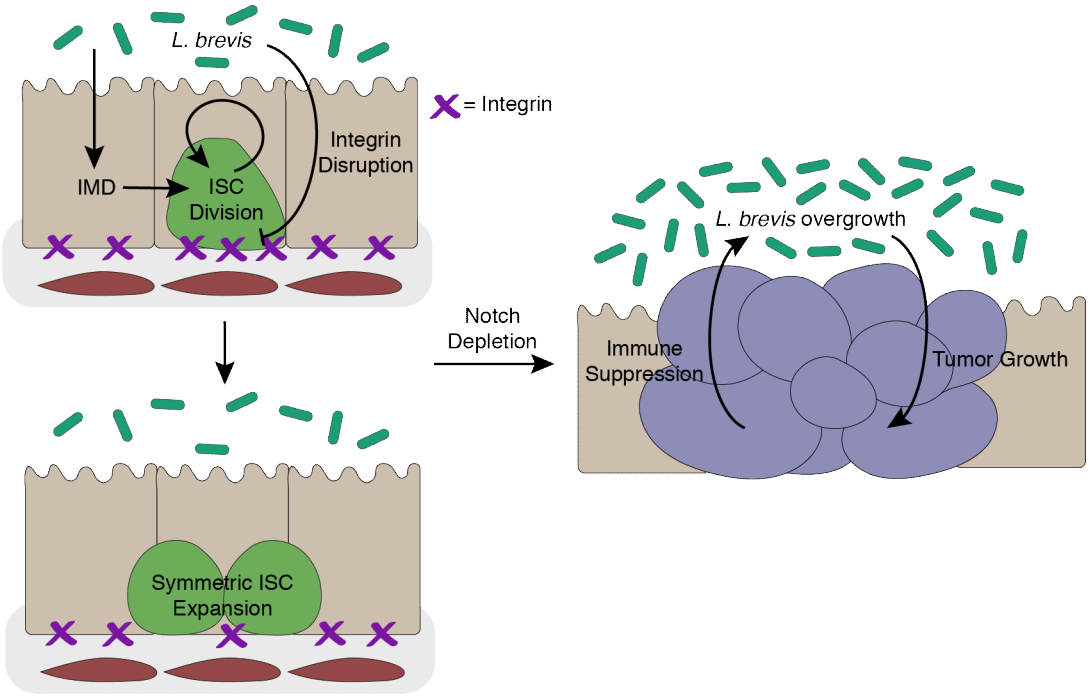

Figure 3.13. Model of *L. brevis* induced proliferation, symmetric stem cell expansion and tumorigenesis. *L. brevis* disrupts the expression and localization of integrins and induces ISC divisions in an IMD-dependent manner, resulting in symmetric ISC expansion. Upon Notch

knockdown in progenitors, tumors form, and the intestine becomes immune suppressed. This leads to *L. brevis* overgrowth and the further promotion of tumorigenesis establishing a feed forward loop between tumor growth and bacterial growth.

Chapter 4

The IMD pathway acts in progenitors to promote intestinal proliferation, differentiation and tumorigenesis

Data in this chapter have been published in:

- Petkau, K., **Ferguson, M**., Guntermann, S., & Foley, E. (2017). Constitutive Immune Activity Promotes Tumorigenesis in *Drosophila* Intestinal Progenitor Cells. *Cell Reports* 20: 1784-1793.
- Shin, M., **Ferguson, M.,** Willms, R. J., Jones, L. O., Petkau, K., & Foley, E. (2022). Immune regulation of intestinal stem cell function in *Drosophila*. *Stem Cell Reports*. 17(4):741-755.

4.1 Summary

Intestinal innate immune pathways control microbial populations in the lumen and defend the host against bacterial insults. However, excessive immune activation contributes to intestinal disease. For instance, chronic inflammation in the intestine contributes to the development of colorectal cancer[195]. Recent studies in mice showed that innate immune pathways act in the intestinal epithelium to modify homeostatic and tumorigenic proliferation of intestinal stem cells[113,114,157,158]. However, it is still unknown if immune pathways function within intestinal stem cells to influence growth. Given the important role ISCs play in intestinal maintenance, homeostasis and tumorigenesis, it is imperative we understand whether immune pathways act directly within intestinal progenitors to modulate their function.

Here, we examined the influence of the IMD pathway in intestinal progenitors of the *Drosophila* intestine. Hyperactivation of IMD in progenitors perturbed the expression of Notch pathway genes, induced enteroendocrine cell specification and promoted intestinal hyperplasia. In addition, chronic IMD activation exacerbated the growth of Notch-deficient tumors, even in the absence of a microbiome, indicating that excessive immune activity in progenitors is sufficient for tumorigenesis. To determine the role of basal IMD activity in progenitors we inhibited IMD and found decreased proliferation and altered expression of critical regulators of ISC division. Blockage of IMD in progenitors also altered expression trajectories of cell maturation genes and perturbed the ability of the intestine to form functional enteroendocrine cells. These data demonstrate the importance of balanced immune signals within progenitors in the context of homeostasis and tumorigenesis.

4.2 Results

4.2.1 IMD pathway components are enriched in intestinal progenitors

IMD is the main antibacterial immune pathway in the *Drosophila* intestine although the effects of IMD are primarily studied within the context of mature epithelial cells such as enterocytes[5,6,110]. However, multiple studies suggest that IMD pathway components are also expressed in progenitor cells[25,88]. To directly compare expression levels of IMD pathway components between different intestinal cell types we performed a single-cell RNA sequencing project of wild-type 10 day old midguts (Fig. 4.1A). We detected all major intestinal cell types based on the expression of known marker genes[25,88]. For example, progenitors had enriched expression

of the marker gene *escargot* (*esg*), regionally defined enterocytes were identified by the expression of various proteases, and enteroendocrine cells highly expressed peptide hormones (Fig. 4.1B). In addition to the enrichment in growth and differentiation factors (Fig. 4.1C), progenitors were also characterized by enrichment in immune factors. Specifically, progenitors expressed high levels of IMD pathway genes such as the peptidoglycan receptor *pgrp-lc*, the NF-κB family transcription factor *relish*, and the IMD pathway target gene *pirk* (Fig. 4.1D). For instance, upwards of 66% of progenitors expressed the NF-κB family transcription factor *relish*, whereas only 23% of non-progenitors expressed *relish* (Fig. 4.1E). Since progenitors have enriched expression of immune genes these data raise the possibility that the IMD pathway plays a fundamental role in progenitor function.

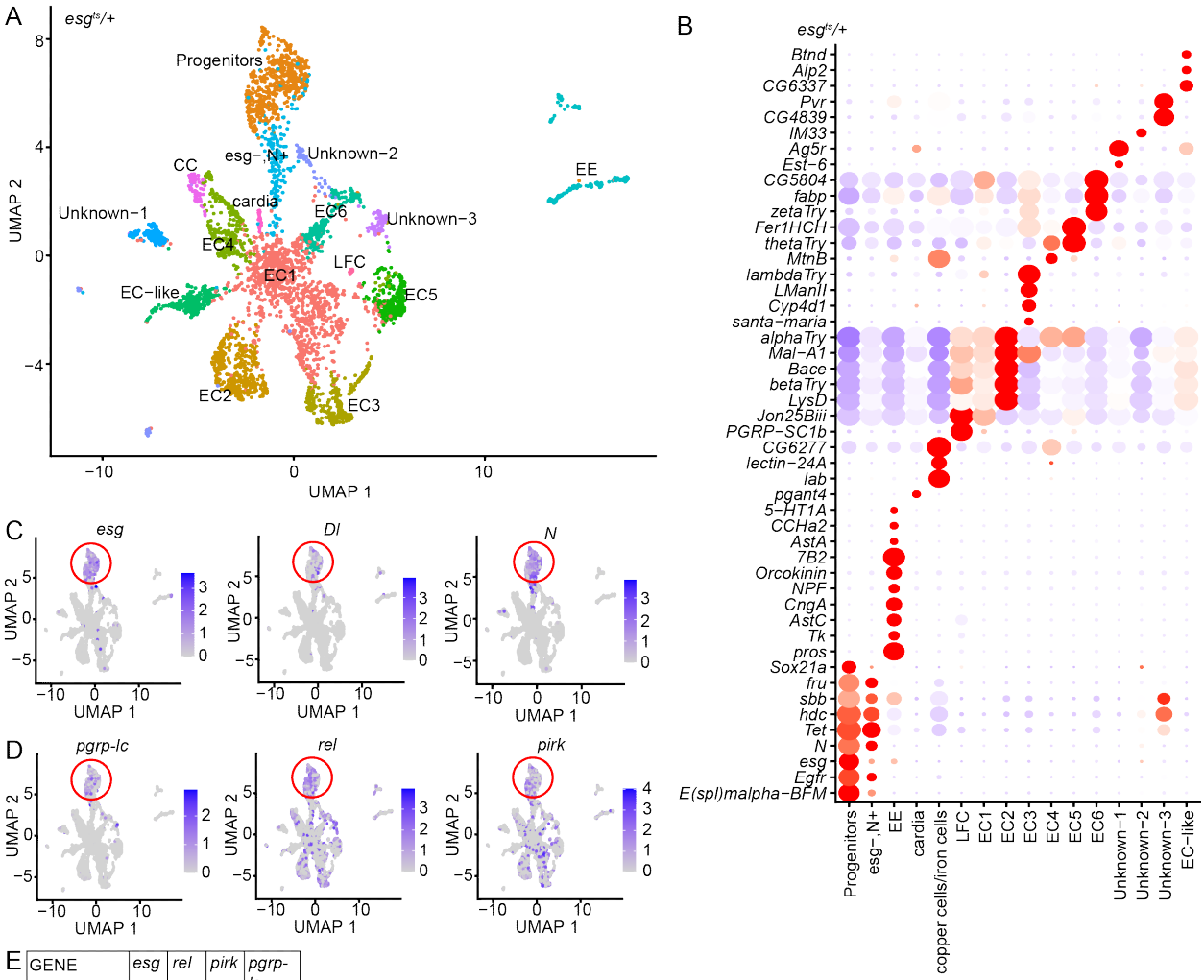

E

GENE	*esg*	*rel*	*pirk*	*pgrp-lc*
% positive in progenitors	68.5	66.1	54.2	49.8
% positive in non-progenitors	3.1	23	18.1	3.8

Figure 4.1 IMD pathway components are enriched in intestinal progenitors. (A) UMAP plot of single cell transcriptomic data from wild-type *esg^{ts}/+* intestines. **(B)** Dotplot of marker genes for each cell cluster from the data in A. Size of the dot represents the proportion of cells within that cluster that express the gene. Colors represent whether that gene is expressed higher (red) or lower (blue) than the average intestinal expression. **(C)** UMAP showing expression of progenitor marker genes. **(D)** UMAP showing expression of IMD pathway genes. Red circles highlight progenitor cells. **(E)** Proportion of progenitors and non-progenitors that express IMD pathway genes. These experiments and analyses were performed by Minjeong Shin.

4.2.2 Constitutive IMD activation induces downstream antimicrobial response

To investigate the impact of IMD activation in progenitors we generated a transgenic fly line that allows for cell-type restricted hyperactivation of IMD. We designed a truncated form of the Imd protein, ImdCA, that uses a start codon at residue 78. This generates an Imd protein that lacks the inhibitory N-terminal amino acids but still contains sequences to interact with FADD. To validate this line, we expressed it in the main humoral immune site of the fly, the fat body (*cgGAL4 ; GAL80^{ts}/UASimdCA (cg^{ts} > CA*)). With this *cg^{ts}* line, transgenes are expressed under the control of a fat body specific driver in a temperature sensitive manner. Here, expression of ImdCA in the fat body by raising flies at 29°C induced expression of the AMPs *dpt* and *att* in the absence of an infection (Fig. 4.2A). Importantly, ImdCA activated AMP expression through the classical IMD pathway, since mutation of *dredd*, the caspase required for downstream Relish activation, blocked ImdCA dependent AMP production (Fig. 3.2A).

Next, we asked if IMD activation could be detected in intestinal progenitor cells. We expressed ImdCA exclusively in intestinal progenitor cells (*esg^{ts}>CA*) and found that intestinal AMP (*dpt* and *att*) expression increased (Fig. 4.2B). These data suggest that ImdCA is sufficient to activate the IMD pathway in intestinal progenitors. Since AMPs are increased with ImdCA expression we asked whether the microbiome composition was affected. To directly compare the two genotypes we generated germ-free *esg^{ts}* and *esg^{ts}>CA* flies and exposed them to a homogenate containing the microbiome of a wild-type fly. We allowed this microbial consortium to associate with the flies over the course of 7 days then shifted flies to 29°C for another 7 days to activate IMD in progenitors (Fig. 4.2C). Intestines dissected from the respective cohorts were processed for 16S deep-

sequencing to identify microbial populations. Although AMP production was increased, there was no effect of IMD activation on microbiome composition (Fig. 3.2C). In each case, intestines were dominated by *Lactobacilli* and *Acetobacter* operational taxonomic units (OTUs). Although IMD activation had little effect on microbiome, activation of IMD in progenitors prolonged the lifespan of flies challenged with lethal doses of the oral pathogen *Vibrio cholerae* (Fig. 4.2D). These data demonstrate that acute IMD activation in progenitors aids the intestine in preventing pathogenic insults but has little impact on the native bacterial composition.

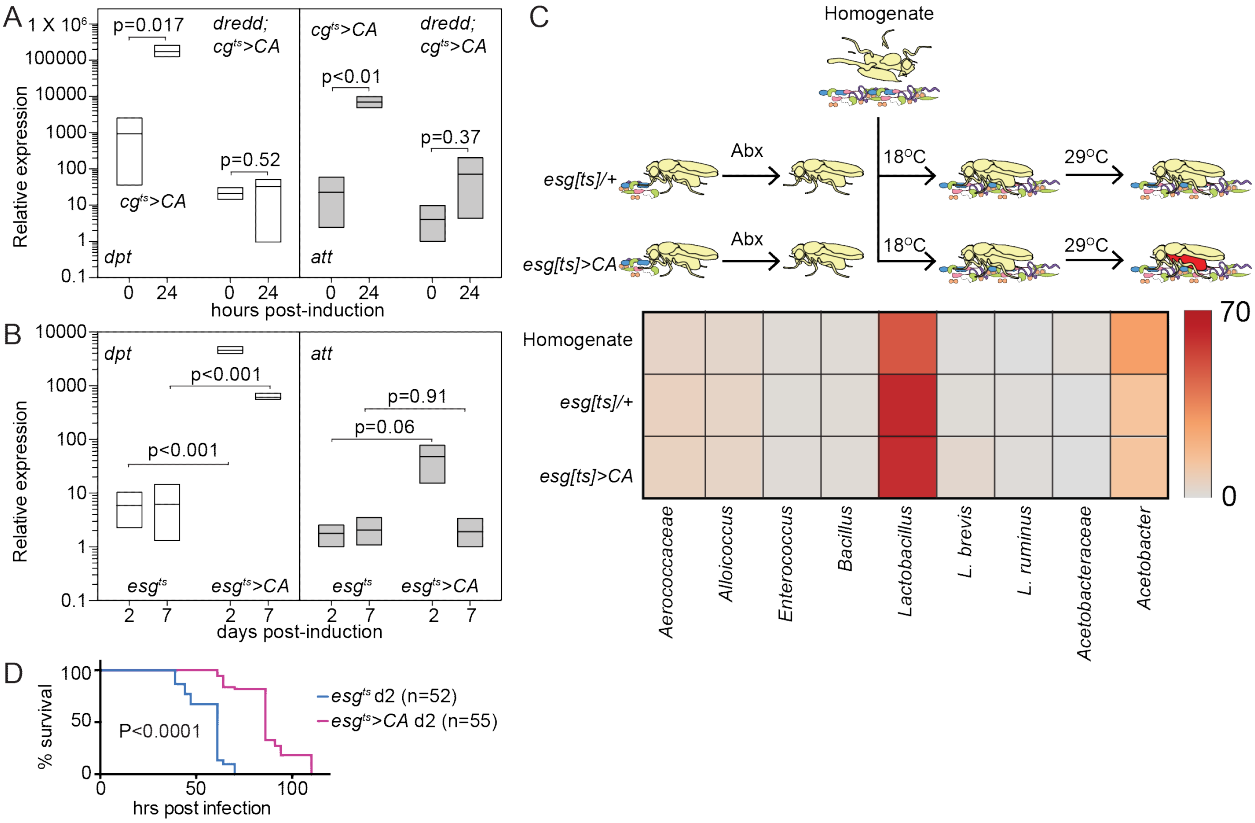

Figure 4.2. Constitutive IMD activation induces downstream antimicrobial response. (A) Expression of the antimicrobial peptides *diptericin (dpt)* and *attacin (att)* after constitutive activation of IMD in the *Drosophila* fat body (cg^{ts}>*CA*) with or without co-expression of *dredd* (*dredd*;cg^{ts}>*CA*). **(B)** Expression of *dpt* and *att* in wild-type (esg^{ts}) intestines or those with active IMD in progenitors (esg^{ts}>*CA*). For A and B significance was found using Students t tests. **(C)** 16S deep sequencing of the microbiome from esg^{ts} and esg^{ts}>*CA* fly intestines. **(D)** Survival of esg^{ts} and esg^{ts}>*CA* flies infected orally with the pathogen *Vibrio cholerae*. These experiments were performed by Kristina Petkau.

4.2.3 Progenitor-specific IMD activation alters expression of growth and differentiation genes.

To characterize the effects of progenitor-specific IMD activation on intestinal physiology we performed a microarray analysis and compared transcriptomic profiles of wild-type *esg^{ts}* and immune active *esg^{ts}>CA* intestines, where IMD was activated for 2 days. In addition, we included intestines from conventionally reared and germ-free animals to compare the effect of IMD activation and the presence of a microbiome. The microbiome downregulated approximately twice as many genes as were upregulated in wild-type *esg^{ts}* flies, however in *esg^{ts}>CA* flies, the microbiome upregulated more genes than were downregulated (Fig. 4.3A). In addition, a smaller proportion of genes were commonly regulated by the presence of the microbiome in both *esg^{ts}* and *esg^{ts}>CA* (Fig. 4.3A). Similarly, IMD activation upregulated many more genes in CR flies than in GF flies however showed similar numbers of genes downregulated in both microbial contexts (Fig. 4.3B). These data suggest that the impacts of the microbiome are altered by the activation of IMD in progenitors and, vice versa, IMD controls different sets of genes dependent on the presence of a microbiome. However, similar biological processes were affected by both the microbiome and IMD activation. For instance, the microbiome and IMD activation altered genes involved in immune response, metabolism, transport and stress response (Fig. 4.3C-D). In addition to these shared effects, IMD activation altered expression of genes involved in stem cell identity and development in CR flies (Fig. 4.3D). This suggests that microbes and the IMD pathway are important regulators of intestinal progenitor cell function.

In addition to these broad effects we noted impacts of progenitor-specific IMD activation on the expression of genes involved in evolutionarily conserved growth, stress and differentiation pathways. These include insulin, Ras, JAK/STAT, Wnt, JNK and Notch signaling pathways, essential regulators of ISC function (Fig. 4.3E). These data match previous reports where the microbiome and Relish alter the expression of growth and stress pathway genes in the intestine[6]. Together this suggests that IMD activation in intestinal progenitors has a profound effect on intestinal physiology including the proliferation and differentiation of ISCs.

A

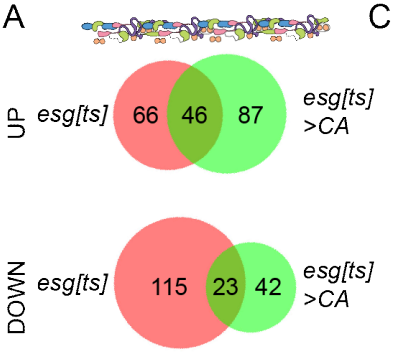

B

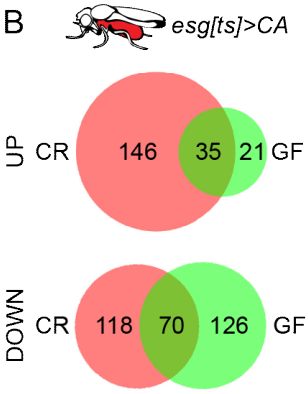

C

Microbiome response.	*esg[ts]*	*esg[ts] >CA*
IMMUNE RESPONSE	15	11
SIGNAL TRANSDUCTION	15	11
METABOLISM	58	40
TRANSPORT	23	11
OXIDATION-REDUCTION	11	11
ION HOMEOSTASIS		4
STRESS RESPONSE	16	5
OTHER	26	19
CHITIN BINDING	8	
STEROL INTERACTING		5

D

esg[ts]>CA response.	CR	GF
IMMUNE RESPONSE	16	11
SIGNAL TRANSDUCTION	38	12
STEM CELL IDENTITY	4	
DEVELOPMENT	9	
METABOLISM	63	31
TRANSPORT	21	19
OXIDATION-REDUCTION	17	11
ION HOMEOSTASIS	5	5
STRESS RESPONSE	26	10
OTHER	19	20
CHITIN BINDING		8
STEROL INTERACTING		6

E

Gene	Function	Fold Change (*esgCA* V *esg*)	ANOVA p-value
MESK2	Ras signaling	-2.15	0.000349
gfzg	Ras signaling	-1.84	0.000116
cdi	Ras signaling	1.59	0.001404
Plzf	Ras signaling	-1.66	0.025787
CG42684	Ras signaling	2	0.000475
dock	Insulin signaling	-1.56	0.016287
srl	Insulin signaling	1.59	0.012109
sug	Insulin signaling	-1.68	0.025726
egr	JNK signaling	1.68	0.001723
Traf4	JNK signaling	1.64	0.000984
nmo	Wnt signaling	-1.98	0.000068
ebd1	Wnt signaling	1.53	0.008942
sfl	Wnt signaling	1.96	0.002488
Prosap	Wnt signaling	-1.53	0.002859
SOCS36E	JAK/STAT	-1.84	0.038907
mahe	Notch signaling	1.54	0.000941
neur	Notch signaling	-1.55	0.001857
Nle	Notch signaling	1.63	0.010107
Rala	Notch signaling	2.07	0.000403

Figure 4.3. Progenitor-specific IMD activation alters expression of intestinal growth and differentiation genes. (A) Number of genes differentially expressed in response to the microbiome in *esg^{ts}* and *esg^{ts}>CA* flies. **(B)** Number of genes differentially expressed in response to progenitor specific IMD activation in conventionally reared (CR) and germ free (GF) flies. **(C)** Biological processes significantly regulated by the microbiome. **(D)** Biological processes significantly regulated by progenitor-specific IMD activation. **(E)** Specific genes significantly altered in *esg^{ts}>CA* flies compared to *esg^{ts}* after 2 days of IMD activation. These analyses were performed by Kristina Petkau.

4.2.4 Activation of IMD in progenitors causes intestinal hyperplasia

Given the effect of progenitor-specific IMD activation on growth and stress pathways in the intestine we determined how IMD activation alters intestinal morphology and proliferation. To address this question, we analyzed the posterior midguts of *esg^{ts}* and *esg^{ts}>CA* flies as they aged. After 2 days of IMD activation in progenitors, *esg^{ts}>CA* intestines are indistinguishable from wild-type intestines (Fig. 4.4A). In both cases, Armadillo (β-catenin ortholog) was localized to cell borders with a regular arrangement around large enterocytes that were interspersed with small prospero-positive enteroendocrine cells (Fig. 4.4A). Both genotypes contained regularly spaced nuclei and evenly distributed progenitor cells.

By 26 days, wild-type intestines show hallmarks of age-dependent dysplasia, including disrupted intestinal cell borders, crowded and uneven spacing of nuclei and irregular clusters of progenitors (Fig. 4.4A). Midgut architecture was further disrupted at this timepoint with progenitor-specific IMD activation. With active IMD there is a near breakdown of epithelial cell borders and organization, densely crowded nuclei and increased numbers of GFP+ progenitors (Fig. 4.4A). Given the increased level of hyperplasia in *esg^{ts}>CA* flies we asked whether intestinal proliferation is altered under this scenario. To measure intestinal proliferation, we counted the number of phospho-histone 3 positive (PH3+) cells per midgut of *esg^{ts}* and *esg^{ts}>CA* flies after 14 and 24 days of IMD activation. Progenitor-specific IMD activation increased the number of mitotic cells compared to wild-type at both timepoints (Fig. 4.4B). Together these data indicate that chronic activation of IMD in progenitors is sufficient to promote hyperplastic growth of the intestine. Importantly the hyperplastic phenotype noted in *esg^{ts}>CA* flies is not due to accelerated ageing of the fly since the lifespan is indistinguishable between *esg^{ts}* and *esg^{ts}>CA* (Fig. 4.4C).

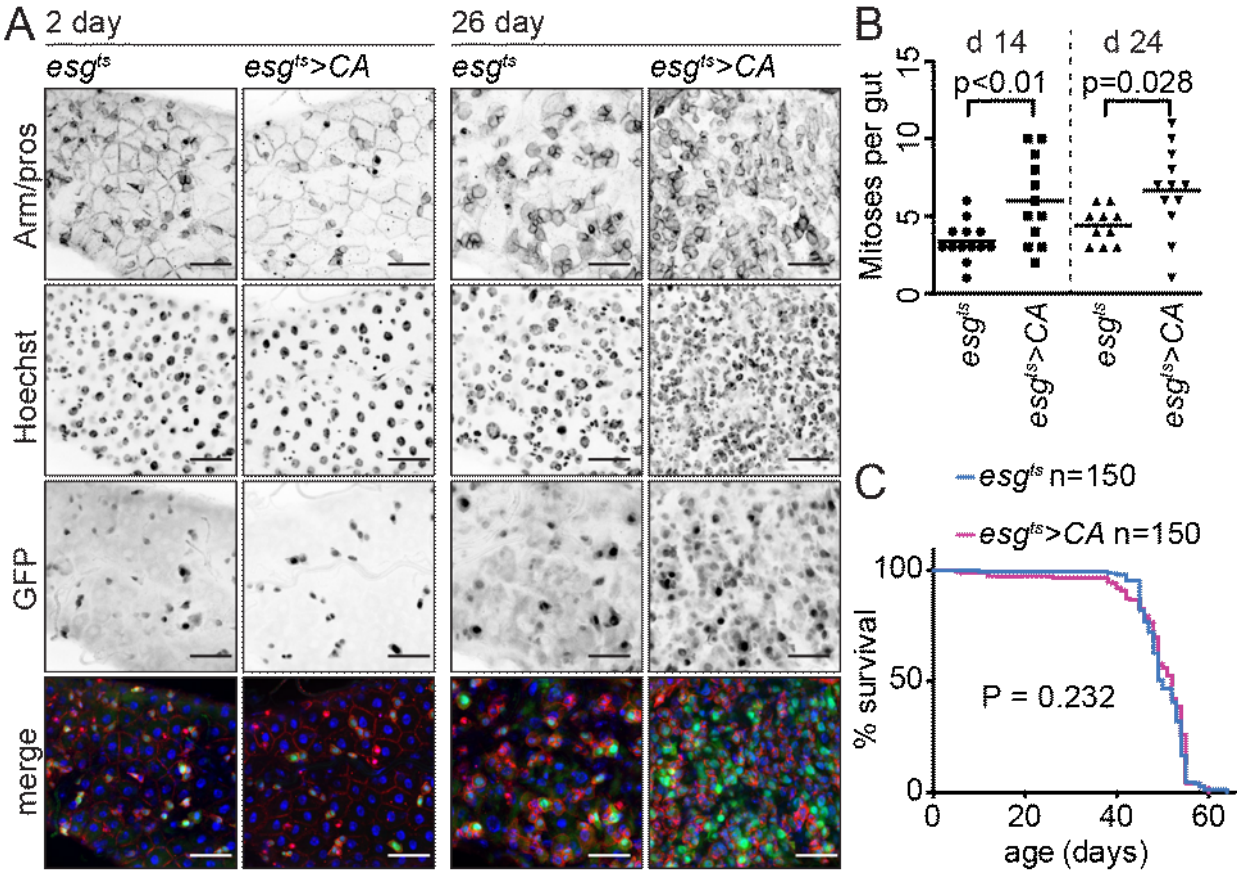

Figure 4.4 Activation of IMD in progenitors causes intestinal hyperplasia. (A) Images of *esg*^{ts} and *esg*^{ts}*>CA* posterior midguts after 2 or 24 days of IMD activation. Armadillo (Arm) labels cell borders (red), prospero (pros) labels enteroendocrine cells (red), Hoescht labels DNA (blue) and GFP labels esg+ progenitors (green). Scale bars 25μm. **(B)** Number of PH3+ mitotic cells per midgut of *esg*^{ts} and *esg*^{ts}*>CA* after 14 or 24 days of IMD activation. Significance found using Students t test. **(C)** Lifespan of *esg*^{ts} and *esg*^{ts}*>CA* flies. Significance determined using Wilcoxen test. These experiments were performed by Kristina Petkau.

4.2.5 IMD activation in progenitors promotes enteroendocrine differentiation

Our microarray results indicate IMD activation in progenitors alters the expression of multiple Notch pathway genes. These observations reflect similar results where IMD pathway mutants have altered Notch activity in the intestine[6]. Since Notch plays an important role in the enterocyte specification of the intestine we determined whether IMD acts in progenitors to control intestinal differentiation. To test whether IMD activation alters differentiation we used MARCM clones. This

technique labels the progeny from individual stem cell divisions to assess subsequent differentiation events. As expected, clones from wild-type flies contained a mixture of small cells, likely progenitors and enteroendocrine cells, as well as large polyploid enterocytes (Fig. 4.5A). In contrast, large polyploid cells were largely absent from ImdCA clones (Fig. 4.5A-B). Instead, ImdCA clones were dominated by small cell aggregates, indicative of dysfunctional enterocyte development.

To determine if progenitor-specific IMD activation alters enteroendocrine differentiation we measured the percentage of enteroendocrine cells after 24 days of ImdCA expression (Fig. 4.5C). In agreement with the effect on intestinal hyperplasia, IMD activation increased the number of nuclei per area of the intestine compared to aged matched wild-type flies (Fig. 4.5D). We also found a significantly greater proportion of nuclei positive for the enteroendocrine cell marker prospero in *esg^{ts}>CA* intestines compared to *esg^{ts}* (Fig. 4.5E). These data show that persistent activation of IMD in progenitors alters the developmental trajectory of progenitor cells and promotes the differentiation of excess enteroendocrine cells.

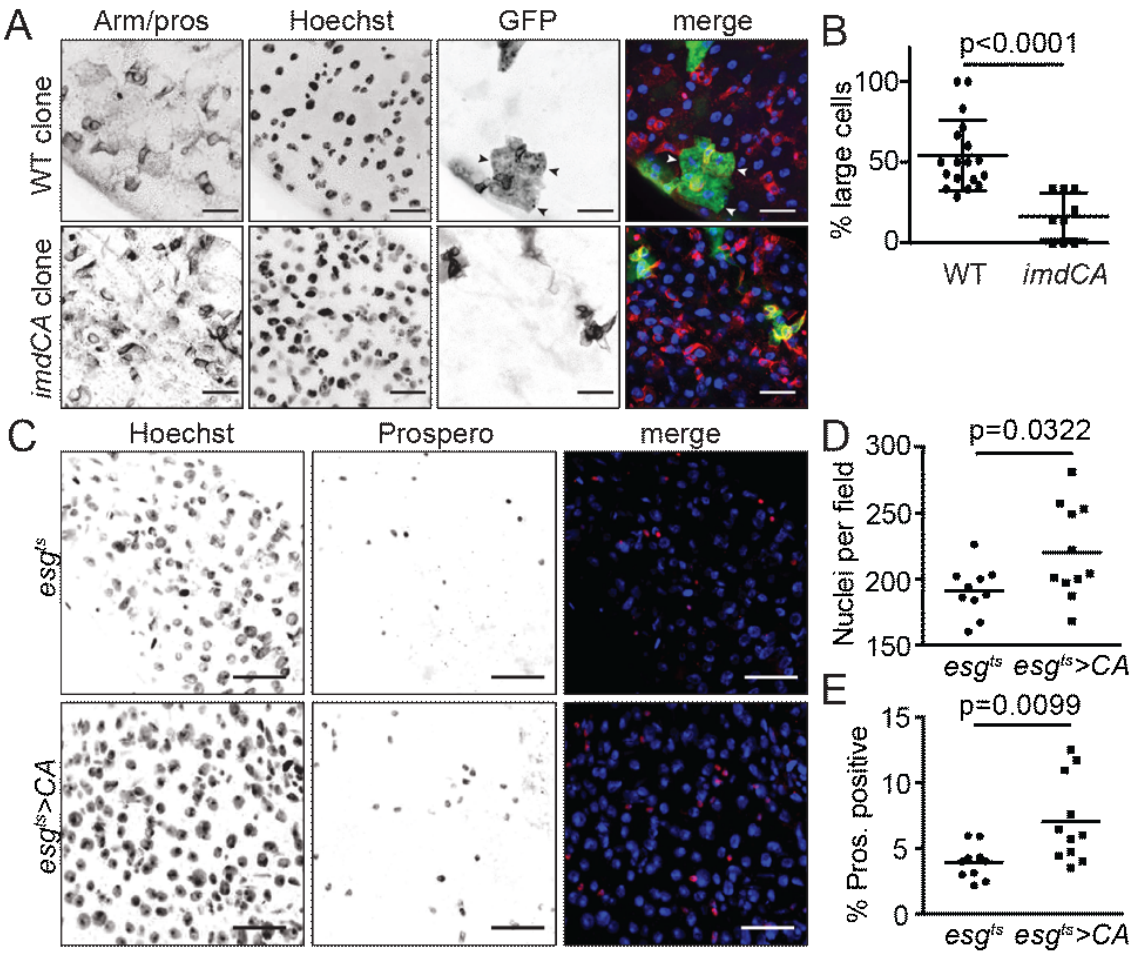

Figure 4.5 IMD activation in progenitors promotes enteroendocrine differentiation. (A) Images of wild-type clones and those with active IMD. Arm/pros labels cell borders and enteroendocrine cells (red), Hoescht labels DNA (blue) and GFP marks the clone (green). Scale bars 15μm. **(B)** Proportion of large cells within wild-type or imdCA clones. **(C)** Images of esg^{ts} and esg^{ts}>*CA* posterior midguts after 20 days of IMD activation. Scale bars 25μm. **(D)** Number of nuclei per field in esg^{ts} and esg^{ts}>*CA* posterior midguts. **(E)** Percent of nuclei that are prospero positive in esg^{ts} and esg^{ts}>*CA* posterior midguts. Significance of B, D and E found using Students t test. These experiments were performed by Kristina Petkau.

4.2.6 Progenitor-specific IMD activation promotes Notch-deficient tumorigenesis

Bacterial insults in flies and mice increase the growth of intestinal tumors. For instance, challenge with pathogenic microbes increases the growth of Notch-deficient tumors in the *Drosophila* intestine[76,156]. Given the impact of ImdCA on Notch pathway targets I determined whether immune activation in progenitors alters tumorigenesis. To answer this question, I knocked down Notch in intestinal progenitors (esg^{ts}/N^{RNAi}) and determined the effect of the microbiome and IMD activation on tumor incidence. As expected, after 8 days of Notch depletion from progenitors, tumors formed that were populated by GFP+ progenitors and pros+ enteroendocrine cells (Fig. 4.6A). Removal of the microbiome reduced tumor severity and decreased the incidence of tumors in esg^{ts}/N^{RNAi} intestines (Fig. 4.6B). These data suggest that immune pathways that respond to microbes promote the expansion of Notch-deficient tumors.

To directly test whether progenitor-specific IMD activation influences tumorigenesis I expressed ImdCA in progenitors alongside Notch depletion ($esg^{ts}>N^{RNAi}$;*CA*) and assessed tumor growth. Compared to N^{RNAi} alone, co-expression of *ImdCA* and N^{RNAi} in progenitors exacerbated tumorigenesis. IMD activation resulted in large disorganized patches of progenitors and enteroendocrine cells (Fig. 4.6C), whereas with Notch depletion alone, tumors are smaller with more distinct boundaries. To determine whether IMD activation is sufficient for tumorigenesis I examined intestines from germ-free $esg^{ts}>N^{RNAi}$;*CA* flies. Similar to the conventionally reared, IMD activation caused germ-free intestines to produce large disorganized tumors populated by progenitors and enteroendocrine cells (Fig. 4.6D). To quantify the effects of IMD activation and the microbiome on Notch-deficient tumorigenesis I determined intestinal tumor incidence. I devised a grading system

to classify intestines with no visible tumors as grade 1, intestines with only progenitor populated tumors as grade 2, and those with progenitor and enteroendocrine cell tumors as grade 3. With this classification system I found that approximately 60% of conventionally reared $esg^{ts}>N^{RNAi}$ intestines contained grade 3 tumors while removal of the microbiome decreased incidence of grade 3 tumors to 10% (Fig. 4.6E). Co-expression of *ImdCA* increased tumor incidence, where now over 75% of intestines contained grade 3 tumors independent of whether the flies were made germ-free (Fig. 4.6E). These data indicate that activation of IMD in progenitors is sufficient to promote tumorigenesis, even in the absence of a microbiome.

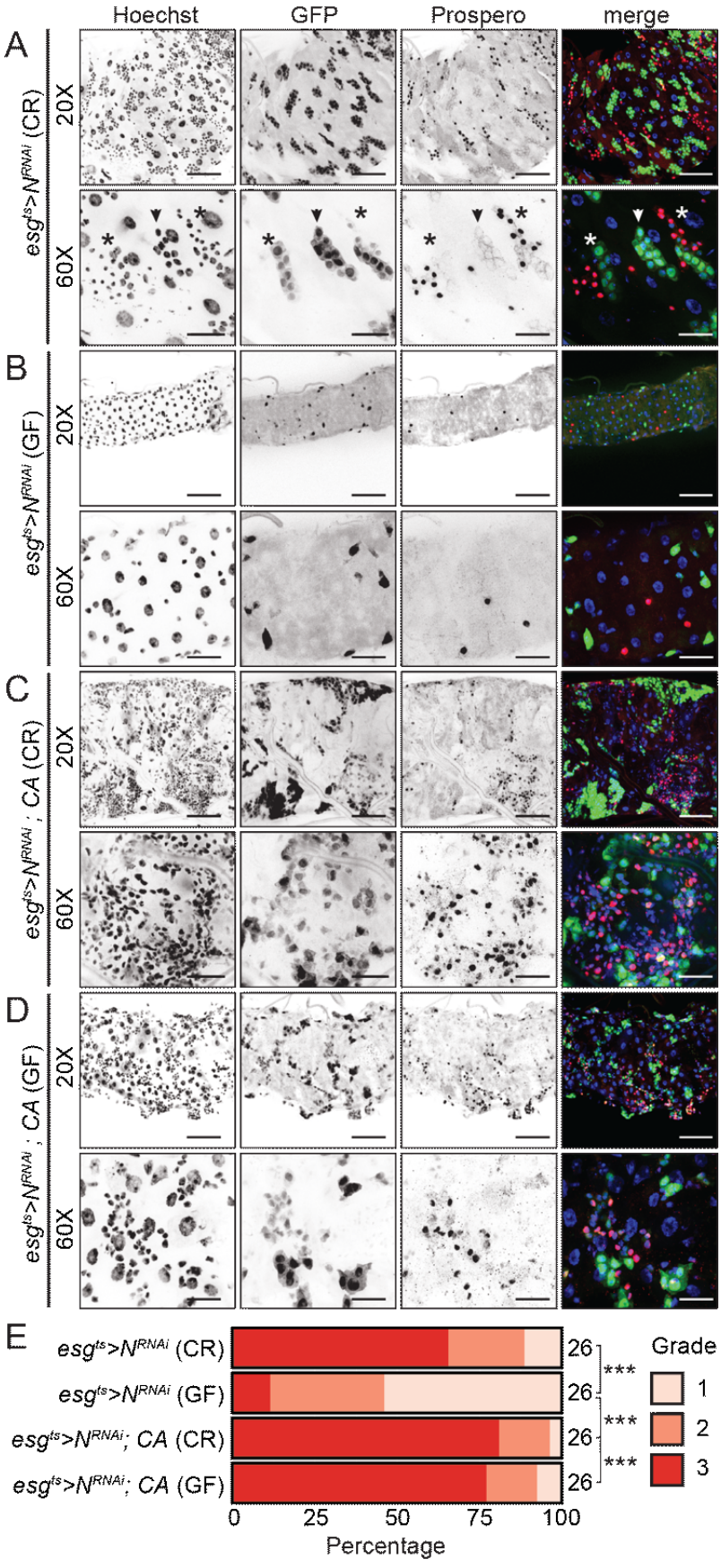
Hoechst
GFP
Prospero
merge
A
esg^ts>N^RNAi (CR)
20X
60X
B
esg^ts>N^RNAi (GF)
20X
60X
C
esg^ts>N^RNAi ; CA (CR)
20X
60X
D
esg^ts>N^RNAi ; CA (GF)
20X
60X
E
esg^ts>N^RNAi (CR)
esg^ts>N^RNAi (GF)
esg^ts>N^RNAi; CA (CR)
esg^ts>N^RNAi; CA (GF)
26
26
26
26
***
***
***
Grade
1
2
3
0
25
50
75
100
Percentage

Figure 4.6 Progenitor-specific IMD activation promotes Notch-deficient tumorigenesis. (A-B) Images of *esg^{ts}>N^{RNAi}* intestines after 8 days of Notch knockdown in CR (A) or GF (B) flies. Asterisks highlight a grade 3 tumor containing prospero-positive enteroendocrine cells and GFP-positive progenitors. Arrowhead points to a level 2 tumor only populated by progenitors. **(C-D)** Images of *esg^{ts}>N^{RNAi};CA* intestines after 8 days of Notch knockdown and IMD activation in CR (C) or GF (D) flies. Scale bars for A-D 50μm for 20X images and 15μm for 60X images. **(E)** Tumor incidence in *esg^{ts}>N^{RNAi}* and *esg^{ts}>N^{RNAi};CA* intestines from CR and GF flies. Grade 1 = no visible tumors, grade 2= tumors populated by progenitors grade 3 = tumors populated by progenitors and enteroendocrine cells. Significance found using chi squared test. *** = $p < 0.001$.

4.2.7 IMD acts in stem cells to promote intestinal proliferation

Activation of IMD in progenitors results in intestinal hyperplasia and exacerbation of tumorigenesis. However, as this is a constitutive activation of the pathway, homeostatic roles for IMD activity in progenitors are difficult to elucidate. Therefore, we used a transgenic fly line to inactivate the IMD pathway. Activation of the Imd protein requires proteolytic cleavage and removal of the N-terminal 30 amino acids by the caspase Dredd[196]. Mutation at residue 30 from an aspartic acid to an alanine results in a non-cleavable form of Imd (ImdD30A), acts as a dominant negative and prevents downstream signal transduction[196]. To determine the role of the IMD pathway in progenitors we expressed ImdD30A in progenitors using the *esg^{ts}* driver and assessed proliferation and progenitor dynamics in the posterior midgut. Young wild-type intestines (*esg^{ts}/+)* have very few PH3+ cells, and as flies age proliferation increases (Fig. 4.7A). Expression of ImdD30A in progenitors (*esg^{ts}/D30A*) for 5 days showed no difference in the amount of mitoses compared to age matched controls, however, proliferation did not increase as a result of age (Fig. 4.7A). Here, IMD inactivation resulted in significantly fewer mitotic events compared to aged wild-type flies. Similarly, knockdown of either IMD receptor, the cell surface PGRP-LC or intracellular PGRP-LE PGN sensor, resulted in fewer mitotic cells in aged flies (Fig. 4.7B-C).

To determine whether IMD in progenitors impacts growth via Relish dependent signaling I knocked down the IKKγ ortholog *kenny* or the NF-κB family transcription factor *relish* in progenitors. Wild-type young intestines contain a regular lattice of evenly spaced nuclei, progenitors and enteroendocrine cells (Fig. 4.7D). As wild-type intestines age, epithelial organization becomes

disrupted, with crowded nuclei and clustered progenitor cells (Fig. 4.7E). With *relish* knockdown, aged intestines resemble healthy young guts with organized epithelial landscape (compare Fig. 4.7D and E). In addition to the effects on overall intestinal organization, *relish* or *kenny* depletion in progenitors decreased the number of mitotic cells throughout the intestine compared to aged wild-type controls (Fig. 4.7F-G). In addition, inactivation of Relish impaired the generation of mitotic clones in the posterior midgut, confirming that genetic inhibition of Relish dependent IMD signaling blocks intestinal proliferation (Fig. 4.7H). Together, these data suggest that basal IMD pathway activity is required in progenitors for age-dependent increases in intestinal proliferation and hyperplasia.

In addition to the number of mitotic cells, the number of progenitor cells and ISCs increases over time in wild-type flies, but this does not occur upon progenitor-specific IMD inactivation (Fig. 4.7I-J). Instead there are fewer esg+ progenitor cells and Delta+ ISCs upon 30 days of IMD inactivation compared to wild-type controls (Fig. 4.7I-J). Similarly, knockdown of *relish* decreased the proportion of progenitors in the posterior midgut of aged flies (Fig. 4.7K). Knockdown of the adapter protein Fadd, required for signaling downstream of Imd activation, also reduced the number of Dl+ ISCs in old flies, confirming the proliferative role of IMD in progenitors (Fig. 4.7L). To identify which progenitor cell type IMD acts in to promote proliferation we blocked IMD activity in either ISCs or enteroblasts. Similar to progenitor wide blockage, expression of ImdD30A in ISCs (*ISC^{ts}/D30A*) reduced the number of mitoses in aged flies (Fig. 4.7M). However, inhibition of IMD solely in enteroblasts (*Su(H)^{ts}/D30A*) had no effect on proliferation (Fig. 4.7N). These data indicate that the IMD pathway acts cell autonomously in ISCs to control intestinal proliferation upon ageing.

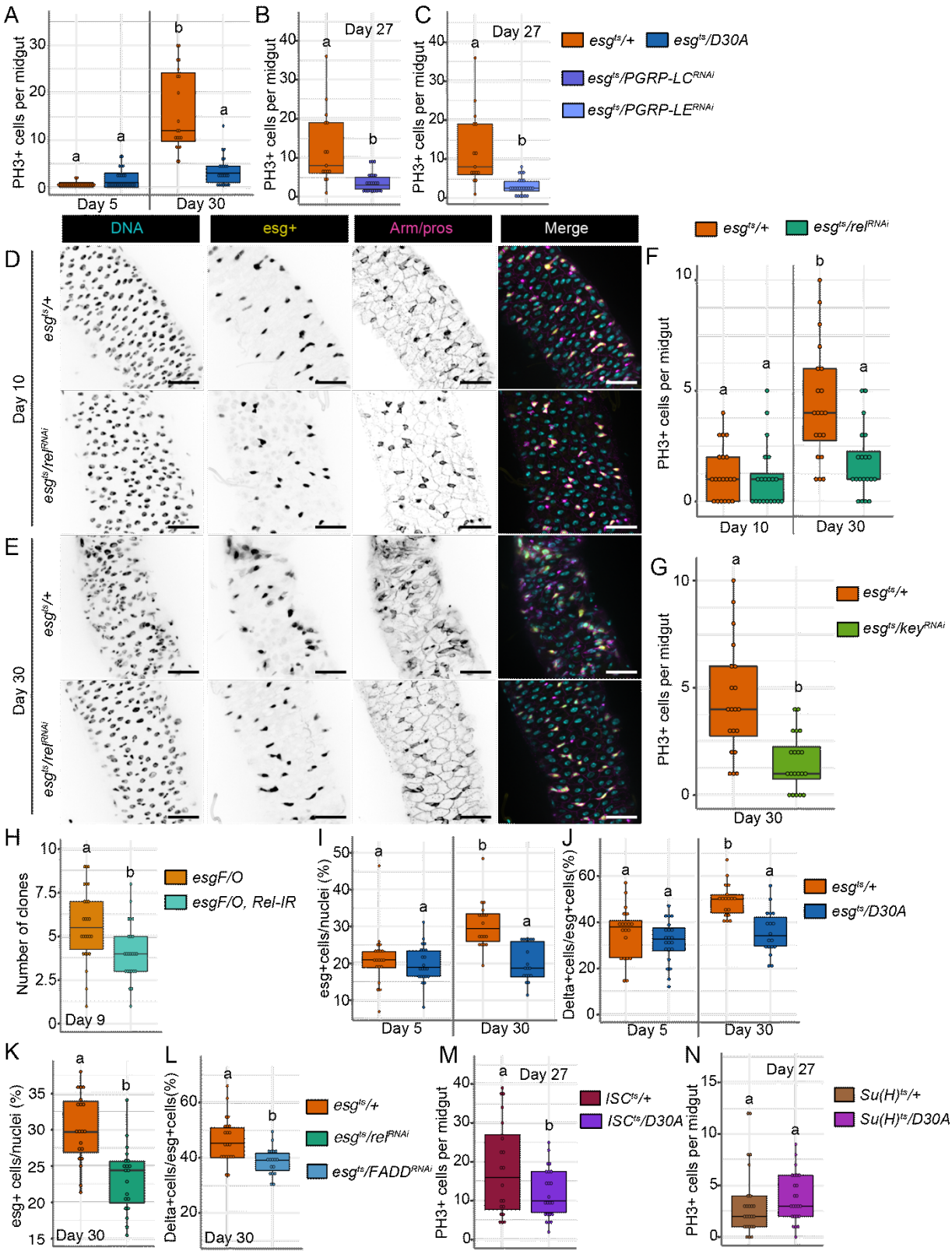

Figure 4.7 IMD acts in stem cells to promote intestinal proliferation. (A-C) Number of PH3+ mitotic cells per midgut after blocking IMD (*esg^{ts}/D30A*) (A) or knocking down the IMD receptors

(*esg^{ts}/PGRP-LC^{RNAi}* (B), *esg^{ts}/PGRP-LE^{RNAi}* (C)). **(D-E)** Images of wild-type *esg^{ts}/+* intestines and those with Relish knocked down in progenitors (*esg^{ts}/rel^{RNAi}*) after 10 (D) or 30 (E) days of Relish depletion. DNA stained by Hoescht (cyan), esg+ progenitors (yellow) and Arm/pros (magenta). Scale bars 25μm. **(F-G)** PH3+ cells per midgut after progenitor specific Relish (F) or Kenny (G) knockdown. **(H)** Number of wildtype and Relish deficient clones per midgut 9 days after clone induction. **(I)** Percent of nuclei that are esg positive progenitors upon ageing and IMD inactivation. **(J)** Percent of esg+ progenitors that are Delta (Dl) positive stem cells upon age and IMD inactivation. **(K)** Progenitors per nuclei upon progenitor specific Relish knockdown. **(L)** Stem cells per progenitors upon progenitor specific FADD knockdown. **(M)** Number of PH3+ cells per midgut upon ISC-specific IMD inactivation. **(N)** Number of PH3+ cells upon enteroblast specific IMD inactivation. Panels A-C, H-J and L-N were performed by Minjeong Shin. For A, F, I and J significance found using ANOVA followed by multiple pairwise Tukey tests. For B, C, G, H, K-N significance found using Students t test. Different letters denote significant difference of $p < 0.05$.

4.2.8 Progenitor-specific IMD inactivation impacts intestinal expression profiles

The intestine is composed of multiple specialized cell types that originate from multipotent ISCs. Although our data implicate IMD acts in progenitors to control proliferation we do not yet know the consequences for blocking IMD in progenitors for the remainder of the intestine. To determine the impacts of progenitor-specific IMD inhibition on individual cell lineages we performed a single-cell RNA sequencing analysis of 10 day old *esg^{ts}/+* and *esg^{ts}/D30A* midguts (Fig. 4.8A). After exclusion of dead cells and doublets, 3,675 cells from *esg^{ts}/+* and 3,654 cells from *esg^{ts}/D30A* were integrated into one dataset using Seurat for direct comparison (Fig. 4.8B). Using unbiased clustering of cells that share transcriptional profiles we identified all previously described intestinal cell types, including progenitors, enteroendocrine cells, enterocytes, copper cells, and cardia[25,88]. Overall, progenitor-specific IMD inhibition had mild effects on intestinal composition. For example, there are fewer EC-like cells and more cardia in *esg^{ts}/D30A* intestines compared to *esg^{ts}/+* (Fig. 4.8C). In addition to these general effects on epithelial composition, blockage of IMD in progenitors altered the expression of critical intestinal regulators in mature cell types. IMD inhibition in progenitors altered expression of genes involved in metabolism, translation, transport, stress response, and RNA

processing in enterocytes whereas genes involved in wounding response, precursor metabolites, and protein ubiquitination were perturbed in enteroendocrine cells (Fig. 4.8D).

To determine direct effects of IMD inactivation on progenitor cells we compared expression profiles of progenitors from *esg^{ts}/+* and *esg^{ts}/D30A*. IMD inhibition results in increased expression of genes involved in autophagy, Hippo signaling, growth, polarity, and cell cycle with decreased expression of genes involved in proteolysis, metabolism and translation (Fig. 4.8D). Of note, IMD inhibition altered expression of genes with critical functions in stem cell identity, division and differentiation. For instance, IMD inhibition in progenitors increased the expression of the Notch pathway target gene *E(spl)m3-HLH*, decreased expression of the Notch signaling modifier *Npc2f*, decreased expression of the septate junction component *Snakeskin* (*Ssk*) and increased expression of the α integrin *scab* (*scb*), two cell adhesion genes with important roles in stem cell maintenance and division (Fig. 4.8E)[36,44,197]. Consistent with data shown in figure 4.7, these results indicate inhibition of IMD in progenitors significantly alters progenitor cell homeostasis.

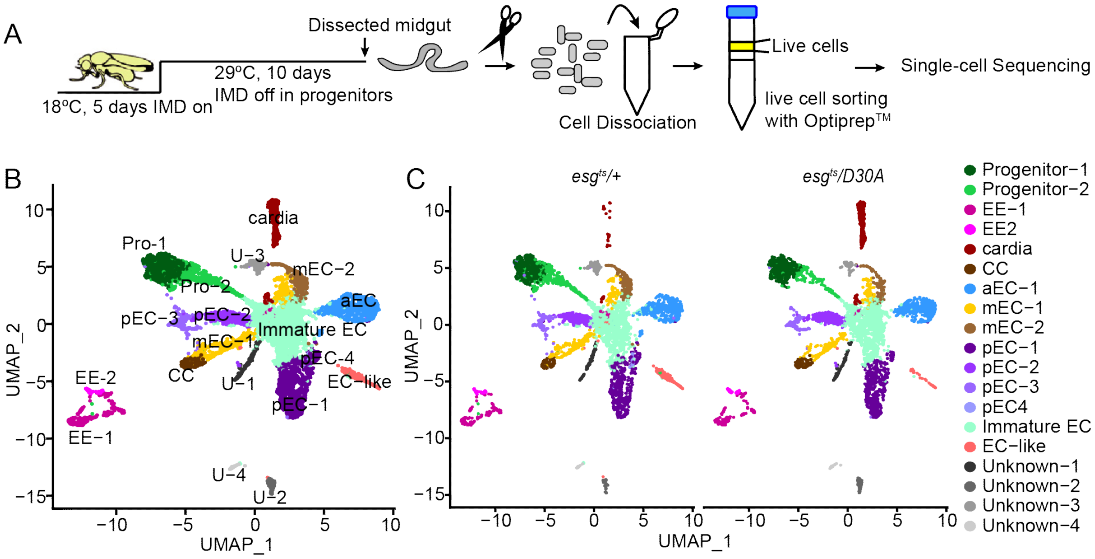
A
Dissected midgut
29°C, 10 days
IMD off in progenitors
18°C, 5 days IMD on
Cell Dissociation
Live cells
live cell sorting
with Optiprep™
Single-cell Sequencing
B
C
esg^ts/+
esg^ts/D30A
UMAP_1
UMAP_2
Pro-1
Pro-2
cardia
U-3
mEC-2
aEC
pEC-3
pEC-2
Immature EC
mEC-1
pEC-4
CC
U-1
EC-like
EE-2
pEC-1
EE-1
U-4
U-2
Progenitor-1
Progenitor-2
EE-1
EE2
cardia
CC
aEC-1
mEC-1
mEC-2
pEC-1
pEC-2
pEC-3
pEC4
Immature EC
EC-like
Unknown-1
Unknown-2
Unknown-3
Unknown-4

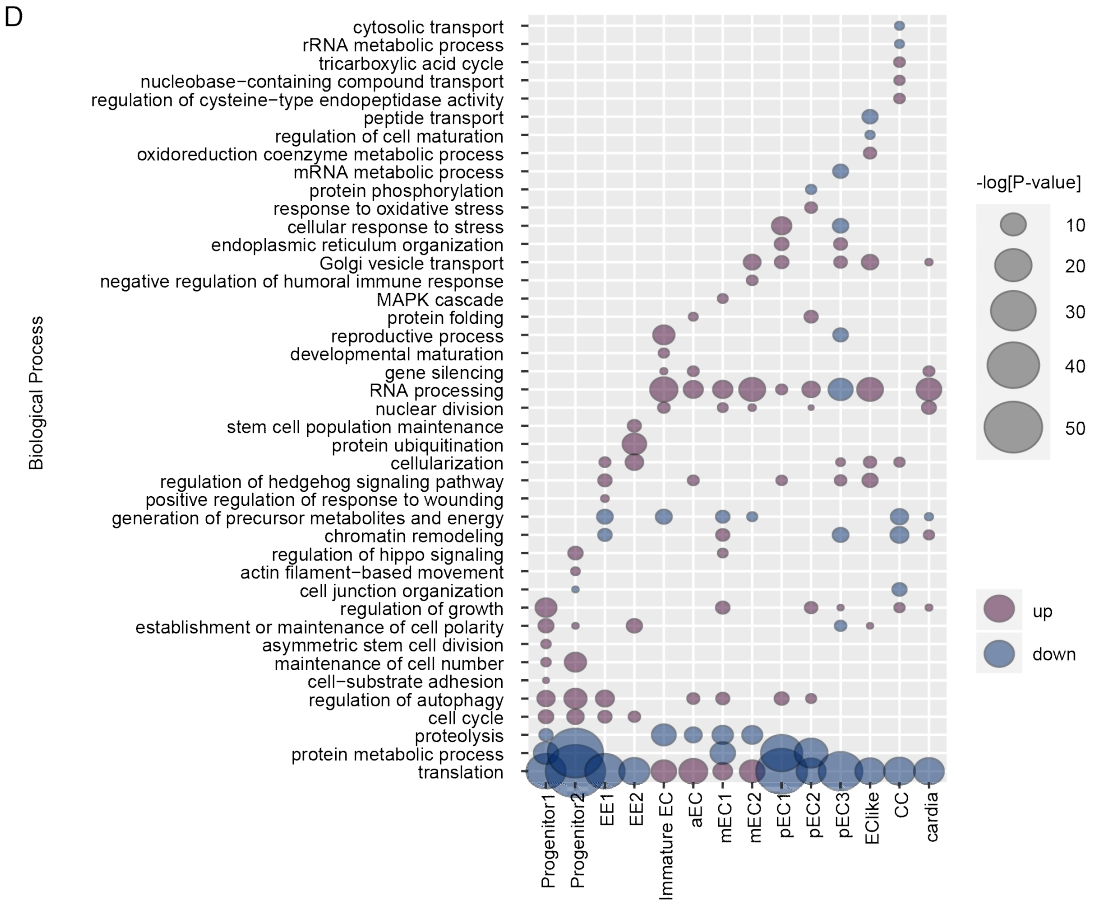
D
Biological Process
cytosolic transport
rRNA metabolic process
tricarboxylic acid cycle
nucleobase-containing compound transport
regulation of cysteine-type endopeptidase activity
peptide transport
regulation of cell maturation
oxidoreduction coenzyme metabolic process
mRNA metabolic process
protein phosphorylation
response to oxidative stress
cellular response to stress
endoplasmic reticulum organization
Golgi vesicle transport
negative regulation of humoral immune response
MAPK cascade
protein folding
reproductive process
developmental maturation
gene silencing
RNA processing
nuclear division
stem cell population maintenance
protein ubiquitination
cellularization
regulation of hedgehog signaling pathway
positive regulation of response to wounding
generation of precursor metabolites and energy
chromatin remodeling
regulation of hippo signaling
actin filament-based movement
cell junction organization
regulation of growth
establishment or maintenance of cell polarity
asymmetric stem cell division
maintenance of cell number
cell-substrate adhesion
regulation of autophagy
cell cycle
proteolysis
protein metabolic process
translation
Progenitor1
Progenitor2
EE1
EE2
Immature EC
aEC
mEC1
mEC2
pEC1
pEC2
pEC3
ECilike
CC
cardia
-log[P-value]
10
20
30
40
50
up
down

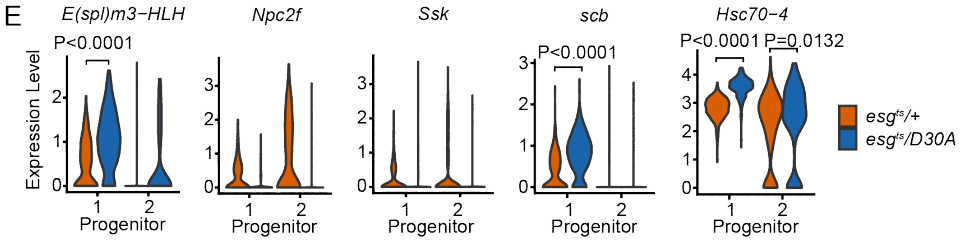
E
E(spl)m3-HLH
Npc2f
Ssk
scb
Hsc70-4
P<0.0001
P<0.0001
P<0.0001 P=0.0132
Expression Level
Progenitor
esg^ts/+
esg^ts/D30A

Figure 4.8 Progenitor-specific IMD inactivation impacts intestinal expression profiles. (A) Schematic of the experimental setup to perform single cell RNA sequencing of *esg^{ts}/+* and *esg^{ts}/D30A* intestines. **(B)** UMAP plot showing cell clusters from integrated transcriptomic datasets from *esg^{ts}/+* and *esg^{ts}/D30A*. Pro = progenitors, EC = enterocytes, EE = enteroendocrine cells, CC = copper cells. **(C)** UMAP from B split by genotype. **(D)** Biological Processes significantly altered in specific cell clusters upon IMD inactivation in progenitors. Size of the dot indicates p value whereas dot color indicates up or down regulation. **(E)** Violin plots of specific genes differentially expressed in progenitors upon IMD inhibition. These experiments and analyses were performed by Minjeong Shin.

4.2.9 Progenitor-specific IMD alters intestinal developmental trajectories

Given the effect of IMD inhibition on the expression of genes required for progenitor-niche interactions and progenitor differentiation I analyzed the impact this has on developmental trajectories of progenitors. To answer this question, I generated unbiased pseudotime developmental trajectories in *esg^{ts}/+* and *esg^{ts}/D30A* intestines using Monocle3. The resulting trajectories successfully re-created known developmental transitions from progenitors to mature progeny in both genotypes (Fig. 4.9A and D). To specifically examine effects of IMD on progenitor development I subset the progenitor populations for each genotype and analyzed the expression of critical developmental regulators across pseudotime (Fig. 4.9B and E). This analysis revealed expression patterns characteristic of developmental transitions for both genotypes. For example, in each case the expression of the stem cell marker Dl was enriched at early stages in pseudotime (Fig. 4.9C and F, Fig. 4.10A). However, IMD inhibition perturbed the expression patterns of differentiation markers. Compared to wild-type, IMD inactivation resulted in premature or prolonged expression of the Notch targets *E(spl)m3-HLH* and *E(spl)malpha-BFM*, the EGF regulator *sprouty* (*sty*), the enterocyte fate regulator *klumpfuss* (*klu*) (Fig. 4.9G-N). In addition, inhibition of IMD in progenitors altered the pseudotime expression profiles of numerous markers of enterocyte maturation (Fig. 4.10B-D). These data indicate that inhibition of IMD in progenitor cells perturbs enterocyte differentiation.

Given the effects of IMD inhibition on enterocyte maturation genes I asked whether enteroblast numbers are affected upon ImdD30A expression. To test if IMD inhibition alters the

transition of ISCs to enteroblasts I monitored the expression of fluorescent markers in *esg^{ts},UAS-CFP,Su(H)-GFP* flies, with or without ImdD30A expression. Here, ISCs are visible as CFP-positive cells whereas enteroblasts are CFP and GFP double positive cells (Fig. 4.9P). Consistent with the effects of IMD inhibition on the expression of Notch pathway genes, *esg^{ts}/D30A* intestines contained increased levels of enteroblasts within the progenitor compartment (Fig. 4.9O). In conjunction with the loss of ISCs upon IMD inhibition (Fig. 4.7J), these data argue that IMD acts in progenitors to promote ISC identity and limit enteroblast differentiation.

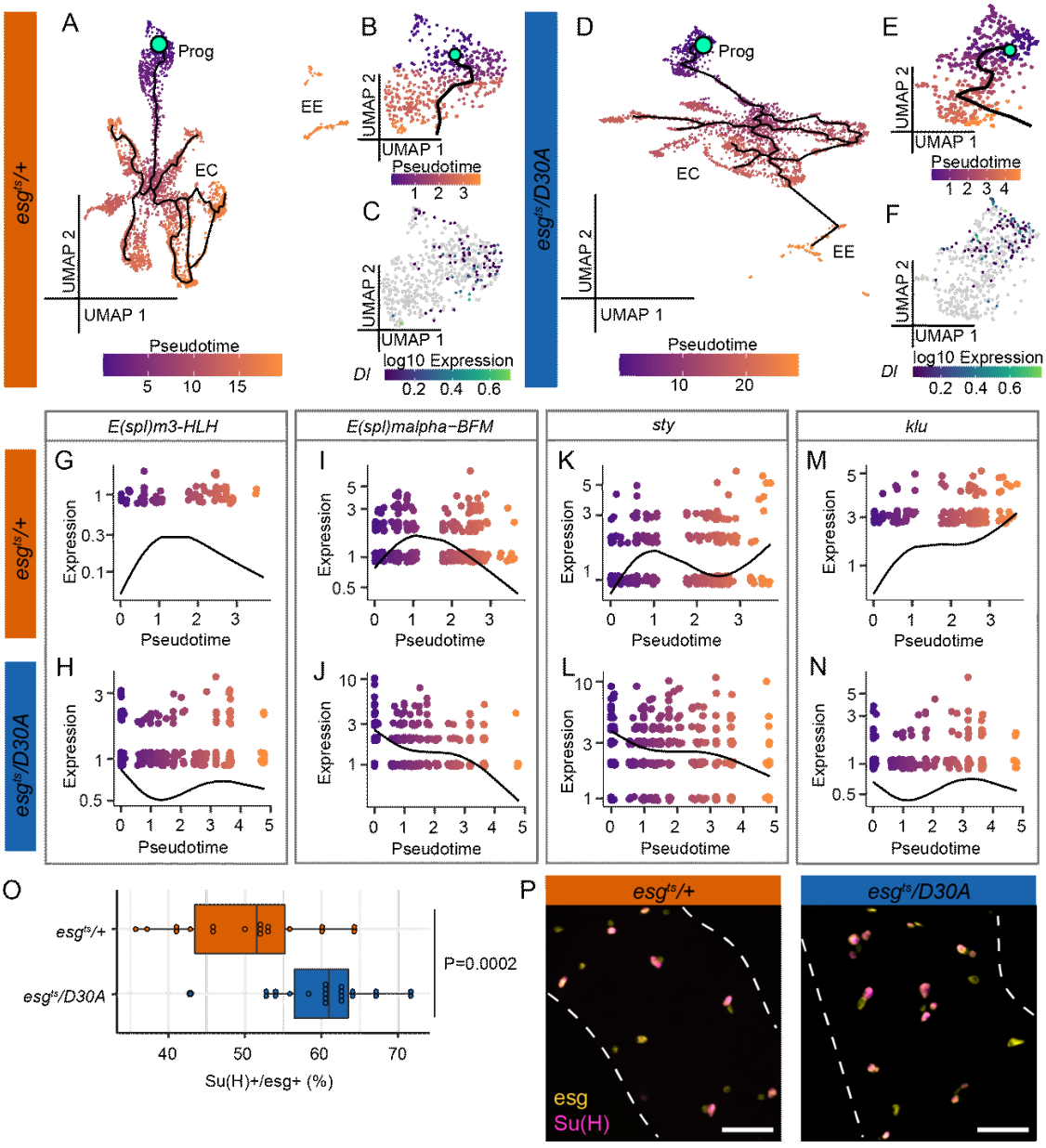

Figure 4.9 Progenitor-specific IMD alters intestinal developmental trajectories. (A-N) Single-cell datasets from Seurat for each individual genotype were analyzed in Monocle3 for pseudotime. For A (*esg^{ts}/+)* and D (*esg^{ts}/D30A*) mint green circles denote root node and the beginning of the intestinal trajectories. Dark purple marks the beginning of pseudotime whereas orange marks cells later in pseudotime. Black lines show trajectories. Prog = progenitors, EC = enterocytes, EE = enteroendocrine cells. **(B and E)** Pseudotime within progenitor subsets of A and D, respectively. **(C and F)** Expression pattern of the ISC marker Delta (Dl) in *esg^{ts}/+* progenitors (C) and in *esg^{ts}/D30A* progenitors (F). Grey dots are those with no detectable expression. **(G-N)** Expression of Notch target genes *E(spl)m3-HLH*, *E(spl)malpha-BFM*, the EGF inhibitor *sprouty* (*sty*), and the EC fate regulator *klumpfuss* (*klu*) over pseudotime within progenitor subsets of the indicated genotypes. **(O)** Percent of esg+ progenitors that are positive for the enteroblast marker Su(H) in *esg^{ts}, UAS-CFP, Su(H)-GFP/+* (n=18) and *esg^{ts}, UAS-CFP, Su(H)-GFP/D30A* (n=22) posterior midguts 14 days after transgene expression. Significance found using Students t test. **(P)** Representative images of intestines used to gather data in (O). Progenitors labelled by esg in yellow and enteroblasts labelled by Su(H) in magenta. Scale bars 25μm.

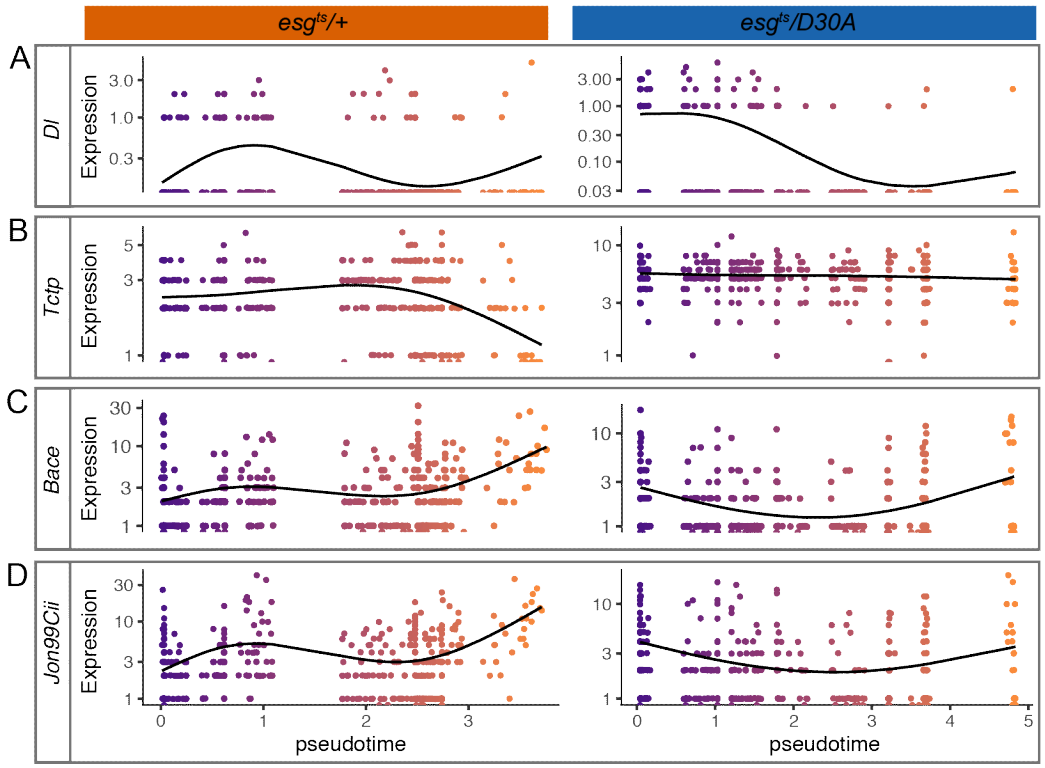

Figure 4.10 Progenitor-specific IMD inhibition alters gene expression across pseudotime. (A-D) Expression of genes involved in stem cell identity and enterocyte maturation across pseudotime trajectories in progenitor subsets from Figure 2.9 B and E.

4.2.10 Progenitor-specific IMD perturbs the generation of enteroendocrine cells

IMD inhibition in progenitors decreases ISC mitoses, alters ISC and enteroblast numbers, and disrupts developmental trajectories of enterocytes suggesting that IMD in progenitors modulates the development of mature epithelial cells. To further elucidate the role of progenitor-specific IMD on epithelial differentiation we examined the transcriptional profiles of enteroendocrine cells from *esg^{ts}/+* and *esg^{ts}/D30A* intestines. Fly enteroendocrine cells have been previously described at a single cell resolution allowing for a detailed comparison between genotypes[88,198]. For instance, enteroendocrine cells can be divided into subsets based on expression of distinct peptide hormones that remain stable during homeostasis or after recovery from infection[199]. To determine if IMD in progenitors impacts enteroendocrine composition we performed unsupervised clustering of enteroendocrine cells from our single-cell sequencing analysis. Five separate enteroendocrine clusters were resolved in both genotypes, each with a signature peptide hormone expression pattern (Fig. 4.11A-B). In two instances, hormone expression profiles were conserved between genotypes. For example, similar to earlier enteroendocrine characterization[199], subset zero from *esg^{ts}/+* and subset two from *esg^{ts}/D30A* expressed *Tk* and *Dh31* (Fig. 4.11C-D). Likewise, subset three from *esg^{ts}/+* and subset one from *esg^{ts}/D30A* had enriched expression of *NPF* and partial expression of *Gpb5* and *CCAP* (Fig. 4.11C-D). In contrast, we did not detect a counterpart for subset zero from *esg^{ts}/D30A* in *esg^{ts}/+* controls and observed minimal conservation of expression profiles from *esg^{ts}/+* subset one, two and four in *esg^{ts}/D30A* (Fig. 4.11C-D). These expression profiles suggest functional differences in enteroendocrine cells between genotypes.

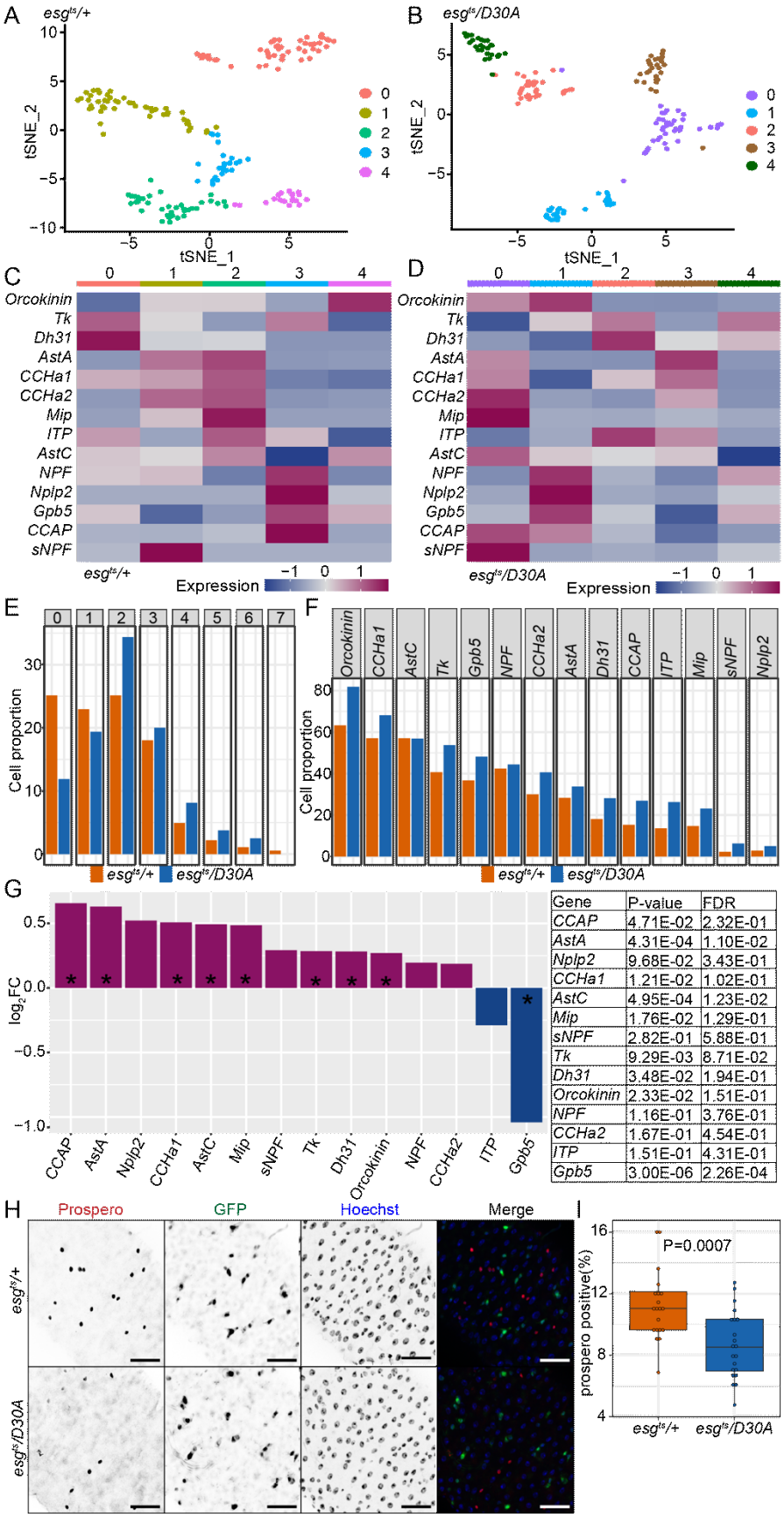

Gene	P-value	FDR
CCAP	4.71E-02	2.32E-01
AstA	4.31E-04	1.10E-02
Nplp2	9.68E-02	3.43E-01
CCHa1	1.21E-02	1.02E-01
AstC	4.95E-04	1.23E-02
Mip	1.76E-02	1.29E-01
sNPF	2.82E-01	5.88E-01
Tk	9.29E-03	8.71E-02
Dh31	3.48E-02	1.94E-01
Orcokinin	2.33E-02	1.51E-01
NPF	1.16E-01	3.76E-01
CCHa2	1.67E-01	4.54E-01
ITP	1.51E-01	4.31E-01
Gpb5	3.00E-06	2.26E-04

4.11 Progenitor-specific IMD perturbs the generation of enteroendocrine cells. (A-B) t-distributed stochastic neighbor embedding (tSNE) plot of enteroendocrine cell subsets in *esg^{ts}/+* and *esg^{ts}/D30A* intestines. **(C-D)** Heatmap showing relative expression of peptide hormones in each enteroendocrine subset. Same colored column bars indicate conservation of peptide hormones across *esg^{ts}/+* and *esg^{ts}/D30A* clusters. **(E)** Quantification of the percentage of enteroendocrine cells that express the indicated number of different peptide hormones in each genotype. **(F)** Quantification of the percentage of enteroendocrine cells that express the indicate peptide hormone in each genotype. **(G)** Quantification of the log2 fold change (log2FC) of peptide hormones in whole intestines comparing the *esg^{ts}/D30A* to *esg^{ts}/+*. Sequences obtained by bulk-seq of intestinal tissues. Asterisks indicate significantly altered genes $p < 0.05$ upon IMD inactivation. **(H)** Images of *esg^{ts}/+* and *esg^{ts}/D30A* after 10 days of IMD inactivation. Prospero labels enteroendocrine cells (red), GFP labels progenitors (green) and Hoescht labels DNA (blue). Scale bars 25μm. **(I)** Percentage of nuclei that are positive for the enteroendocrine marker prospero after 10 days of progenitor-specific IMD inactivation. *Esg^{ts}/+* (n=20) and *esg^{ts}/D30A* (n=21) significance found using Students t test. Panels A-G were done by Minjeong Shin.

We then classified enteroendocrine cells based on the number of hormone peptides they express and observed further differences between *esg^{ts}/+* and *esg^{ts}/D30A* intestines. Upon IMD inhibition, fewer enteroendocrine cells expressed zero or one peptide, and a greater proportion expressed two or more peptides than wild-type controls (Fig. 4.11E). In addition, for thirteen out of the fourteen peptides examined, a greater proportion of the enteroendocrine cells from *esg^{ts}/D30A* expressed the respective peptide than *esg^{ts}/+* (Fig. 4.11F). Together this indicates that inhibition of IMD in progenitors generates enteroendocrine cells with enhanced peptide expression. To directly test the effects of IMD inhibition on peptide expression levels throughout the intestine we performed bulk RNA-seq on whole dissected intestines from *esg^{ts}/+* and *esg^{ts}/D30A*. With the exception of ITP and Gbp5, blocking IMD increased the expression of the remaining twelve peptides throughout the intestine confirming a role of progenitor-specific IMD in the expression of peptide hormones (Fig. 4.11G). Finally, I quantified the number of enteroendocrine cells in the posterior midguts of *esg^{ts}/+* and *esg^{ts}/D30A* by staining for the enteroendocrine cell marker prospero (Fig. 4.11H). Inhibition of IMD decreased the proportion of enteroendocrine cells by approximately 20% compared to controls

(Fig. 4.11I). Together, our results show that inhibition of IMD in progenitors disrupts peptide hormone patterns in mature enteroendocrine cells, decreases the amount of total enteroendocrine cells and increases the expression of most peptides, suggesting progenitor-specific IMD is required for the proper development of enteroendocrine cell lineages.

4.3 Conclusions

Intestinal immune activity regulates the actions of intestinal progenitor cells. For instance, TLR activity in the intestinal epithelium of mice promotes progenitor proliferation and differentiation and in humans, chronic immune activation is associated with the development of colorectal cancer[2,195]. However, it is unclear whether immune pathways act directly within progenitors to alter intestinal homeostasis and disease. I used *Drosophila* to determine the role of the IMD pathway in progenitors in the context of homeostasis, ageing and tumorigenesis. I found that IMD pathway components are enriched in intestinal progenitor cells and upon chronic activation of the IMD pathway in progenitors, intestines become hyperproliferative and dysplastic. In addition, IMD activation results in the perturbation of Notch pathway genes resulting in increased levels of enteroendocrine cell differentiation. Together this suggests that IMD activation in progenitors promotes their division and secretory lineage specification.

Given the role of progenitor-specific IMD on proliferation and Notch pathway genes I asked whether IMD activation impacts the growth of Notch-deficient tumors in the intestine. As the microbiome promotes tumorigenesis, I hypothesized that immune activation induces tumor growth. Indeed, IMD activation caused extensive tumorigenesis in Notch-deficient intestines, even in the absence of a microbiome. These data indicate that hyperactivation of the IMD pathway specifically in progenitors is sufficient to promote tumor growth.

To determine whether basal levels of IMD activity in progenitors governs intestinal homeostasis we blocked IMD activity in progenitors and monitored progenitor identity, proliferation, and differentiation. Inhibition of IMD resulted in fewer stem cells, progenitors and mitoses in aged flies, indicative of a central role for immune signaling in the regulation of progenitor cell function. In addition to growth defects, IMD inhibition in progenitors resulted in perturbed expression patterns of genes involved in differentiation and maturation of mature epithelial cell types. In agreement with this, IMD inhibition lead to increased levels of enteroblasts at the expense of enteroendocrine cell

numbers. Together this suggests that basal levels of IMD are required to promote intestinal proliferation upon age and for the proper differentiation and maturation of enteroendocrine lineages (Fig. 2.12). However, if immune pathways become hyperactive, this can lead to intestinal hyperplasia and exacerbation of tumorigenesis (Fig. 2.12). Therefore, a regulated balance of immune activity is required in progenitor cells to allow for homeostatic differentiation and proliferation while limiting hyperplastic and tumorigenic disease.

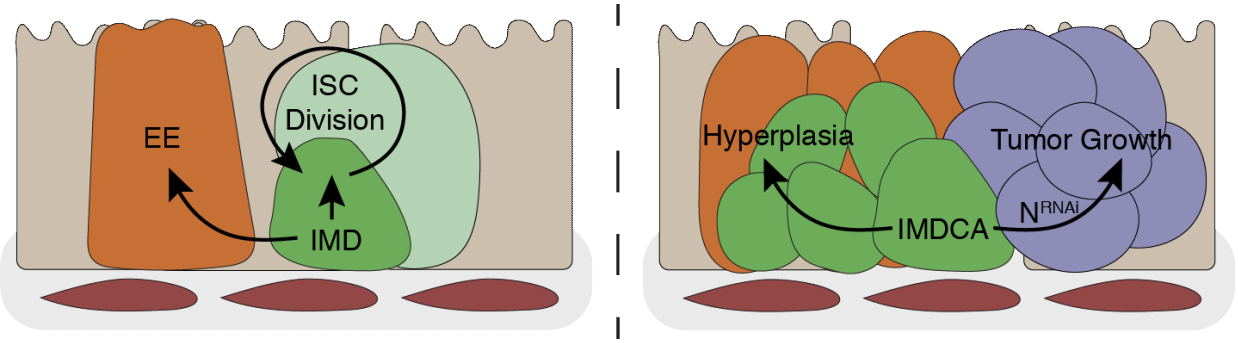

Figure 4.12 IMD in progenitors promotes enteroendocrine differentiation, ISC division, hyperplasia and tumorigenesis. Basal levels of IMD are required in intestinal progenitors for the proper differentiation and maturation of enteroendocrine (EE) cells. Basal IMD in ISCs promotes age-dependent increases in intestinal proliferation. Upon hyperactivation of IMD (IMDCA) in progenitors, intestines become hyperplastic with increased levels of enteroendocrine cells and progenitors. In the context of Notch-deficient intestines, IMD activation exacerbates tumor growth.

Chapter 5

The NF-κB transcription factor Relish acts in stem cells to regulate intestinal repair

Data in this chapter have yet to be published but is deposited online in preprint form:

- **Ferguson, M.,** Shin, M., & Foley, E. (2022). Relish/NF-κB acts in intestinal stem cells to promote epithelial repair in *Drosophila. Biorxiv*
  doi: https://doi.org/10.1101/2022.09.29.510182.

5.1 Summary

Intestinal stem cells (ISCs) divide and differentiate in response to intestinal damage to replace dying cells and maintain an effective epithelial barrier[1]. Immune pathways modify how the epithelium responds to extrinsic stress and immune perturbation alters the effectiveness of epithelial repair. For example, mice mutant for TLRs have defective intestinal repair and are more susceptible to colitis like disease[2,112,129,130]. Despite the importance of immune activity in intestinal repair, we know little about ISC-intrinsic requirements for immune signals to protect the epithelium against acute insults. As ISCs are critical for epithelial maintenance it is important we understand the extent to which immune signals act within ISCs to directly impact their function.

To determine the role of immune signals in ISCs during intestinal repair I analyzed the intestinal response to the damaging agent dextran sodium sulfate (DSS) upon ISC-specific perturbation of the NF-κB family transcription factor Relish. DSS is commonly used in mice to model colitis and in flies, DSS damages the intestine and elicits a proliferative response from ISCs to repair the injury[55,73,200–203]. I discovered that damage response pathways activate NF-κB in ISCs, leading to Ras-dependent promotion of ISC survival and enhanced generation of enteroblasts poised to replace dead and dying enterocytes. Targeted inactivation of NF-κB in ISCs caused death of damaged ISCs and their progeny, resulting in a failure to produce enterocyte precursors, compensatory ISC hyperproliferation, and enhanced lethality in response to damage. This work expands our appreciation of how immune signals alter epithelial maintenance and highlight an intrinsic requirement for NF-κB in ISCs where it promotes cell survival and effective repair.

5.2.1 ISC-specific NF-κB restricts proliferation upon damage

As my results from chapter 4 implicate progenitor-specific NF-κB in ISC proliferation, I determined the consequences of compromised progenitor cell immunity for epithelial responses to acute damage. To do this, I used the *esg^{ts}* driver that allows for temperature specific induction of transgenes in progenitors alongside GFP expression. Specifically, I characterized progenitor dynamics in *esg^{ts}/rel^{RNAi}* and control *esg^{ts}/+* flies that I fed dextran sodium sulfate (DSS), a toxic polysaccharide that disrupts the epithelium, promoting a compensatory burst of ISC divisions. Specifically, DSS damages the basement membrane in the fly intestine and provokes ISC divisions through growth modulators such as Hippo, Myc and Sox21a [55,73,201–203]. Progenitor-restricted

inactivation of *rel* had no visible effect on intestinal physiology in unchallenged, ten-day-old flies (Fig. 5.1A). Unchallenged flies had regularly spaced nuclei interspersed with progenitors independent of *relish* knockdown. This suggests that progenitor-specific Relish has little effect on intestinal physiology in young unchallenged flies. DSS caused damage to $esg^{ts}/+$ midguts (Figure 5.1B), leading to extra divisions (Fig. 5.1E) that increased ISC and progenitor numbers throughout the posterior midgut (Fig. 5.1C-D). I observed similar amounts of epithelial damage (Fig. 5.1B), and expansion of ISC and progenitor populations (Fig. 5.1C-D) in DSS-treated esg^{ts}/rel^{RNAi} guts. However, I also uncovered a distinct effect of *rel* inactivation on damage-dependent proliferation. Specifically, I found that depletion of *rel* from progenitors nearly doubled the mitotic activity of ISCs in flies challenged with DSS compared to wild-type controls (Fig. 5.1E). Notably, progenitor-specific loss of *rel* also significantly increased the frequency of ISC proliferation in flies orally challenged with the enteric pathogen *Ecc15* (Fig. 5.1F), indicating a general requirement for NF-κB to regulate ISC proliferation after ingestion of harmful agents.

To identify the exact progenitor cell type where NF-κB acts to control damage-dependent growth, I knocked down *rel* exclusively in ISCs (ISC^{ts}/rel^{RNAi}) or enteroblasts ($Su(H)^{ts}/rel^{RNAi}$) and measured DSS-mediated ISC proliferation. Like progenitor-wide knockdown, ISC-specific loss of *rel* (Fig. 5.2A), or the IKKγ ortholog *key* (Fig. 5.2B) increased mitoses in response to DSS compared to wild-type controls, demonstrating an ISC-autonomous role for IKK/NF-κB activity in damage-responsive proliferation. Supporting a direct role for *rel* in the control of ISC proliferation, I also found that ISC-restricted expression of a constitutively active *rel* variant (*relVP16*) was sufficient to prevent DSS-responsive proliferation (Fig. 5.2C). In contrast, *rel* depletion from enteroblasts failed to increase ISC proliferation in DSS-treated flies (Fig. 5.2D), suggesting that *rel* acts primarily in ISCs to regulate damage-dependent proliferation.

Since rapid, orderly epithelial repair is essential to survive acute tissue damage, I measured the effect of ISC-specific loss of *rel* on survivability upon DSS exposure. Loss of *rel* did not affect the short, or long-term viability of unchallenged flies (Fig. 5.2E-F). However, depletion of *rel* from ISCs significantly impaired the ability of flies to survive ingestion of DSS (Fig. 5.2E), confirming an essential role for Relish in ISC responses to damaging agents.

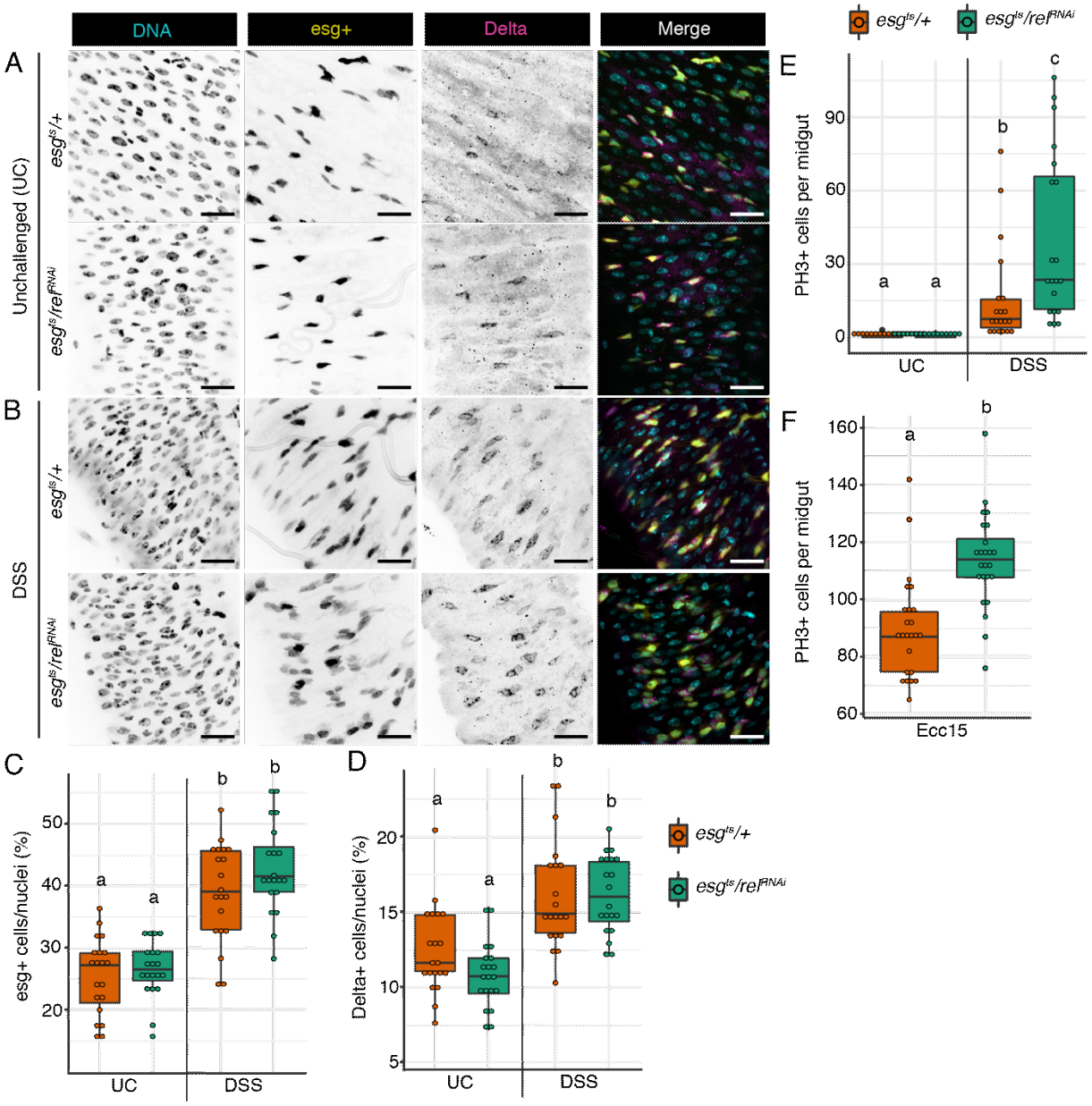

Figure 5.1 Progenitor-specific NF-κB depletion increases ISC divisions in response to acute damage. (A) Images of unchallenged *esg*^{ts}*/+* and *esg*^{ts}*/rel*^{RNAi} intestines. **(B)** Images of *esg*^{ts}*/+* and *esg*^{ts}*/rel*^{RNAi} intestines challenged with DSS for 48hrs. DNA stained with Hoeschst (cyan), esg+ progenitors (yellow) and Delta+ ISCs (magenta). Scale bars = 15μm. **(C)** Proportion of nuclei that are esg+ progenitors upon DSS challenge and progenitor-specific *rel* knockdown. **(D)** Proportion of nuclei that are Delta+ ISCs upon DSS challenge and progenitor-specific *rel* knockdown. **(E)** PH3+ cells per midgut upon DSS challenge and progenitor-specific *rel* knockdown. **(F)** PH3+ cells per midgut upon challenge with the pathogen *Ecc15* and progenitor-specific *rel* knockdown.

Significance for C-E found by ANOVA followed by multiple pairwise Tukey tests. Significance for F found using Students t test. Different letters denote significance of $p < 0.05$.

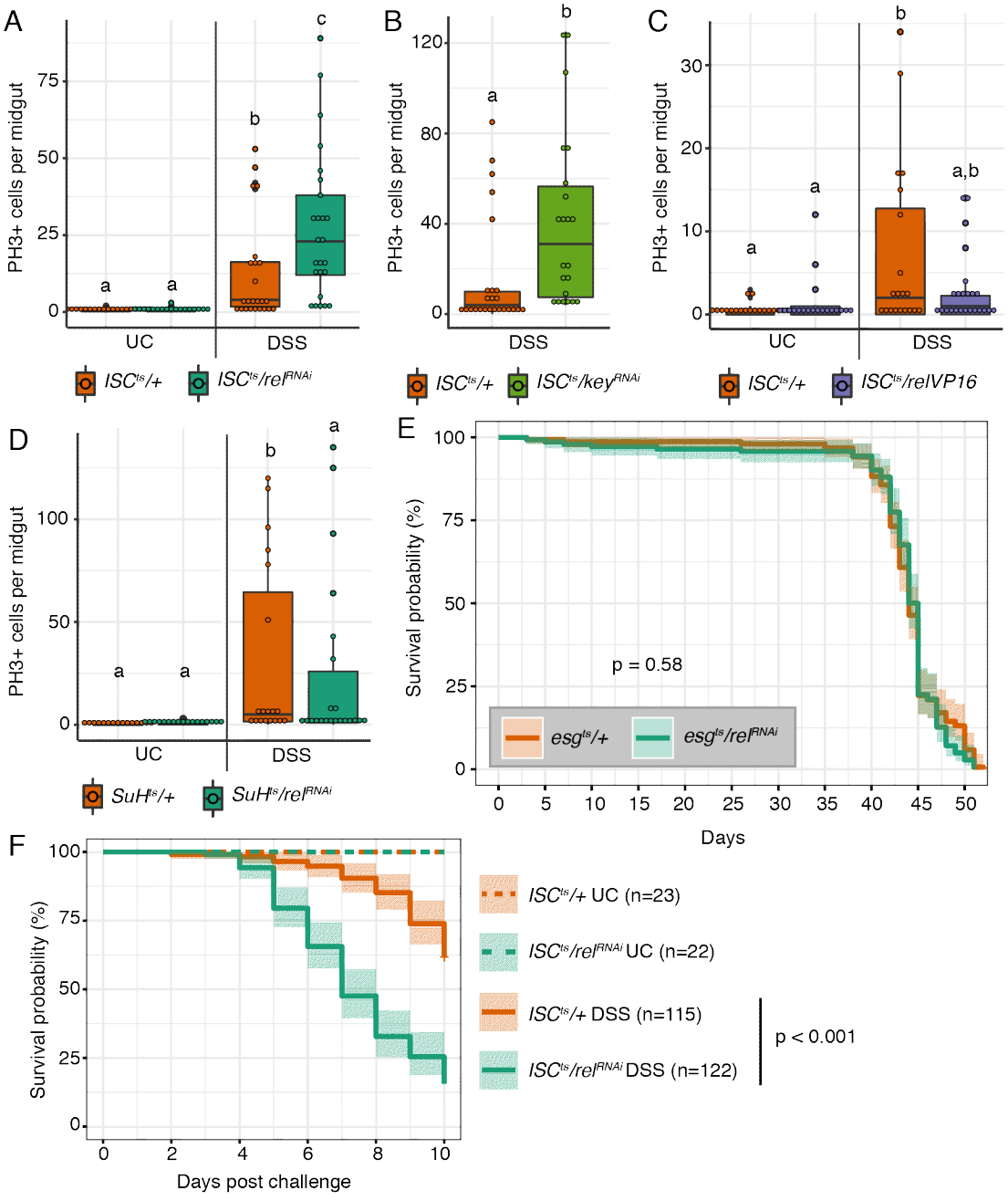

Figure 5.2 ISC-specific NF-κB restricts proliferation upon damage. (A) PH3+ cells per midgut upon DSS challenge and ISC-specific *rel* knockdown. **(B)** PH3+ cells per midgut upon DSS challenge and ISC-specific *key* knockdown. **(C)** PH3+ cells per midgut upon DSS challenge and ISC-specific Relish activation. **(D)** PH3+ cells per midgut upon DSS challenge and enteroblast-specific *rel* knockdown.

(E) Lifespan of wild-type *esg^{ts}/+* flies and those with progenitor-specific *rel* knockdown (*esg^{ts}/rel^{RNAi}*). **(F)** Survival of flies upon 10% DSS challenge and ISC-specific *rel* knockdown. Significance for A, C-D found using ANOVA followed by multiple pairwise Tukey tests. Significance for B found using Student t test. Significance for E-F found using log rank test.

5.2.2 ISC-specific NF-κB is required for enterocyte renewal upon damage

To understand how NF-κB regulates stem cell proliferation in times of acute tissue damage, I analyzed RNA abyndance from individual cells from midguts dissected from unchallenged, or DSS-treated, *ISC^{ts}/+* and *ISC^{ts}/rel^{RNAi}* flies. Specifically, flies were raised in the presence or absence of DSS for 48 hours prior to dissection, mechanical disruption of intestinal tissue, and preparation of cell suspension. Cells were assessed for viability, used to generate single cell libraries and sent for sequencing. Single cell transcriptomes were filtered based on RNA counts and mitochondrial reads to remove cell doublets and dead cells. I selected the *ISC^{ts}* driver line for this experiment, as it permits inactivation of *rel* exclusively in ISCs, while marking ISCs with YFP. As a result, I was able to resolve the impacts of ISC-restricted *rel* inactivation on all intestinal cell types, including the stem cell. In agreement with Figures 5.1 and 5.2, transcriptional states within unchallenged ten-day-old *ISC^{ts}/+* and *ISC^{ts}/rel^{RNAi}* midguts were broadly similar. In both instances, I identified approximately equal ratios of progenitor, enteroendocrine, and enterocyte lineages, as well as specialist acid-producing copper and large flat cells that produce IMD pathway inhibitors in the middle midgut (Fig. 5.3A-B). I also discovered a transcriptionally distinct cell population that expressed classical progenitor markers such as *esg* and *E(spl)m3-HLH*, alongside enterocyte markers such as the *trypsin* family of proteases (Fig. 5.3B, 5.4A). In each case, marker expression was at an intermediary level between that seen in progenitors and enterocytes (Fig. 5.4B-C), suggesting that these cells represent a transition state between undifferentiated progenitors and mature enterocytes. Therefore, I have labeled these cells premature enterocytes (preECs).

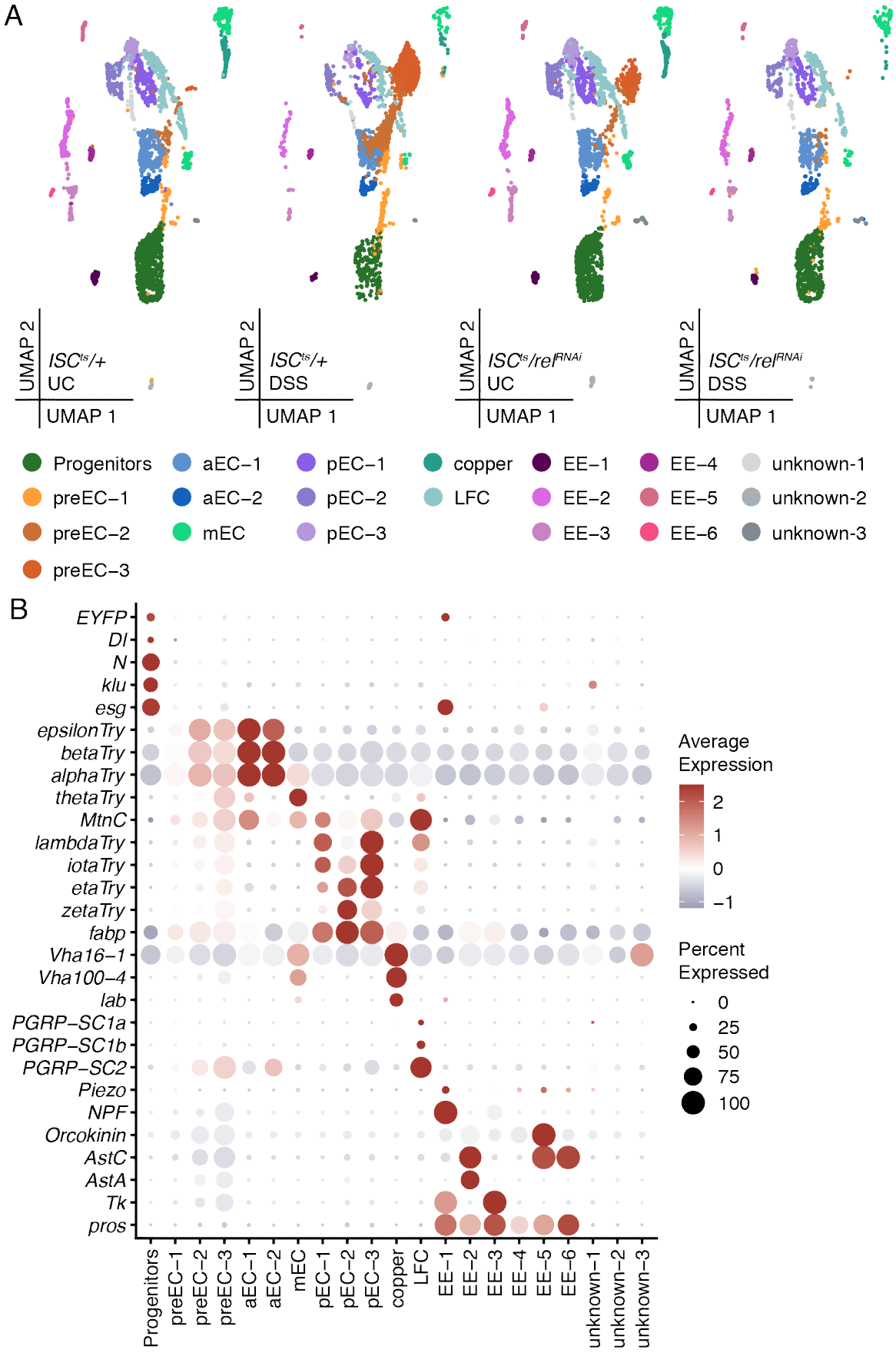
A
UMAP 2
ISCts/+
UC
UMAP 1
UMAP 2
ISCts/+
DSS
UMAP 1
UMAP 2
ISCts/relRNAi
UC
UMAP 1
UMAP 2
ISCts/relRNAi
DSS
UMAP 1
Progenitors
preEC–1
preEC–2
preEC–3
aEC–1
aEC–2
mEC
pEC–1
pEC–2
pEC–3
copper
LFC
EE–1
EE–2
EE–3
EE–4
EE–5
EE–6
unknown-1
unknown-2
unknown-3
B
EYFP
Dl
N
klu
esg
epsilonTry
betaTry
alphaTry
thetaTry
MtnC
lambdaTry
iotaTry
etaTry
zetaTry
fabp
Vha16–1
Vha100–4
lab
PGRP–SC1a
PGRP–SC1b
PGRP–SC2
Piezo
NPF
Orcokinin
AstC
AstA
Tk
pros
Progenitors
preEC–1
preEC–2
preEC–3
aEC–1
aEC–2
mEC
pEC–1
pEC–2
pEC–3
copper
LFC
EE–1
EE–2
EE–3
EE–4
EE–5
EE–6
unknown–1
unknown–2
unknown–3
Average Expression
2
1
0
–1
Percent Expressed
0
25
50
75
100

Figure 5.3 Single-cell RNA sequencing of intestines upon damage and ISC-specific NF-κB depletion. (A) UMAP plots from integrated transcriptomic single cell data from *ISC^{ts}/+* and *ISC^{ts}/rel^{RNAi}* intestines unchallenged (UC) or challenged with DSS. preEC = premature enterocytes, EC = enterocytes (aEC anterior, mEC middle, pEC posterior), EE = enteroendocrine cells, LFC = large flat cells, copper = copper cells. **(B)** Dotplot of markers genes for the clusters from the 4-way integrated data in A. Size of the dot represents the proportion of cells within that cluster that express the indicated gene. Dot color indicates average expression of that gene per cluster.

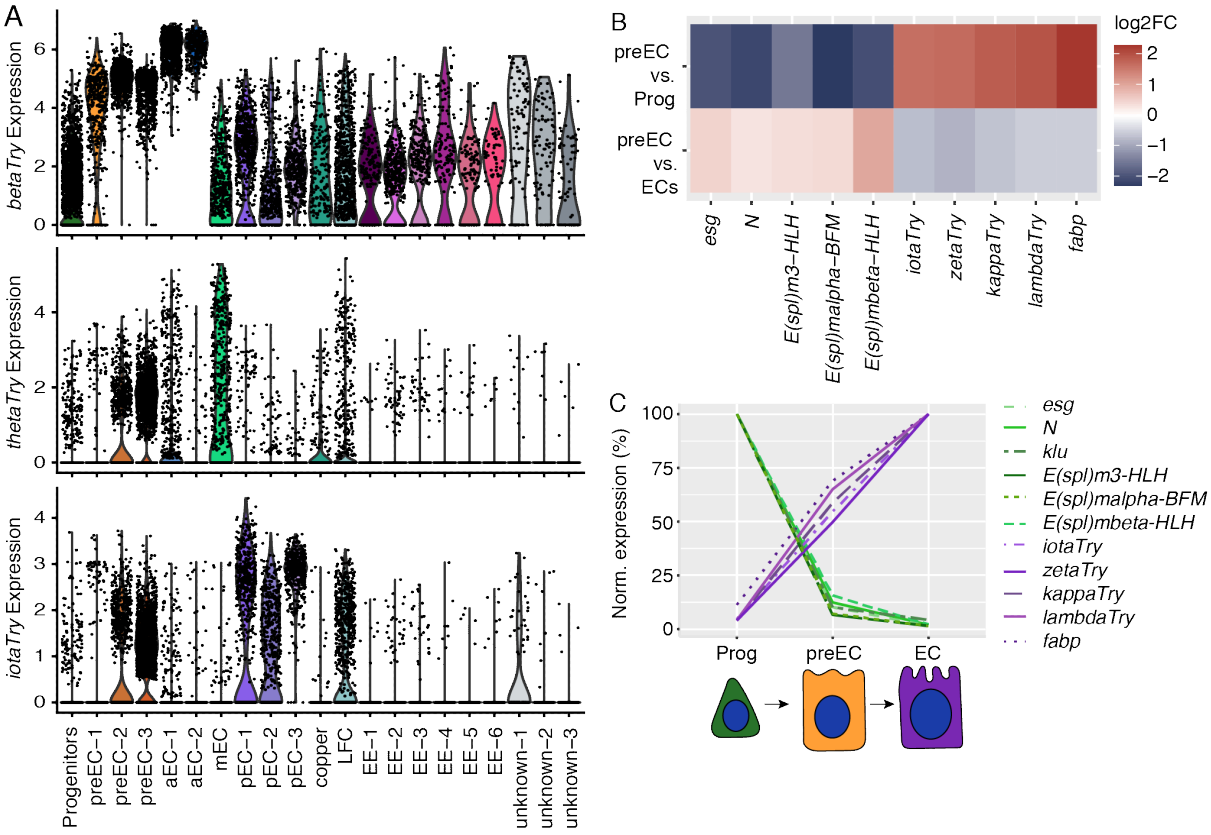

Figure 5.4 Premature enterocytes are an intermediate cell state between progenitors and enterocytes. (A) Violin plots showing expression of anterior (*betaTry*), middle (*thetaTry*) and posterior (*iotaTry*) enterocyte markers across cell clusters showing enrichment of markers in preECs. **(B)** Direct comparison of gene expression between preECs and progenitors or preECs and enterocytes. All genes shown are $p < 0.05$. **(C)** Average normalized expression of selected genes

across developmental cell states from progenitors to preECs to enterocytes. Green lines are progenitor markers and purple lines are enterocyte markers.

In the absence of an extrinsic insult, preECs accounted for roughly 6% of all profiled cells in *ISC^{ts}/+* midguts and 12% of all profiled cells in *ISC^{ts}/rel^{RNAi}* midguts (Fig. 5.5A). Consistent with the extensive tissue renewal required to survive epithelial damage, ingestion of DSS caused a massive spike of preEC numbers in *ISC^{ts}/+* flies. After 48h, 74% of all profiled cells in DSS-treated *ISC^{ts}/+* guts expressed preEC markers, indicating accumulation of cells poised to replace dead and dying enterocytes (Fig. 5.5A). Notably, depletion of *rel* in stem cells resulted in an apparent failure to accumulate cells that expressed preEC markers. In marked contrast to midguts of *ISC^{ts}/+* flies, only 6% of all profiled cells from DSS-treated *ISC^{ts}/rel^{RNAi}* midguts expressed preEC markers (Fig. 5.5A), suggesting a possible failure of *rel*-deficient ISCs to generate preECs in response to damage.

My initial results established that DSS caused a greater proliferative response in *rel*-deficient ISCs than wild-type counterparts (Fig. 5.1-5.2). However, my transcriptional data indicated an apparent absence of preECs, prompting me to ask if the hyperproliferation observed in DSS-challenged, *rel*-deficient ISCs productively contributes to epithelial renewal. To address this question, I measured cell death and enteroblast numbers in midguts of flies that I challenged with DSS. To assess apoptosis, I stained DSS-treated *ISC^{ts}/+* and *ISC^{ts}/rel^{RNAi}* midguts with TUNEL and found that depletion of *rel* from ISCs significantly increased the amounts of TUNEL+ ISCs and epithelial cells (Fig. 5.5B), indicating that *rel* activity in ISCs supports intestinal epithelial cell viability.

Under normal conditions, ingestion of DSS prompts the accumulation of enteroblasts as the gut initiates proliferative responses that replenish dying enterocytes[202]. The absence of cells that express preEC markers upon ISC-specific *rel* knockdown prompted me to ask whether *rel*-deficient ISCs generated enteroblasts upon damage. To quantify enteroblast numbers in response to damage I used the *esg^{ts},UAS-CFP, Su(H)-GFP/rel^{RNAi}* line to mark enteroblasts with CFP and GFP while depleting *rel* from progenitors. I found that progenitor-specific loss of *rel* significantly reduced the number of enteroblasts upon DSS exposure when compared to wild-type controls (Fig. 4.5C-D). Taken together, my data show that NF-κB-deficient ISCs are more prone to cell death and are impaired in their ability to generate enteroblasts and renew the intestine after exposure to DSS.

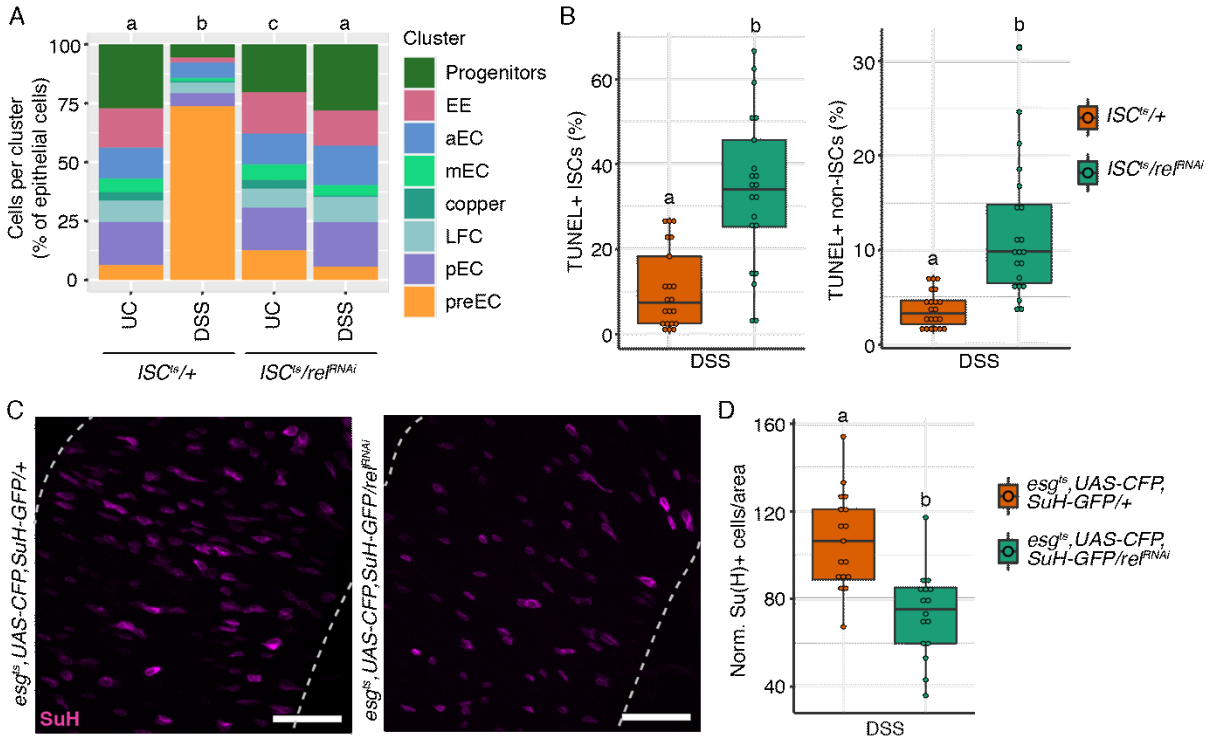

Figure 5.5 ISC-specific NF-κB is required for enterocyte renewal upon damage. (A) Cells per cluster as a proportion of total epithelial cells upon DSS challenge and ISC-specific *rel* knockdown. Significance found using chi squared followed by pairwise proportions tests. **(B)** Proportion of TUNEL positive cells within the YFP+ ISCs or YFP- non-ISC epithelial cells upon DSS challenge and ISC-specific *rel* knockdown. **(C)** Images of SuH+ enteroblasts upon DSS challenge and progenitor-specific *rel* knockdown. Scale bars = 25μm. **(D)** Number of SuH+ enteroblasts per area of the intestine upon DSS and progenitor-specific *rel* knockdown. Significance for B and D found using Students t test.

5.2.3 ISC-specific NF-κB alters Hippo and EGF/Ras pathway expression in response to damage

To resolve the mechanistic basis for NF-κB-dependent control of epithelial proliferative responses to damage, I compared the transcriptional responses of *ISC^{ts}/+* and *ISC^{ts}/rel^{RNAi}* midguts to DSS. First, I established cell-type specific transcriptional responses of a wild-type intestine to damage by identifying differentially expressed genes in an integrated data set generated from expression profiles of unchallenged and DSS-treated wild-type *ISC^{ts}/+* midguts. As expected, DSS ingestion resulted in lineage-specific impacts on expression of numerous genes involved in growth, differentiation, and cell migration (Fig. 5.6A). In particular, progenitors responded to DSS with decreased expression of Notch targets and increased expression of EGF, Hippo, JNK, and JAK-STAT

regulators, central elements of the proliferative epithelial repair pathway (Fig. 3.6B) [1]. Notably, DSS treatment also elevated expression of the Relish targets *pirk* and *PGRP-SC2* in progenitors (Fig. 3.6B), confirming that damage activates NF-κB in progenitors.

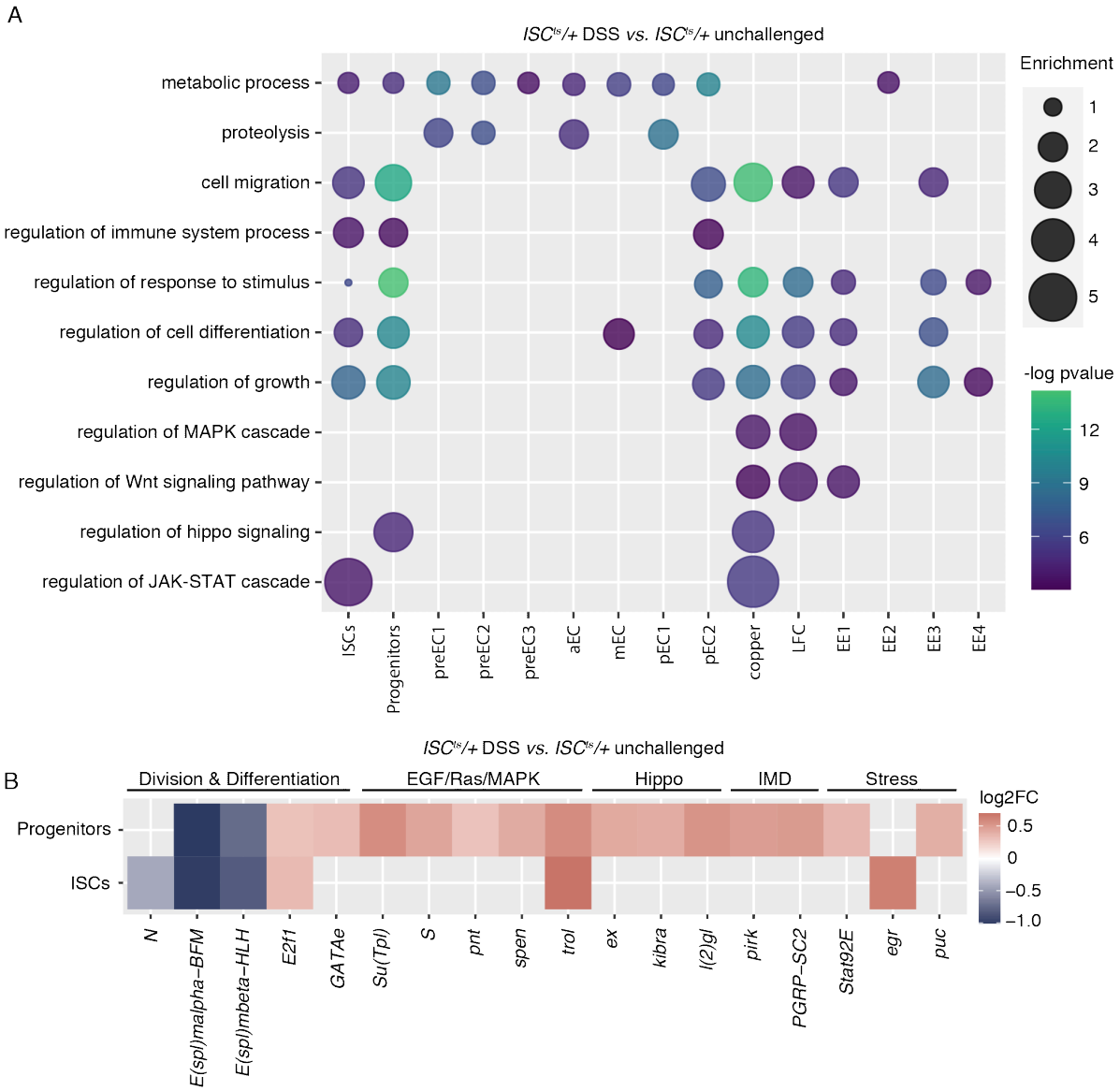

Figure 5.6 Wild-type intestines activate growth and stress response throughout the epithelium upon damage. (A) Biological process GO terms significantly altered in cell clusters from wild-type (*ISC^{ts}/+*) intestines in response to DSS challenge. Size of the dot represents the enrichment score for that GO term and the color of the dot represents the p value. **(B)** Specific genes differentially expressed in wild-type progenitors and YFP+ ISCs in response to DSS challenge. All genes shown are $p < 0.05$.

To determine how ISC-specific loss of NF-κB affects the gut response to damage, I then compared gene expression in DSS-treated *ISC^{ts}/+* and *ISC^{ts}/rel^{RNAi}* single-cell transcriptomes. Among progenitors, ISC-specific loss of *rel* significantly affected DSS-dependent expression of genes required for cell migration, differentiation, and stem cell proliferation (Fig. 5.7A). Conversely, loss of *rel* in ISCs primarily impacted DSS-dependent expression of genes linked with metabolism in enteroendocrine cells and enterocytes (Fig. 5.7A). This indicates that ISC-specific NF-κB knockdown primarily alters epithelial renewal in a cell-autonomous fashion, although I did find evidence that blocking *rel* in ISCs affects certain immune and growth genes in other intestinal cell types, including the Hippo pathway in copper cells (Fig. 5.8). A more detailed comparison of wild-type and *rel*-deficient progenitor transcriptomes showed that NF-κB depletion decreased expression of *relish* and its target genes, confirming successful knockdown of *rel* (Fig. 5.7B). In addition to effects on immune response regulators, NF-κB knockdown altered expression of multiple Hippo and EGF/Ras regulators in progenitors, including the EGF inhibitor *sprouty (sty)*, the signaling regulator *Star* (*S*), and the EGF/Ras-responsive transcription factor *pointed* (*pnt*) (Fig. 5.7B), suggesting possible links between NF-κB and EGF/Ras signaling in progenitors.

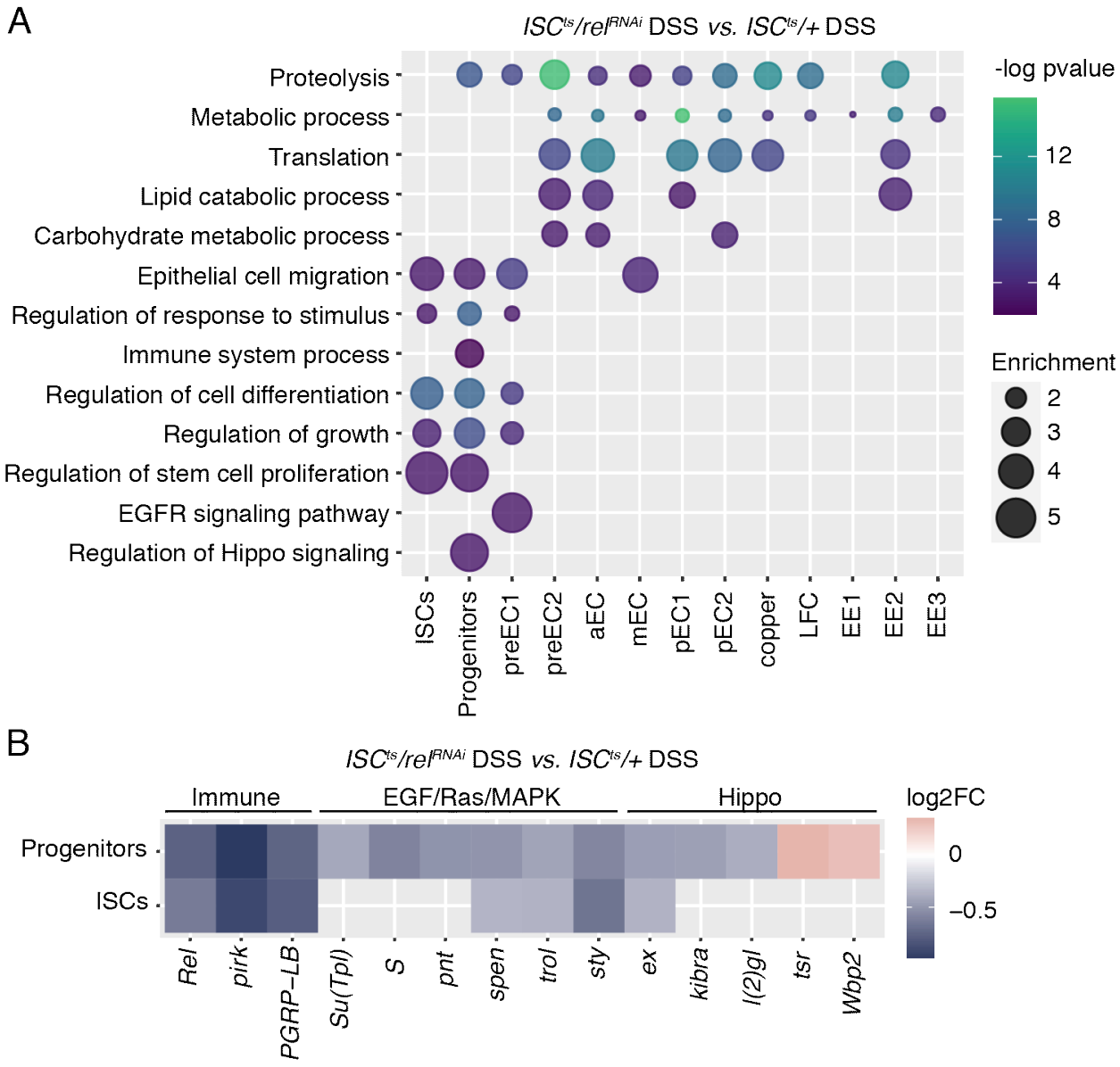

Figure 5.7 ISC-specific NF-κB alters Hippo and EGF/Ras pathway expression in response to damage. (A) Biological process GO terms significantly altered in cell clusters in DSS treated *ISC^{ts}/rel^{RNAi}* intestines compared to DSS treated *ISC^{ts}/+* intestines. Size of dot represents enrichment score and color of dot represents p value. **(B)** Specific genes differentially expressed in progenitors and YFP+ ISCs comparing *ISC^{ts}/rel^{RNAi}* DSS treated to *ISC^{ts}/+* DSS treated intestines. All genes shown are $p < 0.05$.

ISC^{ts}/relRNAi DSS vs. *ISC^{ts}/+* DSS

Cluster	Gene	pvalue	log2FC
Progenitors	*Myc*	2.02E-04	-0.45
Progenitors	*klu*	2.80E-03	-0.48
preEC1	*spi*	2.41E-05	0.90
preEC1	*esg*	2.60E-05	1.08
preEC1	*Dl*	1.56E-03	0.82
preEC1	*E(spl)malpha-BFM*	1.88E-03	0.27
preEC1	*Ras85D*	1.92E-03	0.83
preEC1	*l(2)gl*	1.96E-03	0.58
preEC1	*E(spl)mbeta-HLH*	2.69E-03	0.82
preEC1	*Egfr*	5.14E-03	0.49
preEC1	*sli*	1.62E-02	0.79
preEC2	*PGRP-SC2*	1.67E-13	-1.14
preEC2	*Rel*	6.77E-04	-0.28
preEC2	*Ubx*	2.26E-03	-0.38
preEC2	*Ras85D*	3.02E-02	-0.38
preEC2	*shn*	4.40E-02	-0.42
aEC	*E(spl)mbeta-HLH*	2.25E-07	-0.46
aEC	*PGRP-LE*	1.08E-02	0.34
aEC	*sty*	4.62E-02	-0.52
mEC	*l(2)gl*	4.05E-04	-2.47
mEC	*Socs36E*	2.26E-02	-1.93
mEC	*pnt*	3.29E-02	-1.63
mEC	*wts*	3.29E-02	-1.64
pEC1	*E(spl)mbeta-HLH*	2.00E-04	-0.52
pEC2	*PGRP-SC2*	1.22E-03	-0.89
pEC2	*Rel*	4.71E-03	-0.44
pEC2	*trol*	3.88E-02	-0.32
pEC2	*puf*	4.68E-02	-0.25
copper	*kibra*	1.27E-02	-1.21
copper	*Diap1*	4.21E-02	0.35
LFC	*E(spl)mbeta-HLH*	1.83E-06	-0.27
LFC	*sty*	7.83E-03	-0.30
LFC	*aPKC*	1.35E-02	0.34
LFC	*Myc*	4.28E-02	-0.39
EE1	*pan*	5.31E-05	-1.70
EE1	*hyd*	7.70E-04	-0.71
EE1	*goe*	7.70E-04	-1.81
EE1	*Diap2*	1.08E-03	-0.77
EE1	*ewg*	1.66E-02	-1.63
EE1	*dco*	2.11E-02	-0.27
EE1	*Psi*	2.34E-02	-0.63
EE1	*puf*	8.19E-03	-0.64
EE2	*Rel*	1.03E-05	-0.41
EE2	*PGRP-SC2*	1.64E-05	-1.07
EE2	*ago*	1.81E-05	-0.31
EE2	*kibra*	1.13E-03	-0.25
EE2	*cv-2*	1.57E-03	-0.41
EE2	*mod*	1.57E-03	-0.27
EE2	*mtd*	3.71E-02	0.62
EE3	*ebi*	3.91E-03	-0.87
EE3	*hep*	1.61E-02	-1.04
EE3	*dco*	1.81E-02	-1.12
EE3	*mod*	3.49E-02	-0.65
EE3	*esg*	4.28E-02	-0.60

log2FC

log2FC
1.25
1
0.75
0.5
0.25
0
-0.25
-0.5
-0.75
-1
-1.25
-1.5
-1.75
-2
-2.25
-2.5

Figure 5.8 ISC-specific NF-κB alters immune, growth and stress genes throughout the epithelium in response to damage. Differentially expressed genes across cell clusters involved in IMD pathway, ISC division, differentiation, stress and homeostasis. All genes shown are $p < 0.05$.

5.2.4 Ras acts downstream of NF-κB in ISCs to regulate intestinal repair

EGF/Ras controls proliferation, differentiation, and survival in progenitors[23,31,75,192]. Therefore, I asked if Ras acts downstream of NF-κB in the control of stem cell proliferation. To determine if NF-κB impacts Ras activity I first visualized phosphorylated ERK (pERK) in DSS-treated *ISC^{ts}/+* and *ISC^{ts}/rel^{RNAi}* midguts as a measure of Ras activation (Fig. 5.9A,B). With DSS exposure ~40% of wild-type ISCs are pERK+, however, this decreases to ~5% upon ISC-specific *rel*-depletion (Fig. 5.9D), suggesting that NF-κB is necessary for Ras activation in ISCs upon damage.

Next, I asked whether inhibition of Ras alone alters proliferation in response to DSS. Consistent with earlier reports[31,75,204], progenitor-wide inhibition of Ras (*RasN17/+;esg^{ts}/+*) blocked mitosis upon DSS exposure (Fig. 5.9E). However, inactivation of Ras in ISCs (*RasN17/+;ISC^{ts}/+*, Fig. 5.9C) increased proliferation in response to DSS when compared to wild-type intestines (Fig. 5.9F), a phenotype similar to ISC-specific *rel* depletion. In addition, and similar to the consequences of *rel* depletion, ISC-specific inactivation of Ras increased the number of apoptotic cells in intestines of DSS-treated flies (Fig. 5.9G), suggesting that Ras may act downstream of Relish in ISCs to control epithelial viability and proliferation responses to DSS.

Since *relish* knockdown prevented Ras activation, and ISC-specific Ras inhibition phenocopies several aspects of Relish depletion, I next asked if Ras acts downstream of NF-κB in the context of damage. To determine the relationship between NF-κB and Ras in ISCs I knocked down *rel* and activated Ras concurrently in ISCs of flies that I challenged with DSS (*ISC^{ts},rel^{RNAi}/+;RasV12/+*). Ras activation alone in ISCs had no effect on the number of cells undergoing apoptosis or mitosis upon DSS exposure (Fig. 5.9H-I). Conversely, ISC-specific depletion of *rel* increased the numbers of apoptotic cells and promoted proliferation in response to DSS (Fig. 5.9H-I). Interestingly, when I activated Ras in *rel*-deficient ISCs the apoptotic and hyperproliferative phenotype associated with *rel* knockdown was rescued, and instead, these intestines matched the levels of apoptosis and mitoses in a wild-type fly (Fig. 5.9H-I). Together these results indicate that NF-κB acts in ISCs to promote cell survival by activating the Ras pathway. In the absence of Relish, Ras activity is diminished which induces apoptosis and provokes ISCs to divide excessively to compensate for the lack of effective repair.

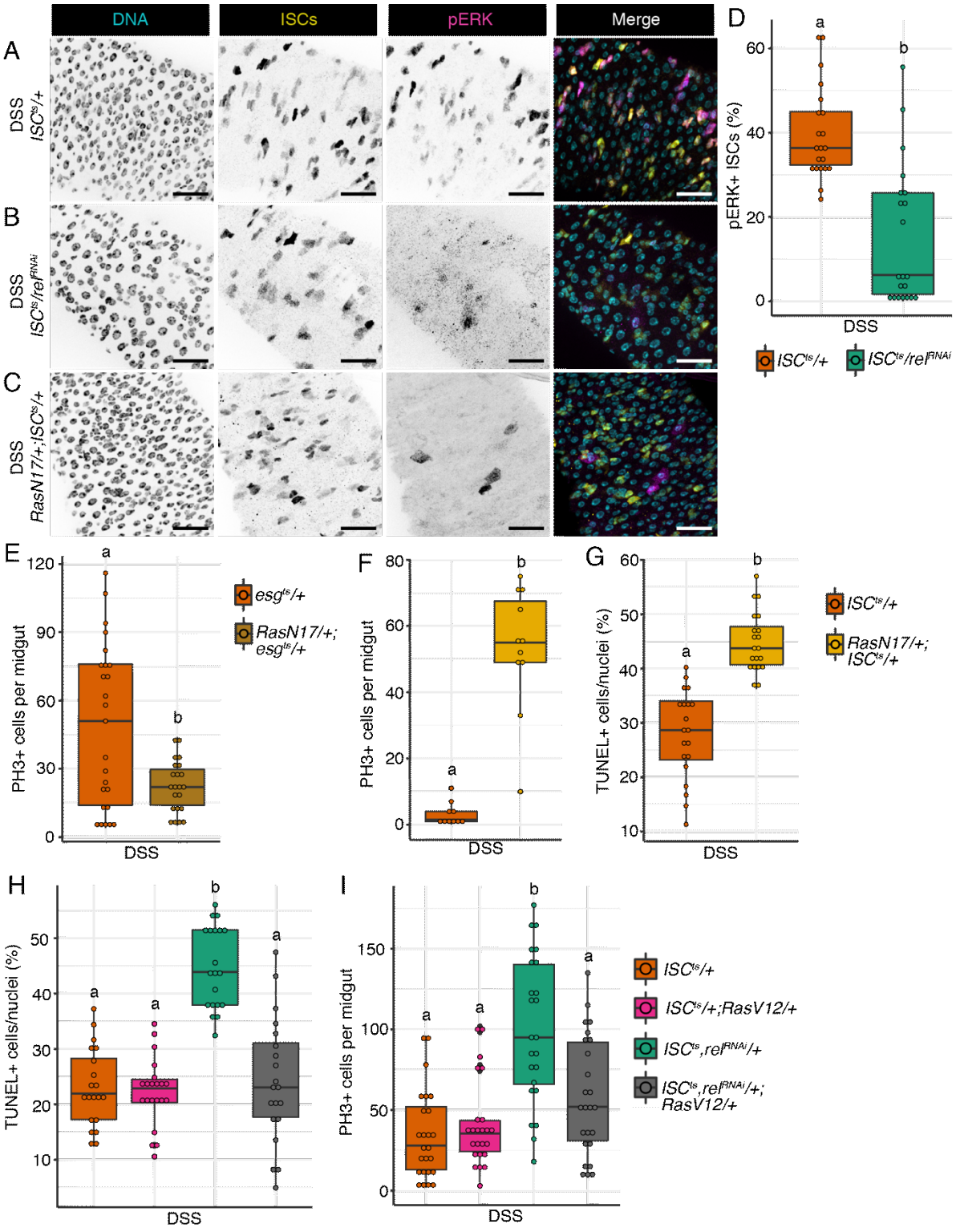

Figure 5.9 Ras acts downstream of NF-κB in ISCs to regulate intestinal repair. (A-C) Images of wild-type *ISC^{ts}/+* (A), ISC-specific *rel* knockdown (*ISC^{ts}/rel^{RNAi}*) (B) and ISC-specific Ras inhibition (*RasN17/+;ISC^{ts}/+)* after DSS treatment. DNA labelled by Hoescht (cyan), YFP+ ISCs (yellow) and

pERK (magenta) to monitor Ras activation. Scale bars = 25μm. **(D)** Proportion of YFP+ ISCs that are pERK positive upon DSS challenge and ISC-specific *rel* knockdown. **(E)** PH3+ cells per midgut upon DSS challenge and progenitor-specific Ras inhibition (*RasN17/+;esg^{ts}/+).* **(F)** PH3+ cells per midgut upon DSS challenge and ISC-specific Ras inhibition. **(G)** TUNEL+ cells per nuclei in posterior midguts upon DSS challenge and ISC-specific Ras inhibition. **(H)** TUNEL+ cells per nuclei in posterior midguts upon DSS challenge and ISC-specific *rel* knockdown (*ISC^{ts},rel^{RNAi}/+)* and Ras activation (*ISC^{ts}/+;RasV12/+)* alone or in conjunction (*ISC^{ts},rel^{RNAi}/+;RasV12/+).* **(I)** PH3+ cells per midgut upon DSS challenge and ISC-specific *rel* knockdown and Ras activation alone or in conjunction. Significance found for D-G using Students t test. Significance for H-I found using ANOVA followed by multiple pairwise Tukey tests.

5.3 Conclusions

Intestinal stem cells adapt their physiology in response to immune signals. For example, pattern recognition receptors act within the intestinal epithelium to modify ISC survival and proliferation in times of acute stress[170,171]. This highlights the importance of immune activity in ISC function. However, since the intestine is a heterologous tissue comprised of multiple specialist cell types it is important to accurately resolve the contributions of ISC-specific immune activity on gut function. As ISCs are essential for intestinal maintenance it is important we understand the contributions of ISC-intrinsic immune function in response to intestinal damage.

To examine links between ISC immunity and intestinal repair I depleted the IKK/NF-κB orthologs *kenny* and *relish* and monitored repair dynamics upon exposure to DSS. Using a combination of imaging, genetics and single-cell transcriptomics I uncovered an essential role for Relish in ISCs in regulating ISC survival and subsequent epithelial maintenance and proliferation. I found that ISC restricted loss of *rel* resulted in extensive stress dependent cell death throughout the epithelium and impaired the generation of premature enteroblasts poised to replace damaged and dying enterocytes. Lack of effective repair upon loss of *rel* results in compensatory ISC hyperproliferation and fly lethality. Mechanistically my data implicate Ras/ERK as a key mediator of Rel-dependent ISC viability. Loss of Ras activity phenocopies the survival and proliferative defects seen with loss of *rel* in ISCs. Furthermore, activation of Ras in ISCs rescued the hyperproliferative defect and cell lethality seen with *rel* depletion alone. Together, these observations suggest that

epithelial stress activates NF-κB in ISCs, leading to Ras/ERK activation, which promotes the viability of ISCs and their progeny, permitting the adequate generation of premature enterocytes and epithelial repair (Fig. 5.10). In the absence of *rel*, Ras/ERK activity is abolished, leading to cell death, ineffective repair, compensatory hyperproliferation and fly lethality (Fig. 5.10). This work deepens our understanding of how immune signals alter ISC function and highlights the importance of regulated immune activity for effective intestinal repair.

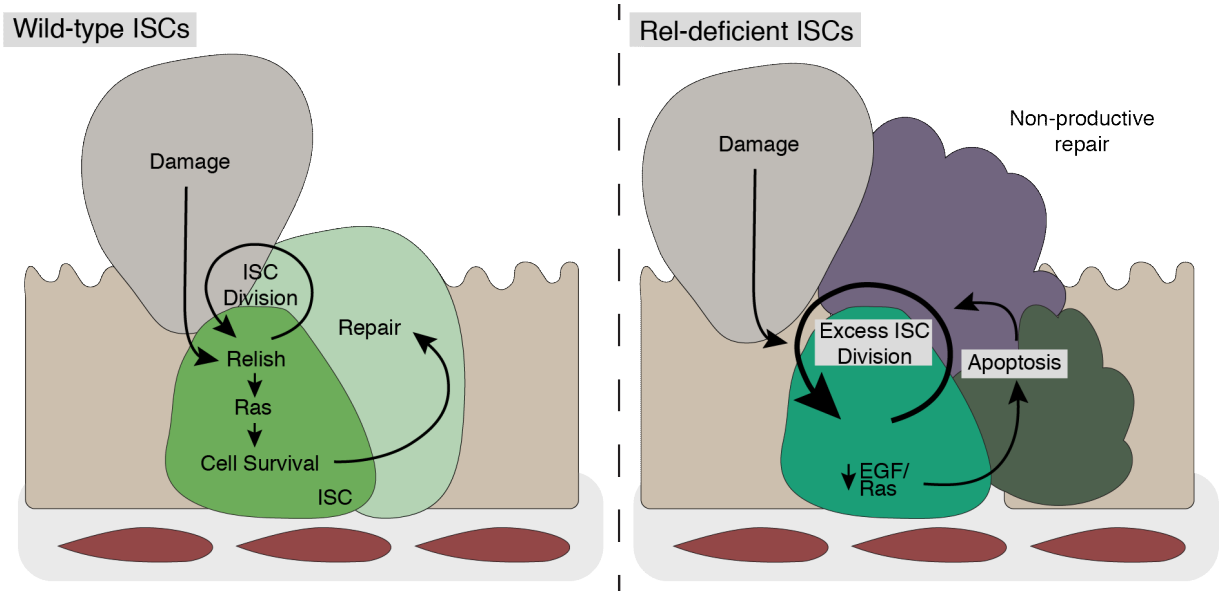

Figure 5.10 The NF-κB transcription factor Relish acts in stem cells to regulate intestinal repair. In wild-type ISCs, damage activates Relish which leads to Ras activation and promotes cell survival. ISCs and their progeny receive survival signals and effectively repair the intestine. Upon Relish depletion, Ras activity declines leading to excess apoptosis of ISCs and their progeny. Apoptotic cells send cues to ISCs to divide leading to hyperproliferation, non-productive repair and fly lethality.

Chapter 6

Discussion

This chapter contains content from the following sources:

- **Ferguson, M.**, Petkau, K., Shin, M., Galenza, A., Fast, D., & Foley, E. (2021). Differential effects of commensal bacteria on progenitor cell adhesion, division symmetry and tumorigenesis in the *Drosophila* intestine. *Development*. 148(5): 1-14
- Shin, M., **Ferguson, M.,** Willms, R. J., Jones, L. O., Petkau, K., & Foley, E. (2022). Immune regulation of intestinal stem cell function in *Drosophila*. *Stem Cell Reports*. 17(4):741-755.

6.1 Chapter 3 discussion

In chapter 3, entitled "Commensal bacteria modify intestinal stem cell adhesion, division symmetry and tumorigenesis", I identified commensal *L. brevis* as a potent stimulator of ISC divisions and tumor growth. In addition, I discovered a feed forward loop where Notch-deficient tumor growth enhances the growth of *L. brevis* in the intestine, which further fuels tumorigenesis. Mechanistically, I found that *L. brevis* altered the expression and subcellular localization of integrins in progenitor cells, leading to the symmetric expansion of ISCs and increased replicative capacity of the intestine. Together this demonstrates that individual bacterial species of the microbiome can have profound effects on ISC function.

6.1.1 Commensal bacteria and intestinal growth

Excess microbiota derived cues support the development of inflammatory diseases and hyperplastic expansion of cells that bear oncogenic lesions[13]. To understand how the microbiome causes progenitor dysplasia I measured growth in *Drosophila* intestines that were mono-associated with common *Lactobacillus* commensals. *L. brevis* and *L. plantarum* were chosen for this work as they have established roles in *Drosophila* intestinal homeostasis[93–96,101,205–207]. In general, my work matches literature that defines context-dependent effects of *Lactobacillus* commensals on juvenile growth, intestinal physiology and adult longevity. I identified *L. brevis* as a potent stimulator of intestinal tumorigenesis. Interestingly, *L. plantarum* did not promote tumor growth even though it grew to similar levels in the intestine. In support of this, *L. plantarum* had minimal effects on the transcriptome of progenitors, while *L. brevis* had a profound impact on progenitor gene expression, especially on genes involved in cell polarity and growth. This suggests that the strain of *L. plantarum* used fails to stimulate or actively inhibits ISC division and suggests that different *Lactobacillus* species have the potential to elicit opposing proliferative responses from ISCs.

It is not fully understood how the intestine distinguishes between different *Lactobacillus* species, although structural differences and bacterial metabolites are strong candidates. Although *L. plantarum* and *L. brevis* are both Gram-positive, they do have different cell wall compositions. For instance, *L. plantarum* contains DAP-type peptidoglycan, known activator of the IMD pathway and more commonly associated with Gram-negative bacteria, while *L. brevis* contains Lys-type peptidoglycan, which activates systemic Toll signaling[3]. Therefore, differential activation of IMD

and Toll may determine downstream ISC divisions. In support of this, *L. brevis* cell wall is sufficient for tumor growth. However, Toll is inactive in the *Drosophila* intestine and the IMD target genes PGRP-SC1a and PGRP-SC1b are highly expressed in progenitors in response to *L. brevis*. In addition, Imd is required for *L. brevis* mediated proliferation. Therefore, it seems *L. brevis* stimulates the IMD pathway and this activation is required for *L. brevis*-induced ISC divisions (Fig. 6.1). However, given that *L. brevis* contains Lys-type peptidoglycan it is unclear how *L. brevis* activates IMD to elicit such a response and whether IMD activation differs between *L. brevis* and *L. plantarum*.

In addition to peptidoglycan differences, *L. brevis* also differs from *L. plantarum* with its use of an S-layer[208,209]. S-layers assemble at the outermost layer of the bacterial cell and form a two-dimensional crystalline array of S-layer protein[210]. S-layers are found on Gram-positive, and Gram-negative bacteria, including pathogens such as *Clostridium difficile* and *Bacillus anthracis*, and are quite prevalent in archaea[210]. S-layers function to facilitate bacterial adherence, interact with innate immune receptors such as TLR4, prevent complement binding, and resist bacteriophage predation[211]. For instance, work on *C. difficile* demonstrated that its S-layer proteins induced dendritic cell maturation and the production of TNFα in a TLR4 dependent manner[212]. This suggests that S-layer proteins themselves modulate immune activity and are potential mediators of immune activation in the intestine. However, it is unclear whether the S-layer of *L. brevis* is required for immune modulation or ISC divisions in *Drosophila*.

Although the cell wall of *L. brevis* was sufficient for tumor growth it is possible that differences in microbial metabolites modulate ISC division in *L. brevis* compared to *L. plantarum*. For instance, *L. brevis* derived uracil promotes the generation of ROS through the enzyme Duox, a process that damages the intestine and activates growth pathways to initiate repair[95,97–99]. Likewise, *L. plantarum* releases lactate which stimulates ROS production via the enzyme Nox, leading to intestinal dysplasia[94,96,206]. Interestingly, while others have found growth promoting effects of *L. plantarum*, myself and others in our lab found that *L. plantarum* does not promote homeostatic or tumorigenic growth[101]. It is possible our strain of *L. plantarum* isolated from the fly intestine differs from the strains used in other studies. Regardless, *L. brevis* and *L. plantarum* produce distinct sets of metabolites capable of altering intestinal physiology, although it is unclear whether these differences reflect tumorigenic capacities of each bacteria.

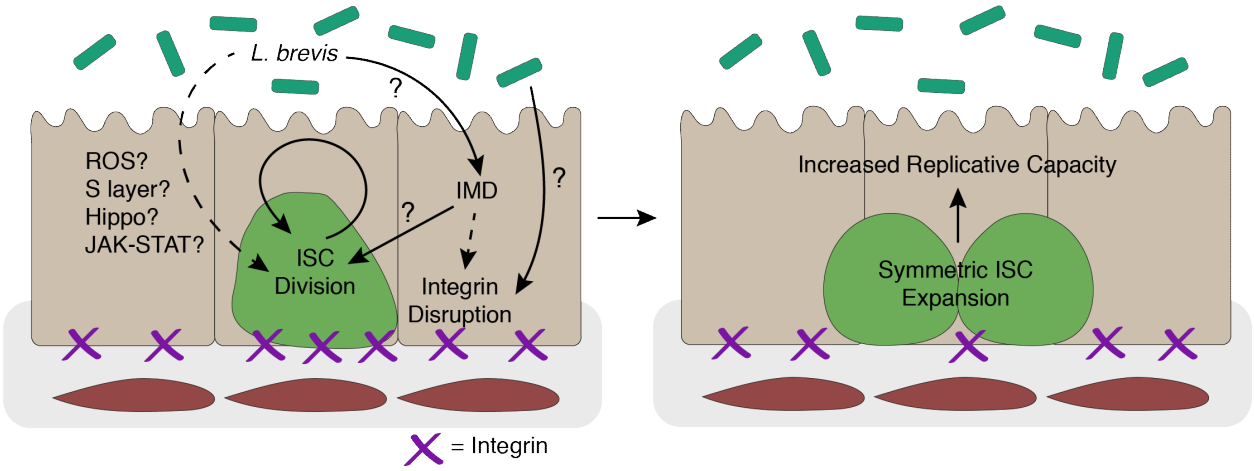

Figure 6.1 *L. brevis* disrupts integrins and promotes ISC symmetric divisions. *L. brevis* activates ISC divisions in an IMD-dependent manner. *L. brevis* may also disrupt integrins via IMD. *L. brevis* mediated integrin disruption causes ISC symmetric divisions and expands the ISC pool. *L. brevis* potentially alters ISC divisions through additional mechanisms.

6.1.2 Bacterial effects on integrins

To determine how *L. brevis* affects intestinal proliferation, I characterized mRNA levels in midgut progenitors of flies inoculated with *L. brevis*. I observed significant effects of *L. brevis* on the expression and subcellular localization of integrins, crucial regulators of stem cell niche interactions and stem cell maintenance[36,44,45,213–217]. Typically, integrins accumulate at basolateral margins on intestinal progenitors and anchor interphase progenitors to the extracellular matrix. In many tissues, including the fly intestine, integrins organize the stem cell division plane by orienting the mitotic spindle. Progenitors mainly divide at angles greater than 20° to the basement membrane, leading to asymmetric divisions, after which basal daughter cells remain in the niche and retain stemness, whereas apical daughters exit the niche and differentiate[27,193]. Approximately 20-40% of divisions in the young adult intestine under homeostasis occur symmetrically, yielding clonal lineages of stem cells or enteroblasts[35,37,193,194]. Over time, enteroblast clones differentiate into mature enterocytes that eventually die. However, clonal stem cell lineages retain the capacity to grow and establish regional dominance within the epithelium. In some cases, symmetric divisions facilitate adaptive responses to environmental fluctuations allowing the intestinal environment to tune proliferative needs to extrinsic factors. For instance, rapid changes in nutrient availability or

ingestion of toxic doses of paraquat increase the frequency of symmetric divisions that expand the stem cell pool, allowing for a rapid regenerative response[35,193]. Similarly, integrin depletion from intestinal progenitors alters division angles, increases symmetric divisions and promotes expansion of ISCs[36]. Therefore, *L. brevis*-mediated integrin depletion may be a mechanism of adaptive growth in the intestine. Because my focus was on intestinal progenitors it is unclear whether *L. brevis* also alters integrins in mature epithelial types. As integrin loss in enterocytes causes delamination and subsequent stress-induced tumor growth[68], it is important to understand whether the actions of *L. brevis* on integrins is specific to progenitors or if enterocytes are also affected.

How *L. brevis* disrupts integrins and promotes stem cell divisions requires clarification. As stem cells derive cues from the surrounding epithelium to direct their growth, it is likely that mature epithelial cells, such as enterocytes, sense *L. brevis* and transduce signals to ISCs to promote growth. My transcriptional profiling of progenitors suggests that, in addition to changes in integrin expression, *L. brevis* alters mRNA levels indicative of Hippo inhibition and JAK-STAT activation, pathways known to mediate regenerative proliferation in response to intestinal damage or the microbiome[5,6,73,74,76,203,218,219]. In addition, *L. brevis* activates the expression of IMD target genes in progenitors and *L. brevis* fails to induce ISC divisions in *imd* mutants. This suggests that the IMD pathway is required for *L. brevis* mediated growth. This raises the possibility that IMD impacts integrins in the intestine. In support of this, exposure of insect cells to MAMPs upregulates integrins in an IMD dependent manner *in vitro*[87]. Interestingly, changes in integrin expression and other cytoskeletal genes in response to bacterial MAMPs is dependent on Tak1 and JNK, but not Relish[87]. This suggests that IMD activation alters integrin expression through JNK. In addition, data from chapter 4 shows that IMD inhibition in progenitors leads to increased integrin expression (Fig. 4.8E). This is in contrast to findings *in vitro* where IMD activation increased integrin expression, however these discrepancies may be due to the differential requirements for integrins by stem cells within a tissue versus cells in a dish. Nevertheless, our *in vivo* data suggest that IMD activity in progenitors acts to inhibit integrin expression. Therefore, I speculate that *L. brevis* activates IMD to inhibit integrin expression, leading to the symmetric expansion of ISCs (Fig. 6.1). In parallel with, or downstream of IMD, *L. brevis* activates growth and stress pathways and promotes ISC divisions, leading to intestinal proliferation and exacerbation of tumorigenesis (Fig. 6.1). However, a direct link between *L. brevis*, IMD and integrins has yet to be established.

6.1.3 Intestinal tumors and bacterial growth

Quantification of host-associated bacteria suggests that physiological disruptions associated with Notch deficiency promote the accumulation of *L. brevis* in the intestine, which fuels continued growth of Notch-deficient tumors. A similar feed-forward loop was recently described in a BMP-deficient tumor model[61], suggesting a conserved relationship between tumor growth and microbiota expansion in flies. My transcriptional data raise the possibility that inactivation of Notch partially increases *L. brevis* loads by suppressing the expression of IMD pathway regulators (Fig. 6.2). Along these lines, flies mutant for negative regulators of the IMD pathway have increased bacterial abundance and intestinal hyperplasia[109]. However, given the massive increase in bacterial numbers observed upon Notch knockdown compared with the more moderate increases observed associated with *imd* mutants, I hypothesize that additional mechanisms underlie the increased *L. brevis* loads seen upon Notch deficiency.

As Notch is required for proper intestinal differentiation, the mis-differentiated epithelium upon Notch knockdown may be incapable of fully limiting bacterial accumulation in the intestine. Notch inactivation changes the intestinal composition and possibly gene expression of differentiated cells in the intestine[68]. Altered intestinal composition may introduce environmental niches that allow for better bacterial growth, adherence or survivability. For instance, Notch controls the differentiation of copper cells, specialized cells in the middle midgut that attenuate bacterial growth by establishing a stomach-like region of low pH[22,220]. Thus, Notch-deficiency impairs the ability of the intestine to eradicate bacteria in the copper cell region due to perturbed acidification, leading to bacterial overgrowth (Fig. 6.2). In addition to the lack of copper cells, Notch inactivation increases the number of enteroendocrine cells in the intestine, important producers of peptide hormones that regulate feeding behaviour and fly metabolism[198,199]. Therefore, it is possible that the increased abundance of enteroendocrine cells alters the metabolic profile of the intestine in such a way that favours *L. brevis* growth (Fig. 6.2). Alternatively, increased numbers of enteroendocrine cells and the increased energy demands of tumor growth in the intestine may trigger flies to eat more, thus ingesting more bacteria from the food (Fig. 6.2). Together, I speculate that Notch-deficient intestines are impaired in their ability to control bacterial abundance in the intestine due to a multifactorial network of perturbed immunity and mis-differentiation of mature epithelial cells (Fig. 6.2).

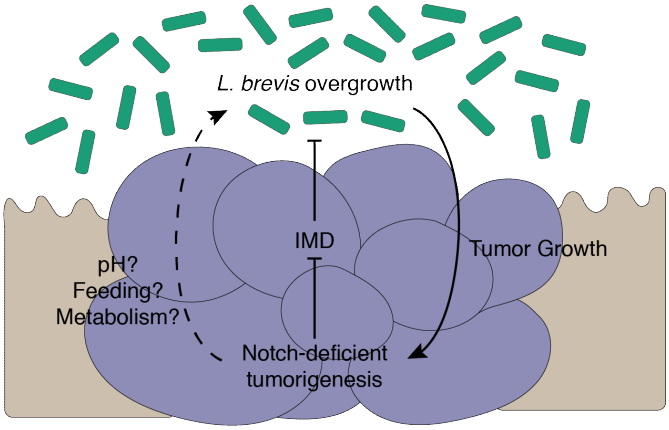

Figure 6.2 Feed forward loop between tumorigenesis and bacterial growth. Notch-deficient tumors repress IMD activity, resulting in *L. brevis* overgrowth. *L. brevis* overgrowth fuels tumor growth. Notch-deficient tumors may also promote *L. brevis* overgrowth via additional mechanisms.

6.2 Chapter 4 discussion

In chapter 4 entitled "The IMD pathway acts in progenitors to promote intestinal proliferation, differentiation and tumorigenesis" I characterized the role of the IMD pathway in intestinal progenitor cells. I found that chronic activation of the IMD pathway in progenitors resulted in intestinal hyperplasia and exacerbated Notch-deficient tumorigenesis. In addition, inhibition of IMD in progenitors decreased proliferation and altered the differentiation and maturation of epithelial cells, leading to decreased enteroendocrine cell numbers. Collectively, these data highlight the importance of regulated immune signals in progenitors in the context of homeostasis and tumorigenesis.

6.2.1 Progenitor-specific IMD promotes intestinal hyperplasia and tumorigenesis

Innate defenses mitigate threats from pathogenic bacteria but chronic inflammation is associated with increased risk of intestinal diseases such as colorectal cancer[195]. To determine effects of immune activation exclusively in intestinal progenitors I compared intestinal physiology of wild-type *Drosophila* to those with a constitutively active IMD pathway in progenitor cells. Persistent IMD activation in progenitors resulted in intestinal hyperplasia without a significant shift in microbiome composition. This indicates that IMD activation promotes progenitor dysfunction directly, not as a consequence of dysbiosis. In agreement with this, mature cells types in the intestine produce antimicrobial peptides in response to infection but stem cells do not[25]. This indicates that IMD does not have antimicrobial functions in progenitors, instead it modulates ISC divisions. Along

these lines, IMD activation recapitulated certain transcriptional events that occur in response to bacteria. For instance, conserved regulators of growth and differentiation such as JAK-STAT and Notch pathways were perturbed upon IMD activation and similar effects have been noted in response to both pathogenic and commensal microbes[5,6,83]. This indicates that microbes activate IMD in progenitors to modify growth and differentiation.

Given the changes to Notch pathway components upon IMD activation I determined whether IMD activation altered the growth of Notch-deficient tumors. Here, IMD activation exacerbated tumorigenesis and even promoted tumor growth in flies without a microbiome. This suggests that IMD activation in progenitors is sufficient for Notch-deficient tumorigenesis (Fig. 6.3). However, we still do not know how IMD promotes hyperplasia and subsequent tumor growth. Our transcriptional analysis suggests growth pathways such as Ras, Insulin, JNK, Wnt or JAK-STAT may be involved. Data from chapter 5 suggests that Ras acts downstream of Relish in ISCs (Fig. 5.9) and given the important role Ras has in tumor growth[77,156] is a likely candidate for future experimentation. Regardless of the lack of mechanistic insight, these observations have important implications in the context of intestinal ageing, immune activity and tumorigenesis. As flies age the microbiome becomes dysbiotic and immune activity increases in the intestine[22,190]. In addition, spontaneous accumulation of mutations at the Notch locus is linked to age-dependent development of intestinal tumors[71]. Therefore, I speculate that age-dependent increases in IMD activity promote tumor growth in wild-type flies.

6.2.2 Progenitor specific IMD and intestinal proliferation

Highly conserved growth pathways such as EGF, JAK-STAT and WNT direct the proliferation of ISCs in vertebrates and invertebrates[18,19,21,30,66,121,221]. In contrast, the role of innate immune pathways on progenitor function and epithelial homeostasis is unclear. In flies, IMD has context dependent effects on proliferation. For instance, *V. cholerae* infection blocks ISC divisions in an IMD-dependent manner while trypanosome infection induces IMD-dependent proliferation[103,124,126]. In some cases, proliferative changes are partly due to microbiome changes. For example, *relish* mutants have increased proliferation, but this change does not occur in germ-free flies, which suggests mutation of *relish* alters the microbiome in such a way that promotes proliferation[5]. However, Relish controls the expression of over 50% of the microbiome

induces genes, including those involved in ISC divisions, and pro-growth roles for Relish have also been elucidated[6]. Here, overexpression of the peptidoglycan receptor PGRP-LC in enterocytes promotes ISC divisions in a Relish dependent manner[110]. Presently, we report a pro-growth role for the IMD pathway in progenitors. Blockage of IMD or knockdown of downstream pathway components, including Relish, in progenitors reduced intestinal proliferation in aged flies. Interestingly, these effects are mediated through ISCs, not enteroblasts. This indicates that ISCs respond to microbial stimuli and activate immune pathways to regulate ISC function cell autonomously, however the mechanisms remain unclear (Fig. 6.3).

In addition to cell autonomous mechanisms for IMD-dependent ISC divisions, our data propose that IMD impacts intestinal composition, which may indirectly alter ISC dynamics. For example, IMD inhibition in progenitors decreases the number of enteroendocrine cells and increases the abundance of enteroblasts. As enteroendocrine cells and enterocytes produce paracrine factors that influence ISC fate[1,30,50,75,222,223], it is possible that the altered intestinal differentiation upon IMD inactivation produces an intestinal landscape with perturbed growth and stress signaling. Our transcriptional profiling also describes how IMD alters the maturation of enteroblasts and the expression of peptide hormones in enteroendocrine cells. Together, IMD may not only alter cell composition but also the functionality of mature cell types, with potential consequences for ISC divisions.

In the context of ageing, IMD activity rises in the *Drosophila* intestine and correlates with ISC dysfunction and hyperplastic phenotypes[22,190]. Since hyperplasia does not occur upon ISC specific IMD inhibition it is likely that in wild-type flies, the hyperplastic phenotype associated with age is due to increased immune activity in ISCs. However, it is unclear whether immune activity changes specifically in ISCs over the flies lifetime. In addition, it is unknown how microbial signals reach ISCs to modify their function. ISCs are basally located in the epithelium and do not make frequent contact with the gut lumen and the abundance of bacterial pattern. However, peptidoglycan is not confined to the lumen in flies or vertebrates. Peptidoglycan crosses the epithelial barrier, even in an undamaged healthy intestine, and multiple mechanisms exist to prevent peptidoglycan accumulation in the fly hemolymph[109,224–227]. Therefore, it is likely that passive or active transport mechanisms allow the passage of bacterial patterns from the lumen to basally located ISCs. Along these lines, several vertebrate TLRs have a specific apical-basal localization in

different contexts. For instance, TLR4 is enriched apically in villi but basolaterally in crypts of the human colon[228]. This indicates that mature epithelial cells detect MAMPs in the lumen while progenitors detect basally located MAMPs that have crossed the epithelial barrier. Apical and basal stimulation also leads to the activation of differential downstream effectors of TLR activation. For example, apical stimulation of TLR9 leads to JNK activation, whereas basolateral TLR9 stimulation leads to NF-κB activation and IL-8 secretion[229]. Together this suggests that mechanisms to detect and respond effectively to basally located MAMPs are evolutionarily conserved and these responses may differ from the detection of apically located MAMPs. This may represent an adaptive measure for intestines to respond effectively to invading pathogens while tolerating the commensal microbes in the lumen.

The fly intestine has functionally specialized regions that regulate distinct aspects of digestion and absorption. IMD pathway components and downstream targets of IMD activation are also regionally defined. For instance, activation of IMD in the anterior midgut results in antimicrobial peptide production, while activation in the posterior midgut results in the expression of genes that dampen IMD signals[20,89–91]. Along these lines, loss of IMD inhibitors or overexpression of PGRP-LC in enterocytes increases proliferation in the posterior midgut[109,110]. This suggests that antibacterial defenses predominate in the anterior intestine while the posterior midgut is designed to tolerate microbes and limit IMD dependent proliferation. We found that IMD inactivation in progenitors reduced proliferation and hyperplasia in the posterior midgut, however it is unclear whether IMD acts in progenitors from the anterior or middle midgut to control proliferation (Fig. 6.3). Since the posterior midgut is the most highly proliferative area of the intestine and IMD negative regulators act there to restrict IMD dependent proliferation, it is likely that IMD acts mainly in ISCs of the posterior midgut to promote growth, however further experimentation is required to elucidate the functions of IMD in ISCs along the entire rostral-caudal axis.

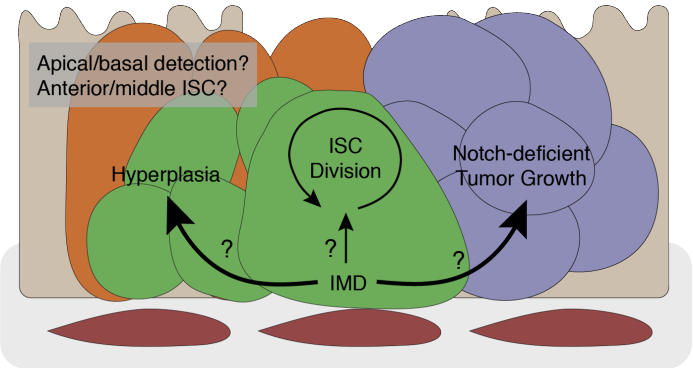

Figure 6.3 IMD in progenitors promotes intestinal growth. IMD promotes ISC divisions under homeostasis. Hyperactive IMD (thicker arrows) causes intestinal hyperplasia and promote tumor growth. Mechanism and specifics of ISC immune activation are unknown.

6.2.3 Progenitor-specific IMD and intestinal differentiation

Intestinal differentiation is governed by evolutionarily conserved pathways such as Notch, and immune activity modulates Notch to alter intestinal differentiation[66,230]. For instance, commensal bacteria stimulate enterocyte differentiation and *relish* mutants have decreased expression of Notch genes[6]. This suggests that bacteria act through the IMD pathway to stimulate Notch and promote enterocyte lineage development. In contrast to these epithelium wide perturbations, we found that active IMD in progenitors promotes the expansion of enteroendocrine lineages. Along these lines, IMD inhibition in progenitors leads to increased expression of Notch pathway targets and increased numbers of enteroblasts. This suggests that IMD in progenitors inhibits Notch to promote enteroendocrine differentiation. Interestingly, data from chapter 5 show that knockdown of *relish* in progenitors has the opposite effect and instead decreases the number of enteroblasts. In agreement, a recent study shows that *relish* knockdown in progenitors increases enteroendocrine numbers in the intestine[100]. It is possible that the discrepancies between these experiments is the mode of IMD inactivation and consequences on downstream signaling. For instance, IMD inactivation would have downstream consequences on JNK and Relish dependent signaling, while *relish* knockdown would not affect IMD-dependent JNK activation. Therefore, I speculate that IMD-dependent JNK signaling inhibits Notch to promote enteroendocrine differentiation while Relish signaling promotes Notch and enterocyte development (Fig. 6.4).

How IMD alters differentiation is unclear. Recent work has identified the Notch ligand Delta as a target gene of Relish in intestinal progenitors[100]. This suggests that Relish induces the expression of Delta on ISCs to activate Notch and promote enterocyte differentiation (Fig. 6.4). In addition, Sox21a, a regulator of ISC division and differentiation, is also a target of Relish in

progenitors[100]. Interestingly, the IMD antagonist Caudal alters differentiation through Sox21a[231]. Similar to Sox21a overexpression, depletion of Caudal from intestinal progenitors leads to an accumulation of premature enterocytes. Mechanistically, Caudal depletion in progenitors activates the JAK-STAT pathway to increase Sox21a expression and promote Notch[231]. Since Sox21a is a target gene of Relish and Caudal is a known repressor of Relish dependent signaling it is possible that the effects of Caudal depletion are mediated through Relish. However, the links between Caudal, Relish, Sox21a and differentiation require further clarification.

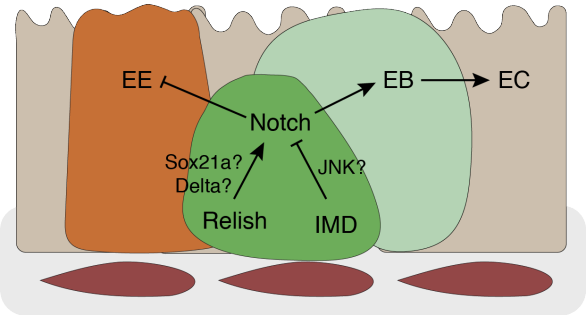

Figure 6.4 IMD in progenitors alters intestinal differentiation. Relish in progenitors activates Notch to promote enteroblast (EB) and enterocyte (EC) differentiation potentially via Sox21a or Delta. IMD inhibits Notch to promote enteroendocrine (EE) differentiation potentially through JNK.

6.3 Chapter 5 discussion

In chapter 5 entitled "The NF-κB transcription factor Relish acts in stem cells to regulate intestinal repair" I determined how Relish depletion in progenitors alters the intestinal response to damage. I found that *relish* knockdown in progenitors or ISCs results in hyperproliferation in response to DSS. Furthermore, *relish* depletion increased epithelial cell death and disrupted enterocyte renewal, resulting in ineffective repair and host lethality. Mechanistically, Ras/ERK acts downstream of Relish in ISCs to promote cell survival and repair. These observations underscore the importance of immune signaling in ISCs for appropriate damage repair responses.

6.3.1 ISC-specific NF-κB promotes intestinal repair

Effective intestinal repair requires the coordinated activation of cellular growth, stress and survival pathways[1]. Immune activity is known to impact intestinal repair effectiveness; however, it is unclear whether immune activation is required specifically in ISCs to modulate repair. In mice, germline encoded pattern recognition receptors, such as TLR4 and NOD2, are enriched in ISCs and modify survival and proliferation during periods of acute stress[170–172]. Similarly, I found that ISC-

specific loss of Relish resulted in extensive stress-dependent ISC death that impaired damage-responsive generation of premature enterocytes. The inability to replace dead and dying enterocytes by Relish deficient ISCs provokes a hyperproliferative response in an attempt to facilitate repair, however effective repair does not occur which leads to host lethality. Together this suggests that NF-κB acts in ISCs to promote cell survival and the generation of premature enterocytes for effective intestinal repair (Fig. 6.5). This is in contrast to the role of Relish in enterocytes where it promotes cellular delamination in response to pathogenic microbes[110]. Along these lines, the AMP Defensin promotes cell death of tumors that are sensitized by TNF, demonstrating that immune activation alters survival dynamics of oncogenic lesions[232]. Similarly, in vertebrates, NF-κB can either promote or inhibit apoptosis depending on the cellular context, however a pro-survival role is most often attributed to NF-κB[233]. For instance, treatment of mouse fibroblasts and macrophages with TNFα induces apoptosis of *RelA-/-* (p65 protein of the NF-κB heterodimer) but not wild-type cells, indicative of a pro-survival role for NF-κB[234]. In addition to cell survival, Relish in progenitors alters differentiation in *Drosophila* intestines. For instance, Relish depletion from progenitors decreases enteroblasts and increases enteroendocrine numbers[100]. Therefore, it is possible that defective enterocyte renewal upon ISC-specific Relish knockdown is due to a combination of cell death and inadequate enterocyte differentiation (Fig. 6.5).

Interestingly, Relish can either promote or inhibit ISC divisions in different contexts. For instance, as seen in chapter 4, progenitor-specific Relish knockdown inhibits ISC divisions during homeostatic ageing while in chapter 5, ISC-specific Relish knockdown provokes ISC hyperproliferation in response to acute stress. These opposing roles for Relish indicate that ISCs must appropriately balance NF-κB activity to limit age-dependent proliferation while allowing for effective repair responses to acute stress. Similar opposing phenotypes have been noted in the literature. For instance, in one scenario progenitor-specific *relish* knockdown increased proliferation in flies fed LB bacterial broth[124], while in a separate set of experiments *relish* depletion decreased proliferation in flies fed a standard diet[126]. It is possible these discrepancies are due to differential roles for Relish under homeostasis and during times of stress. For instance, feeding flies exclusively LB broth results in fly mortality after approximately 6 days[102]. Therefore, a broth diet likely stresses the intestine and activates the need for Relish in ISCs for effective repair, while on standard food there is little damage and Relish instead promotes homeostatic proliferation.

Together, NF-κB in ISCs promotes homeostatic and limits stress dependent proliferation, however the mechanisms behind the differential downstream impacts of Relish on proliferation are unclear. My data suggests that Relish acts through Ras/ERK to promote cell survival and limit proliferation in response to acute damage, but it is unknown if Relish acts similarly through Ras/ERK during homeostasis to control intestinal growth. In support of this, IMD activation in progenitors results in perturbed expression of Ras signaling components in the absence of damaging chemicals (Fig. 4.3E). In addition to Ras/ERK, I also identified robust alterations to the expression of Hippo pathway components upon ISC-specific Relish knockdown in response to intestinal injury. Hippo is known to act both in enterocytes and progenitors to regulate proliferation cell non-autonomously and autonomously in response to damage[1,73,74,203,223,235]. Interestingly, EGF/Ras and JAK-STAT pathways act downstream of Hippo in both enterocytes and progenitors to mediate proliferative effects and the Hippo pathway transcription factor Yorkie is required in progenitors to promote proliferation in response to DSS[73,203,219,223]. Given the alterations to the Hippo pathway upon ISC-specific Relish depletion and the corresponding inhibition in Ras, it is possible that Relish acts through Hippo to mediate downstream effects on Ras activation, cell survival and repair, however further experimentation is required to determine the role of Hippo in Relish mediated repair responses.

6.3.2 Crosstalk between NF-κB and Ras/ERK signaling in ISCs

To determine factors that act downstream of Relish in ISCs to impact intestinal repair I compared expression of growth and stress regulators in progenitors upon DSS exposure and *relish* knockdown. I found that Relish controlled the expression of multiple EGF/Ras regulators and that Relish is required in ISCs for ERK phosphorylation in response to DSS. Interestingly, inactivation of Ras specifically in ISCs caused hyperproliferation and increased apoptosis in response to DSS, phenotypes similar to Relish depletion. Additionally, I found that genetic activation of Ras exclusively in stem cells overrides the hyperproliferative and pro-apoptotic phenotype associated with Relish-deficiency. In agreement with this, active Ras in human colorectal neoplasms correlates with decreased levels of apoptosis suggesting that Ras activation has an evolutionarily conserved pro-survival role in the intestinal epithelium[236,237]. From these results, I speculate that epithelial stress engages NF-κB in ISCs, leading to Ras/ERK activation, which promotes stem cell viability, attenuates

stem cell proliferation and permits generation of adequate premature enterocyte numbers to protect the interior from excess damage (Fig. 6.5).

Currently, it is unclear how Relish activates Ras/ERK, or whether links between cell viability and proliferation are correlative or causative. Epithelial cell death triggers stress dependent ISC divisions to repair the damage and maintain barrier integrity[1]. Although cell death positively correlated with increased ISC divisions upon Relish depletion, it is possible that divisions are a consequence of additional ISC intrinsic alterations. For instance, Ras/ERK may directly suppress ISC divisions instead of proliferation being a product of increased cell death, however further investigation is required to determine the exact role of Ras/ERK specifically in ISCs. Interestingly, Ras and NF-κB activity have evolutionarily conserved links. In vertebrates, NF-κB acts downstream of Ras to protect from apoptosis and potentiate proliferation[238]. Similarly, in *Drosophila*, activation of Ras in wing discs and salivary glands increases the expression of IMD target genes[239]. Conversely, infection activates Ras in intestinal progenitors where it suppresses IMD in the intestine through expression of the negative regulator Pirk[240]. These observations indicate that Ras activity modulates NF-κB and can either promote or suppress NF-κB dependent on the tissue or context. However, to date there is little evidence that Ras acts downstream of NF-κB, although EGF signaling is activated in response to immune stimulation. For instance, TLR4 is required in the intestinal epithelium of mice to induce EGF and promote growth in response to DSS[140]. Similarly in *Drosophila*, oral infection with pathogenic microbes stimulates both IMD and EGF to promote enterocyte shedding and ISC proliferation[110] while *relish* mutants have decreased expression of EGF regulators[6]. However, it remains unclear how immune activation and NF-κB in ISCs alters EGF/Ras/ERK in a cell autonomous fashion specifically in ISCs.

These results also raise an interesting aspect of the role of the EGF/Ras/ERK pathway in fly midgut progenitors. My data agree with earlier reports that progenitor-wide inhibition of Ras blocks the proliferative burst typically seen in midguts of flies exposed to noxious agents[31,75,204]. However, I found that inhibition of Ras exclusively in ISCs significantly increases the rate of damage-responsive proliferation. These observations raise the possibility that Ras alters proliferation via different mechanisms in ISCs and enteroblasts. Interestingly a novel role for Ras in *Drosophila* enteroblasts has been recently discovered. Here, Ras activity in enteroblasts induces enteroblast mitosis, which generates two ISCs to facilitate repair in response to pathogenic infection[241]. This

presents the possibility that Ras acts primarily in enteroblasts to promote proliferation whereas Ras in ISCs enhances epithelial survival upon damage. In support of the pro-survival role for Ras in *Drosophila* ISCs, inactivation of EGF signaling in progenitors induces apoptosis in ISC progeny[192]. Given the importance of Ras in intestinal health it is imperative we further characterize the cell type-specific mechanisms behind Ras-dependent cell proliferation and cell survival. Together these observations suggest that Relish acts through Ras in ISCs to control cell survival in the face of extrinsic insults and are key factors in effective epithelial repair.

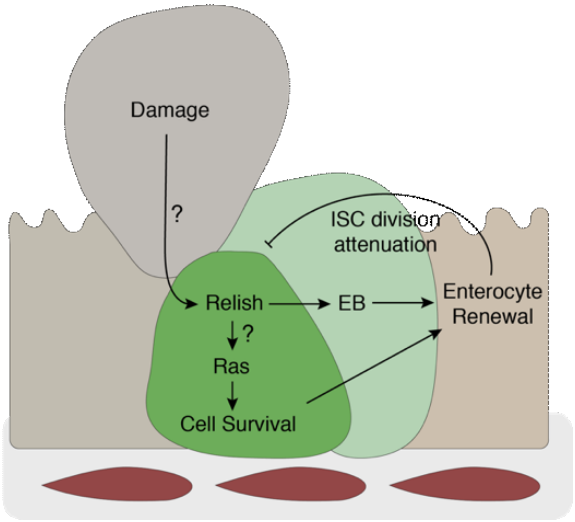

Figure 6.5 Relish acts in ISCs to promote intestinal repair. Damage activates Relish in ISCs via unknown mechanisms. Relish promotes enteroblast differentiation and Ras dependent cell survival leading to enterocyte renewal and the attenuation of ISC divisions. Mechanisms of Relish-dependent Ras activation are unknown.

6.4 Concluding Remarks

Intestinal stem cells govern epithelial maintenance and integrate microbial cues to dictate their functions. Within the scope of my thesis I found that commensal bacteria have profound and specific differential effects on ISC function and tumorigenic capacities. In addition, I found that the IMD pathway and downstream NF-κB family transcription factor Relish act specifically in ISCs to promote homeostatic and tumorigenic proliferation, modulate differentiation and promote cell survival in the face of acute stress. Together this implies that bacterial components are directly sensed by ISCs to alter their function, and that immune activity must be appropriately balanced in ISCs to allow for proper differentiation and repair without provoking excessive growth, hyperplasia and tumorigenesis. Given the constant environmental fluctuations the intestinal lumen is exposed to, I argue that immune signaling in ISCs is used as an adaptive mechanism to tune cell survival, differentiation and proliferation to the specific needs of the epithelium.

Bibliography

1 Jiang H, Tian A & Jiang J (2016) Intestinal stem cell response to injury: lessons from Drosophila. *Cell Mol Life Sci* **73**, 3337–3349.

2 Burgueño JF & Abreu MT (2020) Epithelial Toll-like receptors and their role in gut homeostasis and disease. *Nat Rev Gastroenterol Hepatol* **17**, 263–278.

3 Lesperance DN & Broderick NA (2020) Microbiomes as modulators of Drosophila melanogaster homeostasis and disease. *Curr Opin Insect Sci* **39**, 84–90.

4 Lynch S V. & Pedersen O (2016) The Human Intestinal Microbiome in Health and Disease. *N Engl J Med* **375**, 2369–2379.

5 Buchon N, Broderick NA, Chakrabarti S & Lemaitre B (2009) Invasive and indigenous microbiota impact intestinal stem cell activity through multiple pathways in Drosophila. *Genes Dev* **23**, 2333–2344.

6 Broderick NA, Buchon N & Lemaitre B (2014) Microbiota-Induced Changes in Drosophila melanogaster Host Gene Expression and Gut Morphology. *MBio* **5**, 1–13.

7 Cheesman SE, Neal JT, Mittge E, Seredick BM & Guillemin K (2011) Epithelial cell proliferation in the developing zebrafish intestine is regulated by the Wnt pathway and microbial signaling via Myd88. *PNAS* **108**, 4570–4577.

8 Li Y, Kundu P, Seow SW, Matos CT De, Aronsson L, Pettersson S & Greicius G (2012) Gut microbiota accelerate tumor growth via c-jun and STAT3 phosphorylation in APCMin/+ mice. *Carcinogenesis* **33**, 1231–1238.

9 Zackular JP, Baxter NT, Iverson KD, Sadler WD, Petrosino JF, Chen GY & Schloss PD (2013) The Gut Microbiome Modulates Colon Tumorigenesis. *MBio* **4**, 1–9.

10 Zhai Z, Huang X & Yin Y (2017) Beyond immunity : The Imd pathway as a coordinator of host defense , organismal physiology and behavior. *Dev Comp Immunol*, 1–9.

11 Sodhi CP, Neal MD, Siggers R, Sho S, Ma C, Branca MF, Prindle T, Russo AM, Afrazi A, Good M, Browersinning R, Firek B, Morowitz MJ, Ozolek JA, Gittes GK, Billiar TR & Hackam DJ (2012) Intestinal epithelial toll-like receptor 4 regulates goblet cell development and is required for necrotizing enterocolitis in mice. *Gastroenterology* **143**, 708–718.

12 Matsuoka K & Kanai T (2015) The gut microbiota and inflammatory bowel disease. *Semin Immunopathol* **37**, 47–55.

13 Gagnière J, Raisch J, Veziant J, Barnich N, Bonnet R, Buc E, Bringer MA, Pezet D & Bonnet M (2016)

Gut microbiota imbalance and colorectal cancer. *World J Gastroenterol* **22**, 501–518.

14 Vipperla K & O'Keefe SJ (2016) Diet, microbiota, and dysbiosis: a "recipe" for colorectal cancer. *Food Funct*, 1731–1740.

15 Nishida A, Inoue R, Inatomi O, Bamba S, Naito Y & Andoh A (2018) Gut microbiota in the pathogenesis of inflammatory bowel disease. *Clin J Gastroenterol* **11**, 1–10.

16 Zeller G, Tap J, Voigt AY, Sunagawa S, Kultima JR, Costea PI, Amiot A, Böhm J, Brunetti F, Habermann N, Hercog R, Koch M, Luciani A, Mende DR, Schneider MA, Schrotz-King P, Tournigand C, Tran Van Nhieu J, Yamada T, Zimmermann J, Benes V, Kloor M, Ulrich CM, von Knebel Doeberitz M, Sobhani I & Bork P (2014) Potential of fecal microbiota for early-stage detection of colorectal cancer. *Mol Syst Biol* **10**, 766.

17 Jiang H & Edgar BA (2011) Intestinal stem cells in the adult Drosophila midgut. *Exp Cell Res* **317**, 2780–2788.

18 Jiang H & Edgar BA (2012) Intestinal stem cell function in Drosophila and Mice. *Curr Opin Genet Dev* **22**, 354–360.

19 Casali A & Batlle E (2009) Intestinal Stem Cells in Mammals and Drosophila. *Cell Stem Cell* **4**, 124–127.

20 Buchon N, Osman D, David FPA, Yu Fang H, Boquete JP, Deplancke B & Lemaitre B (2013) Morphological and Molecular Characterization of Adult Midgut Compartmentalization in Drosophila. *Cell Rep* **3**, 1725–1738.

21 Miguel-Aliaga I, Jasper H & Lemaitre B (2018) Anatomy and Physiology of the Digestive Tract of Drosophila melanogaster. *Genetics* **210**, 357–396.

22 Li H, Qi Y & Jasper H (2016) Preventing Age-Related Decline of Gut Compartmentalization Limits Microbiota Dysbiosis and Extends Lifespan. *Cell Host Microbe* **19**, 240–253.

23 Strand M & Micchelli CA (2013) Regional control of Drosophila gut stem cell proliferation: EGF establishes GSSC proliferative set point & controls emergence from quiescence. *PLoS One* **8**, 1–10.

24 Marianes A & Spradling AC (2013) Physiological and stem cell compartmentalization within the Drosophila midgut. *Elife* **2013**, 1–19.

25 Dutta D, Dobson AJ, Houtz PL, GlaBer C, Revah J, Korzelius J, Patel PH, Edgar BA & Buchon N (2015) Regional Cell-Specific Transcriptome Mapping Reveals Regulatory Complexity in the Adult Drosophila Midgut. *Cell Rep* **12**, 346–358.

26 Ohlstein B & Spradling A (2006) The adult Drosophila posterior midgut is maintained by pluripotent stem cells. *Nature* **439**, 470–474.

27 Ohlstein B & Spradling A (2007) Multipotent Drosophila Intestinal Stem Cells Specify Daughter Cell Fates by Differential Notch Signaling. *Science (80-)* **315**, 988–993.

28 Micchelli CA & Perrimon N (2006) Evidence that stem cells reside in the adult Drosophila midgut epithelium. *Nature* **439**, 475–479.

29 Kuraishi T, Binggeli O, Opota O, Buchon N & Lemaitre B (2011) Genetic evidence for a protective role of the peritrophic matrix against intestinal bacterial infection in Drosophila melanogaster. *PNAS* **108**, 15966–15971.

30 Xu N, Wang SQ, Tan D, Gao Y, Lin G & Xi R (2011) EGFR , Wingless and JAK/STAT signaling cooperatively maintain Drosophila intestinal stem cells. *Dev Biol* **354**, 31–43.

31 Biteau B & Jasper H (2011) EGF signaling regulates the proliferation of intestinal stem cells in Drosophila. *Development* **138**, 1045–1055.

32 Barker N, Van Es JH, Kuipers J, Kujala P, Van Den Born M, Cozijnsen M, Haegebarth A, Korving J, Begthel H, Peters PJ & Clevers H (2007) Identification of stem cells in small intestine and colon by marker gene Lgr5. *Nature* **449**, 1003–1007.

33 Barker N, Van Oudenaarden A & Clevers H (2012) Identifying the stem cell of the intestinal crypt: Strategies and pitfalls. *Cell Stem Cell* **11**, 452–460.

34 de Navascués J, Perdigoto CN, Bian Y, Schneider MH, Bardin AJ, Martínez-Arias A & Simons BD (2012) *Drosophila* midgut homeostasis involves neutral competition between symmetrically dividing intestinal stem cells. *EMBO J* **31**, 2473–2485.

35 O'Brien LE, Soliman SS, Li X & Bilder D (2011) Altered Modes of Stem Cell Division Drive Adaptive Intestinal Growth. *Cell* **147**, 603–614.

36 Goulas S, Conder R & Knoblich JA (2012) The Par Complex and Integrins Direct Asymmetric Cell Division in Adult Intestinal Stem Cells. *Cell Stem Cell* **11**, 529–540.

37 Joly A & Rousset R (2020) Tissue adaptation to environmental cues by symmetric and asymmetric division modes of intestinal stem cells. *Int J Mol Sci* **21**, 1–17.

38 Ayyaz A, Li H & Jasper H (2015) Haemocytes control stem cell activity in the Drosophila intestine. *Nat Cell Biol* **17**, 736–748.

39 Chakrabarti S, Dudzic JP, Li X, Collas EJ, Boquete J-P & Lemaitre B (2016) Remote Control of Intestinal Stem Cell Activity by Haemocytes in Drosophila. *PLoS Genet* **12**, 1–24.

40 Morrison SJ & Spradling AC (2008) Stem Cells and Niches: Mechanisms That Promote Stem Cell Maintenance throughout Life. *Cell* **132**, 598–611.

41 Takashima S & Hartenstein V (2012) Genetic Control of Intestinal Stem Cell Specification and Development: A Comparative View. *Stem Cell Rev Reports* **8**, 597–608.

42 Chen AJ, Sayadian A, Lowe N, Lovegrove HE & St Johnston D (2018) An alternative mode of epithelial polarity in the Drosophila midgut. *PLoS Biol* **16**, 1–24.

43 Martin JL, Sanders EN, Moreno-roman P, Koyama LAJ, Balachandra S, Du X & O'Brien LE (2018) Long-term live imaging of the Drosophila adult midgut reveals real-time dynamics of division, differentiation and loss. *Elife* **7**, 1–33.

44 Lin G, Zhang X, Ren J, Pang Z, Wang C, Xu N & Xi R (2013) Integrin signaling is required for maintenance and proliferation of intestinal stem cells in Drosophila. *Dev Biol* **377**, 177–187.

45 Okumura T, Takeda K, Taniguchi K & Adachi-yamada T (2014) Bv Integrin Inhibits Chronic and High Level Activation of JNK to Repress Senescence Phenotypes in Drosophila Adult Midgut. *PLoS One* **9**, 1–14.

46 Jones RG, Li X, Gray PD, Kuang J, Clayton F, Samowitz WS, Madison BB, Gumucio DL & Kuwada SK (2006) Conditional deletion of **β** 1 integrins in the intestinal epithelium causes a loss of Hedgehog expression, intestinal hyperplasia, and early postnatal lethality. *JCB* **175**, 505–514.

47 Lin G, Xu N & Xi R (2008) Paracrine Wingless signalling controls self-renewal of Drosophila intestinal stem cells. *Nature* **455**, 1119–1123.

48 Cordero JB, Stefanatos RK, Scopelliti A, Vidal M & Sansom OJ (2012) Inducible progenitor-derived Wingless regulates adult midgut regeneration in Drosophila. *EMBO J* **31**, 3901–3917.

49 Perochon J, Carroll LR & Cordero JB (2018) Wnt signalling in intestinal stem cells: Lessons from mice and flies. *Genes (Basel)* **9**, 1–19.

50 Cordero JB, Stefanatos RK, Myant K, Vidal M & Sansom OJ (2012) Non-autonomous crosstalk between the Jak/Stat and Egfr pathways mediates Apc1-driven intestinal stem cell hyperplasia in the Drosophila adult midgut. *Development* **139**, 4524–4535.

51 Tian A, Benchabane H & Ahmed Y (2018) Wingless/Wnt Signaling in Intestinal Development, Homeostasis, Regeneration and Tumorigenesis : A Drosophila Perspective. *J Dev Biol* **6**, 1–20.

52 Wang C, Zhao R, Huang P, Yang F, Quan Z, Xu N & Xi R (2013) APC loss-induced intestinal tumorigenesis in Drosophila: Roles of Ras in Wnt signaling activation and tumor progression. *Dev Biol* **378**, 122–140.

53 Krausova M & Korinek V (2014) Wnt signaling in adult intestinal stem cells and cancer. *Cell Signal* **26**, 570–579.

54 Tian A, Wang B & Jiang J (2017) Injury-stimulated and self-restrained BMP signaling dynamically regulates stem cell pool size during Drosophila midgut regeneration. *PNAS*, E2699–E2708.

55 Tian A & Jiang J (2014) Intestinal epithelium-derived BMP controls stem cell self-renewal in Drosophila adult midgut. *Elife* **3**, 1–23.

56 Li Z, Zhang Y, Han L, Shi L & Lin X (2013) Trachea-Derived Dpp Controls Adult Midgut Homeostasis in Drosophila. *Dev Cell* **24**, 133–143.

57 Guo Z, Driver I & Ohlstein B (2013) Injury-induced BMP signaling negatively regulates Drosophila midgut homeostasis. *JCB* **201**, 945–961.

58 Li H, Qi Y & Jasper H (2013) Dpp Signaling Determines Regional Stem Cell Identity in the Regenerating Adult Drosophila Gastrointestinal Tract. *CellReports* **4**, 10–18.

59 Zhou J, Florescu S, Boettcher A, Luo L, Dutta D, Kerr G, Cai Y, Edgar BA & Boutros M (2015) Dpp/Gbb signaling is required for normal intestinal regeneration during infection. *Dev Biol* **399**, 189–203.

60 Cichy W, Klincewicz B & Plawski A (2014) Juvenile polyposis syndrome. *Arch Med Sci* **10**, 570–577.

61 Zhou J & Boutros M (2020) JNK-dependent intestinal barrier failure disrupts host–microbe homeostasis during tumorigenesis. *PNAS* **117**, 9401–9412.

62 Bardin AJ, Perdigoto CN, Southall TD, Brand AH & Schweisguth F (2010) Transcriptional control of stem cell maintenance in the Drosophila intestine. *Development* **137**, 705–714.

63 Biteau B & Jasper H (2014) Slit/Robo Signaling Regulates Cell Fate Decisions in the Intestinal Stem Cell Lineage of Drosophila. *Cell Rep* **7**, 1867–1875.

64 Guo Z & Ohlstein B (2015) Bidirectional Notch signaling regulates Drosophila intestinal stem cell multipotency. *Science (80-)* **350**, aab0988-1-aab0988-8.

65 Zeng X & Hou SX (2015) Enteroendocrine cells are generated from stem cells through a distinct progenitor in the adult Drosophila posterior midgut. *Development* **142**, 644–653.

66 Vooijs M, Liu Z & Kopan R (2011) Notch: Architect, landscaper, and guardian of the intestine. *Gastroenterology* **141**, 448–459.

67 Takashima S, Adams KL, Ortiz PA, Ying CT, Moridzadeh R, Younossi-Hartenstein A & Hartenstein V (2011) Development of the Drosophila entero-endocrine lineage and its specification by the Notch signaling pathway. *Dev Biol* **353**, 161–172.

68 Patel PH, Dutta D & Edgar B a (2015) Niche appropriation by Drosophila intestinal stem cell tumours. *Nat Cell Biol* **17**, 1182–92.

69 Crosnier C, Vargesson N, Gschmeissner S, Ariza-McNaughton L, Morrison A & Lewis J (2005) Delta-

Notch signalling controls commitment to a secretory fate in the zebrafish intestine. *Development* **132**, 1093–1104.

70 Qiao L & Wong BCY (2009) Role of notch signaling in colorectal cancer. *Carcinogenesis* **30**, 1979–1986.

71 Siudeja K, Nassari S, Gervais L, Skorski P, Lameiras S, Stolfa D, Zande M, Bernard V, Frio TR & Bardin AJ (2015) Frequent Somatic Mutation in Adult Intestinal Stem Cells Drives Neoplasia and Genetic Mosaicism during Aging. *Cell Stem Cell* **17**, 663–674.

72 Biteau B, Hochmuth CE & Jasper H (2008) JNK Activity in Somatic Stem Cells Causes Loss of Tissue Homeostasis in the Aging Drosophila Gut. *Cell Stem Cell* **3**, 442–455.

73 Ren F, Wang B, Yue T, Yun E, Ip YT & Jiang J (2010) Hippo signaling regulates Drosophila intestine stem cell proliferation through multiple pathways. *PNAS* **107**, 21064–21069.

74 Shaw RL, Kohlmaier A, Polesello C, Veelken C, Edgar BA & Tapon N (2010) TRASH. *Development* **137**, 4147–4158.

75 Buchon N, Broderick NA, Kuraishi T & Lemaitre B (2010) Drosophila EGFR pathway coordinates stem cell proliferation and gut remodeling following infection. *BMC Biol* **8**, 152.

76 Jiang H, Patel PH, Kohlmaier A, Grenley MO, Donald G & Edgar BA (2009) Cytokine/Jak/Stat signaling mediates regeneration and homeostasis in the Drosophila midgut. *Cell* **137**, 650–657.

77 Nászai M, Bellec K, Yu Y, Román-Fernández A, Sandilands E, Johansson J, Campbell AD, Norman JC, Sansom OJ, Bryant DM & Cordero JB (2021) Ral gtpases mediate egfr-driven intestinal stem cell proliferation and tumourigenesis. *Elife* **10**, 1–33.

78 Chandler JA, Lang J, Bhatnagar S, Eisen JA & Kopp A (2011) Bacterial communities of diverse Drosophila species: Ecological context of a host-microbe model system. *PLoS Genet* **7**.

79 Adair KL, Wilson M, Bost A & Douglas AE (2018) Microbial community assembly in wild populations of the fruit fly Drosophila melanogaster. *ISME J* **12**, 959–972.

80 Broderick NA & Lemaitre B (2012) Gut-associated microbes of Drosophila melanogaster. *Gut Microbes* **3**, 307–321.

81 Koyle ML, Veloz M, Judd AM, Wong AC-N, Newell PD, Douglas AE & Chaston JM (2016) Rearing the Fruit Fly Drosophila melanogaster Under Axenic and Gnotobiotic Conditions. *J Vis Exp* **113**, 1–8.

82 Wong ACN, Chaston JM & Douglas AE (2013) The inconstant gut microbiota of Drosophila species revealed by 16S rRNA gene analysis. *ISME J* **7**, 1922–1932.

83 Buchon N, Broderick NA, Poidevin M, Pradervand S & Lemaitre B (2009) Drosophila Intestinal

Response to Bacterial Infection: Activation of Host Defense and Stem Cell Proliferation. *Cell Host Microbe* **5**, 200–211.

84 Ryu J-H, Ha E-M, Oh C-T, Seol J-H, Brey PT, Jin I, Lee DG, Kim J, Lee D & Lee W-J (2006) An essential complementary role of NF-κB pathway to microbicidal oxidants in Drosophila gut immunity. *EMBO J* **25**, 3693–3701.

85 Buchon N, Broderick NA & Lemaitre B (2013) Gut homeostasis in a microbial world: insights from Drosophila melanogaster. *Nat Rev Microbiol* **11**, 615–626.

86 Myllymäki H, Valanne S & Rämet M (2014) The Drosophila imd signaling pathway. *J Immunol* **192**, 3455–62.

87 Boutros M, Agaisse H & Perrimon N (2002) Sequential Activation of Signaling Pathways during Innate Immune Responses in Drosophila. *Dev Cell* **3**, 711–722.

88 Hung R, Hu Y, Kirchner R, Liu Y, Xu C, Comjean A, Tattikota SG, Li F, Song W, Sui SH & Perrimon N (2019) A cell atlas of the adult Drosophila midgut. *PNAS*, 1–10.

89 Neyen C, Poidevin M, Roussel A & Lemaitre B (2012) Tissue- and Ligand-Specific Sensing of Gram-Negative Infection in Drosophila by PGRP-LC Isoforms and PGRP-LE. *J Immunol* **189**, 1886–1897.

90 Bosco-drayon V, Poidevin M, Boneca IG, Narbonne-Reveau K, Royet J & Charroux B (2012) Peptidoglycan Sensing by the Receptor PGRP-LE in the Drosophila Gut Induces Immune Responses to Infectious Bacteria and Tolerance to Microbiota. *Cell Host Microbe* **12**, 153–165.

91 Ryu J, Kim S-H, Lee H-Y, Bai JY, Nam Y-D, Bae J-W, Lee DG, Shin SC, Ha E-M & Lee W-J (2008) Innate Immune Homeostasis by the Homeobox Gene Caudal and Commensal-Gut Mutualism in Drosophila. *Science (80-)* **319**.

92 Ha EM, Oh CT, Bae YS & Lee WJ (2005) A direct role for dual oxidase in Drosophila gut immunity. *Science (80-)* **310**, 847–850.

93 Iatsenko I, Boquete J-P & Lemaitre B (2018) Microbiota-Derived Lactate Activates Production of Reactive Oxygen Species by the Intestinal NADPH Oxidase Nox and Shortens Drosophila Lifespan. *Immunity* **49**, 929–942.

94 Jones RM, Luo L, Ardita CS, Richardson AN, Kwon YM, Mercante JW, Alam A, Gates CL, Wu H, Swanson PA, Lambeth JD, Denning PW & Neish AS (2013) Symbiotic lactobacilli stimulate gut epithelial proliferation via Nox-mediated generation of reactive oxygen species. *EMBO J* **32**, 3017–3028.

95 Lee KA, Kim SH, Kim EK, Ha EM, You H, Kim B, Kim MJ, Kwon Y, Ryu JH & Lee WJ (2013) Bacterial-

derived uracil as a modulator of mucosal immunity and gut-microbe homeostasis in drosophila. *Cell* **153**, 797–811.

96 Reedy AR, Luo L, Neish AS & Jones RM (2019) Commensal microbiota-induced redox signaling activates proliferative signals in the intestinal stem cell microenvironment. *Development* **146**, 1–7.

97 Xu C, Luo J, He L, Montell C & Perrimon N (2017) Oxidative stress induces stem cell proliferation via TRPA1/RyR-mediated Ca2+signaling in the Drosophila midgut. *Elife* **6**, 1–24.

98 Chen F, Su R, Ni S, Liu Y, Huang J, Li G, Wang Q, Zhang X & Yang Y (2021) Context-dependent responses of Drosophila intestinal stem cells to intracellular reactive oxygen species. *Redox Biol* **39**, 101835.

99 Perochon J, Yu Y, Aughey GN, Medina AB, Southall TD & Cordero JB (2021) Dynamic adult tracheal plasticity drives stem cell adaptation to changes in intestinal homeostasis in Drosophila. *Nat Cell Biol* **23**, 485–496.

100 Liu X, Nagy P, Bonfini A, Houtz P, Bing X-L, Yang X & Buchon N (2022) Microbes affect gut epithelial cell composition through immune-dependent regulation of intestinal stem cell differentiation. *Cell Rep* **38**, 110572.

101 Fast D, Duggal A & Foley E (2018) Monoassociation with Lactobacillus plantarum Disrupts Intestinal Homeostasis in Adult Drosophila melanogaster. *MBio* **9**, 1–16.

102 Fast D, Kostiuk B, Foley E & Pukatzki S (2018) Commensal pathogen competition impacts host viability. *PNAS* **115**, 7099–7104.

103 Fast D, Petkau K, Ferguson M, Shin M, Galenza A, Kostiuk B, Pukatzki S & Foley E (2020) Vibrio cholerae-Symbiont Interactions Inhibit Intestinal Repair in Drosophila. *Cell Rep* **30**, 1088–1100.

104 Hales KG, Korey CA, Larracuente AM & Roberts DM (2015) Genetics on the fly: A primer on the drosophila model system. *Genetics* **201**, 815–842.

105 McGuire SE, Mao Z & Davis RL (2004) Spatiotemporal Gene Expression Targeting with the TARGET and Gene-Switch Systems in Drosophila. *Sci STKE* **2004**, 1–10.

106 Lee T & Luo L (1999) Mosaic analysis with a repressible neurotechnique cell marker for studies of gene function in neuronal morphogenesis. *Neuron* **22**, 451–461.

107 Luo L & Wu JS (2007) A protocol for mosaic analysis with a repressible cell marker (Marcm) in drosophila. *Nat Protoc* **1**, 2583–2589.

108 Yu HH, Chen CH, Shi L, Huang Y & Lee T (2009) Twin-spot MARCM to reveal the developmental origin and identity of neurons. *Nat Neurosci* **12**, 947–953.

109 Paredes JC, Welchman DP, Poidevin M & Lemaitre B (2011) Negative regulation by Amidase PGRPs shapes the drosophila antibacterial response and protects the Fly from innocuous infection. *Immunity* **35**, 770–779.

110 Zhai Z, Boquete J & Lemaitre B (2018) Cell-Specific Imd-NF-kB Responses Enable Simultaneous Antibacterial Immunity and Intestinal Epithelial Cell Shedding upon Bacterial Infection. *Immunity* **48**, 897–910.

111 Hörmann N, Brandão I, Jäckel S, Ens N, Lillich M, Walter U & Reinhardt C (2014) Gut microbial colonization orchestrates TLR2 expression, signaling and epithelial proliferation in the small intestinal mucosa. *PLoS One* **9**, 2–12.

112 Kamdar K, Johnson AMF, Chac D, Myers K, Kulur V, Truevillian K & DePaolo RW (2018) Innate Recognition of the Microbiota by TLR1 Promotes Epithelial Homeostasis and Prevents Chronic Inflammation. *J Immunol* **201**, 230–242.

113 Sodhi CP, Shi XH, Richardson WM, Grant ZS, Shapiro RA, Prindle T, Branca M, Russo A, Gribar SC, Ma C & Hackam DJ (2010) Toll-Like Receptor-4 Inhibits Enterocyte Proliferation via Impaired **β**-Catenin Signaling in Necrotizing Enterocolitis. *Gastroenterology* **138**, 185–196.

114 Santaolalla R, Sussman DA, Ruiz JR, Davies JM, Pastorini C, España CL, Sotolongo J, Burlingame O, Bejarano PA, Philip S, Ahmed MM, Ko J, Dirisina R, Barrett TA, Shang L, Lira SA, Fukata M & Abreu MT (2013) TLR4 Activates the **β**-catenin Pathway to Cause Intestinal Neoplasia. *PLoS One* **8**.

115 Wilson AG & Duff GW (1995) Tumor necrosis factor a Regulates Proliferation in a Mouse Intestinal Cell Line. *Lancet* **345**, 649.

116 Kandori H, Hirayama K, Takeda M & Doi K (1996) Histochemical, Lectin-Histochemical and Morphometrical characteristics of intestinal goblet cells of germ free and conventional mice. *Exp Anim* **45**, 155–160.

117 Bates JM, Mittge E, Kuhlman J, Baden KN, Cheesman SE & Guillemin K (2006) Distinct signals from the microbiota promote different aspects of zebrafish gut differentiation. *Dev Biol* **297**, 374–386.

118 Troll J V, Hamilton MK, Abel ML, Ganz J, Bates JM, Stephens WZ, Melancon E, Vaart M Van Der, Meijer AH, Distel M, Eisen JS & Guillemin K (2018) Microbiota promote secretory cell determination in the intestinal epithelium by modulating host Notch signaling. *Development* **145**, 1–7.

119 Yang Q, Bermingham NA, Finegold MJ & Zoghbi HY (2001) Requirement of Math1 for secretory cell lineage commitment in the mouse intestine. *Science (80-)* **294**, 2155–2158.

120 Fre S, Huyghe M, Mourikis P, Robine S, Louvard D & Artavanis-Tsakonas S (2005) Notch signals

control the fate of immature progenitor cells in the intestine. *Nature* **435**, 964–968.

121 Sancho R, Cremona CA & Behrens A (2015) Stem cell and progenitor fate in the mammalian intestine: Notch and lateral inhibition in homeostasis and disease. *EMBO Rep* **16**, 571–581.

122 Naito T, Mulet C, De Castro C, Molinaro A, Saffarian A, Nigro G, Berard M, Clerc M, Pederson AB, Sansonetti PJ & Pedron T (2017) Lipopolysaccharide from Crypt-Specific Core Microbiota Modulates the Colonic Epithelial Proliferation-to-Differentiation Balance. *MBio* **8**, 1–16.

123 Wang H, Kim JJ, Denou E, Gallagher A, Thornton DJ, Sharif Shajib M, Xia L, Schertzer JD, Grencis RK, Philpott DJ & Khan WI (2015) New role of Nod proteins in regulation of intestinal goblet cell response in the context of innate host defense in an enteric parasite infection. *Infect Immun* **84**, 275–285.

124 Wang Z, Hang S, Purdy AE & Watnick PI (2013) Mutations in the IMD pathway and mustard counter Vibrio cholerae suppression of intestinal stem cell division in Drosophila. *MBio* **4**, 1–9.

125 Hori A, Kurata S & Kuraishi T (2018) Unexpected role of the IMD pathway in Drosophila gut defense against Staphylococcus aureus. *Biochem Biophys Res Commun* **495**, 395–400.

126 Wang L, Sloan MA & Ligoxygakis P (2019) Intestinal NF-κB and STAT signalling is important for uptake and clearance in a Drosophila-Herpetomonas interaction model. *PLoS Genet* **15**, 1–23.

127 Petersson J, Schreiber O, Hansson GC, Gendler SJ, Velcich A, Lundberg JO, Roos S, Holm L & Phillipson M (2010) Importance and regulation of the colonic mucus barrier in a mouse model of colitis. *Am J Physiol - Gastrointest Liver Physiol* **300**, 327–333.

128 Hernández-Chirlaque C, Aranda CJ, Ocón B, Capitán-Cañadas F, Ortega-González M, Carrero JJ, Suárez MD, Zarzuelo A, de Medina FS & Martínez-Augustin O (2016) Germ-free and antibiotic-treated mice are highly susceptible to epithelial injury in DSS colitis. *J Crohn's Colitis* **10**, 1324–1335.

129 Fukata M, Chen A, Klepper A, Krishnareddy S, Vamadevan AS, Thomas LS, Xu R, Inoue H, Arditi M, Dannenberg AJ & Abreu MT (2006) Cox-2 Is Regulated by Toll-Like Receptor-4 (TLR4) Signaling: Role in Proliferation and Apoptosis in the Intestine. *Gastroenterology* **131**, 862–877.

130 Frantz AL, Rogier EW, Weber CR, Shen L, Cohen DA, Fenton LA, Bruno MEC & Kaetzel CS (2012) Targeted deletion of MyD88 in intestinal epithelial cells results in compromised antibacterial immunity associated with downregulation of polymeric immunoglobulin receptor, mucin-2, and antibacterial peptides. *Mucosal Immunol* **5**, 501–512.

131 Cario E, Gerken G & Podolsky DK (2007) Toll-Like Receptor 2 Controls Mucosal Inflammation by Regulating Epithelial Barrier Function. *Gastroenterology* **132**, 1359–1374.

132 Podolsky DK, Gerken G, Eyking A & Cario E (2009) Colitis-Associated Variant of TLR2 Causes Impaired Mucosal Repair Because of TFF3 Deficiency. *Gastroenterology* **137**, 209–220.

133 Fukata M, Michelsen KS, Eri R, Thomas LS, Hu B, Lukasek K, Nast CC, Lechago J, Xu R, Naiki Y, Soliman A, Arditi M & Abreu MT (2005) Toll-like receptor-4 is required for intestinal response to epithelial injury and limiting bacterial translocation in a murine model of acute colitis. *Am J Physiol - Gastrointest Liver Physiol* **288**, 1055–1065.

134 Rose II WA, Sakamoto K & Leifer CA (2012) TLR9 is important for protection against intestinal damage and for intestinal repair. *Sci Rep* **2**, 1–9.

135 Natividad JMM, Petit V, Huang X, De Palma G, Jury J, Sanz Y, Philpott D, Garcia Rodenas CL, McCoy KD & Verdu EF (2012) Commensal and probiotic bacteria influence intestinal barrier function and susceptibility to colitis in Nod1-/-;Nod2-/- Mice. *Inflamm Bowel Dis* **18**, 1434–1446.

136 Couturier-Maillard A, Secher T, Rehman A, Normand S, De Arcangelis A, Haesler R, Huot L, Grandjean T, Bressenot A, Delanoye-Crespin A, Gaillot O, Schreiber S, Lemoine Y, Ryffel B, Hot D, Nùñez G, Chen G, Rosenstiel P & Chamaillard M (2013) NOD2-mediated dysbiosis predisposes mice to transmissible colitis and colorectal cancer. *J Clin Invest* **123**, 700–711.

137 Vijay-Kumar M, Sanders CJ, Taylor RT, Kumar A, Aitken JD, Sitaraman S V., Neish AS, Uematsu S, Akira S, Williams IR & Gewirtz AT (2007) Deletion of TLR5 results in spontaneous colitis in mice. *J Clin Invest* **117**, 3909–3921.

138 Ungaro R, Fukata M, Hsu D, Hernandez Y, Breglio K, Chen A, Xu R, Sotolongo J, Espana C, Zaias J, Elson G, Mayer L, Kosco-Vilbois M & Abreu MT (2009) A novel Toll-like receptor 4 antagonist antibody ameliorates inflammation but impairs mucosal healing in murine colitis. *Am J Physiol - Gastrointest Liver Physiol* **296**, 1167–1179.

139 Guma M, Stepniak D, Shaked H, Spehlmann ME, Shenouda S, Cheroutre H, Vicente-suarez I, Eckmann L, Kagnoff MF & Karin M (2011) Constitutive intestinal NF-kB does not trigger destructive inflammation unless accompanied by MAPK activation. *J Exp Med* **208**, 1889–1900.

140 Hsu D, Fukata M, Hernandez YG, Sotolongo JP, Goo T, Maki J, Hayes LA, Ungaro RC, Chen A, Breglio KJ, Xu R & Abreu MT (2010) Toll-like receptor 4 differentially regulates epidermal growth factor-related growth factors in response to intestinal mucosal injury. *Lab Investig* **90**, 1295–1305.

141 Watanabe T, Asano N, Murray PJ, Ozato K, Tailor P, Fuss IJ, Kitani A & Strober W (2008) Muramyl dipeptide activation of nucleotide-binding oligomerization domain 2 protects mice from experimental colitis. *J Clin Invest* **118**, 545–559.

142 Watanabe T, Kitani A, Murray PJJ, Wakatsuki Y, Fuss IJ & Strober W (2006) Nucleotide Binding Oligomerization Domain 2 Deficiency Leads to Dysregulated TLR2 Signaling and Induction of Antigen-Specific Colitis. *Immunity* **25**, 473–485.

143 Ruder B, Atreya R & Becker C (2019) Tumour Necrosis Factor Alpha in Intestinal Homeostasis and Gut Related Diseases. *Int J Mol Sci* **20**, 1–21.

144 Reinecker HC, Steffen M, Witthoeft T, Pflueger I, Schreiber S, MacDermott RP & Raedler A (1993) Enhanced secretion of tumour necrosis factor-alpha, IL-6, and IL-1**β** by isolated lamina propria mononuclear cells from patients with ulcerative colitis and Crohn's disease. *Clin Exp Immunol* **94**, 174–181.

145 Dionne S, Hiscott J, D'Agata I, Duhaime A & Seidman EG (1997) Quantitative PCR analysis of TNF-**α** and IL-1**β** mRNA levels in pediatric IBD mucosal biopsies. *Dig Dis Sci* **42**, 1557–1566.

146 Cui G, Fan Q, Li Z, Goll R & Florholmen J (2021) Evaluation of anti-TNF therapeutic response in patients with inflammatory bowel disease: Current and novel biomarkers. *EBioMedicine* **66**, 103329.

147 Aardoom MA, Veereman G & de Ridder L (2019) A review on the use of anti-TNF in children and adolescents with inflammatory bowel disease. *Int J Mol Sci* **20**.

148 Neurath MF, Fuss I, Pasparakis M, Alexopoulou L, Haralambous S, Meyer Zum Büschenfelde KH, Strober W & Kollias G (1997) Predominant pathogenic role of tumor necrosis factor in experimental colitis in mice. *Eur J Immunol* **27**, 1743–1750.

149 Bamias G, Dahman MI, Arseneau KO, Guanzon M, Gruska D, Pizarro TT & Cominelli F (2013) Intestinal-Specific TNF**α** Overexpression Induces Crohn's-Like Ileitis in Mice. *PLoS One* **8**, 1–11.

150 Kojouharoff G, Hans W, Obermeler F, Männel DN, Andus T, Schölmerich J, Gross V & Falk W (1997) Neutralization of tumour necrosis factor (TNF) but not of IL-1 reduces inflammation in chronic dextran sulphate sodium-induced colitis in mice. *Clin Exp Immunol* **107**, 353–358.

151 Naito Y, Takagi T, Handa O, Ishikawa T, Nakagawa S, Yamaguchi T, Yoshida N, Minami M, Kita M, Imanishi J & Yoshikawa T (2003) Enhanced intestinal inflammation induced by dextran sulfate sodium in tumor necrosis factor-alpha deficient mice. *J Gastroenterol Hepatol* **18**, 560–569.

152 Al-Sadi R, Guo S, Ye D & Ma TY (2013) TNF-**α** modulation of intestinal epithelial tight junction barrier is regulated by ERK1/2 activation of Elk-1. *Am J Pathol* **183**, 1871–1884.

153 Frey MR, Edelblum KL, Mullane MT, Liang D & Polk DB (2009) The ErbB4 Growth Factor Receptor Is Required for Colon Epithelial Cell Survival in the Presence of TNF. *Gastroenterology* **136**, 217–226.

154 Hilliard VC, Frey MR, Dempsey PJ, Peek RM & Polk DB (2011) TNF-**α** converting enzyme-mediated

ErbB4 transactivation by TNF promotes colonic epithelial cell survival. *Am J Physiol - Gastrointest Liver Physiol* **301**, 338–346.

155 Zhan Y, Chen PJ, Sadler WD, Wang F, Poe S, Núñez G, Eaton KA & Chen GY (2013) Gut microbiota protects against gastrointestinal tumorigenesis caused by epithelial injury. *Cancer Res* **73**, 7199–7210.

156 Apidianakis Y, Pitsouli C, Perrimon N & Rahme L (2009) Synergy between bacterial infection and genetic predisposition in intestinal dysplasia. *Proc Natl Acad Sci U S A* **106**, 20883–20888.

157 Rakoff-Nahoum S & Medzhitov R (2007) Regulation of spontaneous intestinal tumorigenesis through the adaptor protein MyD88. *Science (80-)* **317**, 124–127.

158 Salcedo R, Worschech A, Cardone M, Jones Y, Gyulai Z, Dai RM, Wang E, Ma W, Haines D, O'hUigin C, Marincola FM & Trinchieri G (2010) MyD88-mediated signaling prevents development of adenocarcinomas of the colon: Role of interleukin 18. *J Exp Med* **207**, 1625–1636.

159 Lowe EL, Crother TR, Rabizadeh S, Hu B, Wang H, Chen S, Shimada K, Wong MH, Michelsen KS & Arditi M (2010) Toll-Like Receptor 2 signaling protects mice from tumor development in a mouse model of Colitis-induced cancer. *PLoS One* **5**.

160 Chen GY, Shaw MH, Redondo G & Núñez G (2008) Innate immune receptor nod1 protects the intestine from inflammation-induced tumorigenesis. *Cancer Res* **68**, 10060–10067.

161 Fukata M, Chen A, Vamadevan AS, Cohen J, Breglio K, Krishnareddy S, Hsu D, Xu R, Harpaz N, Dannenberg AJ, Subbaramaiah K, Cooper HS, Itzkowitz SH & Abreu MT (2007) Toll-Like Receptor-4 Promotes the Development of Colitis-Associated Colorectal Tumors. *Gastroenterology* **133**, 1869–1881.

162 Fukata M, Shang L, Santaolalla R, Sotolongo J, Pastorini C, España C, Ungaro R, Harpaz N, Cooper HS, Elson G, Kosco-Vilbois M, Zaias J, Perez MT, Mayer L, Vamadevan AS, Lira SA & Abreu MT (2011) Constitutive activation of epithelial TLR4 augments inflammatory responses to mucosal injury and drives colitis-associated tumorigenesis. *Inflamm Bowel Dis* **17**, 1464–1473.

163 Kim S, Keku TO, Martin C, Galanko J, Woosley JT, Schroeder JC, Satia JA, Halabi S & Sandler RS (2008) Circulating levels of inflammatory cytokines and risk of colorectal adenomas. *Cancer Res* **68**, 323–328.

164 Al Obeed OA, Alkhayal KA, Al Sheikh A, Zubaidi AM, Vaali-Mohammed MA, Boushey R, Mckerrow JH & Abdulla MH (2014) Increased expression of tumor necrosis factor-**α** is associated with advanced colorectal cancer stages. *World J Gastroenterol* **20**, 18390–18396.

165 Stanilov N, Miteva L, Dobreva Z & Stanilova S (2014) Colorectal cancer severity and survival in correlation with tumour necrosis factor-alpha. *Biotechnol Biotechnol Equip* **28**, 911–917.

166 Popivanova BK, Kitamura K, Wu Y, Kondo T, Kagaya T, Kaneko S, Oshima M, Fujii C & Mukaida N (2008) Blocking TNF-**α** in mice reduces colorectal carcinogenesis associated with chronic colitis. *J Clin Invest* **118**, 560–570.

167 Zhao X, Ma L, Dai L, Zuo D, Li X, Zhu H & Xu F (2020) TNF-**α** promotes the malignant transformation of intestinal stem cells through the NF-**κ**B and Wnt/**β**-catenin signaling pathways. *Oncol Rep* **44**, 577–588.

168 Price AE, Shamardani K, Lugo KA, Deguine J, Roberts AW, Lee BL & Barton GM (2018) A Map of Toll-like Receptor Expression in the Intestinal Epithelium Reveals Distinct Spatial, Cell Type-Specific, and Temporal Patterns. *Immunity* **49**, 560–575.e6.

169 Chabot S, Wagner JS, Farrant S & Neutra MR (2006) TLRs Regulate the Gatekeeping Functions of the Intestinal Follicle-Associated Epithelium. *J Immunol* **176**, 4275–4283.

170 Nigro G, Rossi R, Commere PH, Jay P & Sansonetti PJ (2014) The cytosolic bacterial peptidoglycan sensor Nod2 affords stem cell protection and links microbes to gut epithelial regeneration. *Cell Host Microbe* **15**, 792–798.

171 Neal MD, Sodhi CP, Jia H, Dyer M, Egan CE, Yazji I, Good M, Afrazi A, Marino R, Slagle D, Ma C, Branca MF, Prindle T, Grant Z, Ozolek J & Hackam DJ (2012) Toll-like receptor 4 is expressed on intestinal stem cells and regulates their proliferation and apoptosis via the p53 up-regulated modulator of apoptosis. *J Biol Chem* **287**, 37296–37308.

172 Levy A, Stedman A, Deutsch E, Donnadieu F, Virgin HW, Sansonetti PJ & Nigro G (2020) Innate immune receptor NOD2 mediates LGR5+ intestinal stem cell protection against ROS cytotoxicity via mitophagy stimulation. *Proc Natl Acad Sci U S A* **117**, 1994–2003.

173 Petkau K, Fast D, Duggal A & Foley E (2016) Comparative evaluation of the genomes of three common Drosophila-associated bacteria. *Biol Open* **5**, 1305–1316.

174 Pukatzki S, Ma AT, Sturtevant D, Krastins B, Sarracino D, Nelson WC, Heidelberg JF & Mekalanos JJ (2006) Identification of a conserved bacterial protein secretion system in Vibrio cholerae using the Dictyostelium host model system. *Proc Natl Acad Sci U S A* **103**, 1528–1533.

175 Basset A, Khush RS, Braun A, Gardan L, Boccard F, Hoffmann JA & Lemaitre B (2000) The phytopathogenic bacteria Erwinia carotovora infects Drosophila and activates an immune response. *Proc Natl Acad Sci U S A* **97**, 3376–3381.

176 Schindelin J, Arganda-carreras I, Frise E, Kaynig V, Longair M, Pietzsch T, Preibisch S, Rueden C, Saalfeld S, Schmid B, Tinevez J, White DJ, Hartenstein V, Eliceiri K, Tomancak P & Cardona A (2019) Fiji: an open-source platform for biological-image analysis. *Nat Methods* **9**, 676–682.

177 Dutta D, Xiang J & Edgar BA (2013) RNA Expression Profiling from FACS-Isolated Cells of the Drosophila Intestine. *Curr Protoc Stem Cell Biol*, 2F.2.1-2F.2.12.

178 Shin M, Ferguson M, Willms RJ, Jones LO, Petkau K & Foley E (2022) Immune regulation of intestinal-stem-cell function in Drosophila. *Stem Cell Reports* **17**, 741–755.

179 Lyne R, Smith R, Rutherford K, Wakeling M, Varley A, Guillier F, Janssens H, Ji W, Mclaren P, North P, Rana D, Riley T, Sullivan J, Watkins X, Woodbridge M, Lilley K, Russell S, Ashburner M, Mizuguchi K & Micklem G (2007) FlyMine: An integrated database for Drosophila and Anopheles genomics. *Genome Biol* **8**.

180 Thomas PD, Kejariwal A, Campbell MJ, Mi H, Diemer K, Guo N, Ladunga I, Ulitsky-Lazareva B, Muruganujan A, Rabkin S, Vandergriff JA & Doremieux O (2003) PANTHER: A browsable database of gene products organized by biological function, using curated protein family and subfamily classification. *Nucleic Acids Res* **31**, 334–341.

181 Bolger AM, Lohse M & Usadel B (2014) Trimmomatic: a flexible trimmer for Illumina sequence data. *Bioinformatics* **30**, 2114–2120.

182 Kim D, Langmead B & Salzberg SL (2015) HISAT: a fast spliced aligner with low memory requirements. *Nat Methods* **12**.

183 Li H, Handsaker B, Wysoker A, Fennell T, Ruan J, Homer N, Marth G, Abecasis G, Durbin R & Subgroup 1000 Genome Project Data Processing (2009) The Sequence Alignment/Map format and SAMtools. *Bioinformatics* **25**, 2078–2079.

184 Liao Y & Smyth GK (2019) The R package Rsubread is easier , faster , cheaper and better for alignment and quantification of RNA sequencing reads. **47**.

185 Robinson MD, Mccarthy DJ & Smyth GK (2010) edgeR: a Bioconductor package for differential expression analysis of digital gene expression data. *Bioinformatics* **26**, 139–140.

186 Eden E, Navon R, Steinfeld I, Lipson D & Yakhini Z (2009) GOrilla: a tool for discovery and visualization of enriched GO terms in ranked gene lists. *BMC Bioinformatics* **10**, 1–7.

187 Satija R, Farrell JA, Gennert D, Schier AF & Regev A (2015) Spatial reconstruction of single-cell gene expression data. *Nat Biotechnol* **33**, 495–502.

188 Hao Y, Hao S, Andersen-Nissen E, Mauck WM, Zheng S, Butler A, Lee MJ, Wilk AJ, Darby C, Zager

M, Hoffman P, Stoeckius M, Papalexi E, Mimitou EP, Jain J, Srivastava A, Stuart T, Fleming LM, Yeung B, Rogers AJ, McElrath JM, Blish CA, Gottardo R, Smibert P & Satija R (2021) Integrated analysis of multimodal single-cell data. *Cell* **184**, 3573–3587.e29.

189 Trapnell C, Cacchiarelli D, Grimsby J, Pokharel P, Li S, Morse M, Lennon NJ, Livak KJ, Mikkelsen TS & Rinn JL (2014) The dynamics and regulators of cell fate decisions are revealed by pseudotemporal ordering of single cells. *Nat Biotechnol* **32**, 381–386.

190 Clark RI, Salazar A, Pellegrini M, William W, Walker DW, Clark RI, Salazar A, Yamada R, Fitz-gibbon S, Morselli M & Alcaraz J (2015) Distinct Shifts in Microbiota Composition during Drosophila Aging Impair Intestinal Function and Drive Mortality. *CellReports* **12**, 1656–1667.

191 Guo L, Karpac J, Tran SL & Jasper H (2014) PGRP-SC2 Promotes Gut Immune Homeostasis to Limit Commensal Dysbiosis and Extend Lifespan. *Cell* **156**, 109–122.

192 Reiff T, Antonello ZA, Ballesta-Illán E, Mira L, Sala S, Navarro M, Martinez LM & Dominguez M (2019) Notch and EGFR regulate apoptosis in progenitor cells to ensure gut homeostasis in Drosophila . *EMBO J* **38**, 1–15.

193 Hu DJ & Jasper H (2019) Control of Intestinal Cell Fate by Dynamic Mitotic Spindle Repositioning Influences Epithelial Homeostasis and Longevity. *CellReports* **28**, 2807–2823.

194 Jin Y, Patel PH, Kohlmaier A, Pavlovic B, Zhang C & Edgar BA (2017) Intestinal Stem Cell Pool Regulation in Drosophila. *Stem Cell Reports* **8**, 1–9.

195 Ullman TA & Itzkowitz SH (2011) Intestinal inflammation and cancer. *Gastroenterology* **140**, 1807–1816.

196 Paquette N, Broemer M, Aggarwal K, Chen L, Husson M, Ertürk-Hasdemir D, Reichhart JM, Meier P & Silverman N (2010) Caspase-Mediated Cleavage, IAP Binding, and Ubiquitination: Linking Three Mechanisms Crucial for Drosophila NF-κB Signaling. *Mol Cell* **37**, 172–182.

197 Chen HJ, Li Q, Nirala NK & Ip YT (2020) The Snakeskin-Mesh Complex of Smooth Septate Junction Restricts Yorkie to Regulate Intestinal Homeostasis in Drosophila. *Stem Cell Reports* **14**, 828–844.

198 Guo X, Yin C, Yang F, Zhang Y, Huang H, Wang J, Deng B, Cai T, Rao Y & Xi R (2019) The Cellular Diversity and Transcription Factor Code of Drosophila Enteroendocrine Cells. *Cell Rep* **29**, 4172–4185.e5.

199 Beehler-Evans R & Micchelli CA (2015) Generation of enteroendocrine cell diversity in midgut stem cell lineages. *Dev* **142**, 654–664.

200 Wirtz S, Popp V, Kindermann M, Gerlach K, Weigmann B, Fichtner-Feigl S & Neurath MF (2017)

Chemically induced mouse models of acute and chronic intestinal inflammation. *Nat Protoc* **12**, 1295–1309.

201 Howard AM, Lafever KS, Fenix AM, Scurrah CR, Lau KS, Burnette DT, Bhave G, Ferrell N & Page-Mccaw A (2019) DSS-induced damage to basement membranes is repaired by matrix replacement and crosslinking. *J Cell Sci* **132**.

202 Amcheslavsky A, Jiang J & Ip YT (2009) Tissue Damage-Induced Intestinal Stem Cell Division in Drosophila. *Stem Cell* **4**, 49–61.

203 Karpowicz P, Perez J & Perrimon N (2010) The Hippo tumor suppressor pathway regulates intestinal stem cell regeneration. *Development* **137**, 4135–4145.

204 Jiang H, Grenley MO, Bravo MJ, Blumhagen RZ & Edgar BA (2011) EGFR/Ras/MAPK signaling mediates adult midgut epithelial homeostasis and regeneration in drosophila. *Cell Stem Cell* **8**, 84–95.

205 Combe BE, Defaye A, Bozonnet N, Puthier D, Royet J & Leulier F (2014) Drosophila microbiota modulates host metabolic gene expression via IMD/NF-κB signaling. *PLoS One* **9**.

206 Jones RM, Desai C, Darby TM, Luo L, Wolfarth AA, Scharer CD, Ardita CS, Reedy AR, Keebaugh ES & Neish AS (2015) Lactobacilli Modulate Epithelial Cytoprotection through the Nrf2 Pathway. *CellReports* **12**, 1217–1225.

207 Storelli G, Defaye A, Erkosar B, Hols P, Royet J & Leulier F (2011) Lactobacillus plantarum promotes drosophila systemic growth by modulating hormonal signals through TOR-dependent nutrient sensing. *Cell Metab* **14**, 403–414.

208 Masuda K & Kawata T (1979) Ultrastructure and Partial Characterization of a Regular Array in the Cell Wall of Lactobacillus brevis. *Microbiol Immunol* **23**, 941–953.

209 Jakava-Vijanen M, Avall-Jaaskelainen S, Messner P, Sleytr UB & Palva A (2002) Isolation of Three New Surface Layer Protein Genes (slp) from Lactobacillus brevis ATCC 14869 and Characterization of the Change in Their Expression under Aerated and Anaerobic Conditions. *J Bacteriol* **184**, 6786–6795.

210 Sleytr UB, Schuster B, Egelseer E & Pum D (2014) S-layers : principles and applications. *FEMS Microbiol Rev* **38**, 823–864.

211 Fagan RP & Fairweather NF (2014) Biogenesis and functions of bacterial S-layers. *Nat Rev Microbiol* **12**, 211–222.

212 Ryan A, Lynch M, Smith SM, Amu S, Nel HJ, McCoy CE, Dowling JK, Draper E, O'Reilly V, McCarthy

C, O'Brien J, Eidhin D, O'Connell MJ, Keogh B, Morton CO, Rogers TR, Fallon PG, O'Neill LA, Kelleher D & Loscher CE (2011) A role for TLR4 in clostridium difficile infection and the recognition of surface layer proteins. *PLoS Pathog* **7**.

213 Ellis SJ & Tanentzapf G (2010) Integrin-mediated adhesion and stem-cell-niche interactions. *Cell Tissue Res* **339**, 121–130.

214 Fernandez-Minan A, Martin-Bermudo MD & Gonzalez-Reyes A (2007) Integrin Signaling Regulates Spindle Orientation in Drosophila to Preserve the Follicular-Epithelium Monolayer. *Curr Biol* **17**, 683–688.

215 Marthiens V, Kazanis I, Moss L, Long K & Ffrench-Constant C (2010) Adhesion molecules in the stem cell niche – more than just staying in shape? *J Cell Sci* **123**, 1613–1622.

216 Toyoshima F & Nishida E (2007) Spindle Orientation in Animal Cell Mitosis: Roles of Integrin in the Control of Spindle Axis. *J Cell Physiol*, 407–411.

217 You J, Zhang Y, Li Z, Lou Z, Jin L & Lin X (2014) Drosophila Perlecan Regulates Intestinal Stem Cell Activity via Cell-Matrix Attachment. *Stem Cell Reports* **2**, 761–769.

218 Beebe K, Lee WC & Micchelli CA (2010) JAK/STAT signaling coordinates stem cell proliferation and multilineage differentiation in the Drosophila intestinal stem cell lineage. *Dev Biol* **338**, 28–37.

219 Shaw RL, Kohlmaier A, Polesello C, Veelken C, Edgar BA & Tapon N (2010) The Hippo pathway regulates intestinal stem cell proliferation during Drosophila adult midgut regeneration. *Development* **137**, 4147–4158.

220 Wang C, Guo X & Xi R (2014) EGFR and Notch signaling respectively regulate proliferative activity and multiple cell lineage differentiation of Drosophila gastric stem cells. *Cell Res* **24**, 610–627.

221 Barker N (2014) Adult intestinal stem cells: Critical drivers of epithelial homeostasis and regeneration. *Nat Rev Mol Cell Biol* **15**, 19–33.

222 Scopelliti A, Cordero JB, Diao F, Strathdee K, White BH, Sansom OJ & Vidal M (2014) Local control of intestinal stem cell homeostasis by enteroendocrine cells in the adult Drosophila midgut. *Curr Biol* **24**, 1199–1211.

223 Houtz P, Bonfini A, Liu X, Revah J, Guillou A, Poidevin M, Hens K, Huang HY, Deplancke B, Tsai YC & Buchon N (2017) *Hippo, TGF-, and Src-MAPK pathways regulate transcription of the upd3 cytokine in Drosophila enterocytes upon bacterial infection*.

224 Capo F, Chaduli D, Viallat-Lieutaud A, Charroux B & Royet J (2017) Oligopeptide Transporters of the SLC15 Family Are Dispensable for Peptidoglycan Sensing and Transport in Drosophila. *J Innate*

Immun **9**, 483–492.

225 Gendrin M, Welchman DP, Poidevin M, Hervé M & Lemaitre B (2009) Long-range activation of systemic immunity through peptidoglycan diffusion in Drosophila. *PLoS Pathog* **5**.

226 Troha K, Nagy P, Pivovar A, Lazzaro BP, Hartley PS & Buchon N (2019) Nephrocytes Remove Microbiota-Derived Peptidoglycan from Systemic Circulation to Maintain Immune Homeostasis. *Immunity* **51**, 625–637.e3.

227 Zaidman-Rémy A, Hervé M, Poidevin M, Pili-Floury S, Kim MS, Blanot D, Oh BH, Ueda R, Mengin-Lecreulx D & Lemaitre B (2006) The Drosophila Amidase PGRP-LB Modulates the Immune Response to Bacterial Infection. *Immunity* **24**, 463–473.

228 Fusunyan RD, Nanthakumar NN, Baldeon ME & Walker WA (2001) Evidence for an innate immune response in the immature human intestine: Toll-like receptors on fetal enterocytes. *Pediatr Res* **49**, 589–593.

229 Lee J, Mo JH, Katakura K, Alkalay I, Rucker AN, Liu Y-T, Lee H-K, Shen C, Cojocaru G, Shenouda S, Kagnoff M, Eckmann L, Ben-Neriah Y & Raz E (2006) Maintenance of colonic homeostasis by distinctive apical TLR9 signalling in intestinal epithelial cells. *Nat Cell Biol* **8**, 1327–1336.

230 Fre S, Bardin A, Robine S & Louvard D (2011) Notch signaling in intestinal homeostasis across species: The cases of Drosophila, Zebrafish and the mouse. *Exp Cell Res* **317**, 2740–2747.

231 Wu K, Tang Y, Zhang Q, Zhuo Z, Sheng X, Huang J, Ye J, Li X, Liu Z & Chen H (2021) *Aging-related upregulation of the homeobox gene caudal represses intestinal stem cell differentiation in Drosophila*.

232 Parvy JP, Yu Y, Dostalova A, Kondo S, Kurjan A, Bulet P, Lemaître B, Vidal M & Cordero JB (2019) The antimicrobial peptide defensin cooperates with tumour necrosis factor to drive tumour cell death in Drosophila. *Elife* **8**, 1–26.

233 Dutta J, Fan Y, Gupta N, Fan G & Gélinas C (2006) Current insights into the regulation of programmed cell death by NF-**κ**B. *Oncogene* **25**, 6800–6816.

234 Van Antwerp DJ, Martin SJ, Verma IM & Green DR (1998) Inhibition of TNF-induced apoptosis by NF-**κ**B. *Trends Cell Biol* **8**, 107–111.

235 Ren F, Shi Q, Chen Y, Jiang A, Ip YT, Jiang H & Jiang J (2013) Drosophila Myc integrates multiple signaling pathways to regulate intestinal stem cell proliferation during midgut regeneration. *Cell Res* **23**, 1133–1146.

236 Downward J (1998) Ras signalling and apoptosis. *Curr Opin Genet Dev* **8**, 49–54.

237 Ward RL, Todd A V., Santiago F, O'Connor T & Hawkins NJ (1997) Activation of the K-ras oncogene in colorectal neoplasms is associated with decreased apoptosis. *Cancer* **79**, 1106–1113.

238 Mayo MW, Norris JL & Baldwin AS (2001) Ras regulation on NF-**κ**B and apoptosis. In *Methods in Enzymology* pp. 73–87.

239 Hauling T, Krautz R, Markus R, Volkenhoff A, Kucerova L & Theopold U (2014) A Drosophila immune response against Ras-induced overgrowth. *Biol Open* **3**, 250–260.

240 Ragab A, Buechling T, Gesellchen V, Spirohn K, Boettcher AL & Boutros M (2011) Drosophila Ras/MAPK signalling regulates innate immune responses in immune and intestinal stem cells. *EMBO J* **30**, 1123–1136.

241 Tian A, Morejon V, Kohoutek S, Huang Y, Deng W & Jiang J (2022) Damage-induced regeneration of the intestinal stem cell pool through enteroblast mitosis in the Drosophila midgut . *EMBO J*, 1–16.